

FINAL Report

**Assessment of Hydrocarbon Seepage Detection Methods
On the Fort Peck Reservation, Northeast Montana**

FINAL Technical Report 4

For the time period:
06/15/2000-06/30/2003

By

Lawrence M. Monson

June 30, 2003

DOE Award #: DE-FG26-00BC15192

Assiniboine and Sioux Tribes
Fort Peck Reservation
P.O. Box 1027
Poplar, MT 59255

DISCLAIMER

“This report was prepared as an account of work sponsored by an agency of the United States Government. Neither the United States Government nor any agency thereof, nor any of their employees, makes any warranty, express or implied, or assumes any legal liability or responsibility for the accuracy, completeness, or usefulness of any information, apparatus, project, or process disclosed, or represents that its use would not infringe privately owned rights. Reference herein to any specific commercial product, process, or service by trade name, trademark, manufacturer, or otherwise does not necessarily constitute or imply its endorsement, recommendation, or favoring by the United States Government or any agency thereof. The views and opinions of authors expressed herein do not necessarily state or reflect those of the United States Government or any agency thereof.”

ABSTRACT

This is the FINAL Technical Report for DOE Grant No. DE-FG-26-00BC15192 entitled *“Assessment of Hydrocarbon Seepage on Lands Belonging to Ft. Peck Tribes: Soil Geochemistry Application on Aeromagnetic, Landsat Lineament, and 3D Seismic Anomalies”*. Surface exploration techniques have been employed in separate study areas on the Fort Peck Reservation in northeastern Montana. Anomalies associated with hydrocarbon seepage are documented in all three areas and a variety of surface exploration techniques can be compared. In a small area with established production, Head Gas and Thermal Desorption methods best match production; other methods also map depletion. In a moderate-size area that has prospects defined by 3D seismic data, Head Gas along with Microbial, Iodine, and Eh soil anomalies are all associated with the best hydrocarbon prospect. In a large area that contains many curvilinear patterns observed on Landsat images, that could represent micro-seepage chimneys, results are inconclusive. Reconnaissance mapping using Magnetic Susceptibility has identified a potential prospect; subsequent Soil Gas and Head Gas surveys suggest hydrocarbon potential.

In the final year of this project the principle contractor, the Fort Peck Tribes, completed a second survey in the Wicape 3D Seismic Prospect Area (also known as Area 6 in Phase I of the project) and sampled several Landsat image features contained in the Smoke Creek Aeromag Anomaly Area (also known as Area 1 in Phase II of the project). Methods determined to be most useful in Phases I and II, were employed in this final Phase III of the study. The Southwest Wicape seismic anomaly was only partially confirmed. The abundant curvilinears proposed to be possible hydrocarbon micro-seepage chimneys in the Smoke Creek Area were not conclusively verified as such. Insufficient sampling of background data precludes affirmative identification of these mostly topographic Landsat features as gas induced soil and vegetation anomalies. However relatively higher light gas concentrations were found associated with some of the curvilinears. Based on the findings of this work the Assiniboine & Sioux Tribes of the Fort Peck Reservation intend to utilize surface hydrocarbon exploration techniques for future identification and confirmation of oil and gas prospects.

TABLE OF CONTENTS

Cover Page.....	1
Title Page	2
Disclaimer	3
Abstract.....	4
Table of Contents	5
List of Illustrations.....	6-8
Introduction.....	9-11
Geologic Setting.....	12-13
Executive Summary	14-17
<i>Technical Description of Work</i>	
Experimental Procedures.....	18-26
Results and Discussion.....	27
Phase I.....	27-36
Phase II.....	36-47
Other Phase II.....	47-60
Phase III.....	61
Wicape Southwest.....	61-65
Smoke Creek Revisited.....	66-73
Curvilinear Photos.....	73-77
Phase III Conclusions.....	77-78
Final Conclusions.....	78-79
References.....	80-81
Appendices	
A: Jack Land Report.....	82-88
B: Shurr Smoke Creek Phase II Report.....	89-131
C: Wicape Southwest Data Tables.....	132-143
D: Phase III Smoke Creek Data Tables.....	144-165
E: Phase I Commercial Lab Reports (one copy only)	
F: Phase II Commercial Lab Reports (one copy only)	
G: Phase III Commercial Lab Reports (one copy only)	

LIST OF ILLUSTRATIONS

Figure 1. Proposed sample areas with Fort Peck index map.
Figure 2. Summary poster.
Figure 3. Regional tectonic elements and Fort Peck.
Figure 4. Fort Peck tectonic regimes, structural elements, and seismic profile.
Figure 5. Paleozoic producing formations on Reservation.
Figure 6. Location map, with proposed surface exploration areas.
TABLE 1: Exploration Methods
TABLE 2: Exploration Details
Figure 7. Gas chromatograph used for soil probe analysis.
Figure 8. Field operations.
Figure 9. Field sampling.
Figure 10. Power auger and soil gas probe.
Figure 11. Exploranium KT-9 Kappameter.
Figure 12. Geometrics Model G-856 Magnetometer.
Figure 13. Author and Mr. Land in action with the two magnetic instruments.
Figure 14. Location of Area 7, Palomino Oil Field.
Figure 15. Palomino Nisku structure and wells.
Figure 16. Comparison of soil Propane methods at Palomino Oil Field.
Figure 17. Palomino propane gas comparison graph.
Figure 18. Palomino Field Microbial methods compared.
TABLE 3: DATA ANALYSIS - AREA 7
Figure 19. Location of Area 6.
Figure 20. Wicape 3D seismic time structure map.
Figure 21. Wicape sample grid.
Figure 22. Area 6 field views.
TABLE 4: DATA ANALYSIS - AREA 6
Figure 23. Area 6 propane data comparison.
Fig. 24. AREA 6 propane SOIL GAS COMPARISON graph.
Figure 25. Comparison maps of indirect hydrocarbon indicators for Area 6.
Figure 26. Other Area 6 indirect indicators mapped.
Figure 27. Fort Peck aeromagnetic map.
Figure 28. Fort Peck topography and streams.
Figure 29. Fort Peck TM composite satellite image.
Figure 30. Lineament block model and zones for Fort Peck.
Figure 31. Smoke Geoterrrex aeromagnetic anomaly map.
Figure 32. Deflection of structural folds, and seismic time and isochron contours.
Figure 33. Lineament Zone Intersection.
Figure 34. Other Anomalies over Smoke Creek AeroMag Anomaly.
Figure 35. Satellite tonal anomalies with contoured abundance over SC Mag.
Figure 36. Curvilinears, lineaments, and associated aeromag “fault” lines.
Figure 37. Model and evidence for diagenetic chimneys.
Figures 38 and 39. Smoke Creek area photos.
Figure 40. Area 1, Smoke Creek, magnetic susceptibility survey lines.
Figure 41. Area 1 magnetic susceptibility anomalous areas.

Figure 42. Combined residual field magnetic profiles for Smoke Creek.

Figure 44. Area 1 propane data comparison graph.

Figure 45. Area 1 graph comparison of Head Gas to Eh.

Figure 46. Site 26 map of Magnetic Susceptibility anomaly.

Figure 47. 3D time structure map in vicinity of Site 26.

Figure 48. Site 26 Soil Gas propane map.

Figure 49. Site 26 Head Gas propane map.

Figure 50. Smoke Creek Core Area comparison graph of Mag-Sus and propane.

Figure 51. Smoke Creek Core data validity: a – Soil Gas, b – Head Gas.

Figure 52. Smoke Creek Core Mag-Sus, Microbial, and Iodine.

Figure 53. Lobo West Mag-Sus vs. gas: a – profile overlap, b – correlated pts.

Figure 54. Smoke Creek Area magnetic susceptibility anomalies of Land.

Figure 55. Smoke Creek structural domains of Shurr.

TABLE 5. Smoke Creek structural domain observations of Shurr.

Figure 56. Smoke Creek structural domains, curvilinears, and aeromag anomaly.

Figure 57. Smoke Creek structural domains, curvilinears, and Mag-Sus AIR.

Figure 58. Mag-SusProfile anomalies, AeroMag Anomaly with Lineament Zones.

Figure 59. Magnetic Susceptibility Profile anomalies and satellite curvilinears.

Figure 60. Smoke Creek flux source zones of Shurr.

Figure 61. Site 26 data relationship.

Figure 62. Smoke Creek Core Mag-Sus vs. Gas anomalies highlighted.

Figure 63. Smoke Creek anomalies distribution of data types in space and time.

Figure 64. Diagenetic cap model of Klusman and Saeed (1996).

Figure 65. Smoke Creek hydrocarbon flux model by Shurr.

Figure 66. Wicape SW 3D seismic anomaly.

Figure 67. Wicape SW soil survey grid.

Figure 68. Wicape SW data comparison maps.

Figure 69. Wicape Head Gas data comparison graphs: a – ratio, b- frequency.

TABLE 6: LINE R PROPANE DATA COMPARISON, 2002 vs. 2000.

Figure 70. Wicape SW Line R data comparison graph.

Figure 71. Smoke Creek Phase III sample program.

Figure 72. Repeat of Lineament Zone Block Model.

Figure 73. Smoke Creek folds in Bakken Time display.

Figure 74. Smoke Creek Phase III data validity for all data set.

Figure 75. Smoke Creek Phase III Head Gas propane data graph and summary.

Figure 76. Smoke Creek West curvilinear data.

Figure 77. Smoke Creek Northwest curvilinear data.

Figure 78. Smoke Creek Core curvilinear data.

Figure 79. Smoke Creek West Core curvilinear data.

Figure 80. Smoke Creek East Core curvilinear data.

Figure 81. Smoke Creek Northeast curvilinear data.

Figure 82. Smoke Creek Phase III lineament Head Gas propane data graph.

Figure 83. Distant and close-up views of Curvilinear 1.

Figure 84. Curvilinear 2 viewed to the southwest.

Figure 85. Lineament 1 and Curvilinear 3 viewed southeast.

Figure 86. View southeast of Curvilinear 4.

Figure 87. Curvilinear 5 viewed from the southwest.

Figure 88. Views of Curvilinear 6.

Figure 89. Curvilinear 7 viewed from the southeast.

Figure 90. View southeast across Lineament 2.

FINAL REPORT
Surface Hydrocarbon Exploration
Fort Peck Reservation Assessment

By Lawrence M. Monson

INTRODUCTION

Oil and gas have been produced on the Fort Peck Indian Reservation for fifty years. The Fort Peck Tribes have been actively engaged in exploration and production activity during the past fifteen years. As a part of this on-going effort, data sets have been built and prospects have been generated. This grant from the United States Department of Energy has provided an opportunity to assess the utility of surface exploration technology in prospect characterization.

The primary objective of the DOE grant is to conduct surface geochemical and non-seismic, geophysical sampling of soils above geologic or geophysical anomalies that have hydrocarbon potential. Sampling programs were carried out on Tribal lands in a phased approach. During the initial phase, hydrocarbon detection methods and study areas were identified and assessed. Subsequently, the selected detection methods were applied in a series of progressively larger and more complex study areas.

In this Final Technical Report for DOE Grant # DE-FG26-00BC15192, summaries of previous work for Phases I and II of the project are included from the three Semi-annual Technical Progress Reports, 15192R01,2,3 (Monson, 2000, 2001, 2002). New surface exploration data is also presented for a third 3D seismic prospect and for many of the satellite anomalies located in the Smoke Creek aeromagnetic area thought to possibly represent hydrocarbon micro-seepage chimneys. Finally an attempt was made to establish in-house gas detection capabilities for future Tribal exploration efforts.

Phase I applied and compared several existing commercial techniques for either direct or indirect detection of gas micro-seepage. In the initial grant proposal multiple areas of Tribal land where identified as being prospective for oil exploration.

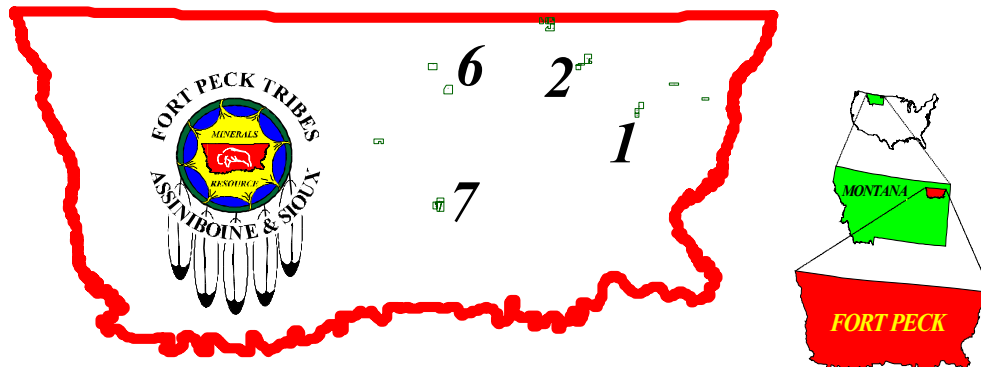


Fig. 1. Proposed sample areas (principle ones numbered) with Fort Peck index map.

An earlier Minerals Assessment funded by the Energy and Minerals Division of the Bureau of Indian Affairs had mapped these sites. That study acquired seismic, well, and other geophysical data for the Assiniboine and Sioux Tribes of the Fort Peck Reservation. In part due to the work of the Tribal Minerals Office geologist on that assessment, the Tribes entered into one of the largest Indian Minerals Development Act (IMDA) agreements in the nation with Gulf Canada. Gulf Canada acquired 85 sections of 3D seismic data in two prospect areas and was the technical sponsoring partner for the Tribes in this DOE funded study. In addition two consultants were included on the team: George Shurr (remote sensing), and Kipp Carroll (surface hydrocarbon exploration). In order to begin evaluating which techniques worked best on the reservation, sampling was done above and an existing oil field and one of the best 3D seismic prospects. As funds were limited, both the oil field and the seismic prospect were selected because of their small areas. Both were required to contain Tribal mineral ownership as well. The Palomino Oil Field and the "Tobago" Prospect in the Wicape 3D survey fit those parameters. Gulf was attempting to find partners to drill the Tobago prospect during and after the geochemical survey was performed. Figure 2 is a summary poster of the proposed project.

Phase II was designed to evaluate the numerous satellite curvilinears concentrated within the Smoke Creek AeroMag Anomaly. Monson and Shurr (1993) suggested that these could represent micro-seepage chimneys as modeled by Land (1991). These anomalies were the primary reason for this DOE funded study. Lying in a nine-township area of the reservation, at the intersection of many geologic trends that included structural, stratigraphic, geomorphic changes, these tonal anomalies needed further analysis. In the second year of this study background samples using the best methods from Phase I were taken around the Smoke Creek AeroMag Anomaly. A comprehensive ground magnetic susceptibility survey was then conducted. Due to the large size of the aeromagnetic anomaly and the wide distribution of the curvilinears, sampling had to be done first only as reconnaissance traverses and then to best minimize the number of samples collected. The magnetic susceptibility survey attempted to collect data over the entire aeromag anomaly rather than focus on individual curvilinears.

Phase III represents new data collected since the third semi-annual report. With the emergence of a new IMDA partner wanting to identify other drilling sites in the Wicape 3D Area, a third anomaly was sampled in the southwest part of the survey. Then a program was conducted to sample as many of the Smoke Creek curvilinears, lineaments, and other structural axes as possible during the past field season. Samples were collected along the perimeters and along one perpendicular profile through the curvilinears. Samples collected for the most favored method were also analyzed in-house. Results from these new operations are discussed in this final report.

PROPOSED SAMPLE SITES
for Hydrocarbon Exploration
using Non-seismic Surface Techniques.
With Geologic Examples.

Project funded by U.S. Dept. of Energy,
National Petroleum Technology Office.

Prime contractor: Assiniboine & Sioux Tribes,
Fort Peck Reservation, Montana.

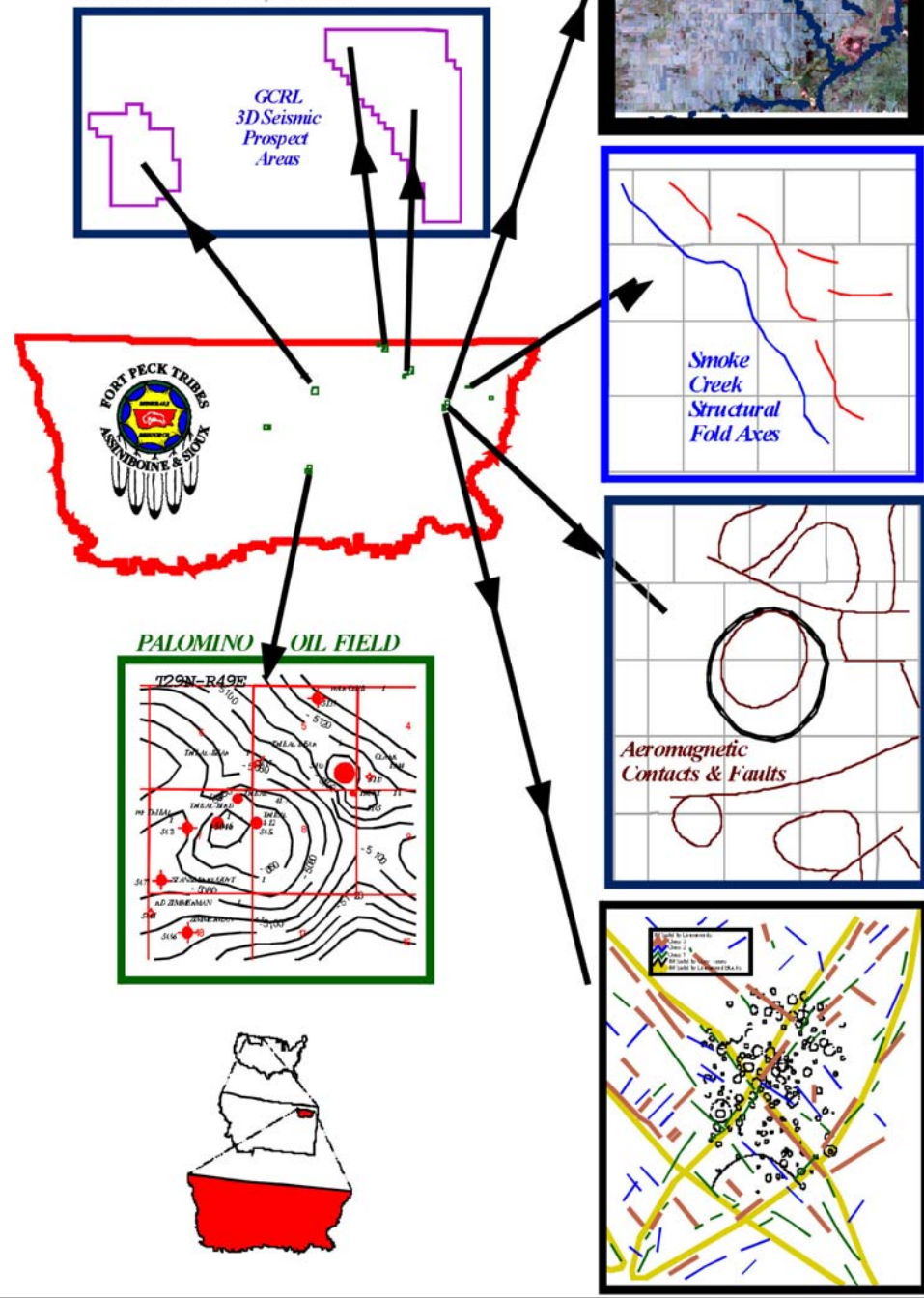


Figure 2. Summary poster.

GEOLOGIC SETTING AND OIL PRODUCTION

The Fort Peck Reservation is part of a regional tectonic element on the western margin of the Williston basin (Figure 3). The marginal tectonic elements were active during deposition of the Zuni Sequence and are made up of a grid of lineament-bound basement blocks (Shurr and others, 1989). Reservation geology is summarized several papers by Monson (see References).

Figure 3. Regional tectonic elements and Fort Peck (modified from Shurr, et al., 1989a).

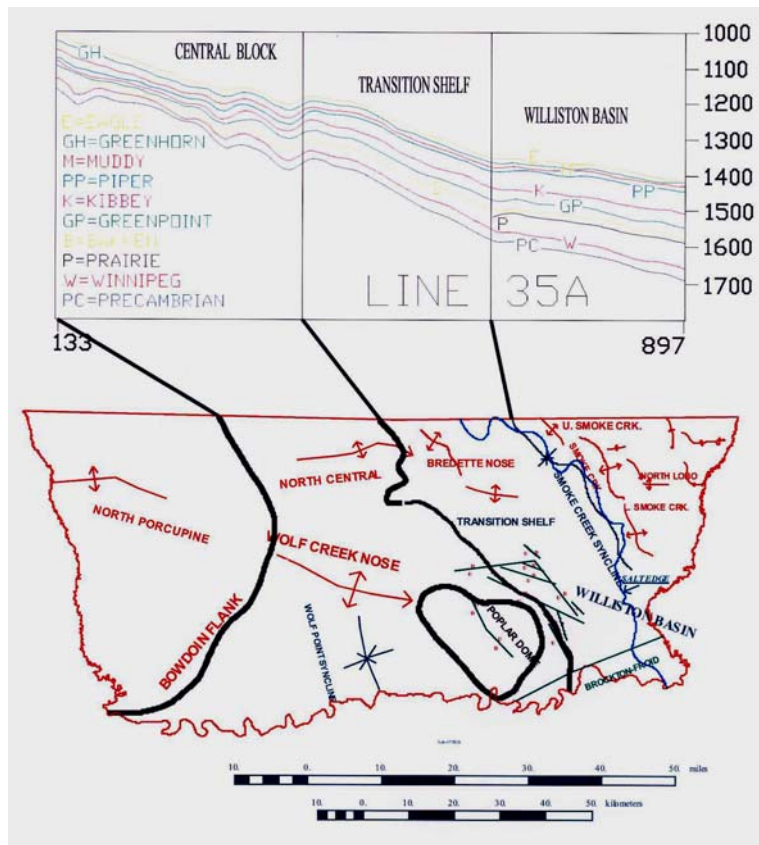
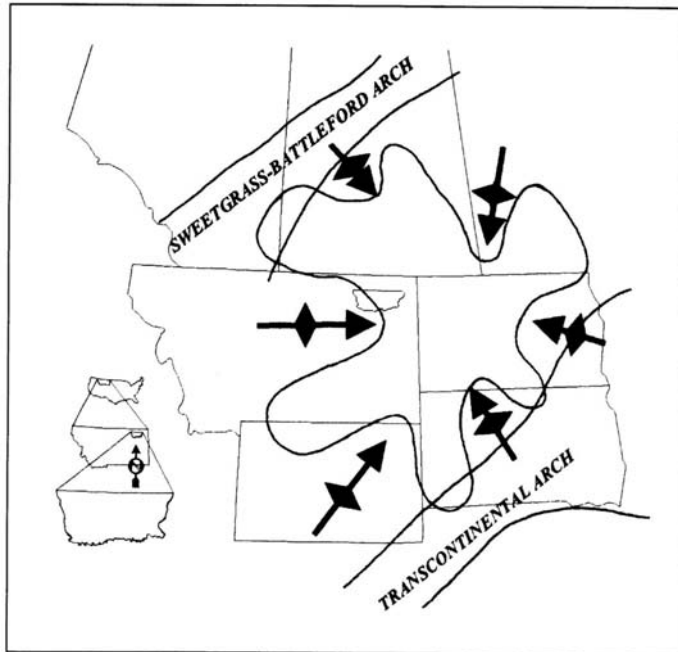
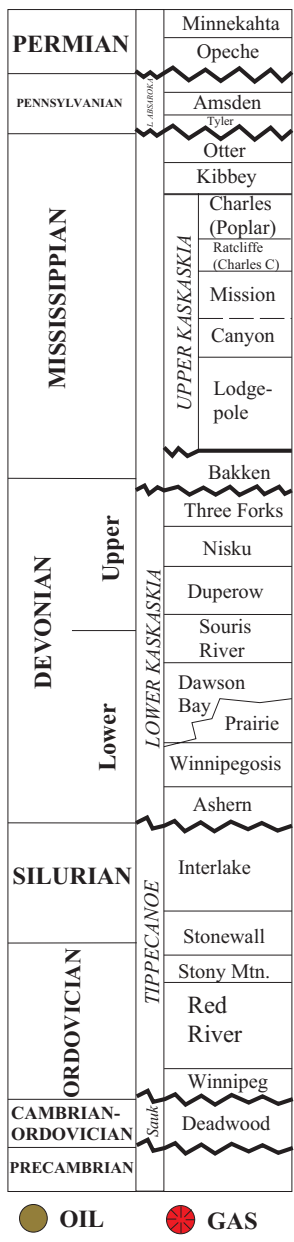


Figure 4. Fort Peck tectonic regimes and structural elements with seismic line profile.

Lineament blocks influenced deposition of reservoir rocks, source beds, and seals and controlled development of structural traps. Three main tectonic subdivisions that are mosaics of basement blocks have been identified on the reservation (Figure 4). The subdivisions have expression on structural and stratigraphic maps, Landsat images, and seismic profiles (Monson and Lund, 1991). Fort Peck Reservation thus has a structural style that is characteristic throughout the basin. Petta, (1999) portrays this transition zone as part of basement controlled suture zone between the Trans-Hudson Province and the Wyoming craton. He advocates that this suture



Zone has numerous prolific oil fields with fractured reservoirs. Hydrocarbon production on the reservation is from Paleozoic formations that are important Williston basin targets.

Paleozoic reservoirs (Figure 5) have produced more than 80 million barrels of oil on the reservation since the first discovery in 1952 (Monson, 1995). About half of the thirty-four fields are still active, including the East Poplar field, which is the largest on the reservation and one of the best in the Williston basin. East Poplar and most of the other active fields are located in the Central tectonic subdivision (Figure 4).

More than 45 million barrels of oil have been produced from the Mississippian Charles Formation where salt solution (Orchard, 1987) has enhanced porosity development over Poplar dome. Total Charles production on the reservation exceeds 56 million barrels.

The Devonian Nisku Formation is another important Paleozoic pay zone in the Williston basin and on Fort Peck Reservation. More than 20 million barrels have been produced from small, prolific fields that are also located in the Central Block although the reservoir could extend into the transition zone (Figure 4). These local structural knobs are thought to be the result of two-stage salt solution (Swenson, 1967).

The three study areas in which surface exploration techniques have been employed on the reservation are all over small seismic structures that have either Nisku production or potential. Surface exploration techniques have been successfully applied to prospects constrained by seismic and Landsat in other parts of the western Williston basin (Andrew and others, 1991)

Figure 5. Paleozoic producing formations on Reservation.

EXECUTIVE SUMMARY

Three study areas (Figure 6) were selected from a group of more than a dozen candidate areas. Reservation-wide databases were employed in the selection process. Subsequently, more detailed local data sets were extracted and displayed to characterize three final study areas. The final three study areas were chosen to represent a spectrum of characteristics, so that work progressed in a phased approach through the three areas. Initial work was done in the Palomino Oil Field. This small area has well-established production that provides a test of utility for the various surface exploration techniques. The Wicape Prospect Area is an intermediate-sized area. Although it has no established production, this area does have well-documented 3D seismic structures that are prospects with excellent potential. The largest study area is the Smoke Creek Area which has a variety of anomalies documented by stratigraphy, structure, geophysics, and remote sensing. Some of these anomalies have potential to be hydrocarbon prospects in an area with a sparse drilling density of only one well per township. As work progressed from the small area with established production to the large area with wildcat potential, a variety of surface exploration techniques were employed and compared.

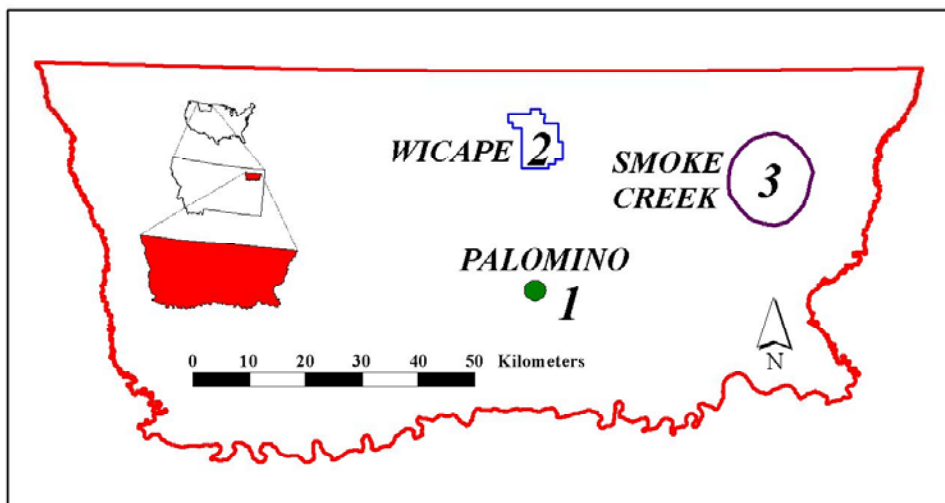


Figure 6. Location of Fort Peck Reservation, northeast Montana, U.S. with surface hydrocarbon exploration areas: 1 – Palomino Oil Field, 2 – Wicape 3D Seismic Prospect Area, 3 – Smoke Creek AeroMag Anomaly.

Phase I (2000): Two of the fifteen proposed areas were selected for surface hydrocarbon exploration on the Fort Peck Reservation in northeastern Montana. These included: 1) Area 7, which lies above a producing oil field, and 2) Area 6, which contains two 3D seismic anomalies. The following hydrocarbon detection methods were chosen for comparison:

1. Free soil gas survey. [SG]
2. Soil acid extraction of gases. [AE]
3. Soil UV Fluorescence. [F1]
4. Soil Magnetic Susceptibility. [MS]

5. Soil Microbial Measurement. [M1]
6. Soil Iodine. [I]
7. Soil head gas analysis of basic hydrocarbons. [HG]
8. Measurement of Soil supplemental indicators: Eh, PH, and Conductivity. [E], [P], [K] respectively.
9. Magneto-Telluric measurement of electromagnetic energy. [MT]

The last method was included free of charge as part of a demonstration prospecting permit and is only available for Area 7. Samples from Area 7 were also sent to a second fluorescence company [F2], to another company utilizing thermal desorption techniques [TD], and to another company for microbial measurement [M2].

The hydrocarbon detection techniques all employ the use of ratios of gases and in one case, detailed statistical normalization. Some companies provided interpretative reports and maps while some companies discounted for only providing the analytical results. All discounted for client field sampling which saved as much as 30% plus transportation costs. The following observations were made for Phase I of the study:

1. ***Head gas*** samples collected by power auger **correlate the best** to oil production and to 3D seismic anomalies.
2. ***Thermal Desorption*** analysis correlates well to production.
3. ***Direct soil gas*** measurements are five to ten times less sensitive and do not correlate as well to either production or to the seismic anomalies.
4. Both ***microbial*** methods show depletion over the oil field, but also have positive anomalies remaining. One 3D anomaly was confirmed in Area 6.
5. ***Acid extract*** gases are depleted over the oil field and correlate partially to the 3D anomalies, but also show a strong halo pattern.
6. ***Iodine, magnetic susceptibility, and UVF*** methods are difficult to interpret. These show depletion and halo anomalies.
7. ***Eh, pH, and Conductivity*** show halo/depletion or inverse anomalies over production and only Eh confirms gas seepage over 3D anomalies.

Area 7 contains the Palomino Oil Field, a Devonian oil reservoir that is among northeast Montana's best and appropriately has Tribal royalty interest in all the producing wells. Although twenty years old, the field still produces under natural pressure, requiring no pump lift assistance. The strong water drive mechanism that continues to force oil into each well bore has undoubtedly maintained constant surface gas micro-seepage. This hypothesis has been verified by the microbial anomalies associated with producing wells even though both microbial analytical sub-contractors claimed that no signature would be present after such a long period of production.

Of primary interest to the Assiniboine & Sioux Tribes is Area 6, which contains two 3D seismic anomalies that ranked high in Gulf Canada's exploration plans. From the results mapped in Area 7, certain methods were again employed in Area 6 based on how well they correlated to the Palomino structure and oil production,

how economical they were, and to the logistics of Tribal personnel sampling for a given method. As highlighted in the initial semi-annual progress report, and a subsequent topical, technical progress report, ***both seismic anomalies have associated surface gas seepage indications.***

Phase II: Phase II of the Fort Peck Tribes project to “Assess Hydrocarbon Seepage on the Reservation utilizing surface exploration techniques” applied the methods, which best correlated to the areas sampled in Phase I. The Head Gas method correlated well to production in the Palomino Oil Field (Area 6) and to 3D seismic anomalies in the Wicape Prospect (Area 7). Because the Tribes acquired Soil Gas chromatograph equipment from Kipp Carroll, who retired, this method was also continued. The Microbial and Iodine methods were the non-gas, indirect hydrocarbon detection methods retained. The Head Gas lab also provides Eh, pH, and K data at little extra charge.

Phase II fieldwork covered the principle reason for this entire study. In 1993 the author published a paper with George Shurr, which focused on the overwhelming set of surface and sub-surface geologic evidence that the Smoke Creek Aeromag Anomaly mapped a subsurface body of tremendous significance. Fold axes, stratigraphic deposition, regional dip, salt dissolution, topographic relief, drainage, soils, satellite lineament/fault blocks, and finally, curved tonal anomalies, all concentrate or hinge on what is buried beneath the eastern plains of the Fort Peck Reservation. A logical explanation of the curvilinears is that they represent hydrocarbon micro-seepage chimneys (Land, 1991).

Because of the size of Area 1 (9 townships) and because of the chimney model, Mr. Land was contracted to conduct a micro-magnetic survey using a Magnetic Susceptibility (MS) meter. His interpretations are included in the appendix along with another report by George Shurr regarding the measurements. MS profiles and maps reveal a complicated data distribution that cannot be correlated to Landsat curvilinears at the scale presented. Three anomalous areas were found, two, which are outside the SC Mag Anomaly. One proved to also have high “background” gas values, which were confirmed by denser sampling. Site 26, as it is named, is a valid oil prospect although it may be structurally low. It does point to hydrocarbons in the area of a 3D defined structure. Hydrocarbons were not confirmed in the other two anomalous MS areas. Microbial and Iodine techniques continue to have merit although not always directly or consistently with the Head Gas method.

Phase III: Encouraged by the apparent confirmation of hydrocarbon micro-seepage above two 3D seismic anomalies in the Wicape Area, another anomaly was sampled during the 2002 field season. This seismic prospect, named Southwest Wicape, lies on the south edge of the 3D survey. A new IMDA partner is interested in identifying additional well sites. Head gas and soil gas samples were collected over approximately 1,760 acres and focused around a 200-acre seismic closure. Fair Head Gas micro-seepage is mapped over the seismic anomaly, however a much stronger propane anomaly exists .5 miles (.8 km) to the west. Eh (redox potential) does not confirm either of these shows as it did in earlier surveys in the study. In-house gas spectrometer analysis of the Head Gas samples mapped the same positive anomaly to the west and a weaker anomaly to the

south, but is not a coincident correlation with the seismic high. Interestingly the probe soil gas method does map a hydrocarbon accumulation over the Wicape SW seismic prospect. This was not the case in other areas except for Site 26 in the northwest part of Area 1 (Smoke Creek). This prospect is scheduled to be the second one drilled in the Wicape IMDA agreement.

Returning to the principle reason for this study, thirteen of the circular, satellite tonal anomalies found in the Smoke Creek AeroMag Area were sampled in 2002. The perimeter and one perpendicular traverse were collected for curvilinears outside and within the core of the aeromag anomaly. Four satellite lineaments were also sampled and soil along part of the principle anticlinal fold axis in the area was also collected. There does not appear to be obvious confirmation that elevated gas micro-seepage occurs within or along the boundary of the curvilinears. As a whole the data set appears to have higher values associated with the perimeter of the curvilinears, but not necessarily for those within the Smoke Creek AeroMag Anomaly. The lineaments average higher propane soil content than the curvilinear centers especially outside the core area. When compared to the Phase II background data for Smoke Creek, the curvilinear perimeters do appear to be anomalous, but considerably more local data is necessary to confirm that observation. Field inspection of the curvilinears reveals that most are elevation closures associated with hills or ridges often along the slopes of the topography or sometimes tracing drainage gullies. They do not appear to be soil color changes or vegetation changes affected by gas seepage. More resistant soil types associated with the micro-seepage chimneys however could cause the topographic highs.

TECHNICAL DESCRIPTION OF WORK

EXPERIMENTAL PROCEDURES

Phase I: Figure 6 displays the sample sites chosen on the Fort Peck Reservation for the comparison of surface hydrocarbon exploration techniques. Area 7 was selected because it lies above the Palomino Oil Field, which is still free flowing under natural water drive and thus an excellent area to test whether hydrocarbon gases have, and are, seeping from the earth. Area 6 is the site of two 3D seismic anomalies mapped by the Tribes' exploration partner, Gulf Canada. These were the only two areas sampled in Phase I.

A comparison of the procedures, analytical techniques, data reported, and comments can be seen in Table 1.

TABLE 1: Exploration Methods
Fort Peck DOE Grant

METHOD	SAMPLING PROCEDURE	ANALYTICAL TECHNIQUE	DATA REPORTED	COMMENTS
1. Free soil gas [SG]	Milled 3 ft. steel pipe with slotted replaceable tip driven into ground with slide hammer. Syringe inserted through replaceable septa and air sample extracted after air is purged from pipe. Syringes transported in padded box.	Soil gas analyzed daily by portable baseline 1030A flame ion gas chromatograph. Empty probe samples run for checks. Output graph and molecular weight by % printed. Quantified in relation to research grade calibration gas.	Methane (ppb) Ethane Propane IsoButane N-Butane	Some samples lost due to power failures. Some gases not detected due to power spikes.
2. Soil Acid Extract [AE]	Soil samples collected from spade hole and placed in steel pint cans with biocide solution. Sealed.	Wesson and Armstrong procedure. Sub-samples retrieved, reacted with HCl and heated. Flame ion detector gas chromatograph used.	Methane (ppm) Ethane Ethylene Propane Propylene I-Butane N-Butane	Benzalconium chloride used as biocide to kill microbial bacteria that might consume H/C molecules.
3. UV Soil Fluorescence [F1]	(same as acid extract)	Sub-samples air-dried for 24 hrs. Polycyclic aromatic compounds extracted with non-polar	Naphthalene (ppb) (2-ring PAC) Phenanthrene	Heavier hydrocarbon molecule indicator. Could be

		solvents. Analysis by spectrophotometer.	(3-ring PAC)	contamination in oil field areas.
4. Magnetic Susceptibility [MS]	Soil sample collected from spade hole.	Meter measures ability of soil minerals to be magnetized.	CGS units reported.	
5. Soil Microbial [M1]	Soil samples collected from spade hole.	Culture only hydrocarbon feeding bacteria with nutrient agar for 72-96 hrs. Measure relative growth by colometric spectrophotometer.	Average raw data density value, relative average, percent ranking and model probability of success.	40 = strong 20 - 30 is significant.
6. Iodine [I]	Soil sample from spade hole.	Dry, sieve to 5 micrometers, weigh, digest to remove organics, titrate, colorimetric analysis.	Iodine (ppm)	Shallow depth.

7. Soil Head Gas [HG]	Soil samples collected by power auger, placed in sealed, double lid on 8 oz. jars separated by septum layer. Jars half filled with water. Lids have center punched 1/8"holes.	Head gas air sample extracted with syringe after gentle agitation. Air analyzed by flame ion detector gas chromatograph.	Methane Ethane Ethene Propane Propene I-Butane N-Butane I-Pentane N-Pentane	Two-inch auger diameter, 36 inches long with replaceable bits.
8a. Eh [E]	Same as Head Gas	Automated specific ion electrode probe analysis.	Millivolts	
8b. PH [P]	Same as Eh	Same as Eh	PH units	
8c. Conductivity [K]	Same as Eh	Same as Eh	Microhos units	
9. Soil Thermal	Spade hole soil sample. Placed	Samples agitated and heated. Analysis by	Methane Ethane	

Desorption [TD]	in glass jar with Teflon sealed, plastic lid.	Flame Ion Detector Gas Chromatograph.	Ethene Propane Propene i-Butanes n-Butane i-Pentane n-Pentane i-Hexane n-Hexane	
10. UV Soil Fluorescence [F2]	Spade hole soil sample.	Soil dried disaggregated, and sieved for fines (clay and silt) fraction. Proprietary solvent added, agitation, centrifuge extract analyzed with synchronous scanning UV fluorescence spectrometer.	Cumulative relative intensity calculated as oil probabilities. Analysis comparison of spectra.	

11. Soil Microbial [M2]	Spade hole soil sample.	Microscopic count of butane oxidizing microbes selectively culled from other organisms present.	Microbial count value.	Samples must be kept cool or dehydrated.
12. Magneto - Tellurics [MT]	Field readings	Portable audio frequency electro-magnetic telluric receiver. (AFMAG). Coupled to digital audiotape. Basically a magnetometer with long antennae dipoles. 10-30 channels collected.	Mud-log type graphs with resistivity plotted vs. depth. Porosity calculated from resistivity in some graphs.	

Table 2 summarizes the theoretical basis behind each hydrocarbon indication method. All samples were collected by Tribal personnel and sent to respective labs for analysis. A sub-contractor did the soil gas survey. All analytical sub-contractors provided data tables by e-mail and, or FAX transfer. The Head Gas sub-contractor supplied detailed and complete statistical analysis and full-color maps for selected data sets. Both Microbial sub-contractors prepared maps and statistical analyses. The Acid Extract company also prepared a thorough statistical review. Details of the sampling procedure and the hydrocarbon indication theory are organized in Table 2.

TABLE 2: Exploration Details
Fort Peck DOE Grant

METHOD	SAMPLE DEPTH	SAMPLE QUANTITY	SAMPLE CONTAINER	H/C INDICATOR	THEORETICAL BASIS
1. SG	61-91 cm	5 cc	syringe	Direct/Semi-Active	Vertical microseepage of light hydrocarbons.
2. AE	15-30 cm	4 cm in pint can	steel can	Direct/Passive	Extraction of occluded light hydrocarbons.
3. F1	15-30 cm	4 cm in pint can	steel can	Direct/Passive	Extraction of fracture migrated medium wt. hydrocarbons.
4. MS	15-30 cm	150 g	zip-loc bag	Indirect/Passive	Reducing environment above H/C seep precipitates ferrous minerals that are more easily magnetized.
5. M1	20 cm	30 g	zip-loc bag	Indirect/Passive	Presence of hydrocarbon feeding bacteria detected above micro-seepage
6. I	3 cm	340 g	zip-loc bag	Indirect/Passive	Hydrocarbon gases free and adsorb iodine from minerals or atmosphere.
7. HG	61-91 cm	625 g	8 oz. jar	Direct/Passive	Extraction of adsorbed light hydrocarbons from soil dissolved in water collected above microseepage.
8a. Eh	61-91 cm	625 g	8 oz. jar	Indirect/Passive	Relatively reducing environment above

					hydrocarbon microseepage.
8b. pH	61-91 cm	625 g	8 oz. jar	Indirect/Passive	Relative higher pH within and even higher pH surrounding H/C seep. Believed to be caused by calcite precipitation where weathered soils are neutralized by light H/C gas adsorption.
8c. K	61-91 cm	625 g	8 oz. jar	Indirect/Passive	Salts precipitated by higher pH soils at margin of microseepage anomaly.
9. TD	15 cm	625 g	Glass jar	Direct/Passive	Extraction of adsorbed hydrocarbons from soils above microseepage.
10. F2	15 cm	625 g	Glass jar	Direct/Passive	Detection of aromatic and double bonded hydrocarbons in soil above microseepage.
11. M2	15-22 cm	30 g	Paper envelope	Indirect/Passive	See M1, #5.

Photographs of the lab and field operations are contained in Figures 7-10.



Figure 7. Gas chromatograph used for soil probe analysis.



Figure 8. Field operations.



Figure 9. Field sampling.



Figure 10. Power auger and soil gas probe.

Phase II: The methods retained for Phase II included: 1) Head Gas, 2) Soil Gas, 3) Microbial (method 2), 4) Iodine and 5) Other indirect measurements provided by the Head Gas Analysis package of services (Eh, pH, and Conductivity). Magnetic Susceptibility measurements were also taken on the soil samples sent for Acid Extract analysis.

New to Phase II was the utilization of reconnaissance micro-magnetic exploration techniques as an investigation tool. The most extensive sampling occurred in the Smoke Creek Area with 1185 Magnetic Susceptibility measurements taken. This study, and this author, benefited greatly from the guidance of John Land. His participation in this project was both fortuitous and appropriate for two reasons: 1) Mr. Land has conducted micro-magnetic surveys for more than 47 years, and thus brought valuable experience and interpretation skills 2) The hydrocarbon seepage model cited in the author's previous work was published by Mr. Land and appears in Figure 36 of this report as well.



To conduct the Magnetic Susceptibility Survey, Mr. Land used an Exploranium KT-9 Kappameter. (See Figure 11). The procedure was simply to record at least three soil contact readings, which were then averaged by the meter. Bare soil was usually prepared by scraping the surface with the heel of a shoe in cultivated or sparsely vegetated soil. Where more dense and undisturbed prairie grasses grew, a small spade was used to open a test hole.

The theory behind using Magnetic Susceptibility measurements as a hydrocarbon exploration tool is that the meter measures how easily the near surface soil is magnetized. Electric currents sent into the soil create a magnetic field that is adsorbed by ferrous minerals in the soil. The indirect inference is that these alteration minerals are more likely formed in a

reducing chemical environment caused by the presence of natural gases in the soil. The tool is primarily a relative indicator (as most surface techniques are) of higher gas levels relative to background levels along the day's profile or adjacent profiles.

On the last three magnetic survey profiles, paths were chosen that best crossed the Smoke Creek Aeromag Anomaly. On these traverses, field magnetic measurements were made with a Geometrics Model G-856 Magnetometer (Figure 12). For each day a similar unit was also set up as a base station to measure the diurnal magnetic variations of the earth in this area. Field measurements were subtracted from the base station readings by synchronizing each unit's time clock and processing the data utilizing post acquisition software.

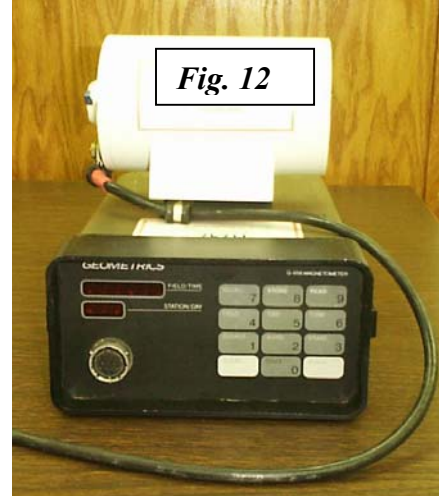




Fig. 13

Figure 13 shows the author and Mr. Land in action with the two magnetic instruments described above. The magnetometer was used to measure local variations in the earth's magnetic field. Although the survey apparently confirmed the overwhelming signature of the Smoke Creek Aeromag Anomaly, subsequent high frequency preservation may provide valuable hydrocarbon traces that could relate to the satellite tonal anomalies (curvilinears).

In all of the magnetic profiles the following sampling distances were employed: 1) Inside the Aeromag Closure - .2 mile (.32 km), 2) within 3 miles (4.8 km) - .3 mile (.48 km), 3) 3-6 miles (4.8 - 9.6 km) - .5 miles (.81 km). The Aeromag Closure is approximately 6 miles (9.6 km) in diameter. Thus each

traverse was approximately 18 miles (29 km). Sampling profiles followed existing roads and trails wherever possible with only a couple short traverses on foot. As with all earlier sampling, GPS locations were mapped and data entered into a laptop computer.

Phase III: The Head Gas package and soil gas probe samples were collected in a similar fashion and grid as were the Area 6 samples in Phase I (offsetting sample survey lines of 1320 feet). Only Head Gas samples were collected over the Smoke Creek satellite anomalies. Approximately 8 sites were selected for each perimeter and the perpendicular traverses collected samples every 1000 feet (305 m) beginning 2000 feet (610 m) outside the curvilinear. The lineaments were also sampled every 1000 feet (305 m). One of the curvilinears (#7) and the fold axis were sampled at 500-foot (152 m) intervals.

In an attempt to establish in-house analytical procedures for the Head Gas sampling method, a separate set of data was collected for each of the 2002 surveys. Problems with the flame ion detector produced inconsistent results for the Wicape SW data. Waiting for repairs and parts for the gas chromatograph and integrator delayed analysis of the Smoke Creek data for almost six months and caused degradation of the samples, which will be discussed later.

RESULTS AND DISCUSSION

Phase I: The Palomino Oil Field (Area 7, Fig. 14), was sampled in four intersecting traverses containing 27 collection points. These were centered on the field's best oil well, Tribal Bird 1-7, which has produced 1.4 million barrels of oil. (Fig. 15.)

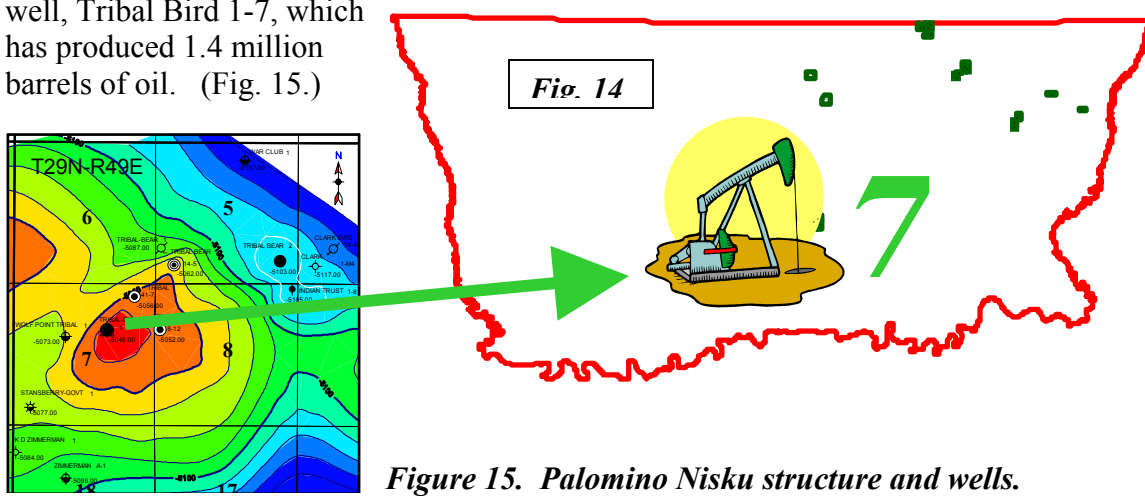


Figure 15. Palomino Nisku structure and wells.

A triplicate sample was taken at the intersection of the traverses. Initially the word "anomaly" refers to contoured map areas of values, usually greater, that indicate gas micro-seepage from the earth. 1.5 times the mean was determined to be a good common anomaly definition. Later reports calculated an anomaly index ratio that will be explained later in this report.

Propane was chosen for comparison purposes and data values were contoured in Figure 16 for each of the four methods, which analyzed for this gas. Head Gas best correlated with oil production. Acid Extract inversely correlated, revealing depletion by 20 years of production. Thermal Desorption partially correlates with production, but has an anomaly perpendicular to the Head Gas trend. This method and the Soil Gas Survey show depletion over the oil field and have elevated gas values to the northwest.

Table 3 is a complete summary of the results for Area 7. For propane, the Head Gas method best correlated with production. The Thermal Desorption method best reproduced propane results in the Triplicate Test. Figure 17 graphs propane for the four methods. The relatively small values and incomplete detection of the Soil Gas Survey data is noticeable. Head Gas and Thermal Desorption are relatively parallel while Acid Extract data is remarkably inverse to these two.

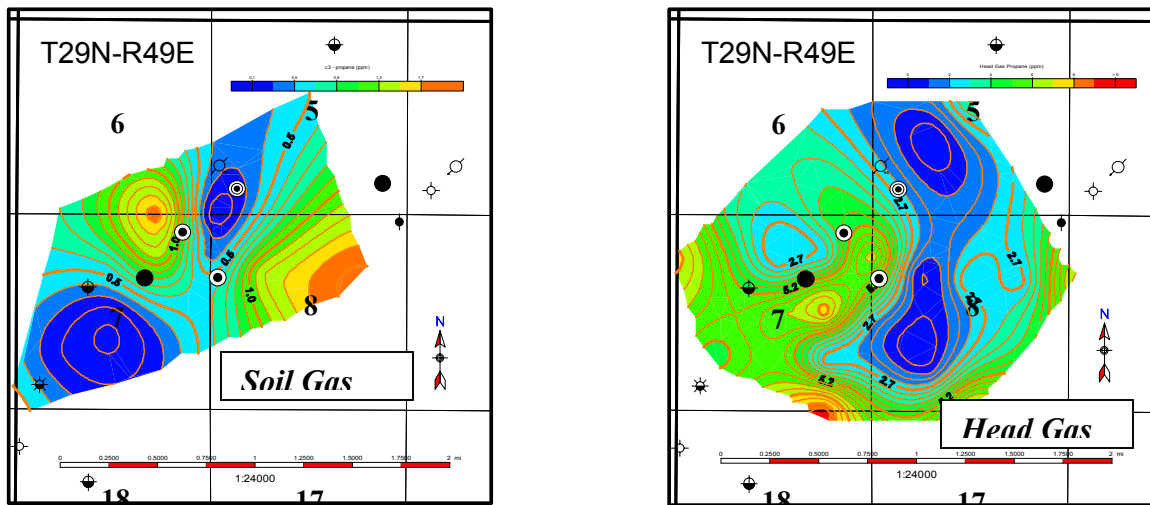
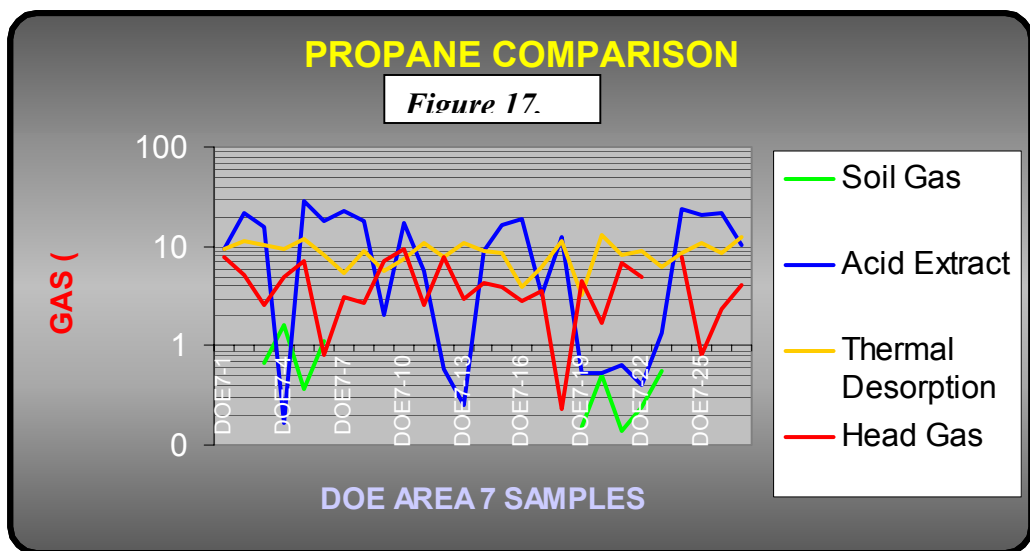
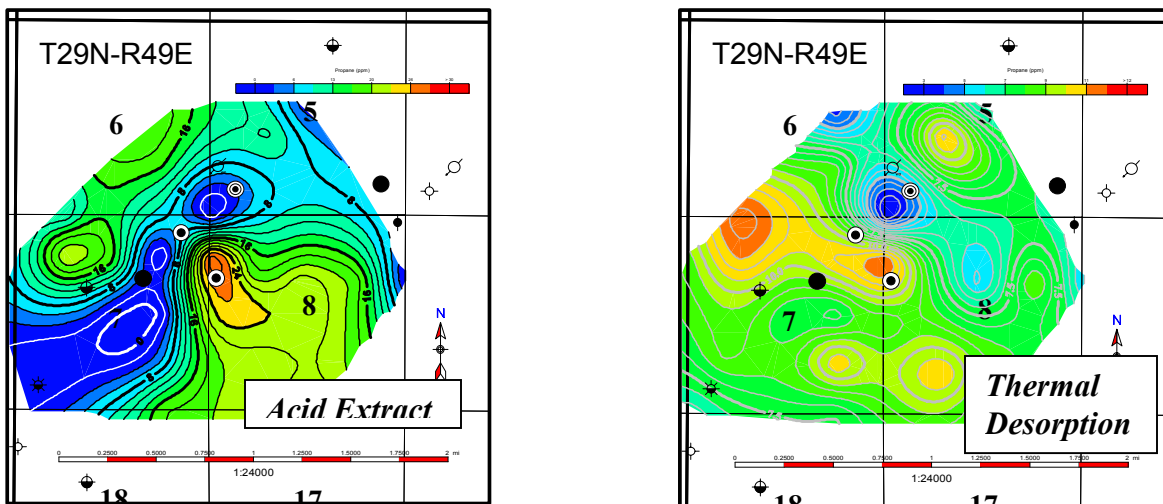


Figure 16. Comparison of soil Propane methods at Palomino Oil Field.



Both Microbial methods are mapped in Figure 18. They show anomalies in different places close to current oil production, but generally confirm depletion over the field. The anomalies may indicate infill or offset drilling locations.

Figure 18. Palomino Field Microbial methods compared.

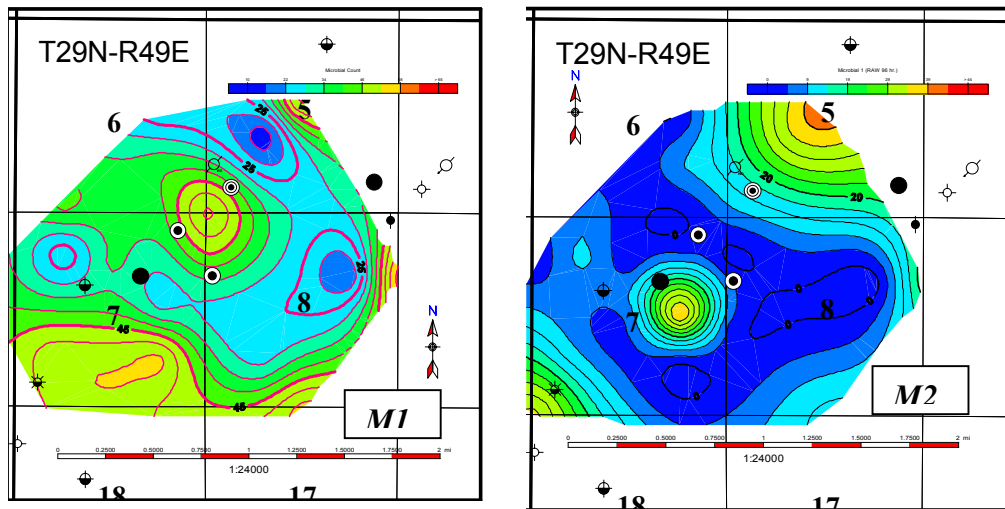


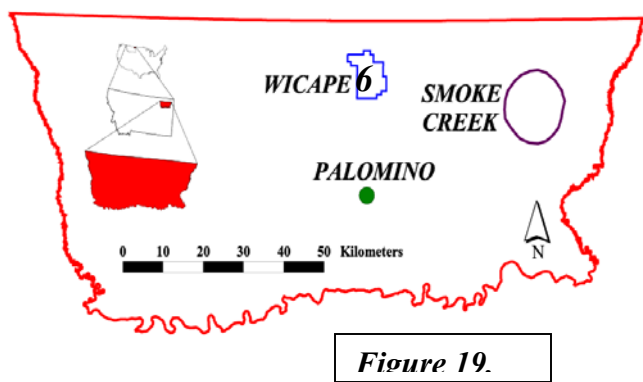
TABLE 3: DATA ANALYSIS - AREA 7

Method	H/C Indicator	Company Validation Technique	Range	Mean	Company Anomaly Technique	Company Anomaly Determination	Company Anomaly Value	Ethane vs. Propane
1. SG	Propane	Inverse relation to Thermal Desorption	0.14-1.64	0.70	Single gas Semi-log Survey log profiles	Slope increase	0.2	Poor
2. AE	Propane	Pearsons Correlation Ethane vs. Propane	0.17-28.38	11.05	Ordered plot single gas	Break in slope (steeper)	3.0	Excellent
3. F1	PAC-3 Ring	NR	11-35	22.81	Ordered plot	Break in slope	23	N/A
4. MS	Magnetization	NR	29-98	56.07	Ordered plot	Break in slope	60	N/A
5. M1	Microbes	Drilling success	-0.65-42.80	10.21	Correlation to production	Experience	20	N/A
6. I	Iodine	Drilling success data duplicates	0.1-6.8	1.7	Mean	Mean	1.7	N/A
7. HG	Propane	Correlation Matrix	0.23-9.43	4.30	Harmonic Mean	Twice Harmonic Mean	4.09	Excellent
8.a. Eh	Eh low	Consistent (-)	-7.30 to -294.50	-46.13	Harmonic Mean	Twice Harmonic Mean	-108.41	N/A
8b. pH	pH double high	Small range	6.47-7.87	7.59	Harmonic Mean	N/R	NR	N/A
8c. K	Halo high	Halo to H/C Highs	392-6460	1151	Harmonic Mean	Twice Harmonic Mean	2302	N/A
9. TD	Propane	Discriminate Analysis	3.22-12.96	8.74	Production Model	Avg. Nearest Samples 4, 5, 13, 20	11.32	Very Good
10. F2	UVF Intensity	Synchronous Spectral Analysis	122-577	253	Oil Probability	Sample 4, 5, 13, 20	100%	N/A
11. M2	Microbes	Standard Statistics	12-62	38	Frequency Histogram	Dual Population	40	N/A
12. MT	Telluric Pay	Structural/Resistivity Correlation	0-28	11	Well Stations	Resistivity Log	0.5	N/A

- (1) Samples surrounding Tribal Bird well, #3, 4, 12, 13, 20, 21
- (2) Compared to Common Anomaly Value: >1, Excellent; .75, Good; .5, Fair; .25, Poor; <.25 Very Poor
- (3) Samples 4, 13, 20 Mean/std. dev. 0-1: Excellent, .1-.25: Very Good, .25: Good, .5: Fair, .75: Poor, >1: Very Poor

Table 3 cont.

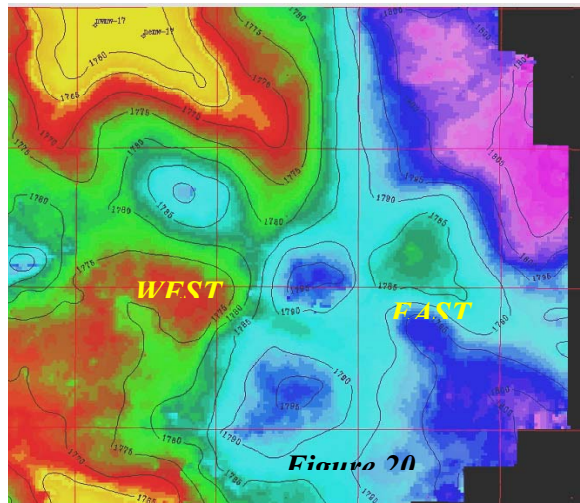
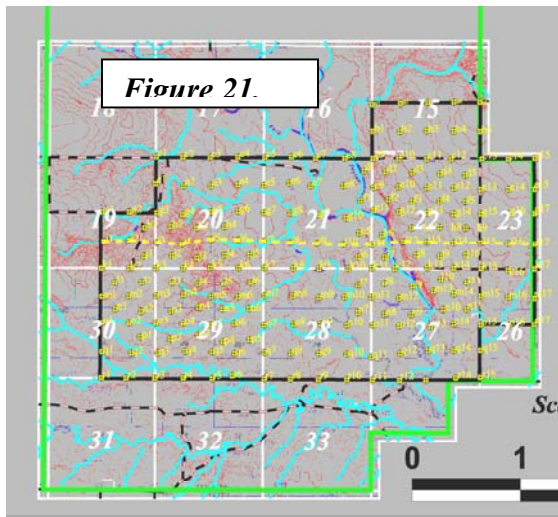
Method	Comparative Common Anomaly Technique	Comparative Common Anomaly Value	Correlation Feature (1)	Correlation Quality (2)	Correlation Type	Triplicate Sample Correlation (3)	Comment
1. SG	1.5 x mean	1.05	Oil Production	0.47-Poor	Inverse?	0.75-Poor	Only 10 samples with both ethane and propane.
2. AE	1.5 x mean	16.57	Oil Production	4.37-Very Poor	Inverse? (Halo)	0.59-Fair	Halo/Depletion
3. F1	1.5 x mean	34	Oil Production	23-Fair	Apical	0.27-Good	Contamination, Bird Well?
4. MS	1.5 x mean	84	Oil Production	47-Poor	Halo	0.11-Very Good	Halo/Depletion
5. M1	1.5 x mean	15.32	Oil Production	13.94-Good	Partial Apical	0.76-Poor	Depletion with one anomalous sample.
6. I	1.5 x mean	2.5	Oil Production	1.1-Poor	Halo	0.3-Good	Halo/Depletion
7. HG	1.5 x mean	6.45	Oil Production	5.09 Good	Apical	0.51-Fair	Best Correlation
8.a. Eh	1.5 x mean	-209.22	Oil Production	-127.51-Poor	Halo	-1.20-Very Poor	Halo/Depletion
8b. pH	Mean + St. Dev.	7.83	Oil Production	7.27-Good	Halo	0.04-Excellent	Well defined Halo
8c. K	1.5 x mean	1726	Oil Production	1177.83-Fair	Inverse	1.18-Very Poor	Inverse/Depletion
9. TD	1.5 x mean	13.12	Oil Production	9.25-Fair	Partial Apical	0.17-Very Good	Good Correlation
10. F2	1.5 x mean	380	Oil Production	286-Fair	Partial Apical	0.12-Very Good	Good Correlation
11. M2	1.5 x mean	56.8	Oil Production	34.5-Fair	Mixed	0.44 Fair	Halo and Apical
12. MT	1.5 x mean	16	Oil Production	21.6-Excellent	Apical	N/A	“Perfect” Correlation



Area 6 is significant to the Assiniboine and Sioux Tribes because it lies within the largest continuous block of land that they own on the Fort Peck Reservation. Figure 19 locates Area 6 in the north-central part of the reservation in an unexplored region. The basis for this selection as a test area is highlighted in Figure 20. The primary 3D seismic anomaly, named

“Tobago”, closes on the east side of the map. A secondary feature, called “Trinidad” occurs 1.5 miles (2.4 km) west, but lacks four-way time closure. These two prospects have been renamed Wicape East and Wicape West, respectively. A large structural nose protruding from the northwest also suggests hydrocarbon trapping potential, but was not sampled due to the large areal extent.

210 locations, along 18 east-west profiles, were sampled for the methods listed in Table 4. (See Figure 21 for the Area 6 base map with sample sites)



Coincidentally, the two 3D anomalies straddle the Poplar River along highlands running parallel to the valley. Figure 22 displays four field views.

Figure 22. Area 6 field views.

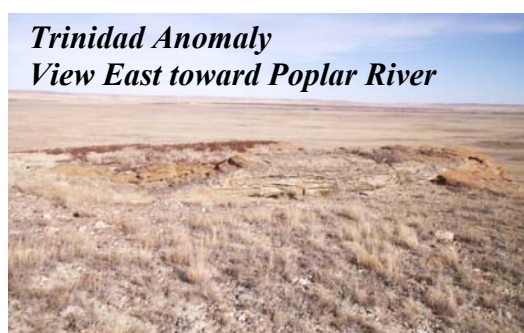
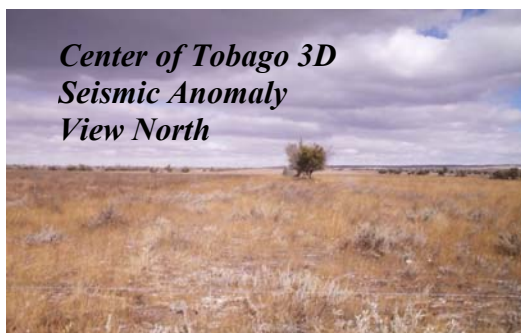


TABLE 4: DATA ANALYSIS - AREA 6

Method	H/C Indicator	Range	Mean	Company Anomaly	Ethane v. Propane	Comparative Common Anomaly Value (1)	West Correlation Feature (2)	Correlation Quality (3)	Correlation Type
1. SG	Propane	0.05-1.91	0.51	0.42	Poor	0.76	3D High	0.42-Fair	Halo?
2. AE	Propane	6.05-50.07	8.69	5.23	Excellent	13.03	3D High	1.73-Very poor	Apical /Small
3. F1	PAC-3 Ring	9-137	33	48	N/A	49	3D High	34-Good	Apical
4. MS	Magnetization	27-135	52	55	N/A	77	3D High	44-Fair	Apical w/Halo
5. M1	Microbes	1.33-4.98	20.66	20	N/A	30.99	3D High	16.64-Fair	Apical
6. I	Iodine	0.00-8.52	0.87	0.85	N/A	1.30	3D High	1.63-Good	Apical/Halo
7. HG	Propane	0.00-46.99	3.97	0.03	Very good	5.96	3D High	5.61-Very good	Apical
8a. Eh	Eh low	-421 to 275	47.08	-137.00	N/A	23.54	3D High	114.03 Poor	Halo
8b. pH	pH double high	6.37-9.28	7.41	7.88	N/A	7.91	3D High	7.53-Good	Halo
8c. K	Conductivity Halo High	144-10,760	1376	1563	N/A	2065	3D High	2165-Good	Inverse Halo?

1 1.5 x mean

2 Average of Samples J3, J4, K4-6, L3-6, M5, M6, N5, N6

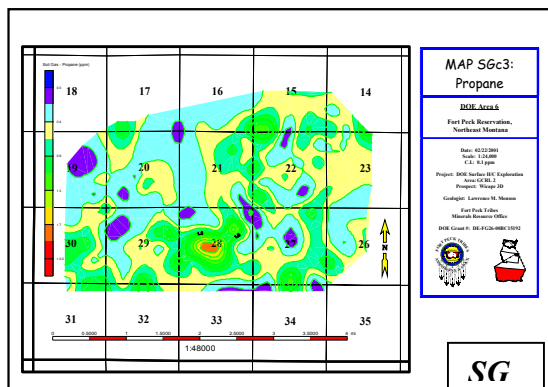
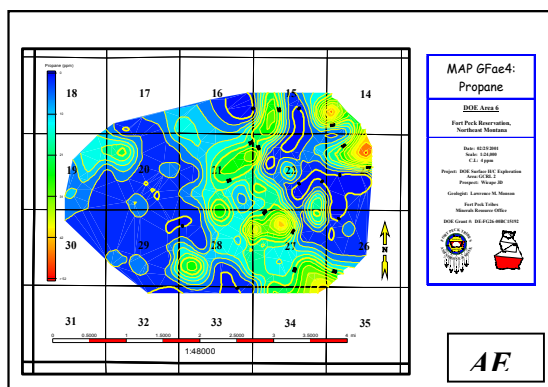
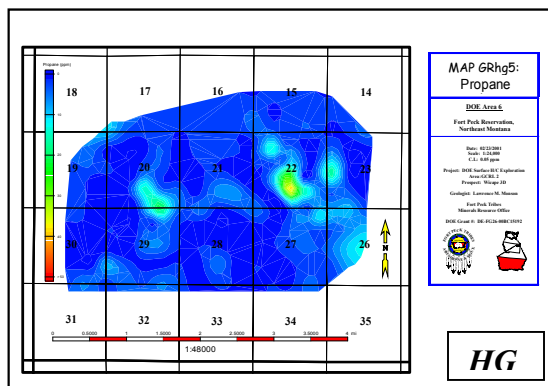
3 (2) compared to (1). >1, Excellent; .75, Good; .5, Fair; .25, Poor; <.25 Very Poor

4 Average of Samples G13, H27, H8, I12, I13, K12-14, L10

5 (4)/(2) See (3) for qualitative description of values.

Method	East Correlation Feature (4)	Correlation Quality (5)	Correlation Type	Comments
1. SG	3D Closure	0.49-Fair	Halo	Possible Halo to seismic prospects.
2. AE	3D Closure	11.16-Good	Apical w/Halo	Very strong Halo around East 3D Prospect.
3. F1	3D Closure	24-Fair	Halo	Off structure areas with stronger anomalies.
4. MS	3D Closure	61-Good	Apical	Halo found around structures also.
5. M1	3D	25.11-	Apical	Other anomalies off structures.

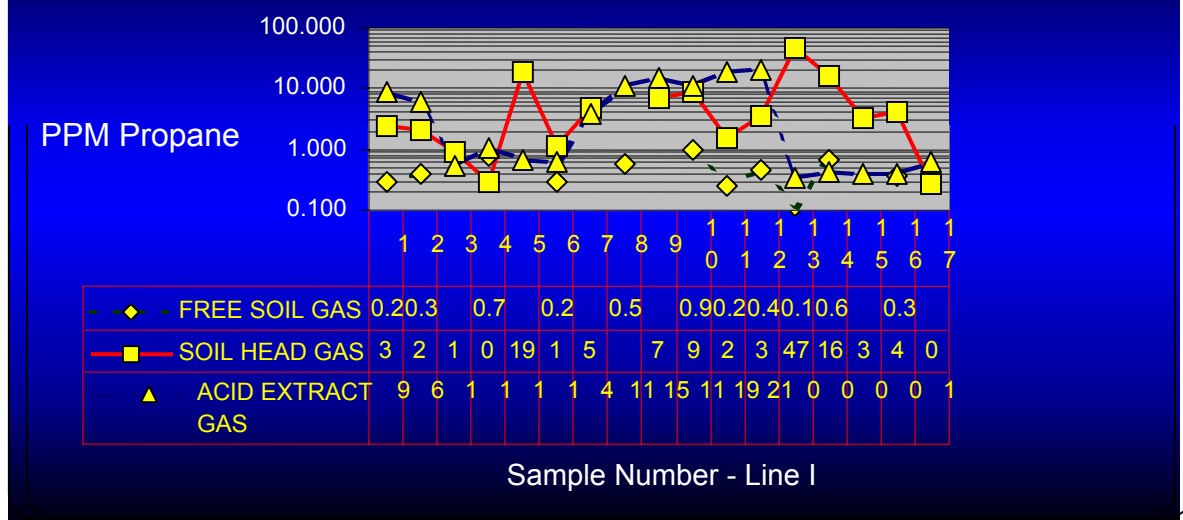
	Closure	Good		
6. I	3D Closure	0.46-Fair	Apical	West Anomaly off structure.
7. HG	3D Closure	10.47-Excellent	Apical	Best correlation to seismic, especially East Prospect.
8a. E	3D Closure	-41.22-Good	Apical	Anomalies west and south of West Prospect.
8b. P	3D Closure	7.14-Fair	Apical/Halo	Topographical Influence?
8c. K	3D Closure	565-None	None	Topographical Influence?



Propane is again the featured gas in Figure 23 that compares the three direct hydrocarbon detection methods employed in evaluating Area 6. The Head Gas (HG) data anomalies strongly correlate with both seismic prospects. Acid Extract (AE) data appears to surround the eastern anomaly as a halo, but closer examination shows this method to have relatively high values over the "Tobago" prospect. The Soil Gas (SG) Survey produced ambiguous results with possibly a small hydrocarbon anomaly over Tobago. Figure 24 graphically compares the propane data along profile line I which intersects both 3D seismic anomalies. The Soil Gas Survey found no propane in some locations and measured values several times smaller than the other two methods. Acid Extract data often plots in an inverse relationship to the Head Gas data suggesting that this method maps a halo anomaly around hydrocarbon seepage.

Figure 23.

Fig. 24. AREA 6 SOIL GAS COMPARISON



Indirect hydrocarbon indicators are mapped in Figure 25: I = Iodine, MS = Magnetic Susceptibility, M1 = Microbial, UVF - UV Fluorescence. All but UVF show elevated values over the eastern 3D anomaly. UVF appears to be higher in the river valley and may be mapping faults that are leaking heavier hydrocarbon gases.

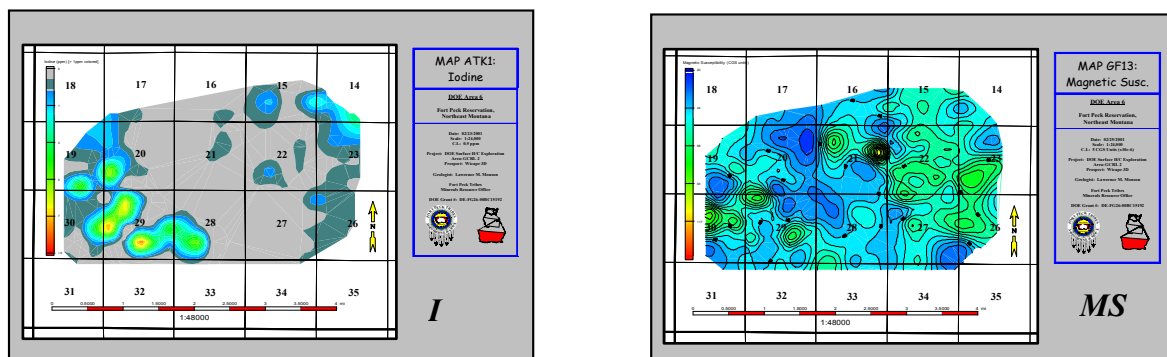
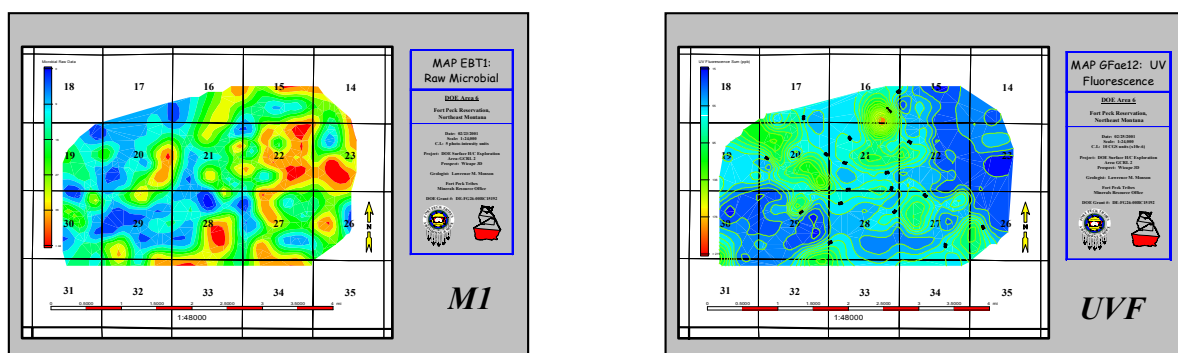
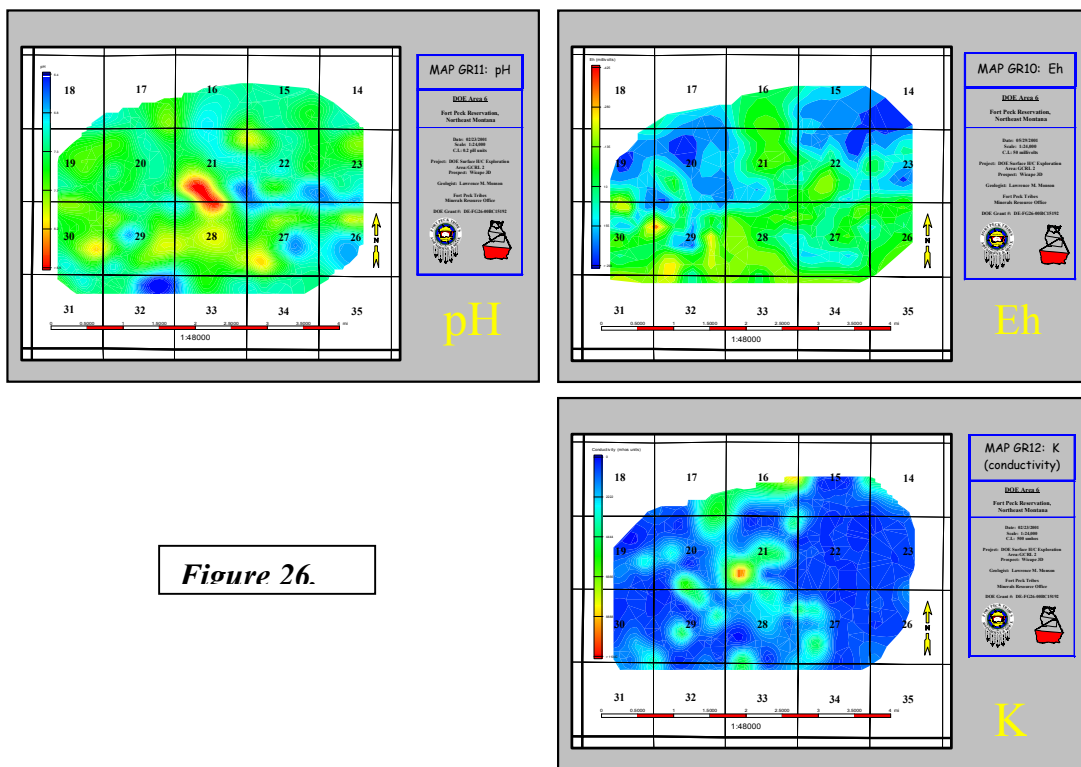


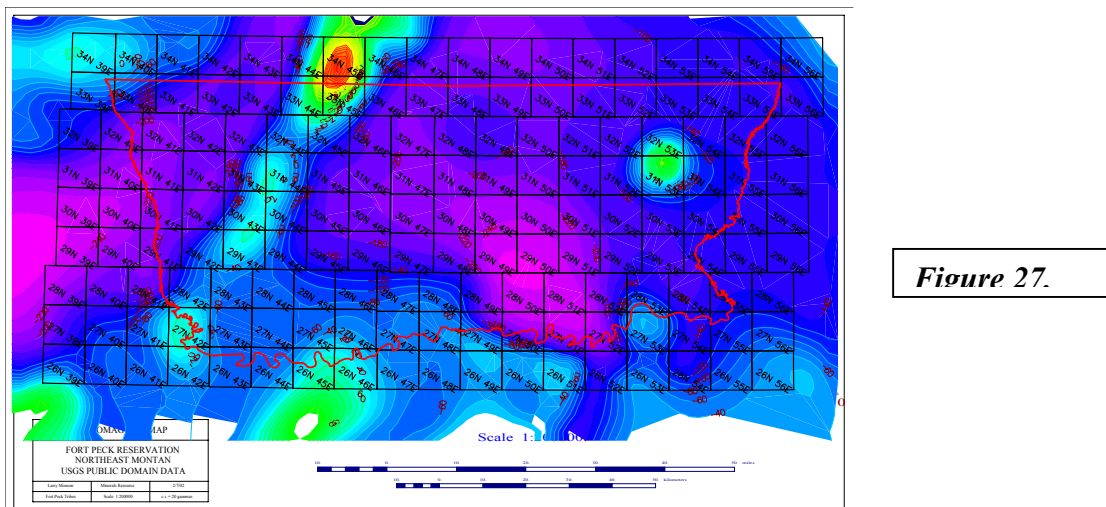
Figure 25.



Three other indirect indicators are displayed in Figure 26. Here only Eh (oxidation/reduction potential) appears useful in delineating hydrocarbon micro-seepage. (See section 22 on the map)



Phase II: Public domain aeromagnetic data was one of the primary data sets acquired by the Fort Peck Tribes in 1990 for their Minerals Assessment Study, funded by the Bureau of Indian Affairs, Energy and Minerals Division. Figure 27 displays two significant aeromag “structures” on the Fort Peck Reservation. The first is a narrow linear trend in the western part of the Reservation. Pertinent to this entire DOE funded project is the circular, “bulls eye” anomaly, which dominates the northeastern part of the Reservation.



When this study began, GCRL, the Tribes IMDA partner and technical matching fund participant of the grant, was more than passively interested in the Smoke Creek Aeromag Anomaly (SC Mag). GCRL's parent company, Gulf Canada, fully appreciated the economic significance of what one explanation for SC Mag could be: an astrobleme. Gulf operates the prolific Steen River Oil Field in Northern Alberta, thought to produce from fractured reservoirs draping a buried meteorite. Other astrobleme fields occur in the Williston Basin, such as Red Wing Field in North Dakota.

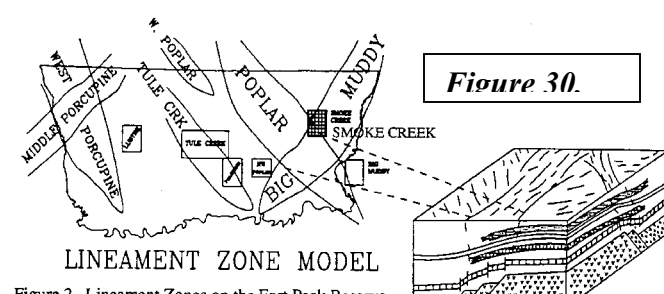
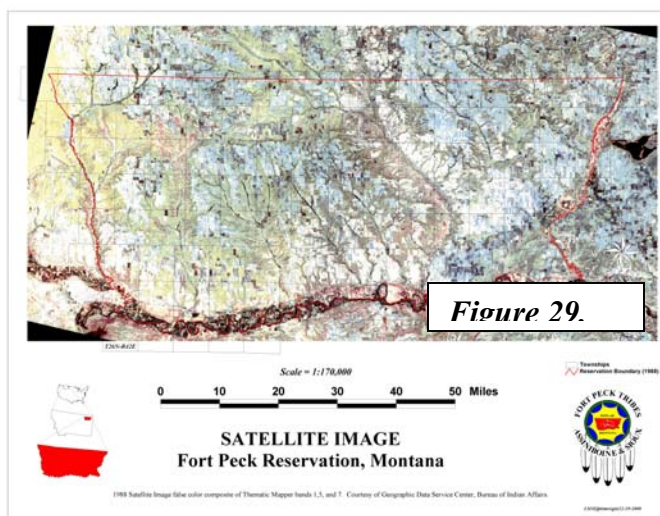
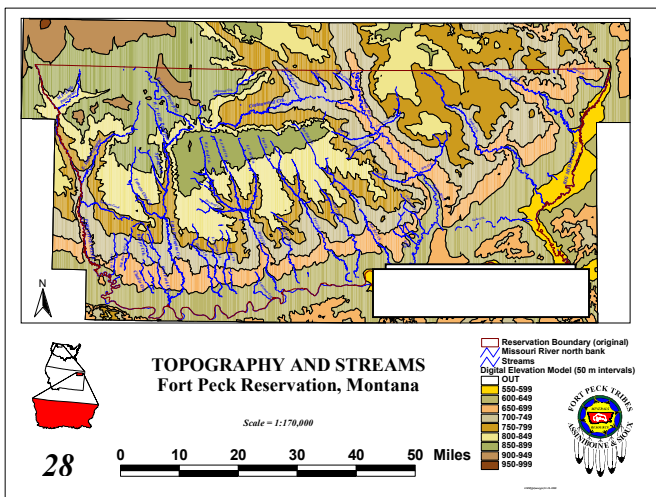
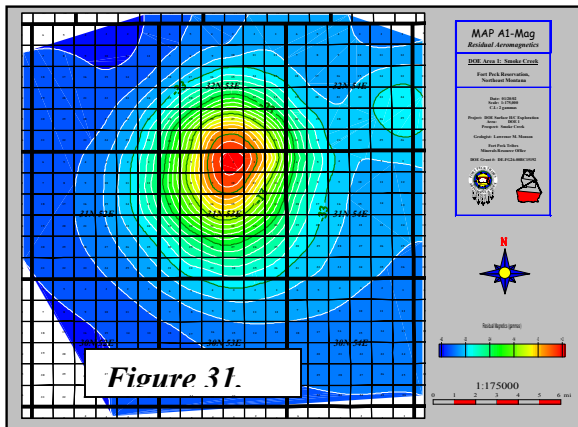


Figure 2. Lineament Zones on the Fort Peck Reservation. Rectangles are enhanced curvilinear study areas.

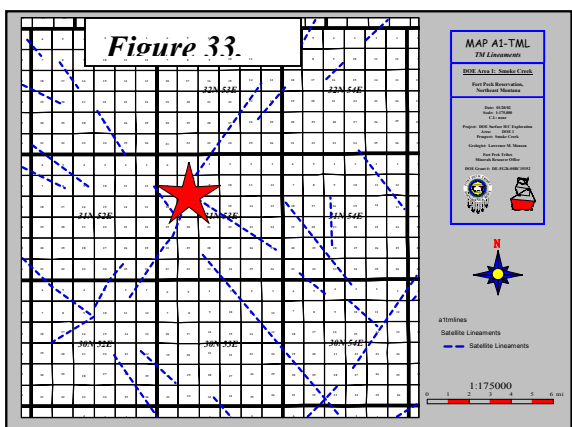
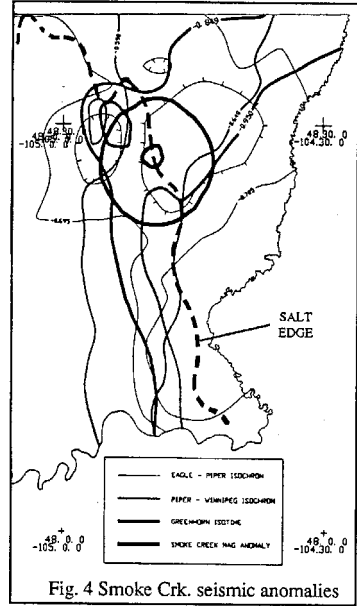
At first the author, from geophysical and petrological training, assumed that SC Mag represented an ultramafic intrusive, perhaps a lopolith formed near the margins of a pre-Paleozoic tectonic suture zone. (Shurr & Monson, 1991, 1993, 1995). These papers document considerable evidence for SC Mag to be more than just an ultramafic intrusion. The historical case began long before when the author was shown Ft. Peck's NW/SE drainage pattern in an

undergraduate geomorphology course (See Figure 28). Note the east-west deflection of Smoke Creek in the northeast part of the Reservation, exactly where SC Mag is located. Taught as a classic example of structurally controlled drainage, within the Williston Basin tectonic framework, Ft. Peck's stream patterns encouraged the author and George Shurr to map satellite lineaments (Figure 29) and propose tectonic blocks. (Figure 30). SC Mag lies at the intersection of the Poplar and Big Muddy Lineament Blocks. It was proposed by Shurr that these lineament zone boundaries represent surface expressions on deep-seated, reactivated faults, which enhance structural drape traps as well as encourage reservoir deposition over tectonic



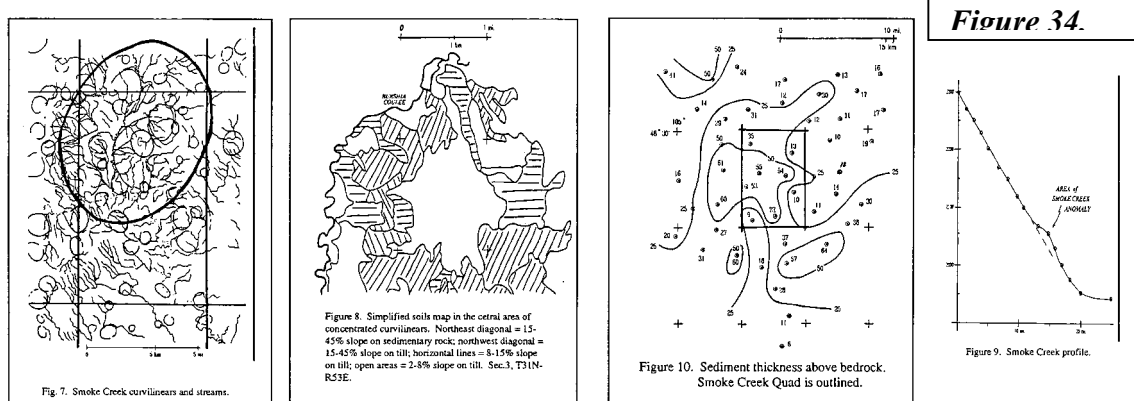
highs. Figure 31 details the SC Mag Aeromag anomaly (from a commercial data acquisition) and became the focus for Shurr and Monson (1993) and this study. That earlier paper documented numerous other anomalies above SC Mag:

Figure 32.



- 1) Figure 32; deflection of structural folds, and seismic time and isochron contours.
- 2) Figure 33; Lineament Zone Intersection

Fig. 4 Smoke Crk. seismic anomalies



4) Figure 35; satellite tonal anomalies (curvilinears) with contoured abundance over SC Mag.

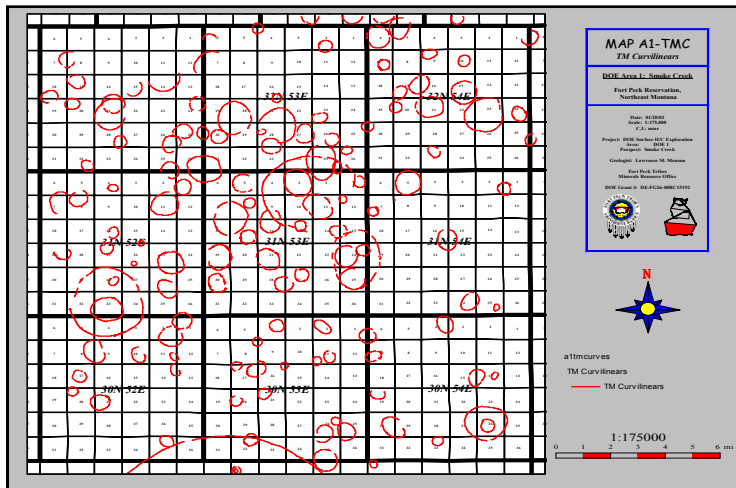


Figure 35.

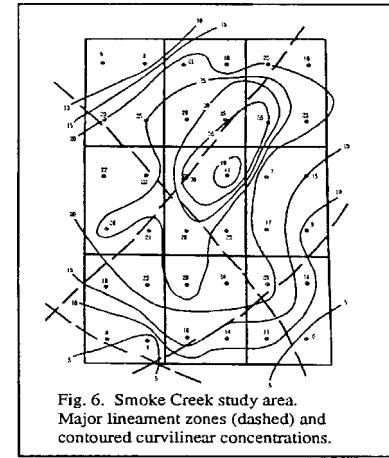


Fig. 6. Smoke Creek study area.
Major lineament zones (dashed) and
contoured curvilinear concentrations.

5) Figure 36; Curvilinears (bubbles) concentrated at lineament intersections and associated with other aeromag structural "fault" lines (Geoterrex, 1990).

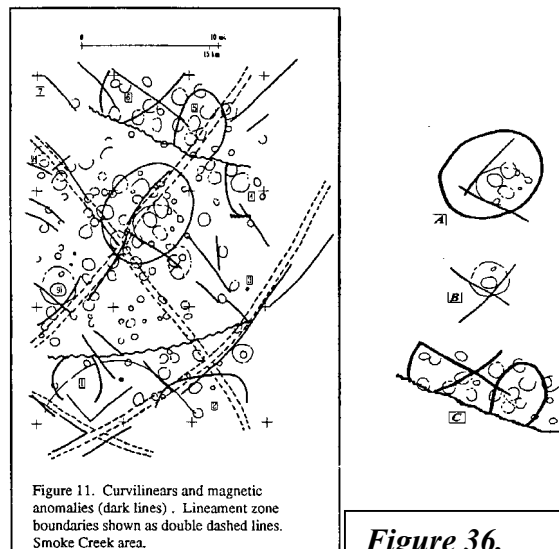


Figure 36.

All of this evidence led Shurr and Monson to propose that the SC Mag curvilinears could be hydrocarbon micro-seepage chimneys as described by Land, 1991 (Figure 37).

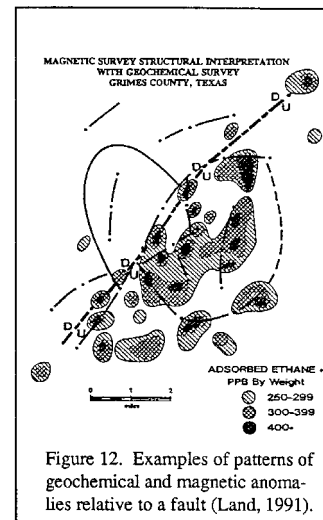


Figure 12. Examples of patterns of geochemical and magnetic anomalies relative to a fault (Land, 1991).

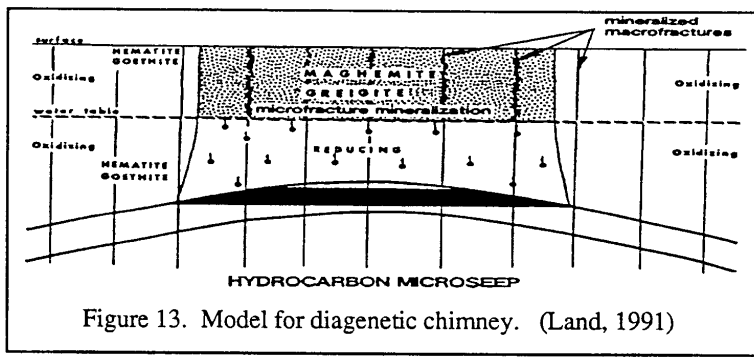


Figure 13. Model for diagenetic chimney. (Land, 1991)

PHASE II FIELD WORK

The surface hydrocarbon exploration methods employed in Phase II of this project are explained in the Experimental Procedures section of this report. Field pictures of a relatively docile Smoke Creek (38), and the east/west portion of the Smoke Creek Valley (39) characterize the terrain traversed. The reddish colored rocks in the second photo bear further investigation. In no other location were these outcrops that color.

Figure 38.



Figure 39.

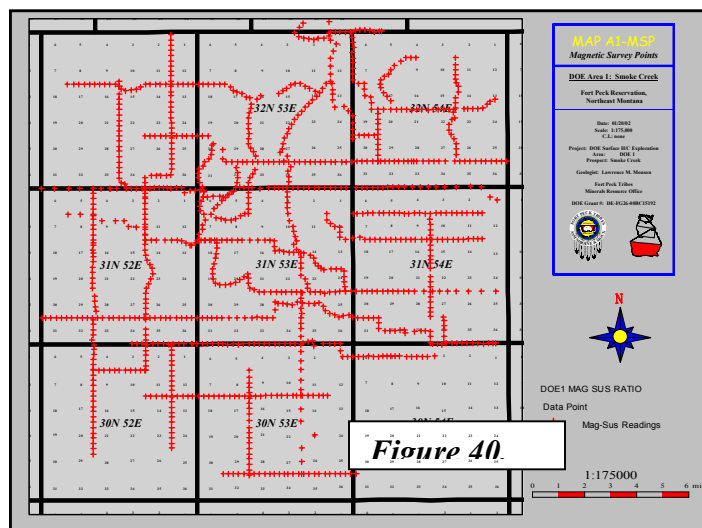


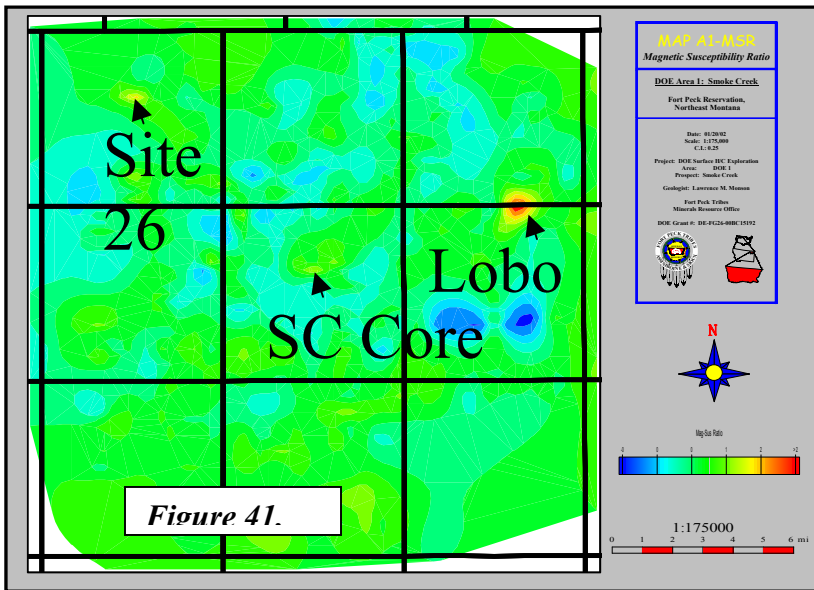
MAGNETIC SURVEY

Magnetic Susceptibility

Although background Soil Gas and Head Gas samples were taken in June, 2001 around the SC Mag, the data was not evaluated until the fall of 2001. Thus we will first examine the results of the Magnetic Susceptibility (MS) reconnaissance, which followed established roads and trails outlined by the sample sites plotted on Figure 40.

Data profiles for all 25 survey lines were plotted in Semi-annual Report #3 (Monson, 2002). As mentioned in the Experimental Procedures, MS values have relative, and not, absolute significance. Specific observations on the MS Profiles were listed in that report. In general there appears to be relatively higher MS values on the northeast and east perimeter of the SC Mag core. The



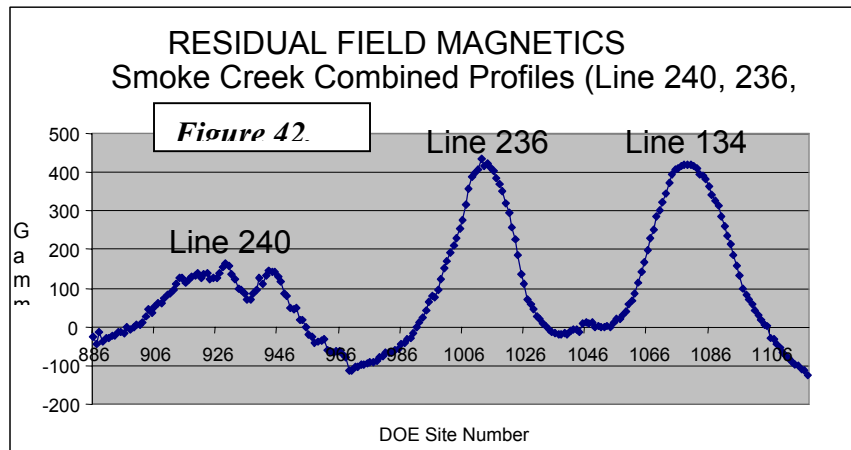


curvilinears proved difficult due to the “noisy” detail of each data set, although that is too be expected if in fact the curvilinears represent overlapping and nested micro-seepage chimneys. The saying of “can’t see the forest for the trees” comes to mind.

Field Magnetics

Field magnetic readings for Lines 134, 236, and 240 were collected to record local variations in the magnetic field, which might be attributed to hydrocarbon modified soil mineralization.

Figure 42 combines

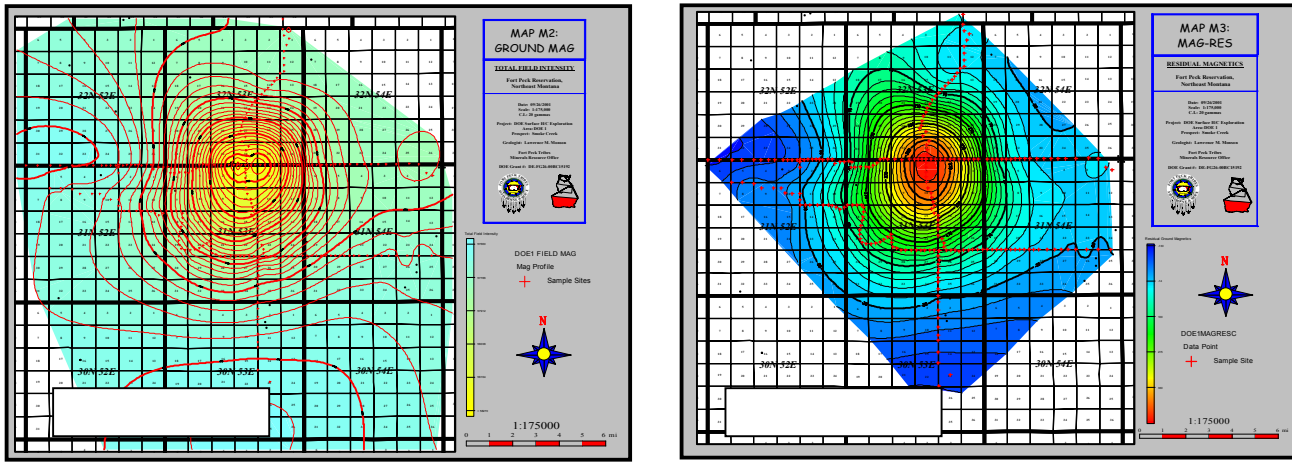


all three as a corrected profile comparison. The sharp peaks of Line 134 and 236 confirm the Smoke Creek Aeromag Anomaly. Line 240 crosses only the southern part of the anomaly and is relatively flatter and undulating. A contour map of the field data is plotted in Figure 43 and enforces this observation (a – Total Field, b – Residual).

Further utility of both the air mag and field mag data lies in reprocessing the data so as to extract the high frequency data, which is normally removed for basement tectonic interpretations. The high frequency “noise” is in fact most desirable information for a micro-seepage hydrocarbon exploration tool. This line of investigation will hopefully be explored in the future.

southwest part of the core also had areas of higher MS values. The most significant increases in MS values, however, were found in the northwest part of the study area, outside the SC Mag anomaly. (See Figure 41: Mag-Sus Ratios)

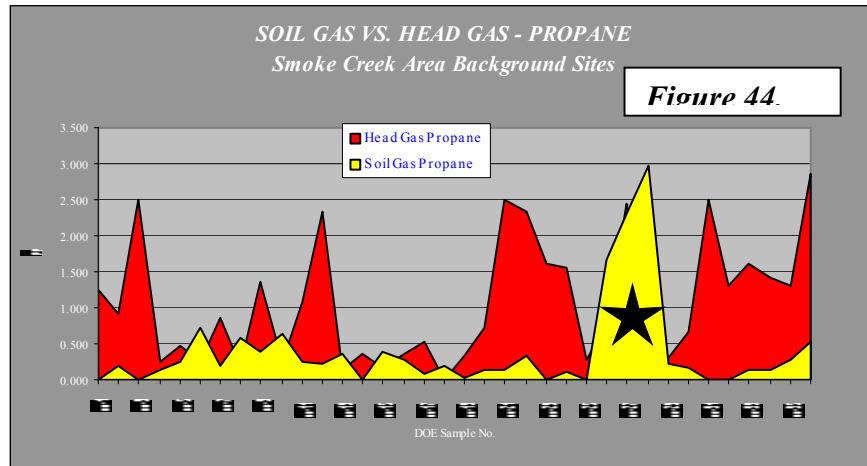
An attempt to relate higher magnetic susceptibility to the



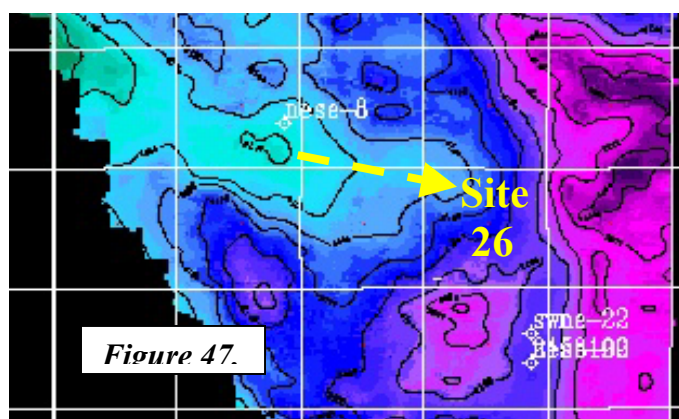
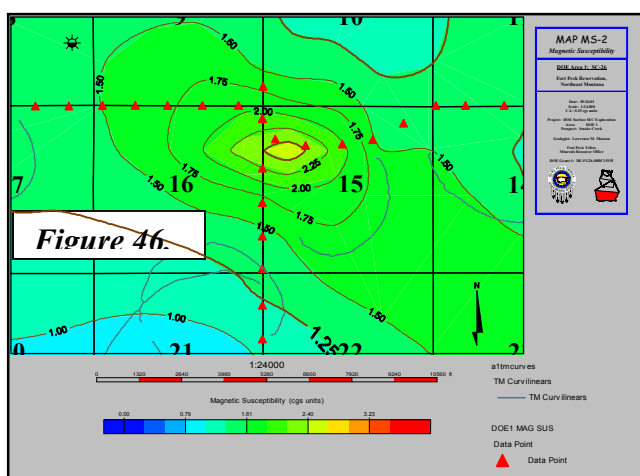
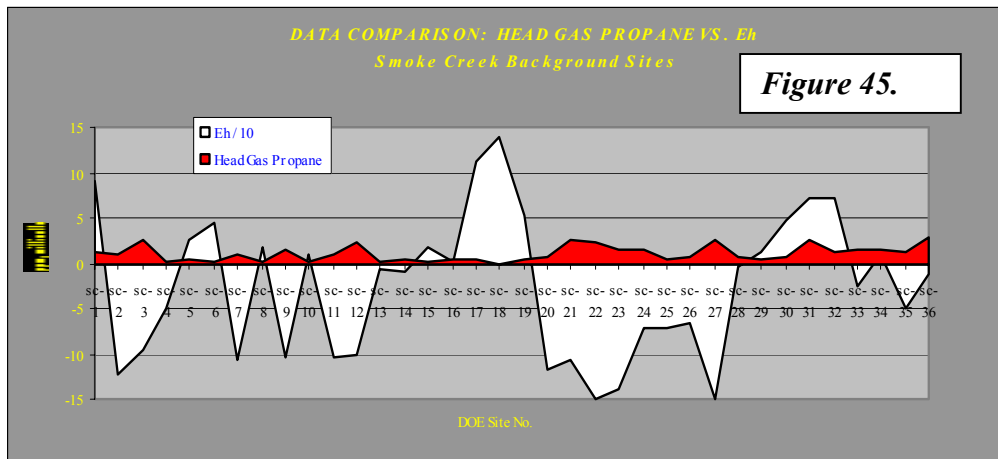
Background Gas Samples

Prior to the MS reconnaissance survey, 36 sites, in eight locations, were sampled around the perimeter of SC Mag in order to establish background data quantities of both Soil Gases and Head Gases. Sampling began in the southwest and proceeded counter clockwise. Because Area 1 encompasses nine townships (324 sq. miles – 843 sq. km, 207,360 acres!) it was beyond the budget of this project to sample the entire area at an appropriate grid. A decision was made to conduct the MS survey as an initial reconnaissance in order to compare the results to the gas background samples and to identify potential anomalies for further soil sampling utilizing the most favorable techniques determined in Phase I.

Figure 44 graphs propane for both the Soil Gas and the Head Gas methods. Surprisingly high values occur in the southwest and especially in the northwest around Site 26. As in Phase I, the Head Gas values are 5-10 times greater than the direct Soil Gas analyses. A notable exception is Propane and Butane Soil Gas at Site 26. This is the only instance to date where Soil Gases were observed to be greater than Head Gases. (See star)

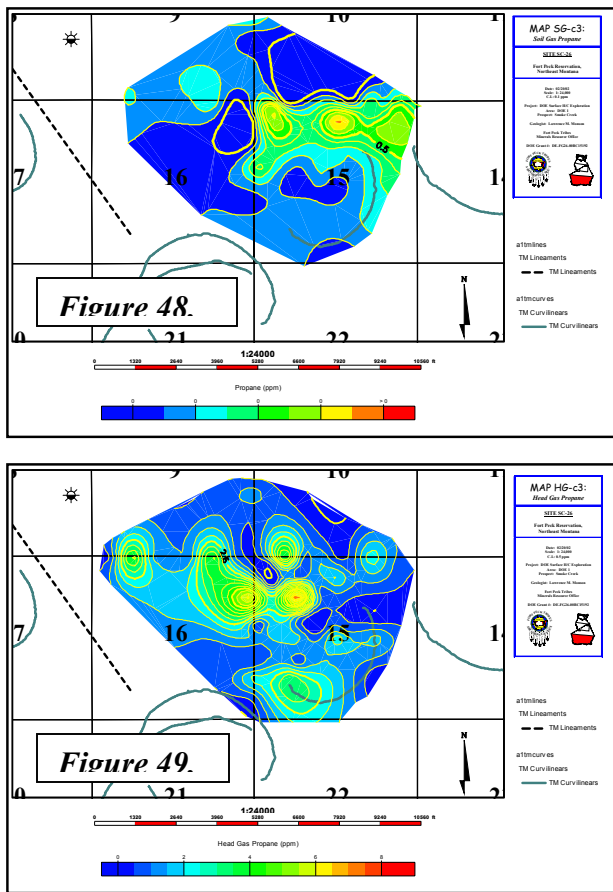


The other indirect indicators, Eh, pH and K were plotted against Head Gas. When Eh is lower the Propane is greater and vice versa, except in sites 30-32 (see Figure 45). This relationship is an excellent correlation and has utility as a hydrocarbon micro-seepage indicator. Eh values were divided by 10 to facilitate similar graph scales. The Background sites were too widely spaced to draw any more specific conclusions.



SITE 26

One of the areas of higher Magnetic Susceptibility in DOE Area 1 is Smoke Creek sample site SC-26. Figure 46 contours this anomaly in the northwest corner of section 15. Map Figure 47 is a time structure map from the Smoke Creek 3D seismic survey. Site 26 lies at the southeast end on a structural nose that has closure in section 8, 1.5 miles (2.4 km) northwest. Recall that the “Background” Soil and Head Gas data also had sharply higher values here. Entirely by coincidence, and outside the primary area of focus (SC Mag Anomaly), independent sampling identified a potential hydrocarbon seepage prospect.



Soil and Head Gas analyses are graphed in Figures 48 and 49, respectively. Among the highest Soil Gas Propane and Butane are found here. The Head Gas Methane values were so large that a log scale had to be used. In the NW/4 samples were collected on offsetting 330 ft, (101 m) spacing. This is the densest grid employed to date in the project. All gases for both methods show elevated light hydrocarbons. The Soil Gas anomalies stretch in a bimodal closure across the north half of Section 15 while the Head Gas closures trend more to the west. No data was collected within the northeast quarter of Section 16 so contour shading there is extrapolated from the section lines.

The indirect techniques applied to Site 26 include: Eh, pH, K, Microbial, and Iodine. The following relationships were observed:

- 1) Eh was not depressed over the gas anomalies, but was low in the southwest of Sec. 15.
- 2) PH contours crudely rim the gas anomalies but not enough background data was present to determine whether the anomaly core was also higher in pH.
- 3) The color scheme on the Conductivity Map is confusing. Higher k values do surround the gas anomaly area (NW/4) thus creating a hole as required by the theoretical basis model.
- 4) Microbial “highs” correlate well to the Head Gas “highs”. There is also an apparent halo around the NW/4.
- 5) Iodine anomalies are present both over and south of the NW/4.

SC Core

In the south central part of the SC Mag core area, a small Magnetic Susceptibility anomaly was detected (See Figure 41). Because this area contained a high concentration of curvilinear “bubbles”, it was selected for a soil sampling profile, and named SC Core.

Some Head Gas values are noticeably lower when compared to the Soil Gas values in this area (See Figure 50). This is not the normal relationship.

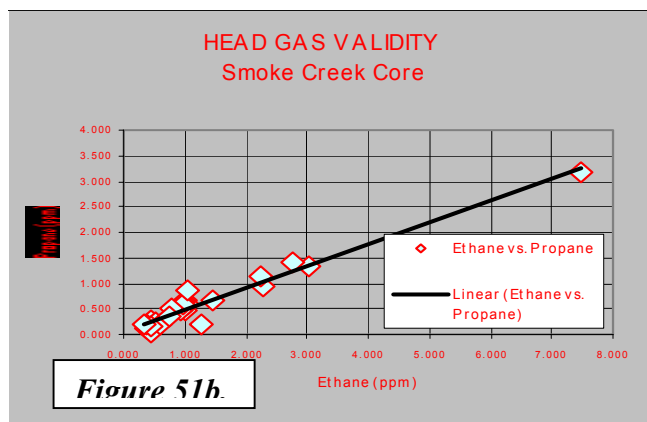
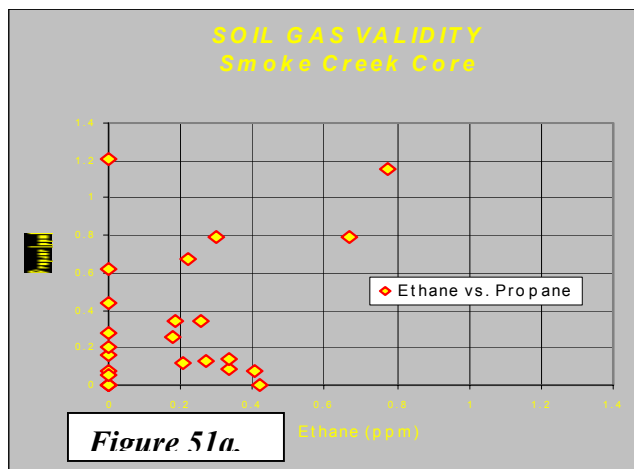
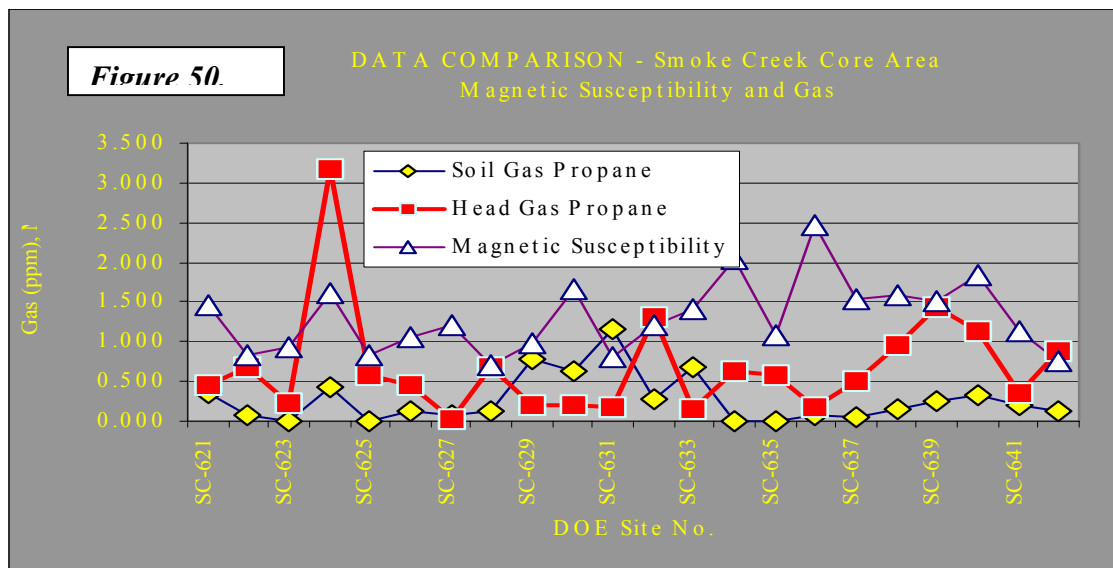
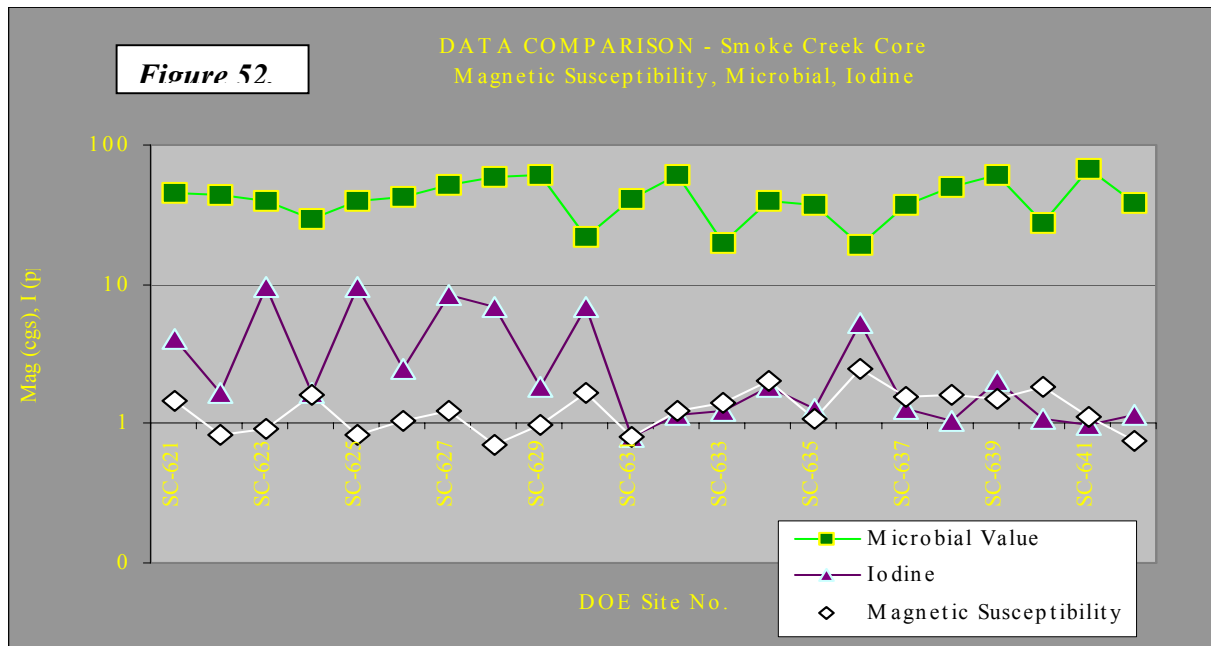


Figure 51a indicates that the Soil Gas data is suspect. In fact, several sites were re-sampled at a later date in order to check the data validity. As usual, the Head Gas data validity is excellent (Fig. 51b). Head Gas Propane does increase in three parts of the 3-mile (4.8 km) traverse. Soil Gas Propane does not correlate very well with the Head Gas values. Figure 50 displays poor gas correlation to the Magnetic Susceptibility data, which of course, prompted the selection of this prospect area in the first place. The only exception is sample site SC-625.

In the western part of the indirect methods profile (right side of Figure 52) Iodine values trace MS values nicely, but Microbial values appear to be antithetic. Mag-Sus, Microbes, Iodine, Eh, pH, and K had no apparent utility in this profile. The MS correlation to Head Gas propane is only good at SC-625 as already mentioned. Microbial values generally track similar to Propane, except at SC-625. Iodine only sometimes correlates to Propane. No maps were made due to insufficient data points.



LOBO WEST

The strongest MS anomaly mapped in the Smoke Creek, DOE Area 1, was found in the northeast, and outside SC Mag. Because this area lies 1-3 miles (1.6 – 4.8 km) west of the abandoned Lobo Oil Field, it was named the Lobo West Prospect Area. An east to west sample traverse was conducted to sample soils for the same methods employed at Site 26 and SC Core. Unlike the SC Core profile, samples for Lobo West were collected at a closer spacing. Therefore the data points do not exactly correspond to those for the MS survey.

In a disturbing reoccurrence, the Soil Gas Data validity was again poor here. However Head Gas data remains valid. ***Head Gas values are disappointingly low in the Lobo West profile.*** When compared to the microbial values an inverse relationship is once again observed. Whether this is significant in an area of such low gas values is debatable. Iodine appears to track the Propane data quite well.

Two profiles were constructed in order to compare Head Gas Propane values to Magnetic Susceptibility. The first, Figure 53a, approximates an overlap of the two data sets sample sites. There is good correlation along Profile 1 for Propane and MS. Even better correlation is displayed in Profile 2 (Fig. 53b), which attempted to match which MS survey points were located next to which Head Gas sample sites.

Figure 53a.

**DATA COMPARISON: Magnetic Susceptibility vs. Gas
Smoke Creek Lobo West - Approximate Profile Overlap**

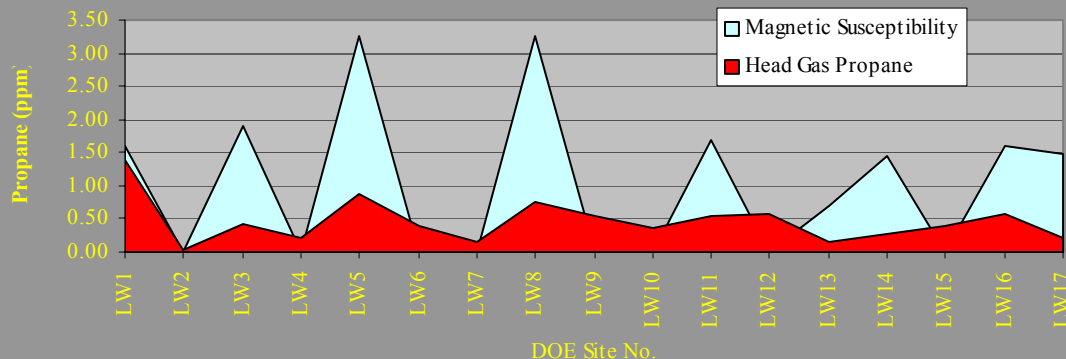
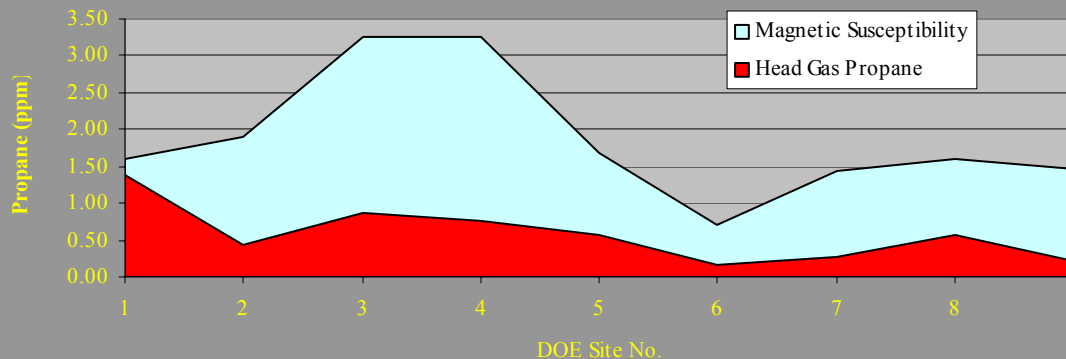


Figure 53b.

**DATA COMPARISON: Magnetic Susceptibility vs. Gas
Smoke Creek Lobo West - Correlated Sample Points**



Again, as with the SC Core area, not enough samples were collected to warrant any maps for Lobo West.

OTHER PHASE II REPORTS FOR SMOKE CREEK

Semi-annual Report #3 did not include Mr. Land's report on the Smoke Creek Magnetic Susceptibility Survey. The appendix of this report includes that report. In addition project consultant, George Shurr also submitted observations on the Smoke Creek Area data and Mr. Land's report. This entire report is also included in the appendix.

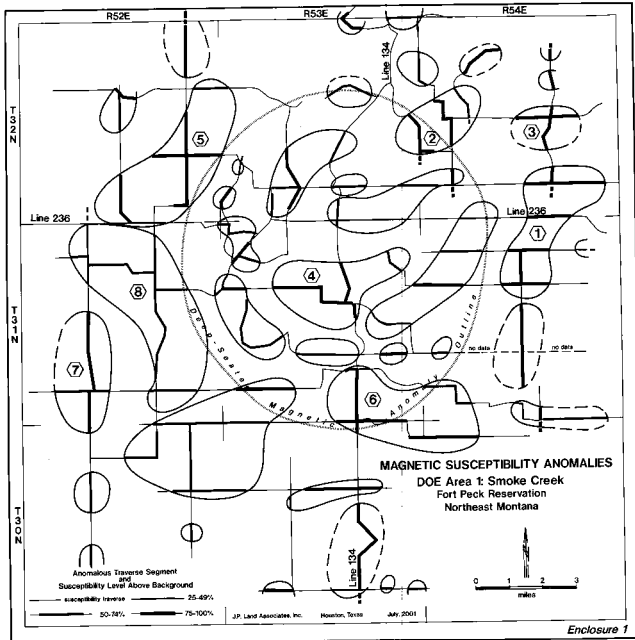
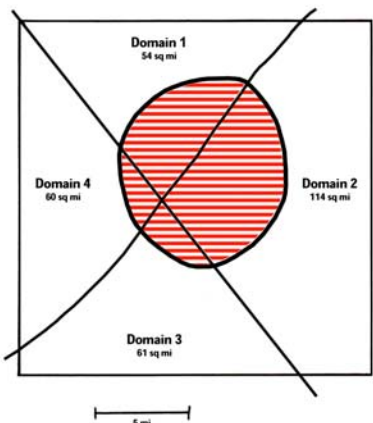


Figure 54

Mr. Land (2002) organized the magnetic susceptibility anomalies into various regions based on their geographic proximity and relative strength compared to background. The stronger anomalies are labeled in Figure 54. He observed that there are more MS anomalies over the deep-seated Smoke Creek magnetic anomaly and that correlates with the reported abundance of curvilinears. Land concluded that the numbered anomalies warranted further investigation perhaps with higher a resolution airborne micromagnetic survey.

Shurr (2002) provides a background on surface exploration by examining the flux mechanisms, plumbing geometries, and flux sources for not only the Smoke Creek area but the other survey areas in Phase I, Palomino and Wicape. From that report, “In the Smoke Creek area, lineament zones and the central aeromagnetic anomaly have influenced the flux mechanisms, plumbing geometries, and flux sources for surface anomalies. Within the lineament zones, macroseepage and ground water movement associated with fracture networks controlled hydrocarbon migration. Areas outside the lineament zones were probably dominated by vertical microseepage. Consequently, patterns of surface anomalies might be expected to be different inside and outside lineament zones. Similarly, anomaly patterns inside and outside the central aeromagnetic anomaly should be different. This would be the result of contrasting hydrocarbon migration and water movement over the flux source versus farther away. In general, the lineament zones and central aeromagnetic anomaly provide a useful geologic subdivision of the Smoke Creek study area. Distinctive patterns in the several types of data are found in each of the subdivisions.”



From the data provided: satellite images, magnetic susceptibility, and Soil and Head Gas, Shurr proposes that large-scale map features relate to four structural domains (see Figure 55). Domain 1 is outside lineament zones, Domains 2 and 4 are within lineament zones, and Domain 3 is at the intersection of lineament zones. For each domain he calculated the density of curvilinears and “bright spots” as mag-sus anomalies (see Table 5).

Figure 55.

Table 5.

Table 1
Summary of Map Observations
See Appendix I

	Domain 1	Domain 2	Domain 3	Domain 4	In	Out
Lineament Zone	None	NE	Both	NW	NA	NA
Area sq mi	54	114	61	60	70	219
Appendix Table A						
Curvilinears per sq mi	0.48	0.38	0.34	0.36	0.51	0.38
Bright spots per sq mi	0.06	0.07	0.07	0.05	0.09	0.06
Bright spots with curvilinears per sq mi	0.04	0.03	0.05	0.03	0.04	0.03
Appendix Table B						
Anomalous linear mi per sq mi	0.41	0.47	0.31	0.4	0.59	0.36
Non-anom linear mi per sq mi	0.5	0.3	0.21	0.25	0.43	0.27
Curvilinears touching anom line per sq mi	0.24	0.21	0.15	0.12	0.33	0.14
Curvilinears NOT touching anom line per sq mi	0.24	0.15	0.15	0.28	0.17	0.2
Appendix Table C						
Total anomalies per sq mi	0.19	0.16	0.13	0.07	0.2	0.11
Total anomalies with curvilinears per sq mi	0.11	0.08	0.18	0.05	0.07	0.06

Large-scale map patterns for the several different data sets reflect the flux source and structural domains. However, comparisons must take into account differences in the size of areas inside and outside the central anomaly and also in each of the four domains. More accurate estimates of area could obviously be made on larger maps employing digital techniques. However, the relative size estimates shown in Figure 55 and Table 5 are adequate for the purpose of normalizing all numerical observations as values per square mile. Actual counts of the various attributes are tabled in the Appendix.

Inside the central anomaly, there are more Landsat curvilinears and more bright spots marking relatively large anomaly values on the magnetic susceptibility ratio map, when compared with outside areas. The area inside the anomaly also shows more linear miles of anomalous magnetic susceptibility profile analyses and more curvilinears touching an anomalous profile segment. Large portions of the area inside the central anomaly have been diagenetically altered because they are directly over the flux source. However, relationships between curvilinears and magnetic susceptibility anomalies are fairly complicated.

Domains 1 and 3 are located outside the lineament zones and within the intersection of lineament zones, respectively. Domain 1 has the maximum number of curvilinears and Domain 3 has the minimum number of curvilinears. However, Domain 3 has the largest numbers of curvilinears that correspond with a bright spot on the magnetic susceptibility ratio map. Domain 1 has the maximum number of linear miles on non-anomalous magnetic susceptibility profiles and Domain 3 has the minimum number of non-anomalous profile miles. It appears that migration pathways producing curvilinears and magnetic susceptibility anomalies are different in these two domains. Domain 1 with no lineament zones favors flux that produces curvilinears, while Domain 3 at the lineament zone intersection shows a correspondence of magnetic susceptibility anomalies and curvilinears.

Domains 2 and 4 are located in the northeast and northwest lineament zones, respectively. Both show about the same number of curvilinears and both have minimum numbers of curvilinears associated with magnetic susceptibility ratio bright spots. Both domains have more miles of anomalous magnetic susceptibility profile than of non-anomalous profile. However, Domain 2 has the maximum number of anomalous profile miles and has more curvilinears touching those anomalous profile segments. Thus, there appear to be some plumbing differences between the northeast and northwest lineament zones.

This overview is intended to summarize patterns and provide some preliminary interpretations. We will now proceed with a discussion of all the details of specific data sets. In addition to the summary Table 5 and figures for each data set, the specific numbers appear in Appendix. However, beyond these general descriptive numbers, there are some distinctive qualitative map patterns that are discussed in each data set. The four structural domains and the central aeromagnetic anomaly provide a framework for all of the descriptions.

Magnetic Susceptibility Contour Maps and Landsat Curvilinears

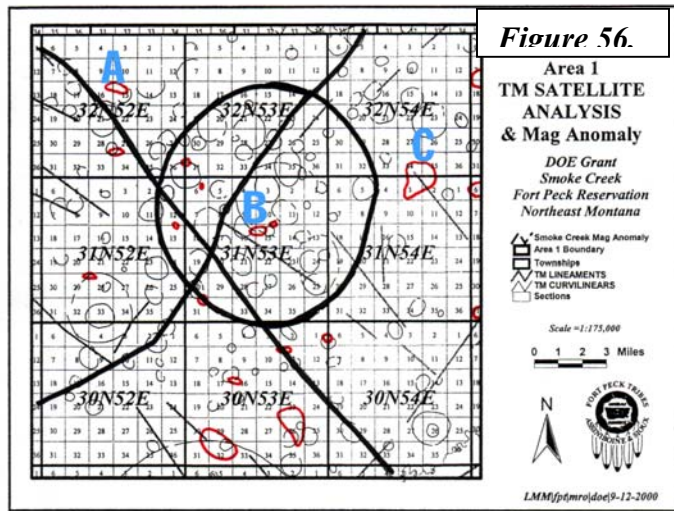


Figure 56.

Landsat curvilinears are displayed with lineament zones and the central aeromagnetic anomaly outline in Figure 56. There is a clustering of curvilinears inside the central aeromag outline. The largest number of curvilinears is inside the aeromag anomaly, but Domain 1, with no lineament zones, is a close second. Domain 3 at the lineament intersection has fewer curvilinears than Domains 2 and 4.

The red outlines on Figure 56 correspond with specific local anomalies that emerge from contouring the magnetic susceptibility ratio. These appear as “bright spots” of yellow and red on an image dominated by the cooler blue and green colors (Monson, 2002, p. 53). Although the number of bright spots is small (see Appendix Table A), there are some interesting patterns. Again, the largest number of bright spots is found within the central aeromagnetic anomaly outline; the rest of the values are all about the same (Table 5). However, Domain 3 is distinctive. Although it has the fewest curvilinears per sq mi, there is a clear correspondence with specific bright spots.

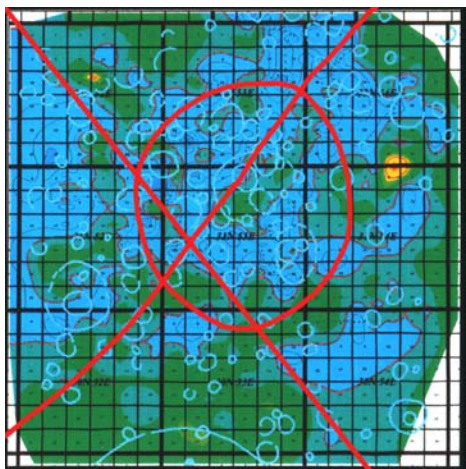


Figure 57.

A good synoptic summary of magnetic susceptibility values is provided by the contour map shown in Figure 57. Lineament zones, the central aeromagnetic outline, and Landsat curvilinears are also displayed. Inside the aeromagnetic outline, magnetic susceptibility values are generally low; the blue contrasts with more extensive green showing higher values outside the outline. Similarly, Domains 2 and 4 in the lineament zones seem to be dominated by low value blue colors. Domain 3 marking the intersection has mostly higher value green.

Magnetic Susceptibility Profiles and Landsat Curvilinears

Magnetic susceptibility data were not only contoured, but were also analyzed in individual traverses or profiles (Land, 2002). Anomalous line segments were then used to outline fairly extensive anomalies (Figure 58). The area inside the central

aeromagnetic anomaly outline has the largest number of anomalous profile miles per sq mi and Domain 3 has the smallest number (Table 5). Domain 1 has the largest number of non-anomalous profile miles per sq mi; it is the only subdivision that has more non-anomalous profile miles than anomalous profile miles. Domains 2 and 4 both have more anomalous than non-anomalous profile miles and have comparable values of anomalous profile miles. The actual numbers used for the summary table are listed in Appendix Table B.

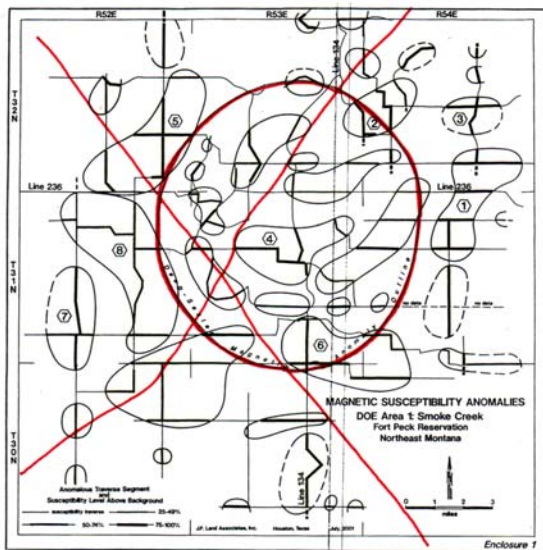


Figure 58. Magnetic Susceptibility Profile anomalies and Smoke Creek Aeromag Anomaly with Lineament Zones.

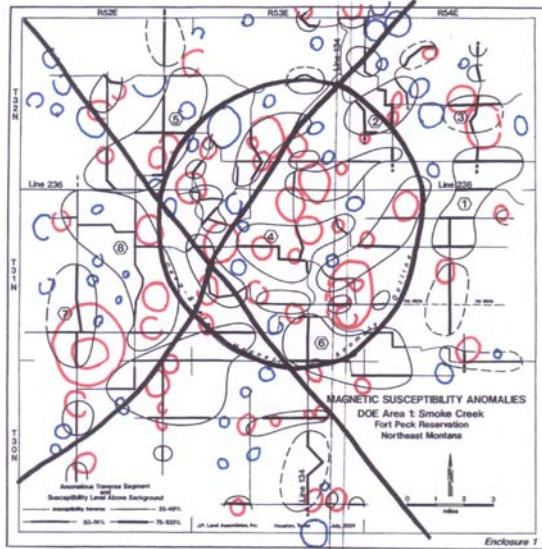
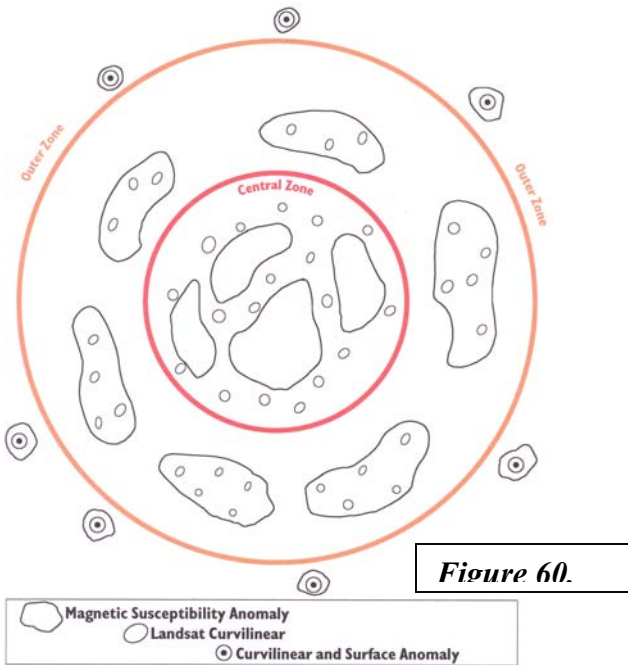


Figure 59. Magnetic Susceptibility Profile anomalies and Smoke Creek Satellite curvilinears.

Magnetic susceptibility traverses and the anomalies based on profile analyses are plotted with Landsat curvilinears in Figure 59. Again, the area inside central aeromagnetic outline has the greatest number of curvilinears touching an anomalous line segment (Table 5). Domains 1 and 3 both have equal numbers of curvilinears touching and not touching anomalous line segments. Domains 2 and 4 do show differences between the northeast and northwest lineament zones. Domain 4 has the smallest number of curvilinears touching anomalous line segments and the largest number not touching an anomalous line segment. Curvilinears in the northwest lineament zone do not seem to be closely associated with magnetic susceptibility anomalies extracted from profile analyses.

Within the outline of the central aeromagnetic anomaly, curvilinears seem to be located outside the outlines of the susceptibility anomalies (Figure 59). This is also reflected in the difference between total anomalies and total anomalies with curvilinears (Table 5). Outside the central aeromagnetic outline, magnetic susceptibility anomalies are larger and less closely packed. In this second zone, the susceptibility anomalies tend to have multiple curvilinears within their outlines. Finally, at the margins of the study area there is a third zone that is characterized by a relatively close correspondence between small



susceptibility anomalies and small, individual curvilinears. These three zones are somewhat similar to patterns of color on Figure 57 map with the superimposed curvilinears. The three zones distributed relative to the flux source are illustrated in Figure 60.

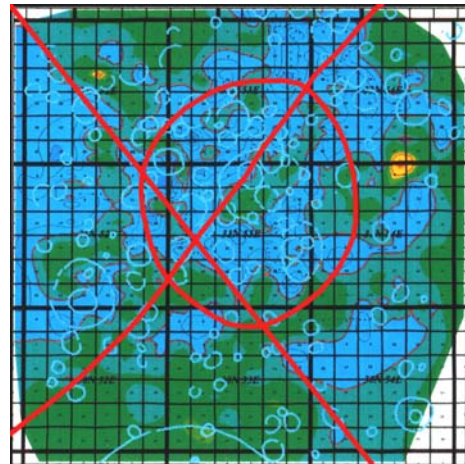
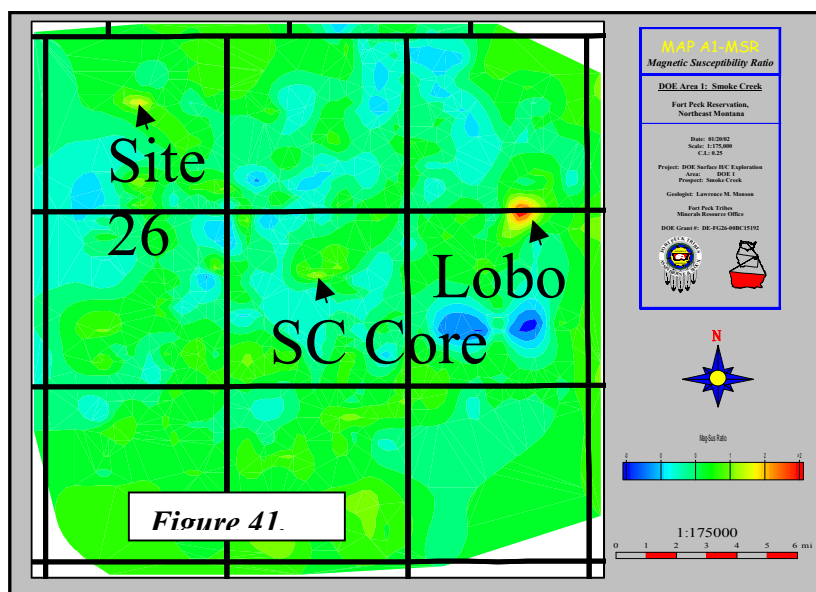


Figure 56.

SMALL-SCALE DATA SETS

Landsat remote sensing and magnetic susceptibility data basically cover the entire Smoke Creek Study Area. These large-scale data are augmented by more detailed measurements of soil gas, head gas, and indirect detection variables. Three areas have closer spaced sampling: Site 26, Smoke Creek Core, and Lobo West (see Figure 41). Work completed in the three areas of detailed sampling is discussed below in the context of the large-scale patterns.



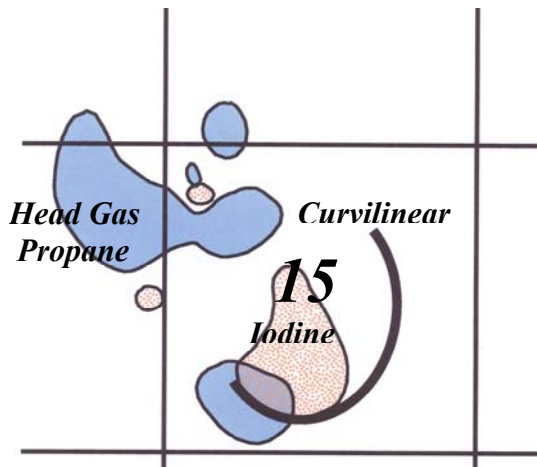


Figure 61. Site 26 data relationship. (Monson, 2002)

Site 26

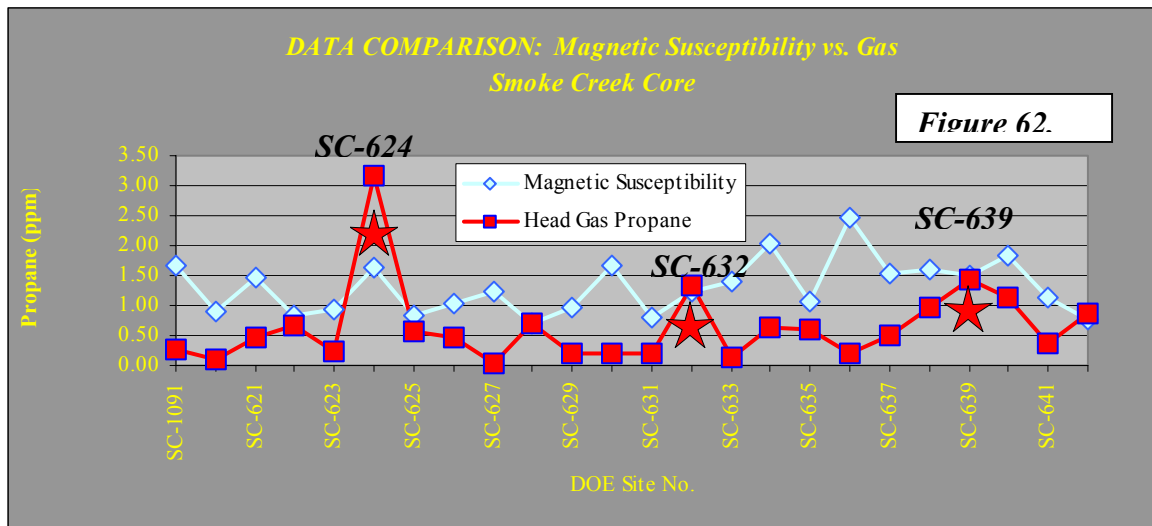
Site 26 is located in Domain 1 near the boundary with the northwest lineament zone. The magnetic susceptibility anomaly in section 15 is located at the open northwest end of a curvilinear arc. In addition, the head gas anomaly in the SW 1/4 of section 15 lies directly on the end of the arc. The arc also outlines an iodine anomaly (Monson, 2002, p. 94). These relative locations are sketched in Figure 61. The close association of a curvilinear, magnetic susceptibility anomaly and a variety of detailed soil and head gas anomalies is significant. Site 26 probably represents a small and simple flux source that

is currently active. The location in Domain 1, where there is no lineament zone, and away from the large central magnetic anomaly is also significant in terms of the general pattern of the Smoke Creek Study Area.

Smoke Creek Core

The Smoke Creek Core area is located in Domain 2, at the extensional corner within the northeast trending lineament zone. This magnetic susceptibility anomaly is near an extremely complex area of curvilinears and is near the center of the central aeromagnetic anomaly outline. Sampling was only done along a single profile that corresponds with line 239 of the magnetic susceptibility data collection. Head gas propane and magnetic

susceptibility values are plotted for comparison in Figure 62. In general, head gas values are low and do not track the magnetic susceptibility data. However, there are some important trends.



A head gas high exactly corresponds with a high magnetic susceptibility value at sample site SC-624. To the west along the profile, another head gas high is located at SC-632 and a third is at SC-639. The average magnetic susceptibility between SC-624 and SC-632 is .928 GGS units; between SC-632 and SC-639 the average is 2.028 CGS units. SC-632 with elevated head gas and magnetic susceptibility seems to be near the border between sections 16 and 17. This is located between specific curvilinears. The area of high magnetic susceptibility between SC-632 and SC-639 approximately corresponds with the green area in section 15 and also has a specific curvilinear. The elevated head gas values on either side of the high magnetic susceptibility values are interpreted to be relatively active seeps leaking along the edges of a large diagenetic cap. This interpretation will be expanded in the “Discussion” section.

Lobo West

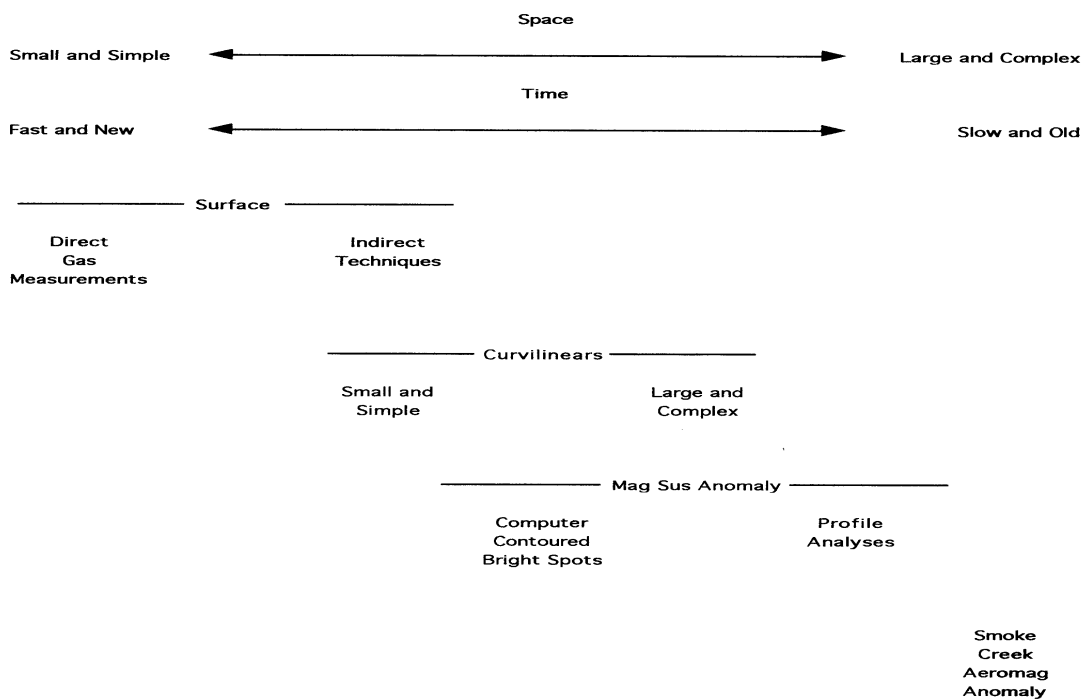
The Lobo West area is located in Domain 2 near the center of the wide, northeast lineament zone. It contains the strongest magnetic susceptibility anomaly mapped in the Smoke Creek Study Area. However, it also has low soil and head gas values. Data are distributed only in a profile and no maps were prepared. This Lobo West anomaly corresponds with the large anomaly ranked as number 1 by J.P. Land Associates, Inc (Figure 58). It is the only large anomaly in zone 2 (Figures 58 and 59) that does not have any curvilinears somewhere within its outline. Furthermore, it is situated at the center of a green area on the contour map that is surrounded by small curvilinears (Figure 57).

The Lobo West anomaly is interpreted to be a large fossil seep that produced a significant area of diagenetic alteration. Subsequent smaller seeps leaked around the edges of this large slab and small curvilinears were formed. If the individual curvilinears have good soil and head gas signatures, then the small seeps are still active. If there are no gas signatures, then the small curvilinears are also fossil seeps. This interrelationship of history, size, and type of anomaly is an example of the interpretations that are discussed in the next section of this report.

DISCUSSION (Shurr, 2002)

The anomalies described for the various types of data fall into a spectrum of space and time characteristics (Figure 63). There is a variation from small and simple anomalies to large and complex. This variation in space is interpreted to also generally reflect a variation in time. The variation in time relates to the flux events ranging from fast, short duration events that are current to slow, long duration events that are old.

Figure 63.
DISTRIBUTION OF DATA TYPES IN SPACE AND TIME

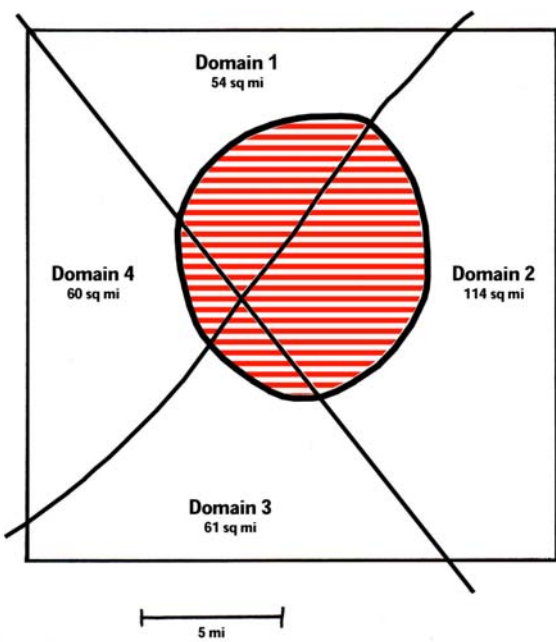


The Smoke Creek Aeromagnetic Anomaly dominates the study area and was probably formed during emplacement of a Tertiary intrusive body. The large magnetic susceptibility anomalies based upon profile analyses were produced by fluid flux patterns associated with the intrusion. Bright spots extracted from contour maps and curvilinears, overlap to provide transition between the large, old anomalies and the small, new ones. They represent flux patterns ranging from diffuse over sizable areas down to those focused in localized areas. Bright spots and complex curvilinears generally require some time for the diagenetic "signal" to buildup. Simple curvilinears and indirect techniques of surface measurement also need time to accumulate the signal, but the required time is shorter. Direct surface gas measurements are the most transitory and are focused in small areas.

These generalizations about the time implications of the several different types of anomaly patterns could be improved substantially with a systematic study of crosscutting relationships. This work would require a better spatial resolution than is available in the small maps used for this report. In effect, the rules used for unraveling sequences of

mineral crystallization in a thin section, using a petrographic microscope, could be applied to the several anomaly types. For example, the distribution of small curvilinears around the margins, but not in the center, of large magnetic susceptibility anomalies, has implications for the timing of the large and small flux sources.

Plumbing Geometry



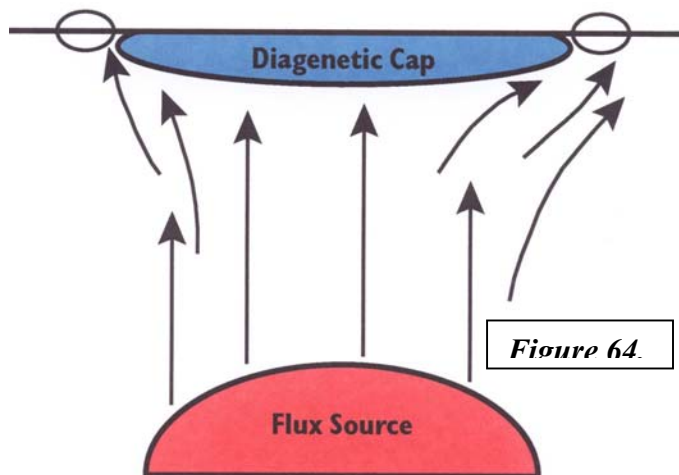
Plumbing geometries can be interpreted from the distribution and attributes of the various anomalies (see Table 5). However, these interpretations are preliminary, speculative, and fairly intuitive. They would be greatly improved by quantitative evaluation of the patterns and by verification of fracture populations. Fundamentally, the four domains in the Smoke Creek Study Area are interpreted to represent different plumbing geometries.

The area with no lineament zones (Domain 1) is relatively unfractured and consequently has no distinctive plumbing geometry. It is characterized by the maximum number of non-anomalous profile miles and by the maximum

number of curvilinears. Many of the curvilinears touch an anomalous profile line and so may have expression in magnetic susceptibility measurements. Focused flow in vertical microseeps over small, simple flux sources is interpreted to be dominant. Site 26 is a typical localized anomaly where surface gas, indirect techniques, magnetic susceptibility and a curvilinear all fall into the same small area. This represents currently active, focused flow over a localized flux source.

At the intersection of two lineament zones (Domain 3), rocks should be extensively fractured. However, there may not be any distinctive plumbing geometry because the intersecting fracture populations would give rise to an essentially homogeneous flow system with no preferential orientation. This area has the minimum number of anomalous profile miles that suggest a diffuse flow. The computer-contoured map of magnetic susceptibilities is dominantly green showing higher values than the lower value blues found in the two adjacent lineament zones. This may be the result of a greater total flux through the area of intersection so that a larger diagenetic buildup produces higher magnetic susceptibility values. Although Domain 3 has a minimum number of curvilinears, many are marked with a bright spot. This localized, focused flow is more similar to Domain 1, than to the two lineament zone domains.

The northeast lineament zone (Domain 2) and the northwest lineament zone (Domain 4) can be expected to have different fracture populations characterized by distinctive modes. Thus, in contrast to Domains 1 and 3, Domains 2 and 4 potentially have more anisotropic flow in unique plumbing geometries. Similar numbers of curvilinears are found in the two lineament zones, but there is only occasional association with a bright spot. Both domains have more anomalous profile miles than non-anomalous, which probably result from the anisotropic flow in distinctive plumbing. Macroseeps dominate in the fracture networks and ground water may contribute a component of horizontal flow.



The Lobo West area is characteristic of the lineament zone domains. Initially in the geologic past, a substantial diagenetic slab was built up to give the magnetic susceptibility anomaly. However, subsequent fluid movement was deflected around the slab so that curvilinears are distributed around the margin. Soil gas values are low over the magnetic susceptibility anomaly because it represents a fossilized macroseep through which no gas is currently moving. This interpretation is

sketched in Figure 64. Klusman and Saeed (1996, p. 166) refer to diversion of microseepage around the diagenetically cemented slab as a mechanism for also producing halo anomalies.

Flux Source

The large Smoke Creek Aeromagnetic Anomaly constitutes a centrally located flux source. If it is positioned above an intrusive igneous body, then the associated pulse of energy and fluid that rose through the sedimentary column may have produced some large surface anomalies. This rising pulse of energy and fluid most likely influenced any local hydrocarbon accumulations to produce small, secondary flux sources.

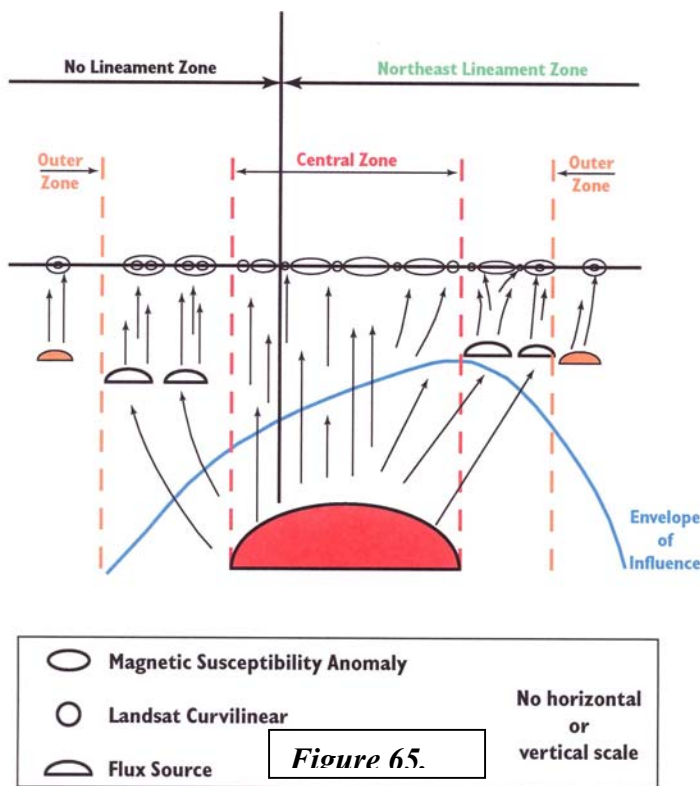
Alternatively, the central aeromagnetic anomaly is located above a huge and complex hydrocarbon accumulation. This structural complex might be an astrobleme, but other interpretations of postulated Williston Basin astroblemes are available (Bridges, 1978 and 1987; Gerhard, et al., 1995). In particular, the location at the intersection of lineament zones that have components of strike-slip displacement argues forcefully for a tectonic origin.

No matter what the origin of the Smoke Creek Aeromagnetic Anomaly may be, it has clearly influenced the development of surface anomalies. Within the outline of the aeromagnetic anomaly, there are more curvilinears, more bright spots, more anomalous profile lines and more magnetic susceptibility anomalies compared with outside areas. In

addition, the area within the outline of the central aeromagnetic anomaly is part of a distinctive qualitative pattern of magnetic susceptibility anomalies and curvilinears.

Magnetic susceptibility anomalies and curvilinears are distributed in three distinct zones around the central Smoke Creek Aeromagnetic Anomaly (see Figure 60). In the center, small curvilinears tend to be located around the margins of the large magnetic susceptibility anomalies. In the second zone surrounding the central zone, small curvilinears are more frequently located within the magnetic susceptibility anomalies. One striking exception is the Lobo West area, which has the curvilinears surrounding the larger anomaly margin (see Figures 56 and 64), but is located outside the central zone in Domain 2. The third zone is out at the margins of the total study area. In this zone, there is a close correspondence between curvilinears, small magnetic susceptibility anomalies and surface measurements. Site 26 is the archetype for this outer zone (see Figure 60).

The three distinct zones of anomalies represent three different sources of hydrocarbon flux (Figure 65). The central zone is located directly above a large and complex flux source. Closely spaced magnetic susceptibility anomalies developed early and are large slabs of diagenetically altered surface material that diverted subsequent microseepage around the margins where curvilinears formed (see Figure 64). In the next zone, curvilinears are found within the anomaly “blobs” suggesting that the diagenetic slab is thinner and/or less extensively developed. Thus, microseeps that formed after the slab was created rose directly through the middle of the anomalies. It is postulated that these are moderate-sized hydrocarbon flux sources and that they were indirectly influenced by flux from the large central source. In the outer zone, small and simple flux sources are located directly below curvilinears that correspond with small magnetic susceptibility anomalies and with surface measurements. In this zone there are minimal influences and complications from either the large central source or from a distinct plumbing geometry such as that associated with the northeast lineament zone.



Interaction between flux sources and plumbing geometries can account for differences between Domain 1 and Domain 2 (Figure 65). Domain 1 outside any lineament zone has no distinctive plumbing geometry and it is dominated by relatively simple vertical hydrocarbon migration above small, localized sources. Influences from the large central flux source may have produced multi-stage histories for some magnetic susceptibility anomalies. Site 26 is an example. In contrast, Domain 2 located within the northeast lineament zone is a corridor of increased fracturing and does have a distinctive plumbing geometry. Influences from the central flux source extend farther out into the lineament zone where fossilized macroseeps, similar to those over the large central source, may form. The Lobo West area is an example.

CONCLUSIONS (Shurr, 2002)

Hydrocarbon seeps associated with the Smoke Creek Aeromagnetic Anomaly have had a variety of life histories and are distributed in distinct patterns. In the center of the area, early and intense flux produced large slabs of diagenetically altered soil that are mapped as magnetic susceptibility anomalies. Subsequently, small seeps were deflected to the margins of the slabs where curvilinears mark their location. Contemporary gas seeps are generally not found within these thick fossil slabs.

Outside the central core area, hydrocarbon migration was influenced by plumbing geometries related to fracture systems in Landsat lineament zones. Large magnetic susceptibility anomalies were formed, but gas continued to flux through most of them so that curvilinears are not just limited to the slab margins. On the outer periphery of the study area, simple small seeps show a correspondence of Landsat curvilinears, magnetic susceptibility anomalies, and gas anomalies.

These interpretative generalizations require the further refinement and clarification that will be available after the next round of data collection has been completed. In the meantime, there are some clear preliminary implications for hydrocarbon exploration: 1) hydrocarbon sources in the sedimentary rocks above the aeromagnetic anomaly may have been depleted long ago; 2) sources surrounding the aeromagnetic anomaly may or may not be depleted, depending upon the plumbing geometry; and 3) the best candidates for exploration are distributed around the periphery as small and simple sources with contemporary seeps.

PHASE III: Wicape SW and Smoke Creek Revisited

The purchase of the Tribes IMDA partner, GCRL, by Conoco/Phillips essentially ended Gulf's participation as a sponsor of this DOE funded project. That left the Wicape 3D Prospect Area untested despite the encouraging results of Phase I that verified two of the 3D seismic anomalies as viable prospects. Fortunately another company entered the play in the summer of 2002 and wanted to confirm additional seismic leads especially along the southwest edge of the 3D survey. Figure 66 locates the Wicape SW prospect in the southwest of section 32.

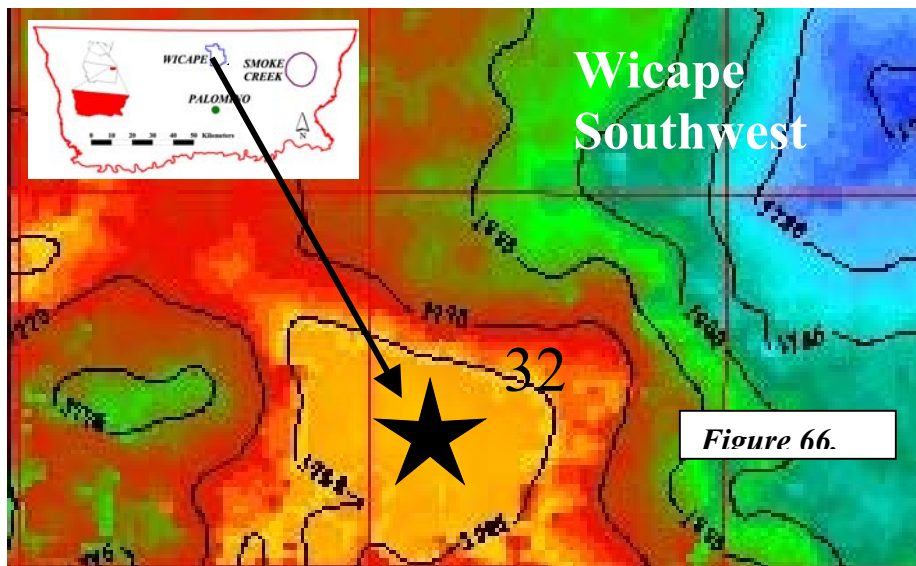
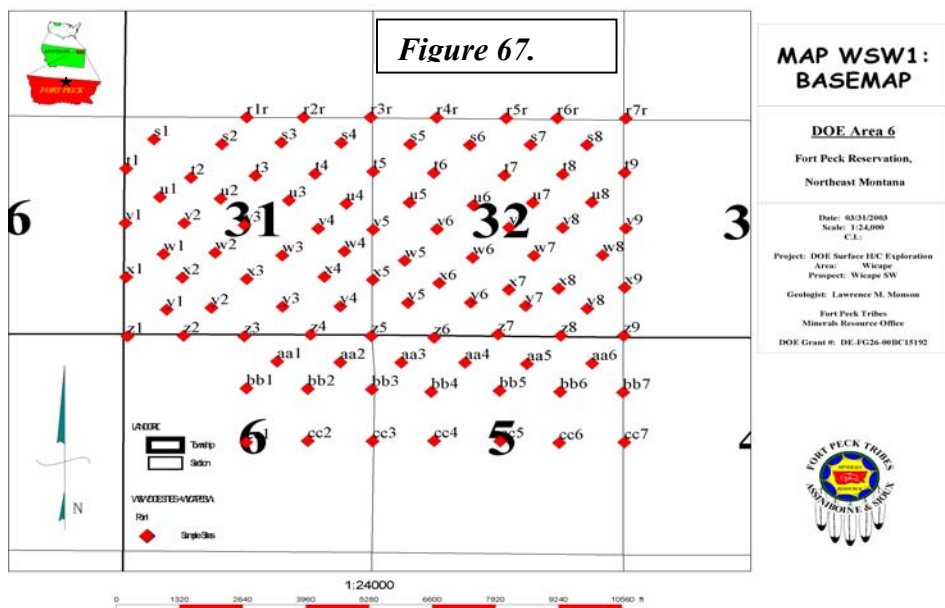
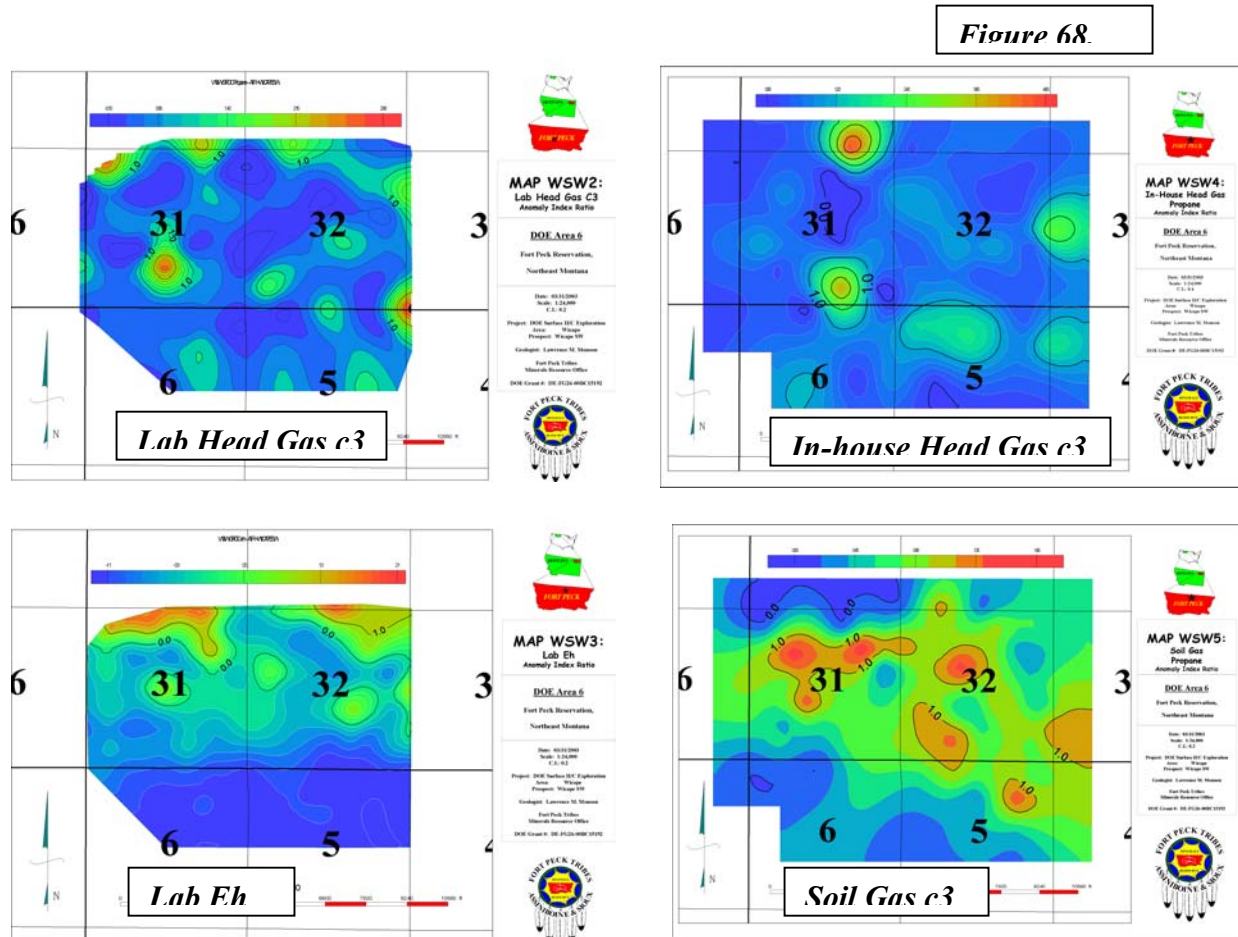


Figure 66.

A sampling grid of offsetting lines with 1320 ft. (433 m) sites was laid out and is displayed in Figure 67.



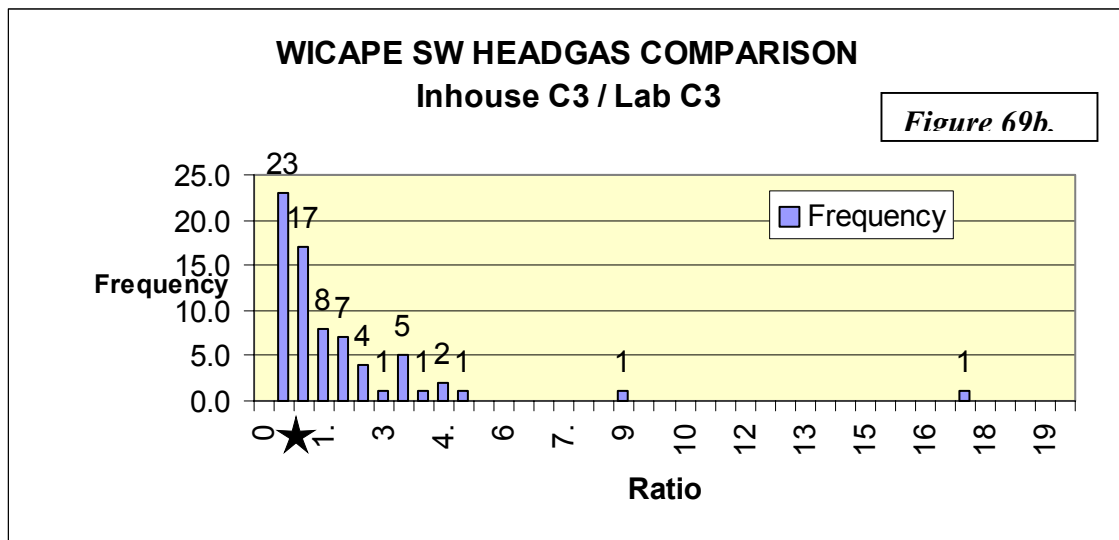
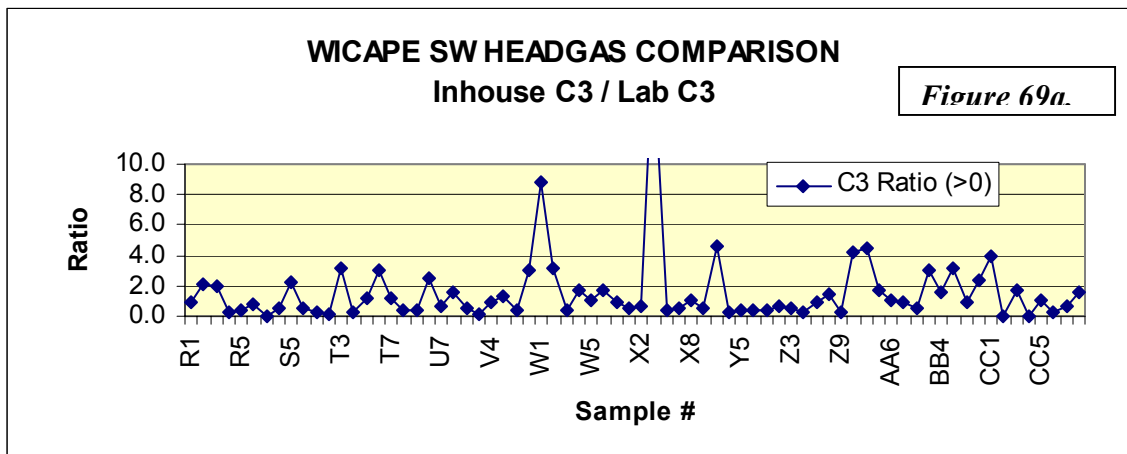
Three propane data sets and Eh are compared for Wicape SW in Figure 68. All display the anomaly index ratio described earlier.



The surface hydrocarbon methods tested here do not so clearly correlate to the seismic anomaly as they did in Phase I at the Wicape East (Tobago) prospect (see Figures 23 – 26). Duplicate Head Gas samples were collected and analyzed; one by the commercial lab employed throughout the project and the other in-house by the modified gas chromatograph used in the Soil Gas analyses. The lab Head Gas map shows a small propane anomaly over the 3D prospect, but has a much stronger anomaly .5 miles (.8 km) to the west. The in-house Head Gas analysis shows higher propane soil values around the 3D anomaly and especially .5 miles to the west, although not exactly where the lab Head Gas anomaly is. Interestingly the probe Soil Gas method confirms a hydrocarbon increase above the 3D prospect. This correlation between Soil Gas and Head Gas data has not been the norm elsewhere in the project except for at Site 26 in the Smoke Creek Area. Eh data is not correlative here at all with only higher values across the northern part of the map where a west-east drainage lies.

Two other data comparisons were made in the Wicape SW Area: 1) Lab vs. In-house Head Gas and, 2) Line R re-sampling. The Head Gas comparison was made to test the feasibility of performing local data analysis for future exploration on Tribal lands. Obviously since the Head Gas method is the preferred technique identified by this study

it is desirable to find a more cost effective way to continue using it and it is necessary to demonstrate that the in-house analysis is as reliable as the commercial lab analysis. The Head Gas comparison is displayed in Figure 69a (raw data) and Figure 69b (frequency distribution).



As seen in Figure 69a there is not a 1:1 correlation between the in-house analyses and the lab analyses. Only 40 of the 70 data points, with a ratio greater than 1.0, (30 in-house samples had no propane reported) plot between 0.5 and 1.5 (star locates the ratio = 1). In general the in-house values were higher than the commercial lab results (average ratio = 1.57). The in-house analyses were relatively erratic as confirmed by the absence of data in 30 samples, something that rarely happens in the reported commercial lab data. Although similar analytical methodology was employed, the commercial lab gas chromatograph normally analyzed 1 cc injections while the in-house GC normally handled 5 cc injections because it was configured to handle less concentrated probe Soil Gas samples. This led to some degradation of the runs perhaps by retention of too much methane. Many plots on the integrator were overwhelmed by the methane peaks, which

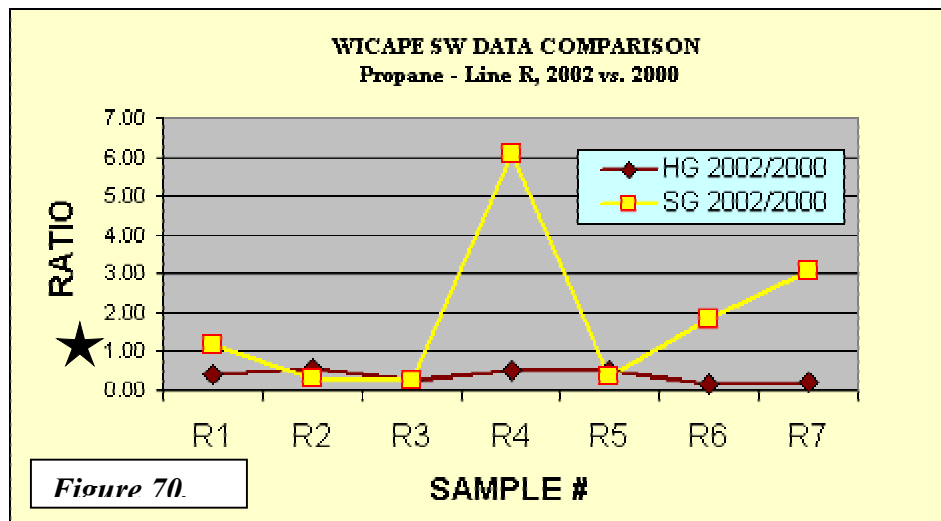
often obscured the ethane peaks and probably some of the propane peaks. It was later determined that the ion detector filament needed replacing when the Smoke Creek samples were run. In addition there was virtually no butane values reported, which strongly suggests that microbial activity consumed the heavier gases and probably some of the lighter gases in the time period between sample collection and analysis.

Another reason for returning to the Wicape Area was to resample sites that had been collected during Phase I, two years earlier. In order for a method to be considered reliable it must be repeatable. Table 6 lists the lab Head Gas and probe Soil Gas data for 2000 and 2002 and calculates a ratio that is graphed in Figure 70.

TABLE 6: LINE R PROPANE DATA COMPARISON, 2002 vs. 2000
DOE Area 6: Wicape Southwest Seismic Prospect

sample#	2002 data		2000		2000		
	LAB HG C3	SG C3	HG C3	02/00 HG C3	SG C3	02/00 SG	
	ppm	ppm	ppm	Ratio	ppm	Ratio	
R1	1.250	0.284	3.130	0.40	0.245	1.16	
R2	4.004	0.295	6.917	0.58	0.925	0.32	
R3	0.427	0.241	1.834	0.23	0.900	0.27	
R4	2.938	2.584	5.514	0.53	0.424	6.09	
R5	1.763	0.438	3.529	0.50	1.175	0.37	
R6	0.941	0.976	6.452	0.15	0.529	1.84	
R7	0.721	1.268	3.984	0.18	0.413	3.07	
	1.721	0.869	4.480	0.37	0.659	1.88	

HG = Head Gas, SG = Soil Gas, C3 = Propane



The 2002 Head Gas values average only 37% of the 2000 data values, but are relatively uniform in their individual ratios ranging from .18 to .58 (again star marks exact correlation of 1). Different soil moisture, air temperature, and barometric pressure could

explain the difference. Again the probe Soil Gas data appears suspect, or at least is not reproducible, as shown by the wide range in ratios between 2002 and 2000 (see yellow line in Figure 70).

SMOKE CREEK REVISITED

Curvilinears

Phase II of this project conducted a reconnaissance magnetic susceptibility survey in an attempt to associate micro-seepage anomalies with the large Smoke Creek AeroMag feature. Sample sites were selected along traverses at an interval described earlier with preference given to curvilinears that appeared on the GPS computer screen. However, the spacing along those profiles was too wide to accurately model hydrocarbon shows above or within the satellite anomalies. Because of the abundance of curvilinears in the Smoke Creek Area, a decision was made to sample as many of them as possible. Figure 71 outlines 4 that were sampled to the west of Smoke Creek, 6 that were sampled within the core of the AeroMag Anomaly, and 3 were examined northeast of the core area.

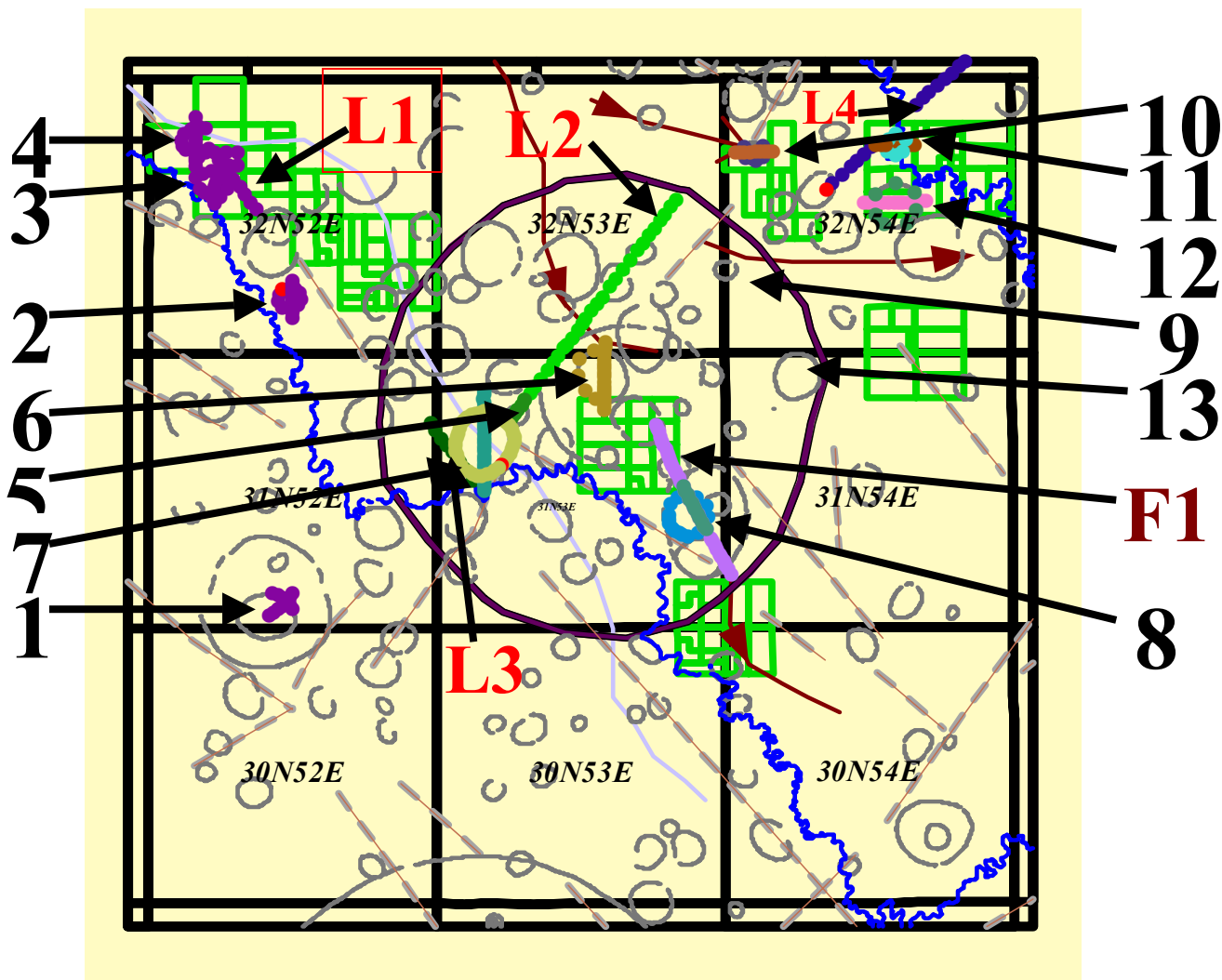


Figure 71. Smoke Creek Phase III sample program. Black numbers label curvilinears sampled. Red numbers label lineaments sampled. F1 is part of the Smoke Creek Anticline axis sampled. Gray lines are curvilinears and lineaments. Light blue line traces the Smoke Creek Syncline axis. Green outlines are tracts in 2D seismic prospects.

The sampling protocol was designed to compare the rims of the curvilinears to a perpendicular traverse that began outside the curvilinear and crossed through as a diameter line bisecting the circle.

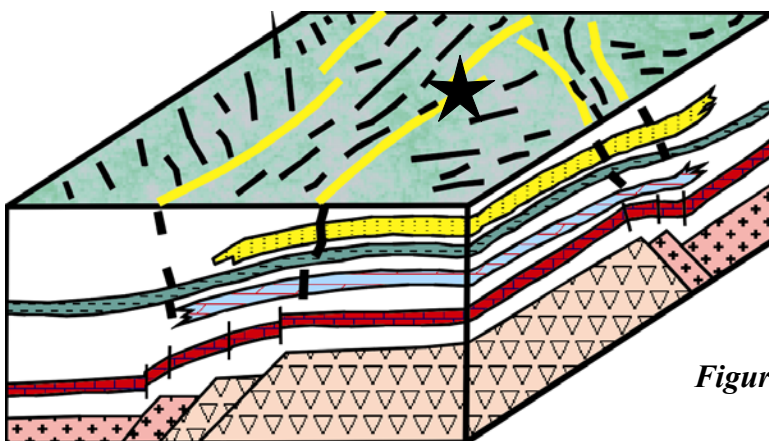


Figure 72.

Lineaments are thought to represent the boundaries of zones containing related linear features that are modeled as basement faults propagated to the surface in Figure 72 (see yellow lines).

The Smoke Creek Anticline parallels a regionally significant syncline with the same name that also marks the edge of the Devonian Prairie Salts (see Figure 73). This subtle structural feature is almost entirely untested by oil wells.

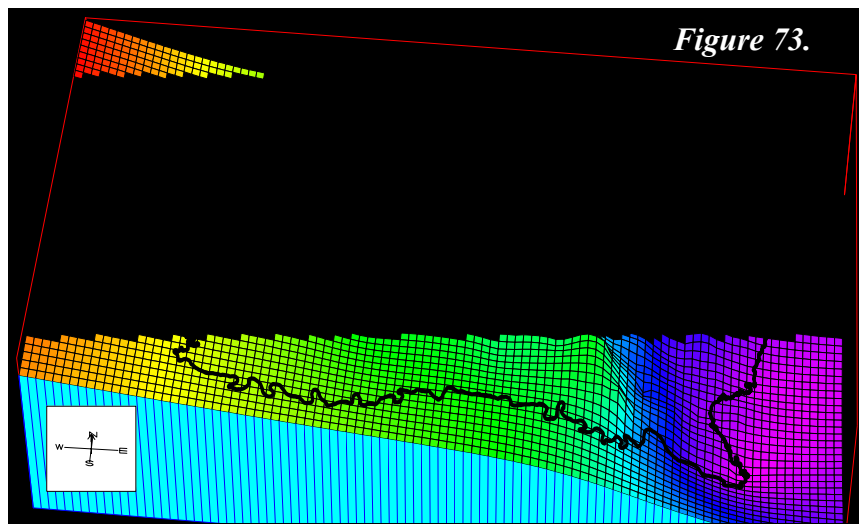


Figure 73.

Figure 74 once again demonstrates the excellent data validity verification of the lab Head Gas data for all four data sets collected in the Smoke Creek area.

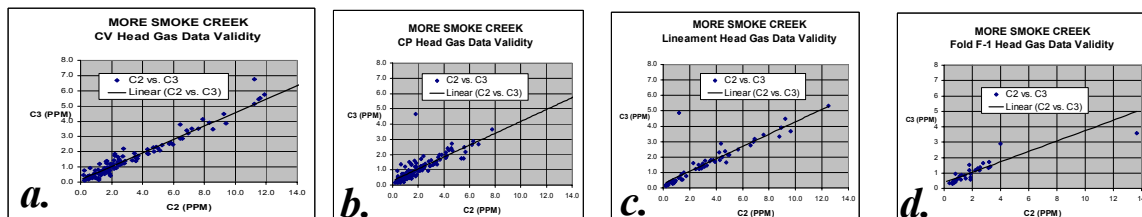
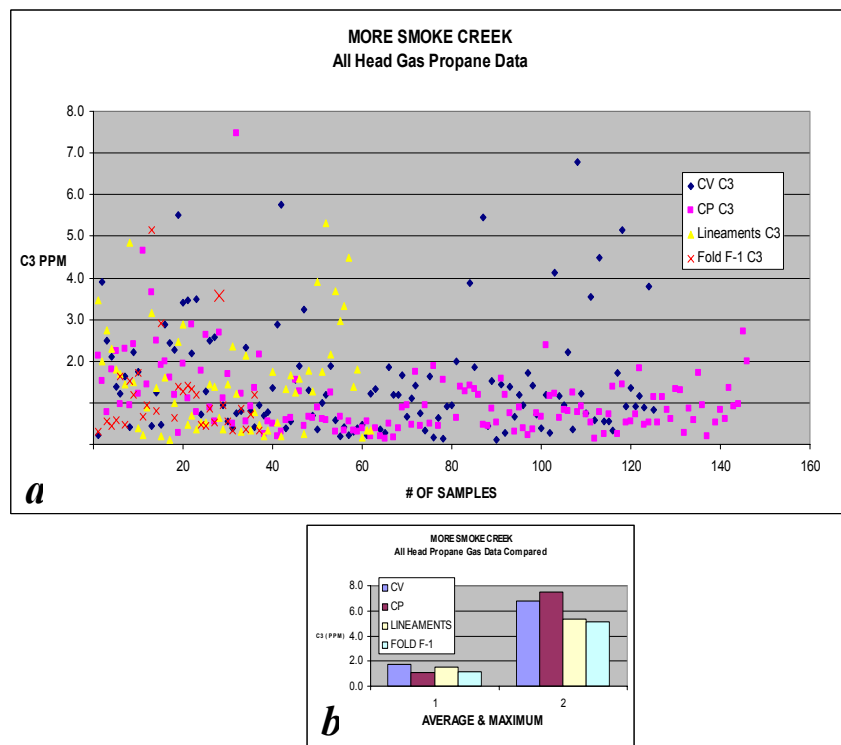


Figure 74. a. CV = Curvilinear rim, b. CP = Curvilinear perpendicular, c. Lineaments, d. Fold.

All the new data collected is plotted in Figure 75a, with each data set summarized in Figure 75b. Graphical inspection suggests that the curvilinear perimeter data (CV) has higher values, followed by the lineaments. The curvilinear perpendiculars (CP) and fold had similar averages. The highest values however were found in one of the CP data sets.

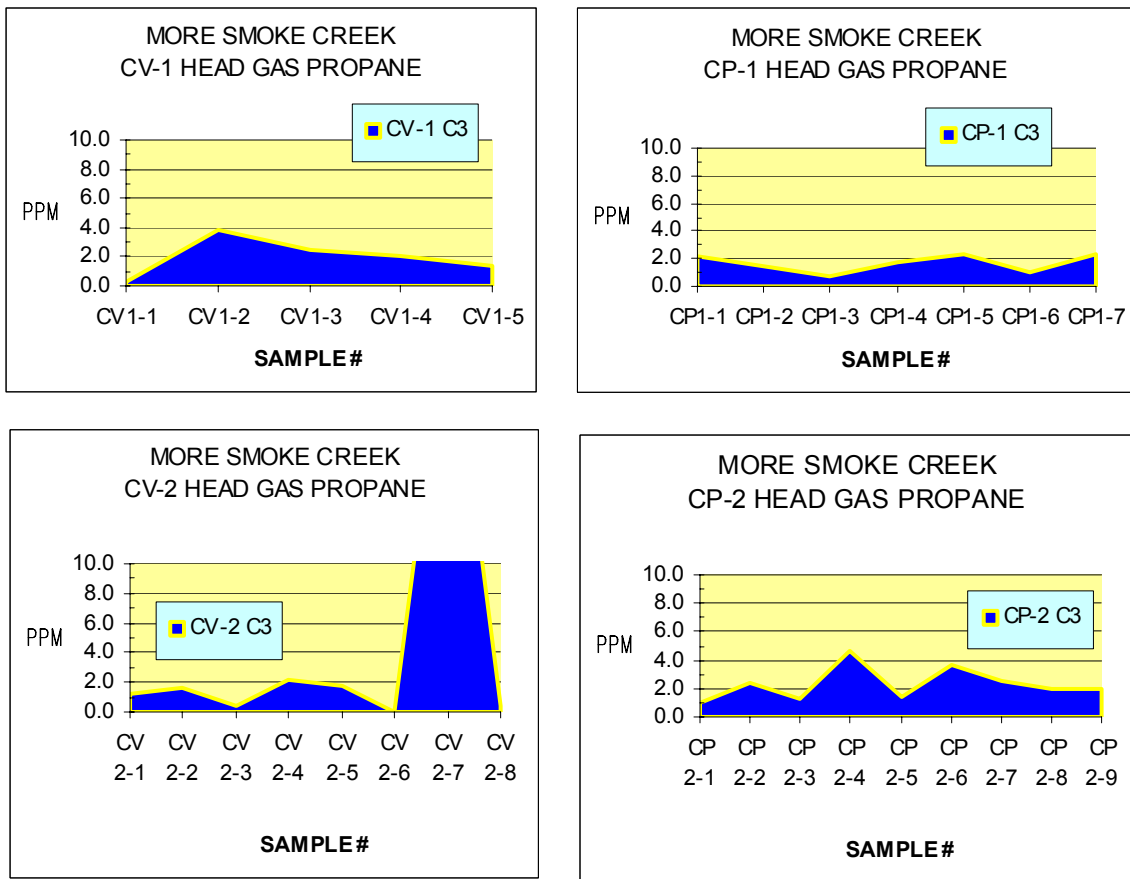
Figure 75. Smoke Creek Head Gas Propane



Propane Head Gas profiles are plotted in Figures 76 – 81 for all the curvilinears that were sampled. These are divided into the following areas in an attempt to compare data collected outside the Smoke Creek AeroMag Anomaly with data collected within the core of the anomaly: Figure 76 – WEST (CV/CP 1 and 2), Figure 77 – NORTHWEST (CV/CP 3 and 4), Figure 78 – CORE (CV/CP 6), Figure 79 – WEST CORE (CV/CP 7), Figure 80 – EAST CORE (CV/CP 8, 9, 13), and Figure 81 – NORTHEAST (CV/CP 10, 11, and 12). Photographs of the curvilinears sampled begin with Figure 83.

CV-1 is a relatively large curvilinear west of the mag anomaly. Only the northwest quarter of the circle was sampled. CV-2, a much smaller anomaly had some of the highest gas values sampled anywhere in the area. See Figure 76 for CV-1 and CV-2 data profiles.

Figure 76. West curvilinear data.



A similar observation can be made for CV-3 in Figure 77, which plots data from curvilinears in the northwest part of the study area. This area had numerous curvilinears, lineaments, and seismic prospects.

Figure 77. Northwest curvilinear data.

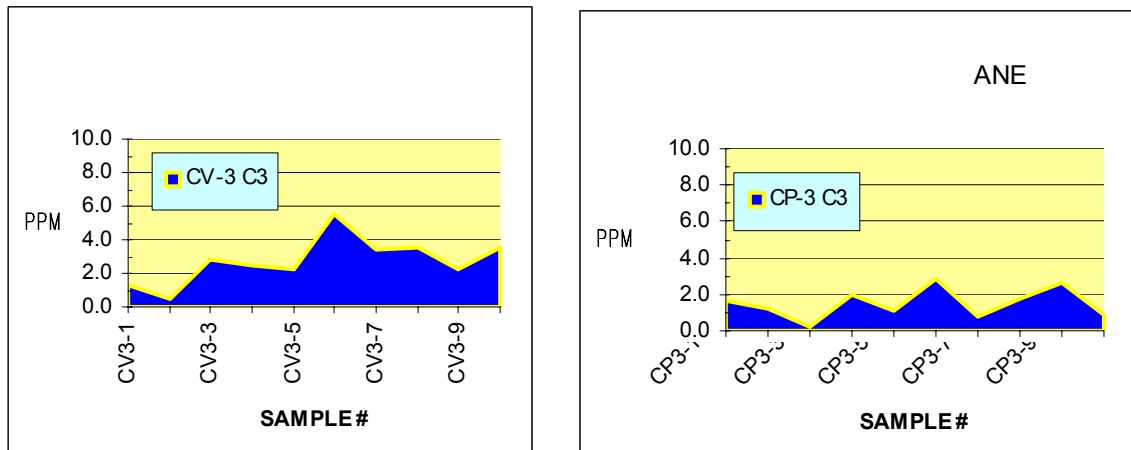
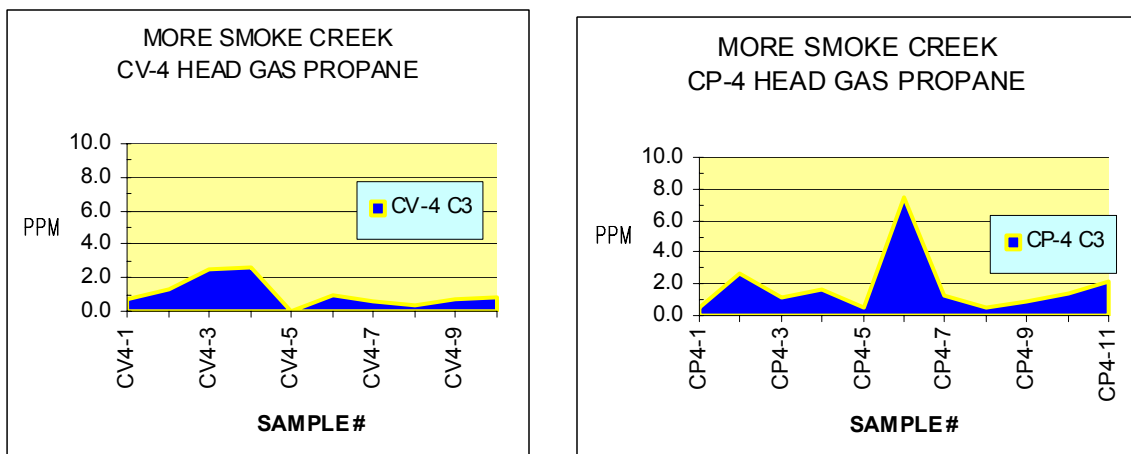
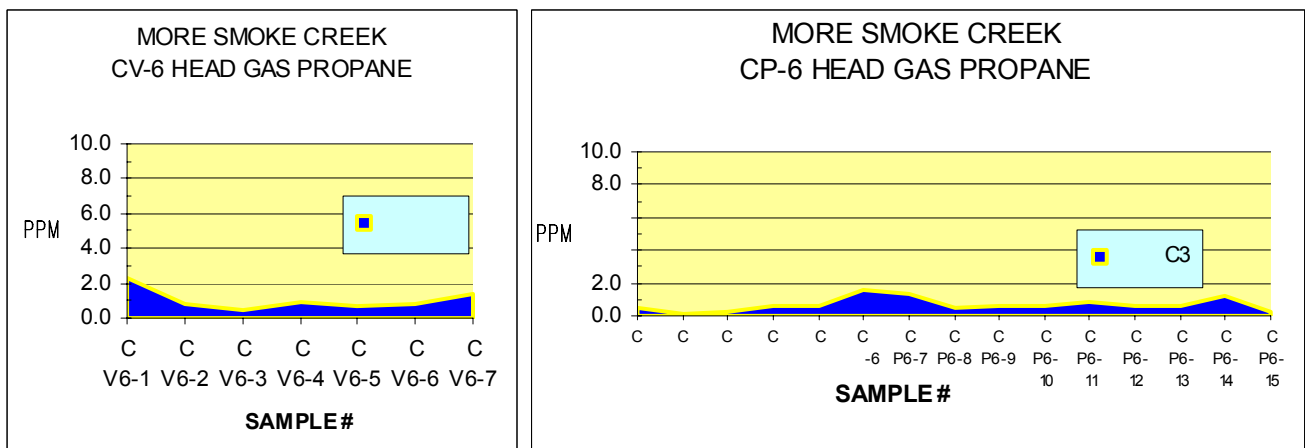


Figure 77 cont. Northwest curvilinear data.



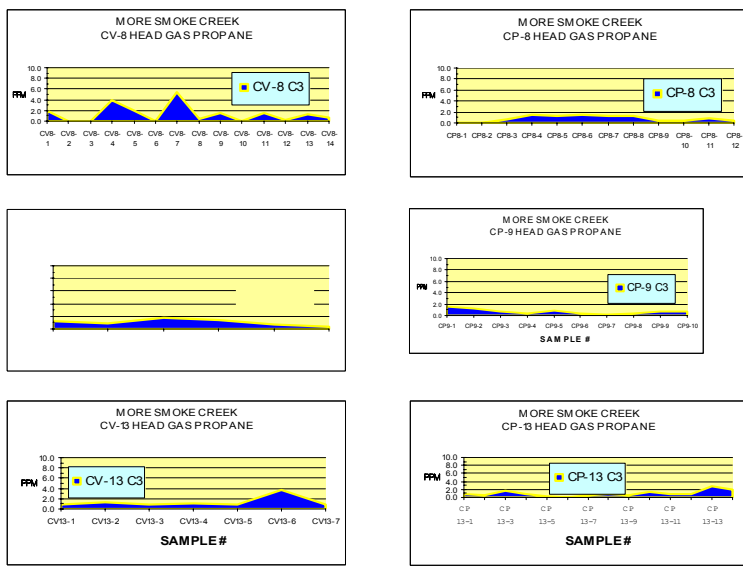
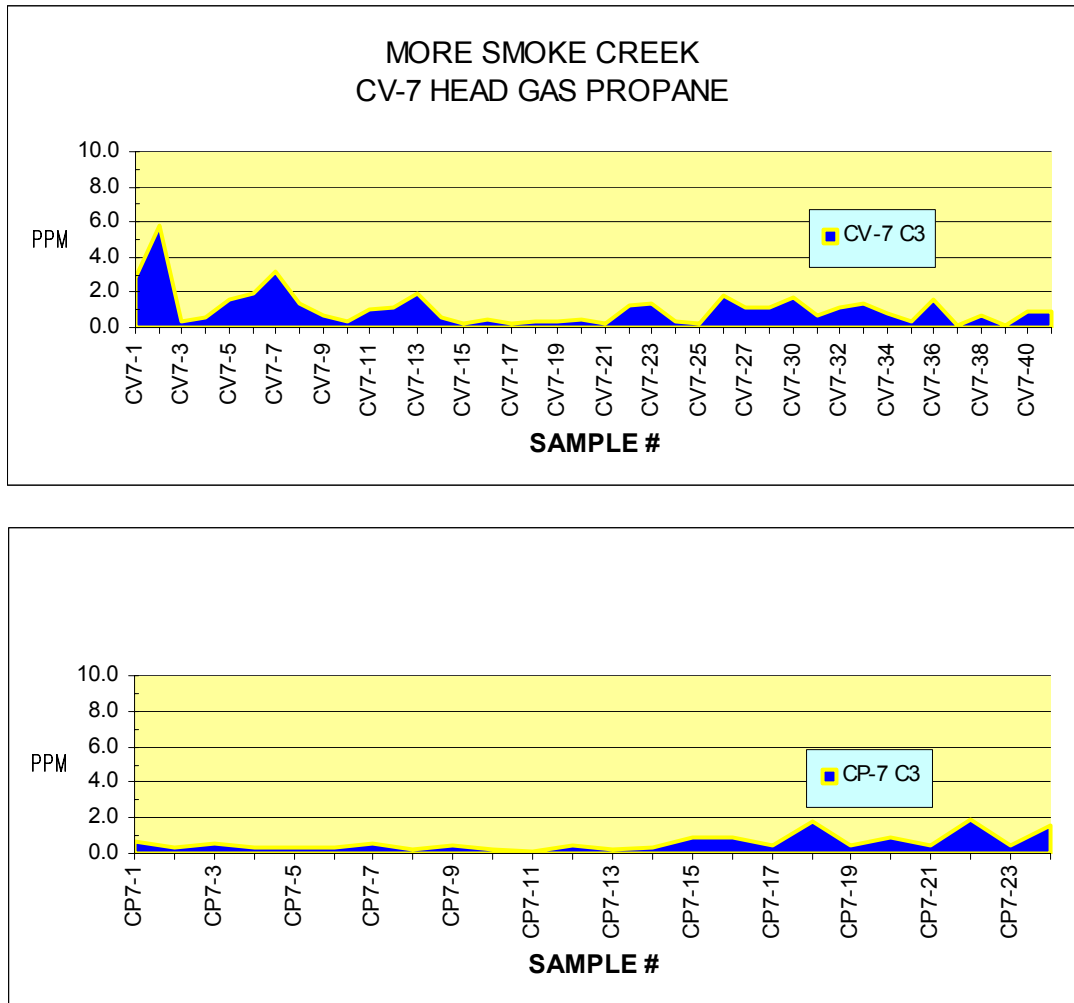
The curvilinear data for the Smoke Creek Core is graphed in Figures 78 through 80. These were separated into the Central Core, West Core, and East Core, respectively. CV-6 lies in the center of a nested curvilinear complex. Figure 78 reveals relatively lower propane values than those encountered in the west and northwest areas. CP-6 has higher values on the north rim as it crosses the curvilinear boundary, but also has higher values within the curvilinear at CP6-6 and then very low values across the south edge.

Figure 78. Smoke Creek Core curvilinear data.



The most densely sampled curvilinear was CV-7 in the West Core area (500 ft., [127 m.] interval). This curvilinear lies at the intersection of two lineament zones and should have gas anomalies if in fact these tonal features represent hydrocarbon micro-seepage. Elevated propane values are recorded in the graphs of Figure 79 particularly around the perimeter and somewhat on the north end of the perpendicular traverse.

Figure 79. West Core curvilinear data.

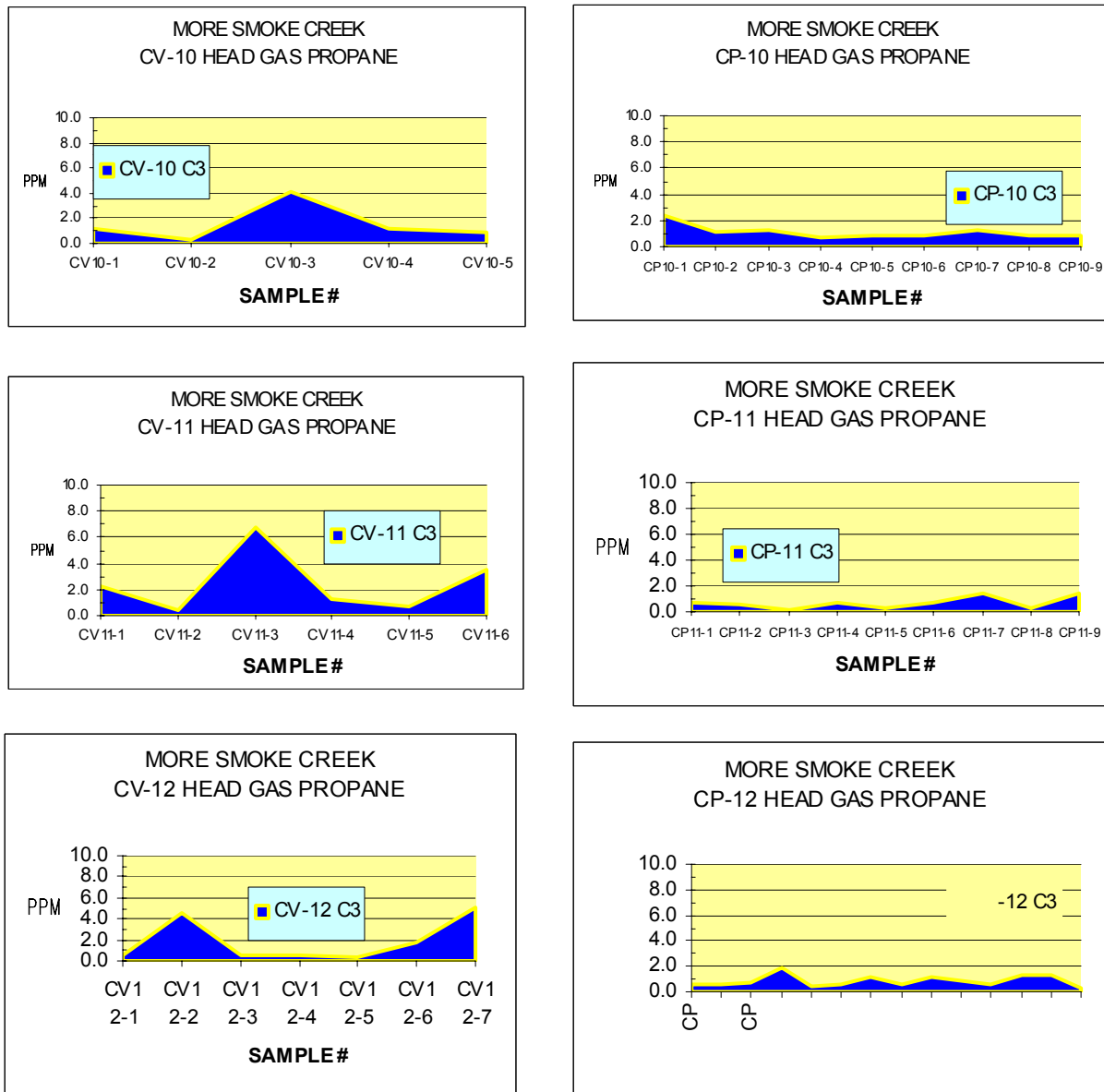


Propane Head Gas data for the three East Core curvilinears are all plotted in Figure 80. Again the perimeters appear to have more sites with higher values, but some of the CP (perpendicular) traverses do have elevated values indicating that the curvilinear cores may be more complex than just a single circular feature.

Figure 80. East Core curvilinear data.

As seen in the West and Northwest curvilinears, those sampled in the Northeast generally have greater propane values in the CV perimeters than in the CP perpendicular traverses. Figure 81 shows this observation in the graphs on the left side of the illustration.

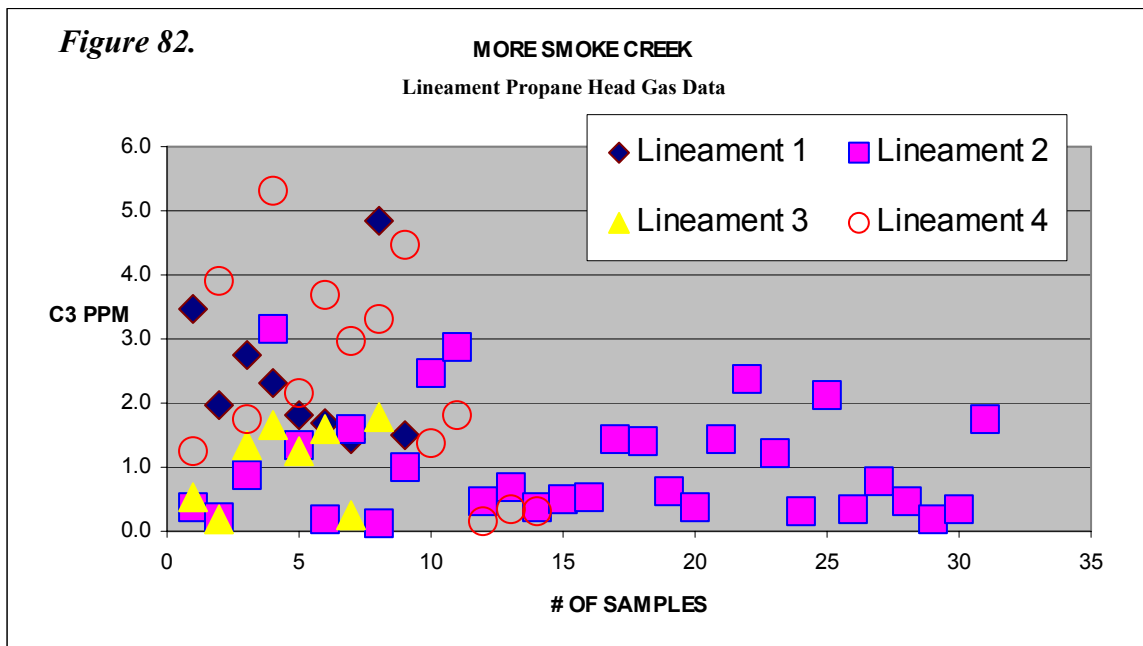
Figure 81. Northeast curvilinear data.



For most of the curvilinears, only half dozen samples were taken above the circle perimeter. This does not constitute a statistically sufficient number of data points. However the rims of the curvilinears appear to have higher gas flux concentrations than either the adjacent area surrounding curvilinears or the diameter traverses. The second conclusion that can be made is that the curvilinears within the core of the Smoke Creek AeroMag Anomaly do not appear to have as high flux rates as those outside the anomaly even though the relative abundance of features is greater inside the core. This could be

explained by Shurr's illustration in Figure 65, which presents a model calling for diagenetically, altered "slabs" sealing the heavily fluxing early history of the area in the core of Smoke Creek. These slabs likely also divert modern flux to the surrounding areas such as Site 26, and the curvilinears in the West, Northwest, and the Northeast areas discussed above.

Figure 82 reinforces this observation for the curvilinears by displaying relatively greater propane Head Gas values for the two lineaments that lie outside the Smoke Creek AeroMag core (Lineaments 1 and 4, dark blue diamonds and red circles, respectively). The fold propane data resembles Lineament 2 with most values less than 2.0 ppm.



Topographic Expression of Curvilinears

One of the important questions regarding the curvilinears is what exactly is the surface characterization of these satellite interpreted tonal anomalies? Do they have topographic expression as hills or valleys? Do they have soil texture and color properties that distinguish them from the surrounding terrain? Or might they even have vegetative expression as places that plants are either enhanced or degraded by escaping hydrocarbons?

Beginning with Figure 83, photographic views are presented to begin to address these questions. The figure caption for each will list pertinent observations.

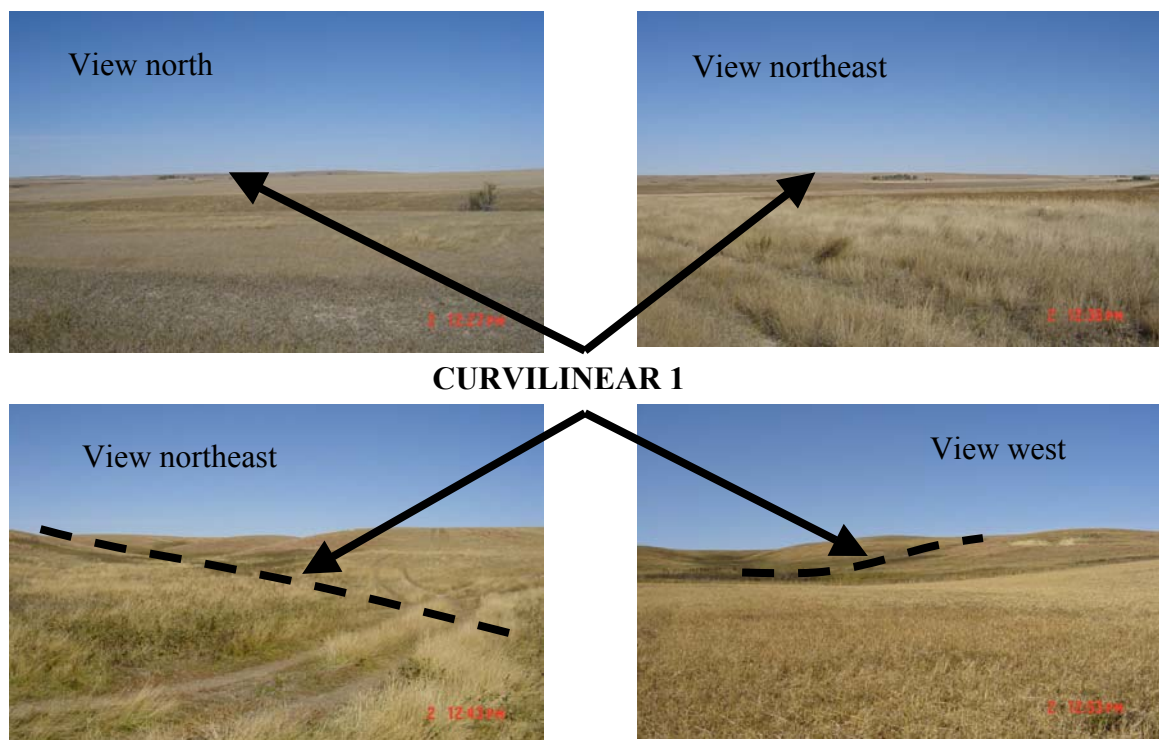


Figure 83. Distant and close-up views of Curvilinear 1. Distant views show a low-relief topographic expression of a circular hill. Close-up views show perimeter line following selected drainages. Note bare ground on hillside associated with this curvilinear perimeter, but not observed in other curvilinears.



Figure 85. Lineament 1 and Curvilinear 3 viewed southeast. Lineament is gentle low relief drainage and CV3 is low relief hill.

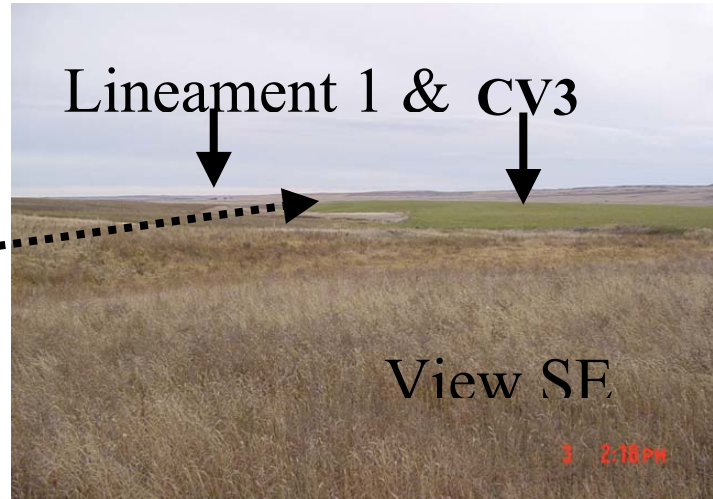


Figure 86. View southeast of Curvilinear 4. Here curvilinear is entirely a stubble wheat field covering a circular hill.

Figure 87. Curvilinear 5 viewed from the southwest at the end of Lineament 2 sampling traverse, which crossed through CV5 as a perpendicular profile. Inset picture shows the steepness of the north and east sides of CV5.

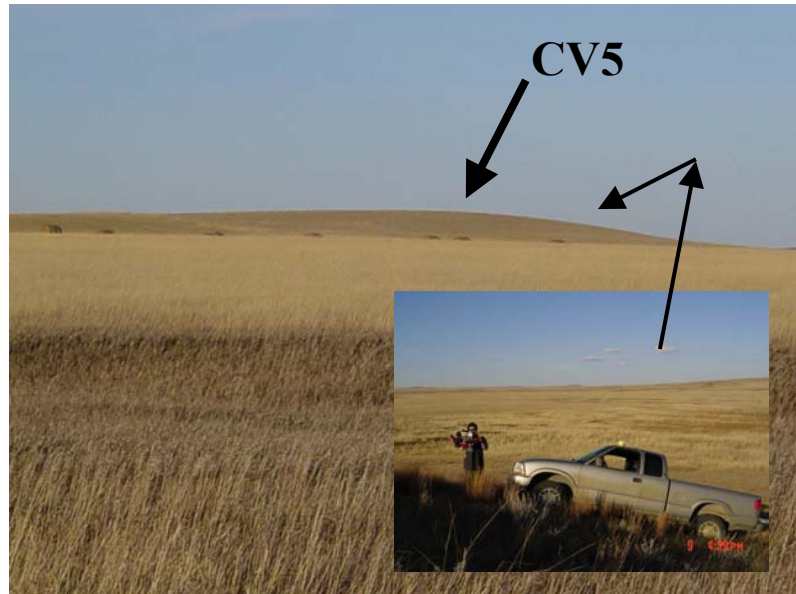


Figure 88. Views of Curvilinear 6 showing topographic circular high with both radial drainage and bounding drainage definition of perimeter.

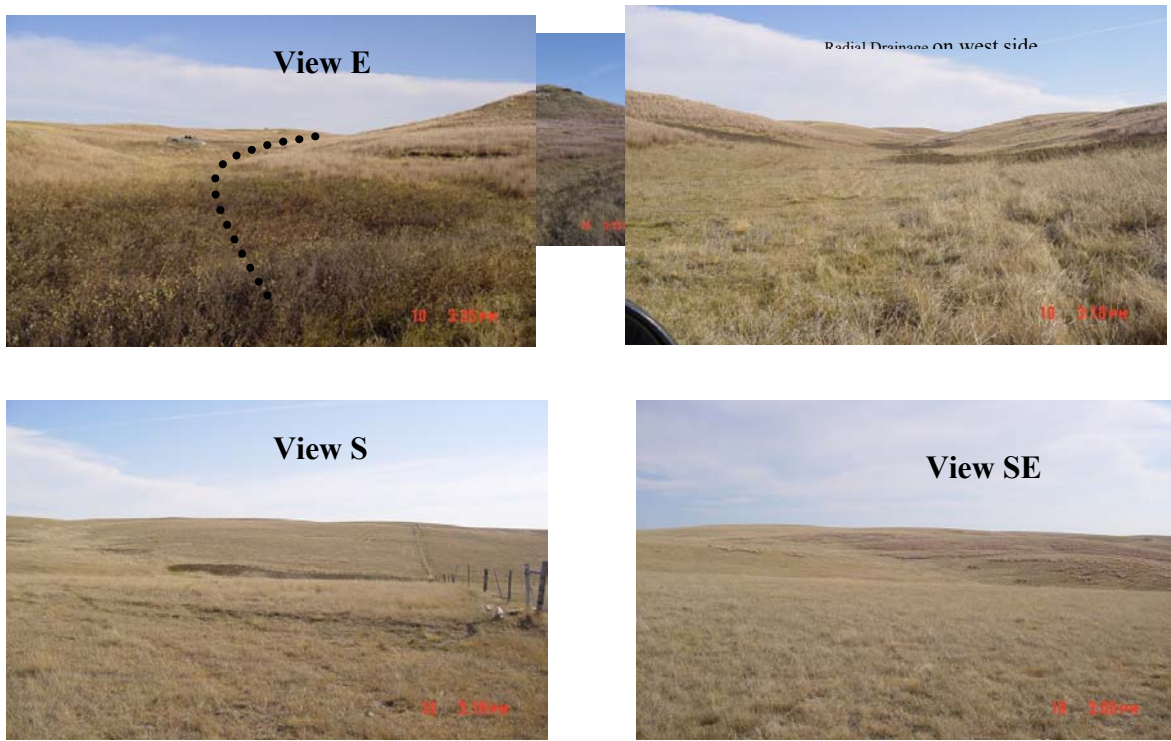




Figure 89. Curvilinear 7 viewed from the southeast. Again anomaly is a topographic high. This curvilinear was sampled at 500 ft. intervals.

Figure 90. View southeast across Lineament 2 (Crazy Horse Creek). Picture taken near north end of sampling traverse.



Smoke Revisited Conclusions

Returning to the principle reason for this study, thirteen of the satellite tonal anomalies found in the Smoke Creek AeroMag Area were sampled in 2002. The perimeter and one perpendicular traverse were collected for curvilinears outside and within the core of the aeromag anomaly. Four satellite linears were also sampled and soil along part of the principle anticlinal fold axis in the area was collected. There does not appear to be obvious confirmation that elevated gas micro-seepage occurs within or along the boundary of the curvilinears. As a whole, the data set appears to have higher values associated with the perimeter of the curvilinears, but not necessarily within the Smoke Creek AeroMag Anomaly. The lineaments average higher propane soil content than the curvilinear centers, especially outside the core area. When compared to the Phase II background data for Smoke Creek, the curvilinear perimeters do appear to be anomalous, but considerably more local data is necessary to confirm that observation. Field

inspection of the curvilinears reveals that most are elevation closures associated with hills or ridges, often along the slopes of the topography, or sometimes tracing drainage gullies. They do not appear to be soil color changes or vegetation changes affected by gas seepage. The topographic highs however could be caused by more resistant soil types associated with the micro-seepage chimneys or diagenetically altered fossil chimneys. The next step should be to sample curvilinears 1, 6, 7, and 12 with a more closely spaced grid.

FINAL CONCLUSIONS

Phase I of this study “*to assess hydrocarbon surface exploration techniques on the Fort Peck Reservation*” determined that the ***best method to employ is the Head Gas procedure***, which collects soil samples from a depth of 1 meter and places them in a sealed jar with water. Gas is extracted for analysis by flame ion gas chromatograph after gentle agitation and heating to 80 degrees Celsius. Although light gas ratios and principle component analysis aids in identifying anomalous data, a standardized comparison ratio was applied for this study to all the data analyzed and *micro-seepage was defined as occurring where the data calculated to be more than 1.5 times the mean of the respective data set*. This anomaly index is named the ***AIR, or anomaly index ratio***. This direct method closely correlated to the oil production at Palomino Field in test Area 7. It also exactly outlined two 3D seismic prospects in Area 6 also known as Wicape. *These will be drilled within the next year as part of a new Indian Mineral Development Act agreement signed by the Tribes this past winter*. Success will of course strongly confirm the Head Gas method as a viable surface exploration technique.

Whether the Head Gas procedure can be adapted for in-house analysis remains to be demonstrated, but preliminary results encourage the pursuit of that capability. Further soil sampling in the southwest part of the Wicape Area tested another 3D prospect, but did not correlate as well. That prospect may also be drilled as part of the new IMDA. Calibrating the in-house gas chromatograph for smaller sample runs that have much higher gas concentrations than the Soil Gas samples the equipment was designed to analyze, remains the principle problem to be solved.

In-house probe Soil Gas investigations, continued after one of the project’s principal consultants retired, did not produce reliable results. One of the basic data validity checks is to plot ethane vs. propane for each data set. In almost all cases the Soil Gas data did not plot as a linear relationship. This questions the analytical accuracy of the in-house gas chromatograph and perhaps the data collection procedure, which often encountered tight soils that gave up little gas during extraction by syringe. The Thermal Desorption method was only tested at Palomino Oil Field and appears to have useful application. Acid Extract analysis mapped what appear to be halo patterns around the apical anomalies mapped by the Head Gas, Eh, and Microbial methods. Undoubtedly it would be much better to employ an in-situ adsorption technique that would collect gas over some time period of at least days. These were deemed too expensive to employ within the grant’s budget. Contracted resistivity methods were not tested for the same reason.

The indirect detection method that appears to have the best utilization potential includes either microbial technique employed. Eh, the reduction/oxidation potential of the soils, appears to also be a good indirect technique to confirm micro-seepage of gas. Iodine results were not easily interpreted and the magnetic susceptibility data did not produce anomalies verified by direct gas detection. If in fact the curvilinears of Smoke Creek are relict, fossil, micro-seepage chimneys as proposed by Shurr, then magnetic susceptibility reconnaissance holds further promise.

Phase II primarily examined the Smoke Creek AeroMag Anomaly area because of the numerous circular satellite anomalies concentrated within the feature. These curvilinears resemble what would be expected from overlapping micro-seepage chimneys reaching the surface of the earth. What ever is causing the significant regional magnetism of the earth in this location appears to also have affected structural and stratigraphic trends in the eastern part of the Fort Peck Reservation. Whether the necessary traps and reservoirs exist at depth remains to be determined. Surface exploration in this phase identified three anomalous magnetic anomalies. Only one of these had confirmed direct gas and indirect indicators in the soils. Since that site lies on the down dip nose of and identified seismic prospect, further surface sampling is warranted. Shurr's analysis of the Phase II data for Smoke Creek advocates a four-part model related to tectonic domains coincident on the intersection of two tectonic lineament zones. The satellite curvilinears within the Smoke Creek core may represent relict chimneys now sealed by diagenetic soil alterations. In that case oil exploration is still encouraged even though modern day flux has decreased or ended, assuming that other timing was correct for oil trapping below.

Phase III returned to examine a third 3D seismic prospect in the Wicape Area. This drill site was not as well correlated as the Phase I sites were. If this well is unsuccessful or not as good as the initial well planned, then the surface exploration observations will also be confirmed. More detailed sampling of the Smoke Creek curvilinears repeats Shurr's Phase II observation that the anomalies outside the core area have higher soil gas flux. The same conclusion can be made from examining the lineament data sets. Confident interpretation of either data set is hampered by the lack of background data and complicated by the overlapping and nested location of the curvilinears. By sampling the perimeter and mostly within each feature the data is biased toward the curvilinear and there is no frame of reference to define what is truly anomalous. A denser sampling grid must be laid out over as many features as possible.

From this project the Fort Peck Tribes are encouraged to apply surface exploration methods to both known prospects and to reconnaissance investigations designed to identify other areas with oil and gas potential.

AKNOWLEDGMENTS

Special thanks to Lee Raffaell, Field Assistant for this project who carried on when the project field geologist bailed out and who covered for me after two medical operations. Without his help and friendship this project would have been impossible.

REFERENCES

Andrew, J.A., D.M. Edwards, R.J. Graf, and R.J. Wold, 1991, Empirical observations relating near-surface magnetic anomalies to high frequency seismic data and Landsat data in eastern Sheridan County, Montana: *Geophysics*, v. 56, p. 1553-1570.

Belt, J.Q. Jr. and G.K. Rice, 1995, Macro Exploration Modeling: A Pragmatic Multidisciplinary Team Process, *Oil and Gas Journal*, June 5, 1995.

Donovan, T.J. et.al., 1986, Near-Surface Magnetic Indicators of Buried Hydrocarbons: Aeromagnetic Detection and Separation of Spurious Signals: *Bull. Association of Petroleum Geochemical Explorationists*. v.12, no.1, p. 1-20.

Elam, J.G., 1990, New Method Helps to Refine Subsurface Interpretations: Electrotelluric Surveying: *World Oil*, June 1990, p. 45-55.

Geoterrex, Schacht, B. and G. Roberts, 1990, Interpretation Report of a High Resolution Aeromagnetic Survey in the Central Williston Basin: Geoterrex Ltd. Project 684.

Klusman, R.W., 1990, Surface and Near-Surface Geochemistry Applied to the Exploration for Petroleum: Short course, Colorado School of Mines.

Land, J.P., 1991, A Comparison of Micromagnetic and Surface Geochemical Survey Results: *Association of Petroleum Geochemical Explorationists Bulletin*, v.7, p. 12-35.

Monson, Lawrence M., 2000, Phase I Interim Report 1, Fort Peck Reservation Assessment of Hydrocarbon Seepage: Semi-Annual Technical Progress Report, Department of Energy Grant Award # DE-FG26-00BC15192.

Monson, Lawrence M., 2001, Phase I Report 2, Fort Peck Reservation Assessment of Hydrocarbon Seepage: Semi-Annual Technical Progress Report, Department of Energy Grant Award # DE-FG26-00BC15192.

Monson, Lawrence M. and G.W. Shurr, 1993, Remote Sensing Applications in the Assessment of Natural Resources on the Fort Peck Reservation, Montana, in Proceedings of the Ninth Thematic Conference on Geologic Remote Sensing: Environmental Research Institute of Michigan, v. 1, p. 431-443.

Monson, Lawrence M., G.W. Shurr, and D.F. Lund, 1991, Importance of Landsat Linear Features in Hydrocarbon Exploration on Fort Peck Reservation, Northeastern Montana, in Proceedings of the Eighth Thematic Conference on Geologic Remote Sensing: Environmental Research Institute of Michigan, v. 1, p. 45-58.

Monson, L.M., 1995, Fort Peck Reservation Oil Summary, Part I: Reservoirs, Production, and Reserves, *in* L.D. Hunter and R.A. Schalla (eds.), Seventh International Williston Basin Symposium: Montana Geological Society, p. 253-264.

Monson, L.M., W. Ewert, and R. Zeier, 1995, Fort Peck Reservation Oil Summary Part II: Exploration Opportunities, *in* L.D. Hunter and R.A. Schalla (eds.), Seventh International Williston Basin Symposium: Montana Geological Society, p. 265-278.

Monson, L.M., 1995, Cretaceous System Stratigraphy and Shallow Gas Resources on Fort Peck Reservation, Northeast Montana *in* L.D. Hunter and R.A. Schalla (eds.), Seventh International Williston Basin Symposium: Montana Geological Society, p. 163-176.

Monson, L.M., 1995, Evaluating Mineral Resource Potential on the Fort Peck Reservation using GIS Analysis, *in* L.D. Hunter and R.A. Schalla (eds.), Seventh International Williston Basin Symposium: Montana Geological Society, p. 367-372.

Monson, L.M. and D.F. Lund, 1991, Breaking into Bakken Formation Potential on the Fort Peck Reservation, in Northeastern Montana, *in* J.E. Christopher and F.M. Haidl (eds.), Sixth International Williston Basin Symposium proceedings: Saskatchewan Geological Society Special Publication No. 11, p. 95-102. Co-author: Lund.

Orchard, D.M., 1987, Structural history of Poplar Dome and the dissolution of Charles Formation salt, Roosevelt County, Montana: *in* C.G. Carlson and J.E. Christopher (eds.), Fifth International Williston Basin Symposium, Saskatchewan Geological Society special publication No. 9, p. 169-177.

Petta, Timothy J., 1999, How fractured reservoirs and a tectonic province boundary relate - clues to possible giant fields: *Oil & Gas Journal*, Jan. 11, 1999, p. 61-66.

Shurr, G.W., L.O. Anna, and J.A. Peterson, 1989, Zuni sequence in Williston Basin – evidence for Mesozoic paleotectonism: *AAPG Bulletin*, v. 73, p. 67-87.

Shurr, G.W., and L.M. Monson, 1995, *Tectonic setting and paleotectonic history of the Fort Peck Reservation in northeastern Montana, in L.D. Hunter and R.A. Schalla, eds. Seventh International Williston Basin Symposium, Montana Geological Society, pp. 11-22.*

Swenson, R.E., 1967, Trap mechanics in Nisku Formation in northeastern Montana: *AAPG Bulletin*, no. 10, p. 1948-1958.

APPENDICES

APPENDIX A: Jack Land Report

Magnetic Susceptibility Survey DOE Area 1: Smoke Creek Northeastern Montana

John P. Land

J.P. Land Associates, Inc.
Houston, Texas

ABSTRACT

To determine the oil and gas potential of the area immediate to a large magnetic anomaly in the Smoke Creek sector of northeastern Montana, various geological, geophysical and geochemical methods are being applied. This report presents the results of a 300 square mile survey involving two geophysical methods, Magnetic Susceptibility and Micromagnetics, testing their applicability to exploring the region.

INTRODUCTION

The upward migration of light hydrocarbons escaping from reservoirs triggers geochemical processes which in turn change the physical properties of the overlying near-surface rocks, changes in their properties such as density, conductivity and magnetism that are geophysically measurable.

The magnetic susceptibility of a rock type is the measure of its ability to be magnetized. Depending on the chemical elements and processes within a gas migration chimney, the near-surface formations develop magnetic susceptibilities different from their immediate surroundings. Such differences are recognizable by the magnetic and magnetic susceptibility survey methods (Foote (1987, 1988 & 1996), Land (1991 & 1999) and Saunders et al (1999).

The large Smoke Creek magnetic anomaly, the subject of this study, was previously mapped by an airborne magnetic survey designed only to map basement topography and structure. To now resolve near-surface, high frequency magnetic anomalies that have the potential of indicating alteration related to hydrocarbon seepage, magnetic susceptibility measurements were made over the entire area. To assist the interpretation of those measurements and to demonstrate the influence of magnetic susceptibility on magnetic anomaly amplitudes, the Earth's magnetic field was measured at the same stations along key traverses.

PROCEDURES

Approximately 1100 magnetic susceptibility measurements were taken along roads and trails at a 0.2 mile interval using a KT-9 digital magnetic susceptibility meter. The Earth's magnetic field was measured at 200 of those locations using a Geometrics proton precession magnetometer. The same type of magnetometer was used at a centrally located base station to continually record the diurnal variations of the Earth's magnetic field. The base station readings were then subtracted from the rover magnetometer readings to produce final total intensity values.

Magnetic susceptibility values were measured along all traverses of the survey. A group of readings were taken at each station and averaged to ensure the validity of that station's value. Magnetic readings were made along several strategic traverses. Enclosures 2 and 3 show both types of measured values along Lines 134 and 236.

Magnetic susceptibility and magnetic profiles were plotted at scales allowing their detailed inspection and interpretation. To increase the visibility of near-surface magnetic responses, events caused by shallow structure and locally anomalous rock properties, a "regional subtractor", a suppressed version of the low frequency total magnetic intensity's curvature, was subtracted from each magnetic value. Opposing arrows designate the approximate limits of anomalous magnetic and magnetic susceptibility zones.

Near-surface anomalies, whether gravity, magnetic, magnetic susceptibility or what, are not simple residual "highs" or "lows". Instead, they are irregularly-surfaced collections of positive and negative high frequency events that vary in how far they depart from "background". The greater the departure (amplitude), the greater the considered potential significance of the anomaly.

To assign priority to each magnetic susceptibility anomaly, the dynamic range of amplitudes along each traverse was determined. For each traverse, values in the lowest 25 percent of the maximum were considered background. The 25 to 49 percentile was considered low priority, the 50 to 74 percentile was considered moderate and the uppermost 25 percentile considered significant.

Enclosure 1 shows the traverse location of magnetic susceptibility anomalies. Light to heavy line weights represent the three percentile groups. Line to line correlation shapes anomalous segments into areas deemed worthy of further investigation.

Hexagons numbered 1 through 8 set apart the eight most prospective anomalies. Their number is the suggested order in which they should be investigated.

OBSERVATIONS

ENCLOSURE 1

Magnetic susceptibility anomalies varying in size and amplitude occupy most of the survey area. There appear to be a greater concentration of anomalies immediate to the outlined deep-seated magnetic anomaly as was the case with curvilinear Landsat anomalies mapped by Shurr.

ENCLOSURES 2 & 3

The generally smooth flow of the total intensity magnetic values suggests that the data is of good quality and free of cultural noise and diurnal disturbances.

Most of the near-surface anomalies of the magnetic profiles correspond well with high amplitude sectors of the susceptibility profiles.

CONCLUSIONS

Past experience in other survey areas has shown there to be a close correlation between higher amplitude magnetic susceptibility anomalies and hydrocarbon and microbial anomalies.

The higher amplitude magnetic susceptibility zones of this survey, those numbered 1 thru 8, are thus considered worthy of further investigation that will determine if any of the features are associated with active hydrocarbon seepage.

The number of susceptibility anomalies and near-surface magnetic anomalies immediate to the deep-seated Smoke Creek anomaly suggest an area where the sedimentary section is structurally disturbed and unstable due to basement relief created by an igneous intrusion that lifted up or broke through pre-existing basement.

RECOMMENDATIONS

If hydrocarbon seepage is found associated with the priority anomalies of this report, an airborne micromagnetic survey of the area is recommended. Such a survey can efficiently provide a solid foundation for the systematic exploration of an area. A regional perspective is produced of the structural grain and alteration zones having the potential of not only indicating hydrocarbon seepage but also locally anomalous velocities, information vital to the optimum processing and interpretation of seismic data.

A survey grid of lines and tie lines at 0.25 mile intervals should also develop a more detailed picture of the deep structural setting of the Smoke Creek magnetic anomaly and insight into the geology of other features such as Landsat linears and curvilinears. Such a survey in the Smoke Creek area is expected to demonstrate the potential and cost

effectiveness of the method for the further reconnaissance of the remainder of the Fort Peck Reservation.

Respectfully submitted,

*J.P. Land
May 6, 2002*

REFERENCES

*Foote, R.S., 1987, Correlations of borehole rock magnetic properties with oil and gas producing areas: Association of Petroleum Geochemical Explorationists Bulletin, **3**, 114-134.*

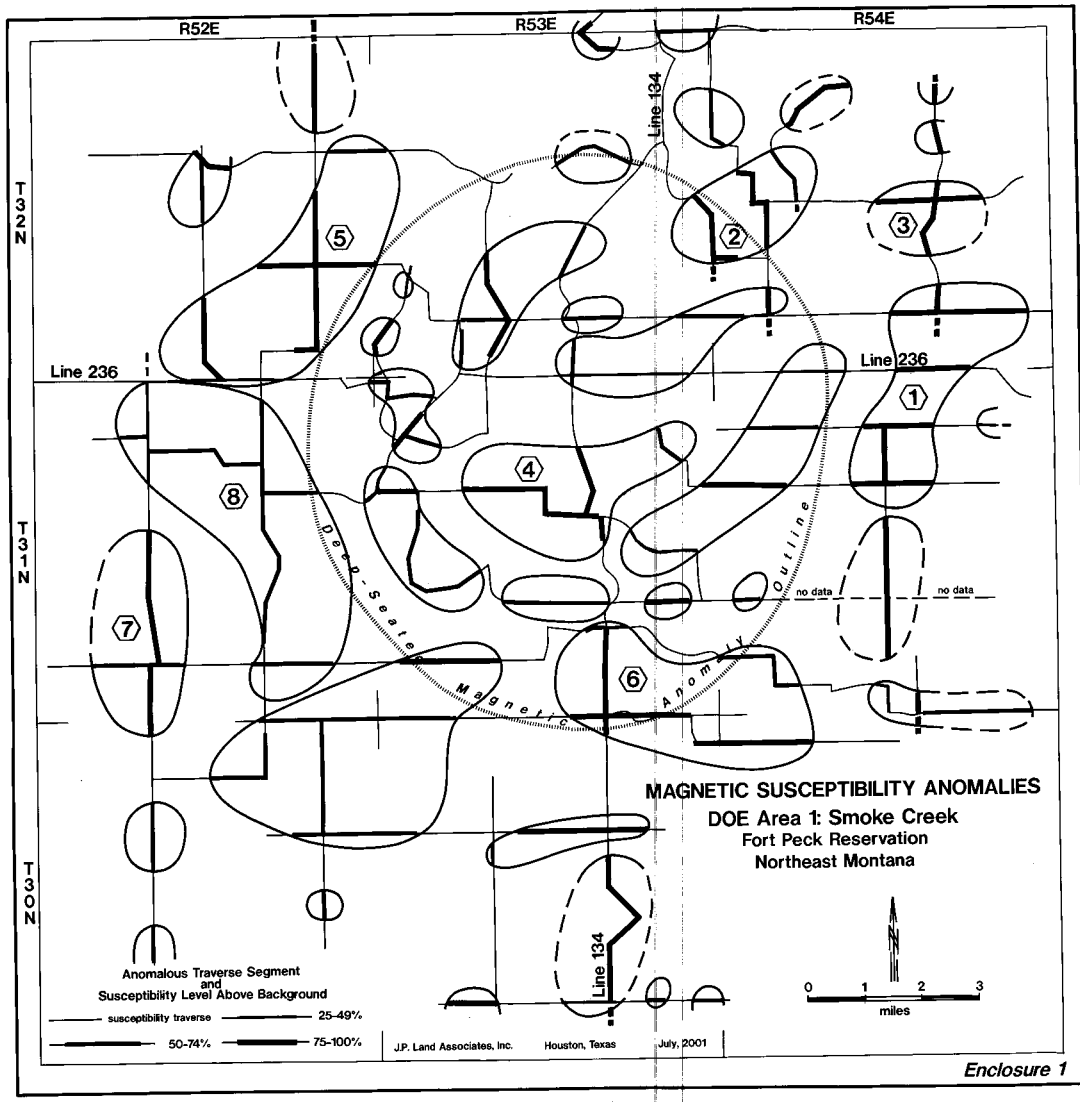
*Foote, R.S., 1988, Correlations of oil and gas producing areas with magnetic properties of the upper rock column, eastern Colorado: Association of Petroleum Geochemical Exploratonists, **4**, 47-61.*

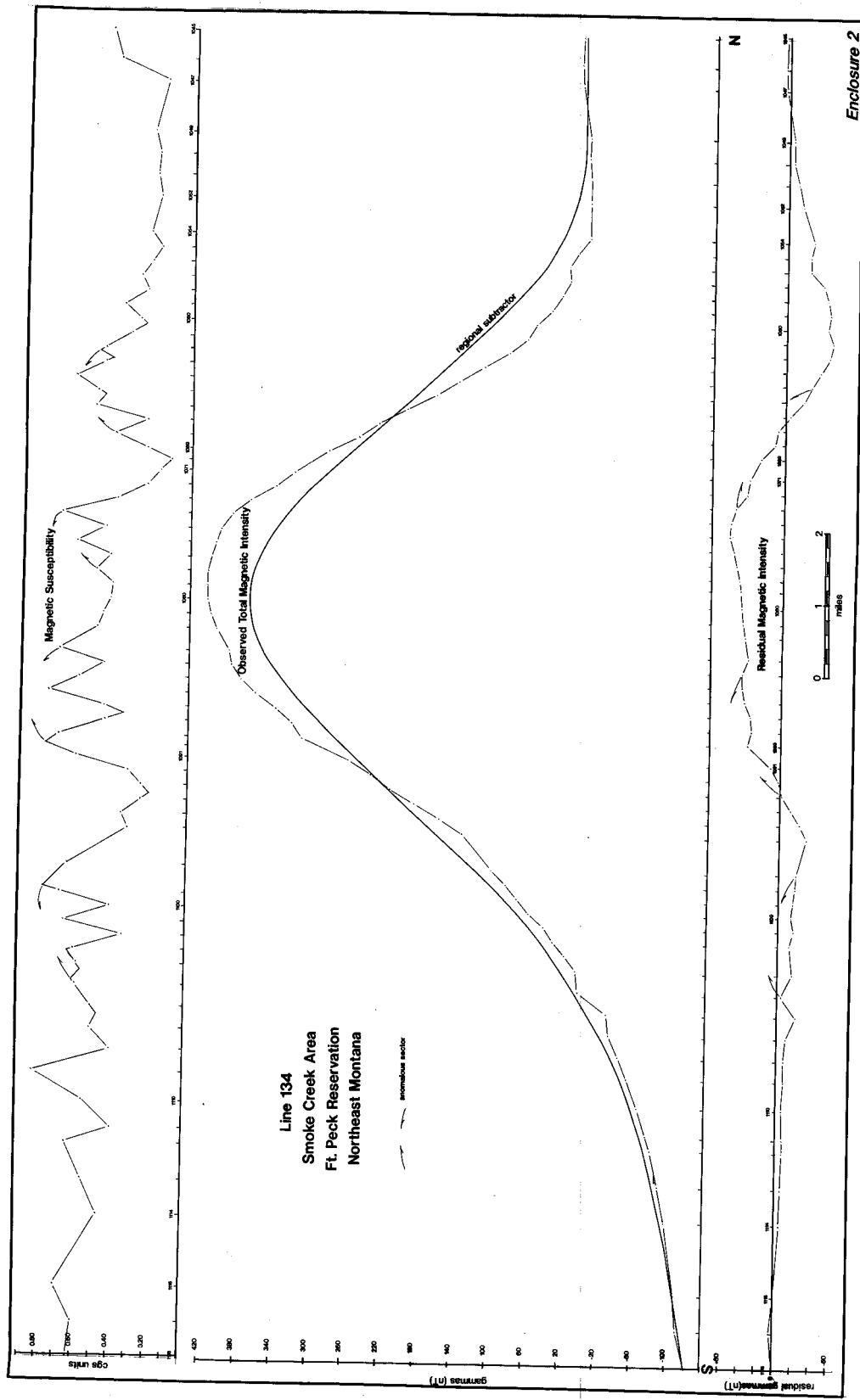
*Foote, R.S., 1996, Relationship of near-surface magnetic anomalies to oil and gas producing areas, in D. Schumacher and M.A. Abrams, eds., *Hydrocarbon migration and its near-surface expression: AAPG Memoir 66*, 107-122.*

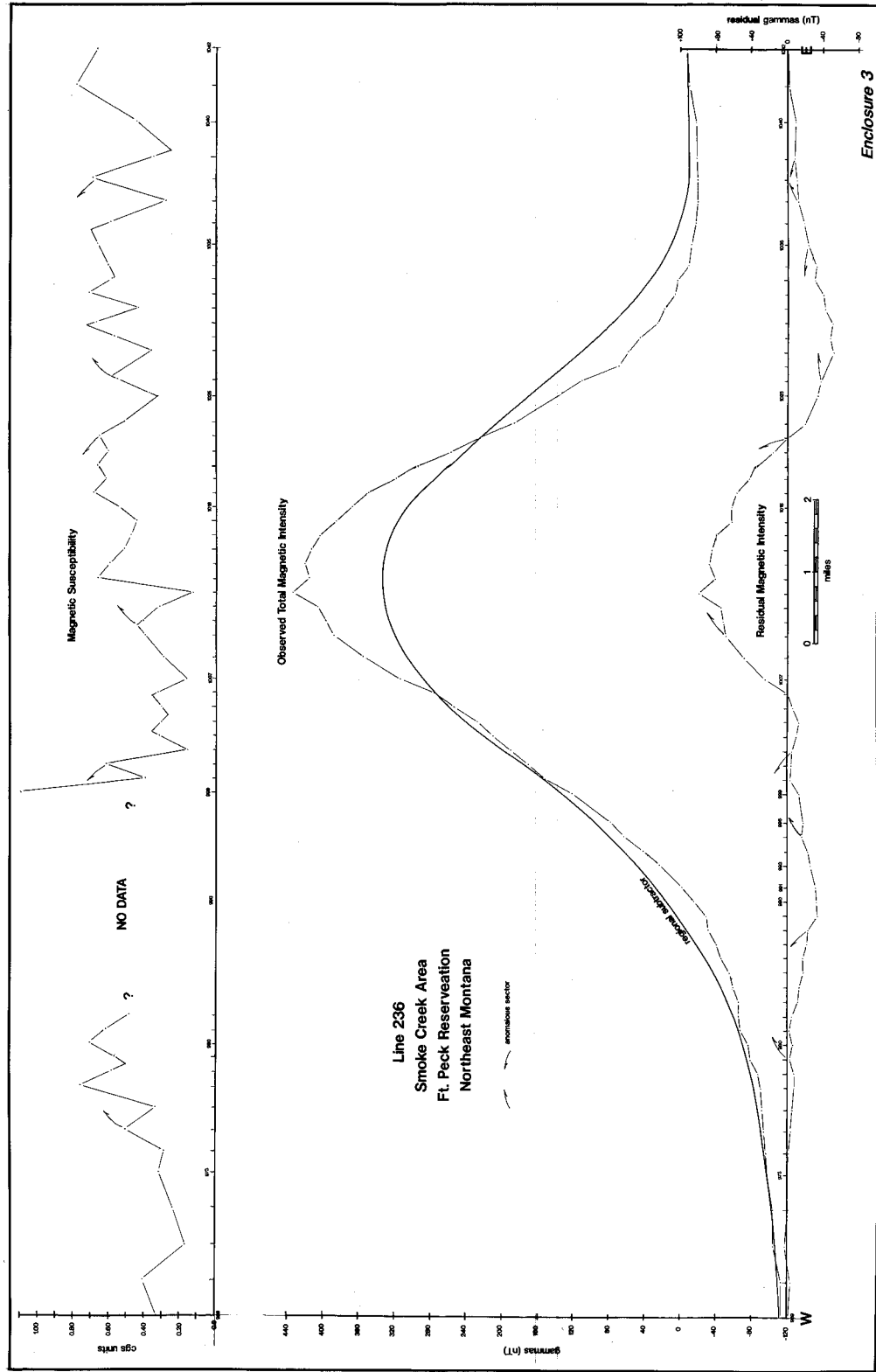
*Land, J.P., 1991, A comparison of micromagnetic and surface geochemical survey results: Association of Petroleum Geochemical Explorationists, **1**, 12-35.*

Land, J.P., 1999, Geophysical evidence of anomalous near-surface rock properties associated with hydrocarbon seepage, the significance and potential (Abstract): Annual meeting of the AAPG, San Antonio, April 1999.

*Saunders, D.F., K.R. Burson, and C.K. Thompson, 1999, Model for hydrocarbon microseepage and related near-surface alterations: AAPG Bulletin, **83**, no. 1, 170-185.*







Appendix B

PRELIMINARY INTERPRETATIONS OF HYDROCARBON GAS CHIMNEYS IN THE SMOKE CREEK STUDY AREA

*A
Report Submitted
to
Minerals Resource Office
Fort Peck Tribes
Poplar, MT*

by

*George W. Shurr
GeoShurr Resources, LLC
Ellsworth, MN*

56129

*George W. Shurr
Rt 1, Box 91-A
Ellsworth, MN*

*507.967.2156
www.geoshurr.com*

geoshurr@prairie.lakes.com

Lawrence M. Monson
FINAL Report 15192R04

Page 89

6/30/2003

EXECUTIVE SUMMARY

The Smoke Creek Study Area is Area 1 of the investigations funded by DOE for the Fort Peck Tribes. Initial pilot studies in other parts of the reservation tested the effectiveness of various surface techniques in mapping hydrocarbon seeps. The best techniques have subsequently been used to study Landsat curvilinears in the vicinity of the Smoke Creek Aeromagnetic Anomaly. It appears that some of the curvilinears correspond with chimneys marking hydrocarbon gas seeps. However, the relationship is complicated by relatively large diagenetic slabs or caps that influence gas migration near the surface.

This report presents initial interpretations of the large amount of data accumulated in the DOE investigations. An initial review of literature and of previous work done on the Reservation provides background on flux mechanisms, plumbing geometries, and flux sources in the Smoke Creek Study Area. This establishes the geologic framework. Three main types of data are employed: Landsat remote sensing, magnetic susceptibility measurements, and soil and head gas observations. These data are summarized in the folios of maps in the DOE reports that document large and small scale patterns in the Smoke Creek Study Area.

Large scale map patterns are related to the geologic framework. Structural domains in the study area are defined by lineament zones and map patterns are arranged around the centrally located aeromagnetic anomaly. Landsat curvilinears are compared with contour maps of magnetic susceptibility values and with anomalies interpreted from profiles of magnetic susceptibility. Small scale data sets focus on three local areas: Area 26, Smoke Creek Core, and Lobo West. Soil gas, head gas, and non-gas surface techniques demonstrate relationships between seeps, diagenetically altered slabs of soil and curvilinears in the three local areas.

The lineament domains correspond with contrasting plumbing geometries. The central aeromagnetic anomaly marks a large and complex source of hydrocarbon flux that has progressively less influence toward the periphery of the study area. Although further investigations are needed to document currently active seeps and quantify the proposed patterns, some exploration implications are clear. The best prospecting potential is in the simple flux sources arranged around the central aeromagnetic anomaly; hydrocarbon sources have probably been depleted in the complex central area.

INTRODUCTION

The Fort Peck Tribe has received DOE funding to “assess hydrocarbon seepage on the Reservation utilizing surface exploration techniques”. During Phase I (Monson, 2000 and 2001) a variety of geochemical and geophysical techniques were tested in several small study areas. Phase II (Monson, 2002) employs the most successful of these techniques to investigate the nature of Landsat curvilinears mapped in and around the Smoke Creek Aeromagnetic Anomaly.

A significant subsurface body is located beneath the large aeromagnetic anomaly. Major stratigraphic and structural patterns reflect the location and Landsat curvilinears are concentrated in the area. It has been suggested (Monson and Shurr, 1993), that the

curvilinears are the surface expression of diagenetic chimneys formed by hydrocarbon seeps. A large number of seeps apparently formed in the vicinity of the subsurface body that has expression as the aeromagnetic anomaly.

A reconnaissance magnetic susceptibility survey has been carried out over the entire Smoke Creek Study Area. These data are summarized in several different formats that can be used to assess the relationships between Landsat linears, magnetic susceptibility anomalies, and hydrocarbon seeps. In addition, soil gas, head gas, and several non-gas techniques are employed in limited areas to document hydrocarbon seeps. The data collection has continued into the fall of 2002.

This report describes the fundamental geologic framework through which the various data sets are distributed. General patterns are identified in a semi-quantitative manner and are related to the geologic framework. Preliminary interpretations are made regarding the sources, migration paths, and flux history for the postulated hydrocarbon seeps.

BACKGROUND ON SURFACE EXPLORATION

Flux Mechanisms

Flux mechanisms are of fundamental importance for surface exploration techniques. Although seismic images of discrete gas chimneys are becoming available (for example, Story, 2002), the exact nature of the flux mechanisms is still not well understood.

Movement as buoyant microbubbles, transport by water, and diffusion are all compared in a recent review of field data and quantitative modeling (Klusman and Saeed, 1996). Movement as buoyant microbubbles is selected as the best explanation for common characteristics of surface anomalies including: 1) position directly over the flux source, 2) sharp definition of the sides, and 3) rapid disappearance after depletion by production. Diffusion has been proposed as most important (Kroos and Leythaeuser, 1996), but this is based mainly on modeling rather than field data.

Discrete droplets or buoyant microbubbles are also favored in an exhaustive review of hydrocarbon migration into surface anomalies (Matthews, 1996a). This review emphasizes the importance of fracture networks that may have more control on macroseeps than on microseeps. For microseeps, capillary flow in the narrow pore throats between mineral grains in mudstone is suggested to account for observed high flow rates and fractures are possibly less significant (Clayton and Dando, 1996). Fast, vertical flux is believed to be influenced by permeability and pressure (Jones and Burtell, 1996). General theoretical considerations (Toth, 1996) and specific field examples (Rostron and Toth, 1996; Holysh and Toth, 1996) clearly demonstrate the potential influence of ground water flow on hydrocarbon flux.

Plumbing Geometries

The distribution and geometry of surface anomalies depend upon the migration route of moving fluids. Microseeps of hydrocarbon gases may represent simple vertical

migration from a buried source. But, macroseeps may involve ground water movement and fracture networks with distinctive geometries. In particular, the plumbing geometries are related to corridors of fractures that characterize lineament zones.

Patterns of high value and low value data stations reflect lineament geometry (Figure 1). In a discussion of the design of sampling programs, Matthews (1996b) illustrates that the majority of high value stations are inside the lineament zone and most of the low value stations are outside. However, some low values are located between fractures within the lineament zone and some high values are found outside the lineament zone. He believes that the background values outside the lineament zone are mainly secondary biogenic gas or are the result of migration in solution and/or diffusion. Both of these migration mechanisms are less dependent upon distinctive plumbing systems and involve horizontal as well as vertical migration. The association of localized anomalies with dominant vertical migration and of more diffuse, widespread anomalies with horizontal migration have also been used as components of a classification of seep styles (Thrasher, et al., 1996). However, this classification is based on crude oil seeps, as well as gas seeps that constitute surface anomalies.

Plumbing geometries that influence fluid movement have been described for several areas in the Northern Great Plains (Shurr and Watkins, 1989). In eastern Montana, fracture corridors have been mapped on Landsat images as lineament zones on and around Cedar Creek Anticline (Shurr 2000). Individual linear features mark specific faults and monoclines along the trend of the anticline (1 through 8, Figure 2) and long linear stream segments perpendicular to the anticline (A and B, Figure 2). At the southeastern end of the anticline, the narrow northwest trending lineament zone intersects a wider lineament zone trending northeast.

At the intersection of the Landsat lineament zones, high altitude photographs (NHAP) are used to map linear features within four separate areas of 9 sq mi each (Figure 3). Area A in the northeast lineament zone has a dominant mode to the northwest but includes a small northeast mode. Area B in the northwest lineament zone has a strong northwest mode. Area C, adjacent to the northeast zone, has smaller modes to both the northwest and northeast. Area D, outside all lineament zones, has a northwest mode, but the azimuths show more variability; the area also has the shortest individual linear features. The largest number (65) of NHAP linear features is in area C which may represent a damage zone adjacent to the northeast lineament zone. Area B, near the intersection of the two lineament zones, has the second greatest number (56) of linear features. Areas A and D have 46 and 45 linear features respectively.

Fluid flow in the northeast lineament zone is suggested by displacement of production patterns down-flow from the structural crests of shallow gas fields. This pattern near the intersection of lineament zones at the southeast end of Cedar Creek Anticline is illustrated in Figure 4. A similar pattern is shown at Little Missouri Field (marked by the star, Figure 2) within the northeast lineament zone in North Dakota (Shurr, 2001).

Landsat lineament zones mapped on Fort Peck (Figure 5) have been shown to subdivide the reservation into a series of structural blocks stepping down off Bowdoin Dome eastward into the Williston Basin (Monson and Lund, 1991). The lineament zones exerted paleotectonic control on patterns of erosion and deposition; post-depositional tectonism along the zones has expression in seismic sections (Shurr and Monson, 1995).

In the eastern part of the reservation, the Smoke Creek Aeromagnetic Anomaly is located at the intersection of the northeast trending Big Muddy Lineament Zone and the northwest trending Poplar River Lineament Zone. A constellation of curvilinears mapped on Landsat images in this area suggest that the central aeromagnetic anomaly is the source of fluid flux that produced a large number of diagenetic chimneys (Monson and Shurr, 1993).

Flux Sources

The Smoke Creek Aeromagnetic Anomaly is the largest and most complex flux source included in the DOE study areas (Monson and Shurr, in review). The smallest and most simple flux source is associated with production in the Palomino Oil Field near the margin of the northwest trending Tule Creek Lineament Zone. The Wicape Prospect Area has a flux source of intermediate size and complexity and is located on the southwestern margin of the Poplar River Lineament Zone which trends northwest.

The Smoke Creek Aeromagnetic Anomaly is mainly located in the extensional corner that results from strike-slip displacements on the intersecting lineament zones (Figure 6). Northeast lineament zones on the Fort Peck Reservation including the Big Muddy Lineament Zone, have been interpreted to have left-lateral displacements and northwest lineament zones, such as the Poplar River Lineament Zone, have right-lateral displacement (Shurr, 1991). Although the large magnetic anomaly has been suggested to be an astrobleme, its position at the extensional corner of intersecting strike-slip zones is consistent with the location of an igneous intrusion. Thus, the tectonic setting would appear to favor the interpretation employed in initial aeromagnetic modeling: the Smoke Creek Aeromagnetic Anomaly is an ultramafic body, perhaps a lopolith, intruded into the crystalline basement.

If the intrusion is part of the Tertiary igneous activity that is extensive in Montana west of the Fort Peck Reservation, then the associated pulse of thermal energy and fluids could have produced some of the postulated diagenetic chimneys. In addition, as the thermal and fluid perturbation moved upward through the sedimentary section, it would greatly influence movement of both ground water and hydrocarbon gases. As a consequence, hydrocarbon traps located near the intrusion or those associated with the lineament zones may have experienced complicated migration histories. Regardless of this speculation, the large number of curvilinears and their distribution suggests multiple flux sources over a large area surrounding the central Smoke Creek Aeromagnetic Anomaly.

Summary

In the Smoke Creek area, lineament zones and the central aeromagnetic anomaly have influenced the flux mechanisms, plumbing geometries, and flux sources for surface anomalies. Within the lineament zones, macroseepage and ground water movement associated with fracture networks controlled hydrocarbon migration. Areas outside the lineament zones were probably dominated by vertical microseepage. Consequently, patterns of surface anomalies might be expected to be different inside and outside lineament zones. Similarly, anomaly patterns inside and outside the central

aeromagnetic anomaly should be different. This would be the result of contrasting hydrocarbon migration and water movement over the flux source versus farther away. In general, the lineament zones and central aeromagnetic anomaly provide a useful geologic subdivision of the Smoke Creek study area. Distinctive patterns in the several types of data are found in each of the subdivisions.

DATA TYPES

Three main types of data are integrated in this report: Landsat remote sensing, magnetic susceptibility values, and surface measurements of gas and other seep indicators. These three data types represent a gradation from large area coverage (Landsat) down to more localized data sets (surface measurements). Original descriptions of data types, compilations of specific values, and synoptic displays of data patterns are all found in the DOE reports, especially Monson (2002).

Landsat

Remote sensing data available on Landsat images has been used to map lineament zones on Fort Peck Reservation (Shurr and Monson, 1995). This work mainly involved simple observation of linear features. More sophisticated digital analysis could be used to classify surface spectral observations from Landsat data in an attempt to map hydrocarbon anomalies (for example, Mello, et al., 1996). Hyperspectral data could probably be handled in a similar way on the Reservation. In the Smoke Creek Study Area, curvilinear features mapped on Landsat data have been related to diagenetic chimneys produced by hydrocarbon seeps (Monson and Shurr, 1993).

Landsat curvilinears that are small circles, are tonal patterns probably associated with variations in vegetation and moisture. These small circles are good candidates for the top of diagenetic chimneys directly above small flux sources. The hydrocarbon flux is probably currently active and consequently the history, as well as the geometry, of the chimney is relatively simple. Small and simple curvilinears might be expected to correspond with individual soil and head gas anomalies.

Large Landsat curvilinears or complexes of large and small circles are, in contrast, older and more complicated. These larger features are usually associated with specific landscape elements, such as curved drainage segments or upland areas, as well as patterns in vegetation and moisture. Large and complex curvilinears are probably associated with relatively extensive areas of diagenetically altered soil and consequently may show an association with magnetic susceptibility anomalies.

Magnetic Susceptibility

Measurements of magnetic susceptibility were made at almost 1200 stations distributed along profiles throughout the Smoke Creek Study Area. Over the nine township area, this represents a sample density of approximately 4 stations per square mile. This sample density is considerably smaller than those used for soil and head gas

surveys, but the magnetic susceptibility profiles do cover most of the study area and provide an ideal reconnaissance survey.

The magnetic susceptibility data are displayed in several different ways. Individual profiles are plotted and anomalous values are interpreted relative to the backgrounds visible within each profile. The map produced by J.P. Land Associates, Inc summarizes these individual profile analyses by outlining anomalous traverse segments. The resulting anomalies are displayed as a map showing irregular "blobs".

In contrast, the contour maps produced in-house at the Ft Peck Reservation provide a synoptic overview of magnetic susceptibility values over the entire study area. The objective, machine contouring extrapolates values between the individual measurement stations. This provides an estimate of the magnetic susceptibility in all parts of the area. Actually, the most useful machine contoured map employs a ratio to an anomaly value defined as 1.5 times the mean for the total data set. Both types of magnetic susceptibility anomalies, i.e. based on profile analyses and based on machine contouring, will be compared with curvilinears mapped on Landsat.

Soil and Head Gas

Soil and head gas surveys were initially done in three localized areas in the Smoke Creek Study Area. All three areas have clear expression on the machine contoured map of ratios to the defined anomaly value. In addition, all three fall within large irregular-shaped anomalies interpreted from the profile analyses.

Area 26 is in the northeastern part of the Smoke Creek Study Area. Sample densities of the soil and head gas surveys are comparable to other surveys done on the Reservation and the data sets are amenable to mapping. In addition to the soil and head gas measurements, Eh, pH, conductivity, microbial data, and iodine techniques were employed.

The Smoke Creek Core is in the central part of the study area. Data are not adequate to display as maps, so profiles are used for basically the same soil gas, head gas, and non-gas data employed in Area 26. The profile in the Smoke Creek Core is important because it is located in an area with many Landsat curvilinears.

The Lobo West area is in the eastern part of the Smoke Creek Study Area. Samples are distributed along a single profile and the data sets are basically the same as in the Smoke Creek Core profile. In both areas, the soil gas data had less validity than the head gas data.

LARGE-SCALE MAP PATTERNS

Intersecting lineament zones subdivide the Smoke Creek Study Area into four separate and discrete structural domains (1-4, Figure 7). Plumbing geometries and flux mechanisms are potentially different in each domain because the fracture patterns and densities are probably different. Domain 1 is located outside the lineament zones; Domain 2 is in the northeast-trending Big Muddy Lineament Zone; Domain 3 corresponds with the lineament zone intersection; and Domain 4 is in the northwest-trending Poplar River Lineament Zone.

The large, central Smoke Creek Aeromagnetic Anomaly subdivides the area on the basis of proximity to flux source (Figure 7). The area inside the circular aeromagnetic anomaly is located directly above the large flux source. Areas outside the central anomaly have more complex migration paths influenced by the lineament zones and are also farther from the primary flux source. Before immersing in the data details, a quick overview summarizes where we are headed.

Overview

Large scale map patterns for the several different data sets reflect the flux source and structural domains. However, comparisons must take into account differences in the size of areas inside and outside the central anomaly and also in each of the four domains (Figure 7). The area shown for Domain 2 does not include most of T 30 N, R 54 E because relatively little magnetic susceptibility data were collected in this southeastern corner of the study area. More accurate estimates of area could obviously be made on larger maps employing digital techniques. However, the relative size estimates shown in Figure 7 and Table 1 are adequate for the purpose of normalizing all numerical observations as values per square mile. Actual counts of the various attributes are tabled in Appendix I.

Inside the central anomaly, there are more Landsat curvilinears and more bright spots marking relatively large anomaly values on the magnetic susceptibility ratio map, when compared with outside areas. The area inside the anomaly also shows more linear miles of anomalous magnetic susceptibility profile analyses and more curvilinears touching an anomalous profile segment. Large portions of the area inside the central anomaly have been diagenetically altered because they are directly over the flux source. However, relationships between curvilinears and magnetic susceptibility anomalies are fairly complicated.

Domains 1 and 3 are located outside the lineament zones and within the intersection of lineament zones, respectively. Domain 1 has the maximum number of curvilinears and Domain 3 has the minimum number of curvilinears. However, Domain 3 has the largest numbers of curvilinears that correspond with a bright spot on the magnetic susceptibility ratio map. Domain 1 has the maximum number of linear miles on non-anomalous magnetic susceptibility profiles and Domain 3 has the minimum number of non anomalous profile miles. It appears that migration pathways producing curvilinears and magnetic susceptibility anomalies are different in these two domains. Domain 1 with no lineament zones favors flux that produces curvilinears, while Domain 3 at the lineament zone intersection shows a correspondence of magnetic susceptibility anomalies and curvilinears.

Domains 2 and 4 are located in the northeast and northwest lineament zones, respectively. Both show about the same number of curvilinears and both have minimum numbers of curvilinears associated with magnetic susceptibility ratio bright spots. Both domains have more miles of anomalous magnetic susceptibility profile than of non-anomalous profile. However, Domain 2 has the maximum number of anomalous profile miles and has more curvilinears touching those anomalous profile segments. Thus, there appear to be some plumbing differences between the northeast and northwest lineament zones.

This overview is intended to summarize patterns and provide some preliminary interpretations. We will now proceed with a discussion of all the details of specific data sets. In addition to the summary Table 1 and figures for each data set, the specific numbers appear in Appendix 1. However, beyond these general descriptive numbers, there are some distinctive qualitative map patterns that are discussed in each data set. The four structural domains and the central aeromagnetic anomaly provide a framework for all of the descriptions.

Magnetic Susceptibility Contour Maps and Landsat Curvilinears

Landsat curvilinears on Fort Peck Reservation were mapped and described in the early nineties (Shurr, 1992). As a part of the recent DOE work, contour maps of magnetic susceptibility were prepared by the staff of the Fort Peck Tribes. The numbers used to describe these data sets are summarized in Table 1 and in Appendix Table A. These are not particularly rigorous descriptions, but do provide a quasi-quantitative basis for comparisons.

Landsat curvilinears are displayed with lineament zones and the central aeromagnetic anomaly outline in Figure 8. There is a clear clustering of curvilinears inside the central aeromagnetic outline. The largest number of curvilinears per sq mi is inside the aeromagnetic anomaly outline, but Domain 1 with no lineament zones runs a close second (Table 1). Domain 3 at the lineament intersection has fewer curvilinears than Domains 2 and 4.

The red outlines on Figure 8 correspond with specific local anomalies that emerge from contouring the magnetic susceptibility ratio. These appear as “bright spots” of yellow and red on an image dominated by the cooler blue and green colors (Monson, 2002, p. 53). Although the number of bright spots is small (see Appendix Table A), there are some interesting patterns. Again, the largest number of bright spots per sq mi is found within the central aeromagnetic anomaly outline; the rest of the values are all about the same (Table 1). However, Domain 3 is distinctive. Although it has the fewest curvilinears per sq mi, there is a clear correspondence with specific bright spots.

A good synoptic summary of magnetic susceptibility values is provided by the contour map shown in Figure 9. Lineament zones, the central aeromagnetic outline, and Landsat curvilinears are also displayed. Inside the aeromagnetic outline, magnetic susceptibility values are generally low; the blue contrasts with more extensive green showing higher values outside the outline. Similarly, Domains 2 and 4 in the lineament zones seem to be dominated by low value blue colors. Domain 3 marking the intersection has mostly higher value green. The less complex Wicape Prospect area also shows correspondence of magnetic susceptibility patterns and the Poplar River Lineament Zone. At Palomino, the distribution of control points doesn’t provide an expression of the Tule Creek Lineament Zone.

The colors provide a generalized impression of data variation, but the distribution of curvilinears relative to the color patterns is also significant (Figure 9). Within the central anomaly, most small curvilinears are located within a field of blue. The central green area is marked by a large curvilinear complex. Domains 1 and 4 seem to have most curvilinears within areas of low value blue. In contrast, Domains 2 and 3 have small circles in higher value green areas, but clustered around the margins of discrete

blue areas. These observations may relate to the timing of the fluxes that produced the curvilinears and the magnetic susceptibility anomalies.

Magnetic Susceptibility Profiles and Landsat Curvilinears

Magnetic susceptibility data were not only contoured, but were also analyzed in individual traverses or profiles. Anomalous line segments were then used to outline fairly extensive anomalies (Figure 10). The resulting anomaly patterns are clearly subjective, although the contractor does have extensive experience in these profile analyses techniques. Still, the contour maps produced by the Tribes do seem to provide a more objective synopsis of magnetic susceptibility values through the study area.

The area inside the central aeromagnetic anomaly outline has the largest number of anomalous linear miles per sq mi and Domain 3 has the smallest number (Table 1). Domain 1 has the largest number of non-anomalous linear miles per sq mi; it is the only subdivision that has more non-anomalous linear miles than anomalous linear miles. Domains 2 and 4 both have more anomalous than non-anomalous linear miles and have comparable values of anomalous linear miles. The actual numbers used for the summary table are listed in Appendix Table B.

Magnetic susceptibility traverses and the anomalies based on profile analyses are plotted with Landsat curvilinears in Figure 11. Again, the area inside central aeromagnetic outline has the greatest number of curvilinears touching an anomalous line segment (Table 1). Domains 1 and 3 both have equal numbers of curvilinears touching and not touching anomalous line segments. Domains 2 and 4 do show differences between the northeast and northwest lineament zones. Domain 4 has the smallest number of curvilinears touching anomalous line segments and the largest number not touching an anomalous line segment. Curvilinears in the northwest lineament zone do not seem to be closely associated with magnetic susceptibility anomalies extracted from profile analyses.

The distinctive expression of Domain 4 is also demonstrated when the anomaly outlines are used, rather than the constituent line segments. Domain 4 has the fewest anomalies and the fewest anomalies that have associated curvilinears (Table 1). The area inside the central aeromagnetic anomaly outline has the most anomalies, but Domain 1 runs a close second. Domain 3 anomalies have the highest number with associated curvilinears. The specific counts and calculations that are summarized in Table 1 are found in Appendix Table C. In addition, there appears to be a qualitative pattern in the susceptibility anomalies and curvilinears.

Within the outline of the central aeromagnetic anomaly, curvilinears seem to be located outside the outlines of the susceptibility anomalies (Figure 11). This is also reflected in the difference between total anomalies and total anomalies with curvilinears (Table 1). Outside the central aeromagnetic outline, magnetic susceptibility anomalies are larger and less closely packed. In this second zone, the susceptibility anomalies tend to have multiple curvilinears within their outlines. Finally, at the margins of the study area there is a third zone that is characterized by a relatively close correspondence between small susceptibility anomalies and small, individual curvilinears. These three zones are somewhat similar to patterns of color on the machine contoured map with

superimposed curvilinears (Figure 9). The three zones distributed relative to the flux source are sketched as a cartoon in Figure 12.

SMALL-SCALE DATA SETS

Landsat remote sensing and magnetic susceptibility data basically cover the entire Smoke Creek Study Area. These large-scale data are augmented by more detailed measurements of soil gas, head gas, and indirect detection variables. Three areas have the close spaced sampling (see Figure 8): Area 26, Smoke Creek Core, and Lobo West. Work completed in the three areas of detailed sampling is discussed below in the context of the large scale patterns. Essentially, the preliminary work in these three areas constitutes a pilot study for the extensive field sampling carried out during the fall of 2002. Results of the most recent data collection will eventually need to be integrated with the large scale patterns described in this report.

Area 26

Area 26 is located in Domain 1 near the boundary with the northwest lineament zone. A relatively complete program of soil gas, head gas, and indirect detection measurements was carried out on a sampling grid that allowed contour maps to be generated. There is good agreement between the location of the magnetic susceptibility anomaly (Monson, 2002, p. 71) and high soil gas propane (Monson, 2002, p. 82), although high soil gas values extend eastward into the NE 1/4 of section 15. All of the soil gas patterns are similar to the propane map. Head gas propane (p. 87) and the other head gas measurements also show good agreement with the magnetic susceptibility anomaly. In addition there is a head gas high in the SW 1/4 of section 15 that also has expression as an Eh low (Monson, 2002, p. 90).

The Area 26 magnetic susceptibility anomaly in section 15 is located at the open northwest end of a curvilinear arc that is shown on all the maps cited in the previous paragraph. In addition, the head gas anomaly in the SW 1/4 of section 15 lies directly on the end of the arc. The arc also perfectly outlines an iodine anomaly (Monson, 2002, p. 94). These relative locations are sketched in Figure 13. The close association of a curvilinear, magnetic susceptibility anomaly and a variety of detailed soil and head gas anomalies is significant. Area 26 probably represents a small and simple flux source that is currently active. The location in Domain 1, where there is no lineament zone, and away from the large central magnetic anomaly is also significant in terms of the general pattern of the Smoke Creek Study Area (see Figure 12).

Smoke Creek Core

The Smoke Creek Core area is located in Domain 2, at the extensional corner within the northeast trending lineament zone. This magnetic susceptibility anomaly is near an extremely complex area of curvilinears and is near the center of the central aeromagnetic anomaly outline. Sampling was only done along a single profile that corresponds with line 239 of the magnetic susceptibility data collection. Head gas

propane and magnetic susceptibility values are plotted for comparison in Figure 14. In general, head gas values are low and do not track the magnetic susceptibility data. However, there are some important trends.

A head gas high exactly corresponds with a high magnetic susceptibility value at sample site SC-624. To the west along the profile, another head gas high is located at SC-632 and a third is at SC-639 (Figure 14). The average magnetic susceptibility between SC-624 and SC-632 is .928 GGS units; between SC-632 and SC-639 the average is 2.028 CGS units. Approximate map locations are obtained by counting data points from the end of the profile. Obviously more detailed locations could be made by directly comparing the profile with the digitized curvilinear locations. SC-632 with elevated head gas and magnetic susceptibility seems to be near the border between sections 16 and 17. This is located between specific curvilinears. The area of high magnetic susceptibility between SC-632 and SC-639 approximately corresponds with the green area in section 15 and also has a specific curvilinear. The elevated head gas values on either side of the high magnetic susceptibility values are interpreted to be relatively active seeps leaking along the edges of a large diagenetic cap. This interpretation will be expanded in the "Discussion" section of this report.

Lobo West

The Lobo West area is located in Domain 2 near the center of the wide, northeast lineament zone. It contains the strongest magnetic susceptibility anomaly mapped in the total Smoke Creek Study Area. However, it also has low soil and head gas values. Data are distributed only in a profile and no maps were prepared. This Lobo West anomaly corresponds with the large anomaly ranked as number 1 by J.P. Land Associates, Inc (Figure 11). It is the only large anomaly in zone 2 (Figures 11 and 12) that does not have any curvilinears somewhere within its outline. Furthermore, it is situated at the center of a green area on the contour map that is surrounded by small curvilinears (Figure 9).

The Lobo West anomaly is interpreted to be a large fossil seep that produced a significant area of diagenetic alteration. Subsequent smaller seeps leaked around the edges of this large slab and small curvilinears were formed. If the individual curvilinears have good soil and head gas signatures, then the small seeps are still active. If there are no gas signatures, then the small curvilinears are also fossil seeps. This interrelationship of history, size, and type of anomaly is an example of the interpretations that are discussed in the next section of this report.

DISCUSSION

The anomalies described for the various types of data fall into a spectrum of space and time characteristics (Table 2). There is a variation from small and simple anomalies to large and complex. This variation in space is interpreted to also generally reflect a variation in time. The variation in time relates to the flux events ranging from fast, short duration events that are current to slow, long duration events that are old.

The Smoke Creek Aeromagnetic Anomaly dominates the study area and was probably formed during emplacement of a Tertiary intrusive body. The large magnetic susceptibility anomalies based upon profile analyses were produced by fluid flux patterns associated with the intrusion. Bright spots extracted from contour maps and curvilinears, overlap to provide transition between the large, old anomalies and the small, new ones. They represent flux patterns ranging from diffuse over sizable areas down to those focused in localized areas. Bright spots and complex curvilinears generally require some time for the diagenetic "signal" to buildup. Simple curvilinears and indirect techniques of surface measurement also need time to accumulate the signal, but the required time is shorter. Direct surface gas measurements are the most transitory and are focused in small areas.

These generalizations about the time implications of the several different types of anomaly patterns could be improved substantially with a systematic study of cross-cutting relationships. This work would require a better spatial resolution than is available in the small maps used for this report. In effect, the rules used for unraveling sequences of mineral crystallization in a thin section, using a petrographic microscope, could be applied to the several anomaly types. For example, the distribution of small curvilinears around the margins, but not in the center, of large magnetic susceptibility anomalies, has implications for the timing of the large and small flux sources.

Plumbing Geometry

Plumbing geometries can be interpreted from the distribution and attributes of the various anomalies (see Table 1). However, these interpretations are preliminary, speculative, and fairly intuitive. They would be greatly improved by quantitative evaluation of the patterns and by verification of fracture populations. Fundamentally, the four domains in the Smoke Creek Study Area are interpreted to represent different plumbing geometries.

The area with no lineament zones (Domain 1) is relatively unfractured and consequently has no distinctive plumbing geometry. It is characterized by the maximum number of non-anomalous profile miles and by the maximum number of curvilinears. Many of the curvilinears touch an anomalous profile line and so may have expression in magnetic susceptibility measurements. Focused flow in vertical microseeps over small, simple flux sources is interpreted to be dominant. Area 26 is a typical localized anomaly where surface gas, indirect techniques, magnetic susceptibility and a curvilinear all fall into the same small area. This represents currently active, focused flow over a localized flux source.

At the intersection of two lineament zones (Domain 3), rocks should be extensively fractured. However, there may not be any distinctive plumbing geometry because the intersecting fracture populations would give rise to an essentially homogeneous flow system with no preferential orientation. This area has the minimum number of anomalous profile miles that suggest a diffuse flow. The machine contoured map of magnetic susceptibilities is dominantly green showing higher values than the lower value blues found in the two adjacent lineament zones. This may be the result of a greater total flux through the area of intersection so that a larger diagenetic buildup produces higher magnetic susceptibility values. Although Domain 3 has a minimum

number of curvilinears, many are marked with a bright spot. This localized, focused flow is more similar to Domain 1, than to the two lineament zone domains.

The northeast lineament zone (Domain 2) and the northwest lineament zone (Domain 4) can be expected to have different fracture populations characterized by distinctive modes. Thus, in contrast to Domains 1 and 3, Domains 2 and 4 potentially have more anisotropic flow in unique plumbing geometries. Similar numbers of curvilinears are found in the two lineament zones, but there is only occasional association with a bright spot. Both domains have more anomalous profile miles than non-anomalous, which probably result from the anisotropic flow in distinctive plumbing. Macroseeps dominate in the fracture networks and ground water may contribute a component of horizontal flow.

The Lobo West area is characteristic of the lineament zone domains. Initially in the geologic past, a substantial diagenetic slab was built up to give the magnetic susceptibility anomaly. However, subsequent fluid movement was deflected around the slab so that curvilinears are distributed around the margin. Soil gas values are low over the magnetic susceptibility anomaly because it represents a fossilized macroseep through which no gas is currently moving. This interpretation is sketched in a cartoon in Figure 15. Klusman and Saeed (1996, p. 166) refer to diversion of microseepage around the diagenetically cemented slab as a mechanism for also producing halo anomalies.

Flux Source

The large Smoke Creek Aeromagnetic Anomaly constitutes a centrally-located flux source. If it is positioned above an intrusive igneous body, then the associated pulse of energy and fluid that rose through the sedimentary column may have produced some large surface anomalies. This rising pulse of energy and fluid most likely influenced any local hydrocarbon accumulations to produce small, secondary flux sources. Alternatively, the central aeromagnetic anomaly is located above a huge and complex hydrocarbon accumulation. This structural complex might be an astrobleme, but other interpretations of postulated Williston Basin astroblemes are available (Bridges, 1978 and 1987; Gerhard, et al., 1995). In particular, the location at the intersection of lineament zones that have components of strike-slip displacement argues forcefully for a tectonic origin.

No matter what the origin of the Smoke Creek Aeromagnetic Anomaly may be, it has clearly influenced the development of surface anomalies. Within the outline of the aeromagnetic anomaly, there are more curvilinears, more bright spots, more anomalous profile lines and more magnetic susceptibility anomalies compared with outside areas (Table 1). In addition, the area within the outline of the central aeromagnetic anomaly is part of a distinctive qualitative pattern of magnetic susceptibility anomalies and curvilinears.

Magnetic susceptibility anomalies and curvilinears are distributed in three distinct zones around the central Smoke Creek Aeromagnetic Anomaly (see Figure 12). In the center, small curvilinears tend to be located around the margins of the large magnetic susceptibility anomalies. In the second zone surrounding the central zone, small curvilinears are more frequently located within the magnetic susceptibility anomalies. One striking exception is the Lobo West area which has the curvilinears

surrounding the larger anomaly margin (see Figures 8 and 15), but is located outside the central zone in Domain 2. The third zone is out at the margins of the total study area. In this zone, there is a close correspondence between curvilinears, small magnetic susceptibility anomalies and surface measurements. Area 26 is the archetype for this outer zone (see Figure 13).

The three distinct zones of anomalies represent three different sources of hydrocarbon flux (Figure 16). The central zone is located directly above a large and complex flux source. Closely spaced magnetic susceptibility anomalies developed early and are large slabs of diagenetically altered surface material that diverted subsequent microseepage around the margins where curvilinears formed (see Figure 15). In the next zone, curvilinears are found within the anomaly "blobs" suggesting that the diagenetic slab is thinner and/or less extensively developed. Thus, microseeps that formed after the slab was created, rose directly through the middle of the anomalies. It is postulated that these are moderate-sized hydrocarbon flux sources and that they were indirectly influenced by flux from the large central source. In the outer zone, small and simple flux sources are located directly below curvilinears that correspond with small magnetic susceptibility anomalies and with surface measurements. In this zone there are minimal influences and complications from either the large central source or from a distinct plumbing geometry such as that associated with the northeast lineament zone.

Interaction between flux sources and plumbing geometries can account for differences between Domain 1 and Domain 2 (Figure 16). Domain 1 outside any lineament zone has no distinctive plumbing geometry and it is dominated by relatively simple vertical hydrocarbon migration above small, localized sources. Influences from the large central flux source may have produced multi-stage histories for some magnetic susceptibility anomalies. Area 26 is an example. In contrast, Domain 2 located within the northeast lineament zone is a corridor of increased fracturing and does have a distinctive plumbing geometry. Influences from the central flux source extend farther out into the lineament zone where fossilized macroseeps, similar to those over the large central source, may form. The Lobo West area is an example.

SUGGESTIONS FOR FURTHER STUDY

The most important next step in further studies near the Smoke Creek Aeromagnetic Anomaly will be to integrate the results of the latest field work with the patterns presented in this report. In particular, are there other examples of the Area 26 study area where curvilinears, small magnetic susceptibility anomalies, and anomalies in surface measurements all closely correspond? And, are these new examples mainly confined to the outermost zone of anomalies? In addition, are there other examples of the Lobo West study area where low gas values characterize the blob anomaly? Do the small curvilinears between the blobs have surface gas anomalies marking local flux sources that are currently active? And, are the additional examples of these fossil macroseeps mainly confined to the central zone and/or the northeast lineament zone? Hopefully some of the recommendations provided for field sampling in my e-mail of September 2, will assist in answering these questions.

Another important step will be to quantify the areal patterns described in a preliminary way in this report. This could be done by employing calculations and digital mapping similar to that done for the Hedberg manuscript. It would be good to objectively verify the pattern differences (see Table 1) recognized for Domains 1 through 4 and for areas inside and outside the outline of the Smoke Creek Aeromagnetic Anomaly. Furthermore, such a quantitative description might help demonstrate subtle domain differences in each of the three anomaly zones (see Figure 12).

Plumbing geometries should be characterized in the lineament zones and their intersection (Domains 2, 3, and 4). This would also provide contrast with the area outside the lineament zones (Domain 1). Fracture systems can be described from measurements in outcrops. Often outcrop observations can be related in a systematic way to lineament zones (for example, see Shurr, et al., 1995, and Shurr, et al., 1996). Outcrop investigations could include detailed surface mapping in local areas, as well as measurement of fracture orientations in outcrops. Linear features mapped on high altitude photographs (for example, Shurr, 2000) or on more detailed air photos can also be used to characterize fracture systems in and around lineament zones.

Magnetic susceptibility anomalies interpreted by J.P. Land Associates, Inc are based upon analyses of individual profiles (see Figure 10). The shape of these blobs should be verified and/or refined by doing more detailed data collection. In addition, the more detailed surveys would be amenable to objective computer contouring such as that used over the entire study area (see Figure 9). Anomalies selected for more detailed sampling should have some particular significance. For example, close association with curvilinears or with anomalies based upon surface gas and indirect techniques.

Finally, the curvilinear, magnetic susceptibility anomalies, and surface measurement anomalies could all be further refined by using additional data sets. Hyperspectral studies of selected anomalies and curvilinears would be of particular interest. Spectral properties of soils would no doubt be influenced by formation of a diagenetic slab and/or by a currently active microseep. This type of remote sensing data would be particularly useful in improving the resolution of anomalies and curvilinears thus far mapped in only a preliminary way. In particular, hyperspectral studies could bridge the scale gap between Landsat curvilinears and anomalies based upon surface measurements. This would be particularly useful for some of the large complexes of multiple curvilinears. But, it would also be significant for small, single-source curvilinears.

CONCLUSIONS

Hydrocarbon seeps associated with the Smoke Creek Aeromagnetic Anomaly have had a variety of life histories and are distributed in distinct patterns. In the center of the area, early and intense flux produced large slabs of diagenetically altered soil that are mapped as magnetic susceptibility anomalies. Subsequently, small seeps were deflected to the margins of the slabs where curvilinears mark their location. Contemporary gas seeps are generally not found within these thick fossil slabs.

Outside the central core area, hydrocarbon migration was influenced by plumbing geometries related to fracture systems in Landsat lineament zones. Large

magnetic susceptibility anomalies were formed, but gas continued to flux through most of them so that curvilinears are not just limited to the slab margins. On the outer periphery of the study area, simple small seeps show a correspondence of Landsat curvilinears, magnetic susceptibility anomalies, and gas anomalies.

These interpretative generalizations require the further refinement and clarification that will be available after the next round of data collection has been completed. In the meantime, there are some clear preliminary implications for hydrocarbon exploration: 1) hydrocarbon sources in the sedimentary rocks above the aeromagnetic anomaly may have been depleted long ago; 2) sources surrounding the aeromagnetic anomaly may or may not be depleted, depending upon the plumbing geometry; and 3) the best candidates for exploration are distributed around the periphery as small and simple sources with contemporary seeps.

REFERENCES CITED

Bridges, L.W.D., 1978, Red Wing Creek Field, North Dakota-a concentricline of structural origin, *in* The economic geology of the Williston Basin: Williston Basin Symposium, Montana Geological Society 24th Annual Conference, p. 315-326.

Bridges, L.W.D., 1987, Red Wing Creek Field, North Dakota-a growth faulted or meteoritic impact structure, *in* J.A. Peterson, D.M. Kent, S.B. Anderson, R.H. Pilatzke, and M.W. Longman, eds., Williston Basin-anatomy of a cratonic oil province: Rocky Mountain Association of Geologists, p. 433-440.

Clayton, C.J., and P.R. Dando, 1996, Comparison of seepage and seal leakage rates, *in* D. Schumacher and M.A. Abrams, eds., Hydrocarbon migration and its near-surface expression: AAPG Memoir 66, p. 169-171.

Gerhard, L.C., S. Anderson, D. Fischer, R. Olea, and L. Robertson, 1995, Western Cold Turkey Creek anomaly-a meteorite impact crater-NOT, *in* L.D.V. Hunter and R. A. Schalla, eds., Proceedings of the Seventh International Williston Basin symposium: Montana Geological Society, p. 179-185.

Holysh, S., and J. Toth, 1996, Flow of formation waters-likely cause for poor definition of soil gas anomalies over oil fields in east-central Alberta, Canada, *in* D. Schumacher and M.A. Abrams, eds., Hydrocarbon migration and its near-surface expression: AAPG Memoir 66, p. 25-277.

Jones, V.T. and S.G. Burtell, 1996, Hydrocarbon flux variations in natural and anthropogenic seeps, *in* D. Schumacher and M.A. Abrams, eds.,

Hydrocarbon migration and its near-surface expression: AAPG Memoir 66, p. 203-221.

Klusman, R.W., and M.A. Saeed, 1996, Comparison of light hydrocarbon microseep mechanisms, *in* D. Schumacher and M.A. Abrams, eds., Hydrocarbon migration and its near-surface expression: AAPG Memoir 66, p. 157-168.

Krooss, B.M., and D. Leythaeuser, 1996, Molecular diffusion of light hydrocarbons in sedimentary rocks and its role in migration and dissipation of natural gas, *in* D. Schumacher and M.A. Abrams, eds., Hydrocarbon migration and its near-surface expression: AAPG Memoir 66, p. 173-183.

Land, J.P., Magnetic susceptibility survey, DOE Area: Smoke Creek, northeastern, Montana: Unpublished Report to the Minerals Resource Office, Fort Peck Tribes, 3 p.

Matthews, M.D., 1996a, Migration-a view from the top, *in* D. Schumacher and M.A. Abrams, eds., Hydrocarbon migration and its near-surface expression: AAPG Memoir 66, p. 139-155.

Matthews, M.D., 1996b, Importance of sampling design and density in target recognition, *in* D. Schumacher and M.A. Abrams, eds., Hydrocarbon migration and its near-surface expression: AAPG Memoir 66, p. 243-253.

Mello, M.R., F.T. Goncalves, N.A. Babinski, F.P. Miranda, 1996, Hydrocarbon prospecting in the Amazon rain forest: application of surface geochemical, microbiological, and remote sensing methods, *in* D. Schumacher and M.A. Abrams, eds., Hydrocarbon migration and its near-surface expression: AAPG Memoir 66, p. 401-411.

Monson, L.M., 2000, Phase I interim report 1, Fort Peck Reservation assessment of hydrocarbon seepage: Semi-annual Technical Progress Report, Department of Energy Grant Award #DE-FG26-00BC15192.

Monson, L.M., 2001, Phase I report 2, Fort Peck Reservation assessment of hydrocarbon seepage: Semi-annual Technical Progress Report, Department of Energy Grant Award #DE-FG26-00BC15192.

Monson, L.M., 2002, Phase II report 3, Fort Peck Reservation assessment of hydrocarbon seepage: Semi-annual Technical Progress Report, Department of Energy Grant Award #DE-FG26-00BC15192.

Monson, L.M., and D.F. Lund, 1991, Breaking into Bakken potential on the Fort Peck Reservation in northeastern Montana, *in* J.E. Christopher and F.M. Haidl, eds., Sixth international Williston Basin symposium: Saskatchewan Geological Society Special Publication Number 11, p. 95-102.

Monson, L.M., and G.W. Shurr, 1993, Remote sensing applications in the assessment of natural resources on the Fort Peck Reservation, Montana, *in* Proceedings of the ninth thematic conference on geologic remote sensing: Environmental Research Institute of Michigan, v. 1, p. 431-443.

Monson, L.M., and G.W. Shurr, in review, Assessment of hydrocarbon seepage on Fort Peck Reservation: a comparison of surface exploration techniques, *in* M. Abrams and J. Whelan, eds., Hedberg Conference: AAPG Memoir.

Rostron, B.J., and J. Toth, 1996, Ascending fluid plumes above Devonian pinnacle reefs-numerical modeling and field example from west-central Alberta, Canada, *in* D. Schumacher and M.A. Abrams, eds., Hydrocarbon migration and its near-surface expression: AAPG Memoir 66, p. 185-201.

Shurr, G.W., 1991, Assessment of geologic significance of Landsat lineament zones on Fort Peck Reservation: Unpublished Report to the Minerals Resource Office, Fort Peck Tribes, 71 p.

Shurr, G.W., 1992, Study of curvilinears on satellite images: Unpublished Report to the Minerals Resource Office, Fort Peck Tribes, 43 p.

Shurr, G.W., 2000, Architectonics of Cedar Creek Anticline, *in* R.A. Schalla and E.H. Johnson, eds., Montana/Alberta thrust belt and adjacent foreland: Montana Geological Society 50th Anniversary Symposium, p. 97-107.

Shurr, G.W., 2001, Basin-margin gas in the Rocky Mountains and adjacent great Plains, *in* D.S. Anderson, J.W. Robinson, J.E. Estes-Jackson, and E.B. Coalson, eds., Gas in the Rockies: Rocky Mountain Association of Geologists, p. 223-239.

Shurr, G.W., 2002, Shallow gas systems in tight reservoirs on basin margins: AAPG Annual Meeting Abstracts, p. A163.

Shurr, G.W., and L.M. Monson, 1995, Tectonic setting and paleotectonic history of Fort Peck Reservation in northeastern Montana, *in* L.D.V. Hunter and R. A. Schalla, eds., Proceedings of the Seventh International Williston Basin symposium: Montana Geological Society, p. 11-22.

Shurr, G.W., and I.W. Watkins, 1989, Basement blocks, tectonics, and fluid movement--"seeping" through the sedimentary cover, *in* Proceedings of the Seventh Thematic conference on Remote Sensing: Environmental Research Institute of Michigan, v. 1, p. 501-517.

Shurr, G.W., A.C. Ashworth, R.B. Burke, and P.E. Diehl, 1995, Tectonic controls on the Lodgepole play in northern Stark County, North Dakota—prospectives from surface and subsurface studies, *in* L.D.V. Hunter and R. A. Schalla, eds., Proceedings of the Seventh International Williston Basin symposium: Montana Geological Society, p. 203-208.

Shurr, G.W., A.C. Ashworth, R. Benton, E.C. Murphy, and R.F. Biek, 1996, Regional framework for Tertiary tectonism in the Northern Great Plains *in* C.J. Paterson and J.G. Kirchner, eds., Guidebook to the geology of the Black Hills, South Dakota: South Dakota School of Mines and Technology Bulletin 19, p. 129-134.

Story, C., 2002, 3-D images active gas changes: AAPG Explorer, June, p. 28-29.

Thrasher, J., A.J. Fleet, S.J. Hay, M. Hovland, and S. Duppenbecker, 1996, Understanding geology as the key to using seepage in exploration: the spectrum of seepage styles, *in* D. Schumacher and M.A. Abrams, eds., Hydrocarbon migration and its near-surface expression: AAPG Memoir 66, p. 223-241.

Toth, J., 1996, Thoughts of a hydrogeologist on vertical migration and near-surface geochemical exploration for petroleum, *in* D. Schumacher and M.A. Abrams, eds., Hydrocarbon migration and its near-surface expression: AAPG Memoir 66, p. 279-283.

L I S T O F T A B L E S

Table 1. Summary of Map Observations.

Table 2. Distribution of data types in space and time.

Appendix 1.

Table A. Magnetic susceptibility ratio contours and Landsat curvilinears.

Table B. Magnetic susceptibility profiles and Landsat curvilinears.

Table C. Magnetic susceptibility profile anomalies and Landsat curvilinears.

L I S T O F F I G U R E S

Figure 1. Distribution of high and low value soil gas stations relative to a lineament zone. Taken from Matthews (1996b).

Figure 2. Lineament zones in green interpreted from Landsat linear features in the area of Cedar Creek Anticline. Specific faults and monoclines are associated with linear features (1-8). Linear features A and B are straight stream segments. Taken from Shurr (2000).

Figure 3. Patterns of linear features near the intersection of lineament zones. Taken from Shurr (2000).

A. Sketch map of Landsat linear features (heavy lines), published surface faults (light lines), and air photo study areas.

B. Rose diagrams of linear features mapped on high altitude air photos (NHAP) in 9 sq mi cells as located in Figure 3-A.

Figure 4. Shallow gas production from the Eagle is displaced to the northeast of structural highs (A and B) within the northeast lineament zone at the intersection with Cedar Creek Anticline. Ground water flow within this corridor of fractures is believed to have produced this pattern. Taken from Shurr (2002).

Figure 5. Landsat lineament zones shown in green on Fort Peck Reservation (map a) are the surface expressions of tectonic basement blocks (sketch b). Taken from Monson and Lund (1991).

Figure 6. Sketch map of the Smoke Creek Aeromagnetic Anomaly located at the intersection of the Big Muddy and Poplar River Lineament Zones.

Figure 7. Geologic framework of the Smoke Creek Study Area. Domain 1 is outside lineament zones, Domains 2 and 4 are within lineament zones, and Domain 3 is at the intersection of lineament zones. The area within the outline of the Smoke Creek Aeromagnetic Anomaly is 70 sq mi and the area outside the anomaly is 219 sq mi.

Figure 8. Curvilinears mapped on Landsat distributed through the lineament zone domains and Smoke Creek Aeromagnetic Anomaly (Monson, 2000). Small areas outlined in red are "bright spots" of high magnetic susceptibility values as mapped on the computer contoured magnetic

susceptibility ratio (Monson, 2002, p. 53). A is Area 26; B is Smoke Creek Core; C is Lobo West.

Figure 9. Landsat curvilinear features superimposed on the computer contoured map of magnetic susceptibility values (Monson, 2002, p. 52). Lineament domains and the central aeromagnetic anomaly are also shown.

Figure 10. Anomalies interpreted from profile analysis of magnetic susceptibility data (Land, 2002). Lineament domains and the central aeromagnetic anomaly are shown in red. Anomalous traverse segments are taken as those with values 50% above background and non anomalous segments are less than 50%.

Figure 11. Landsat curvilinears, lineament domains, and the central aeromagnetic anomaly superimposed on anomalies interpreted from profile analysis (Land, 2002). Red curvilinears touch an anomalous traverse segment and blue curvilinears do not.

Figure 12. Summary sketch of the three zones of anomaly patterns above and around the central flux source associated with the Smoke Creek Aeromagnetic Anomaly.

Figure 13. Cartoon summarizing the relationships of various data sets in Area 26. The heavy line is a Landsat curvilinear. Head gas propane is shown in blue and iodine is patterned in orange (Monson, 2002, p. 87 and 94 respectively).

Figure 14. Comparison of magnetic susceptibility values and head gas propane along the profile through the Smoke Creek Core area (Monson, 2002, p. 119). Point SC-624 has high head gas propane and magnetic susceptibility and is located between curvilinears. Points SC-632 and SC-639 have high propane values and are at the edges of a diagenetic cap characterized by relatively high magnetic susceptibility.

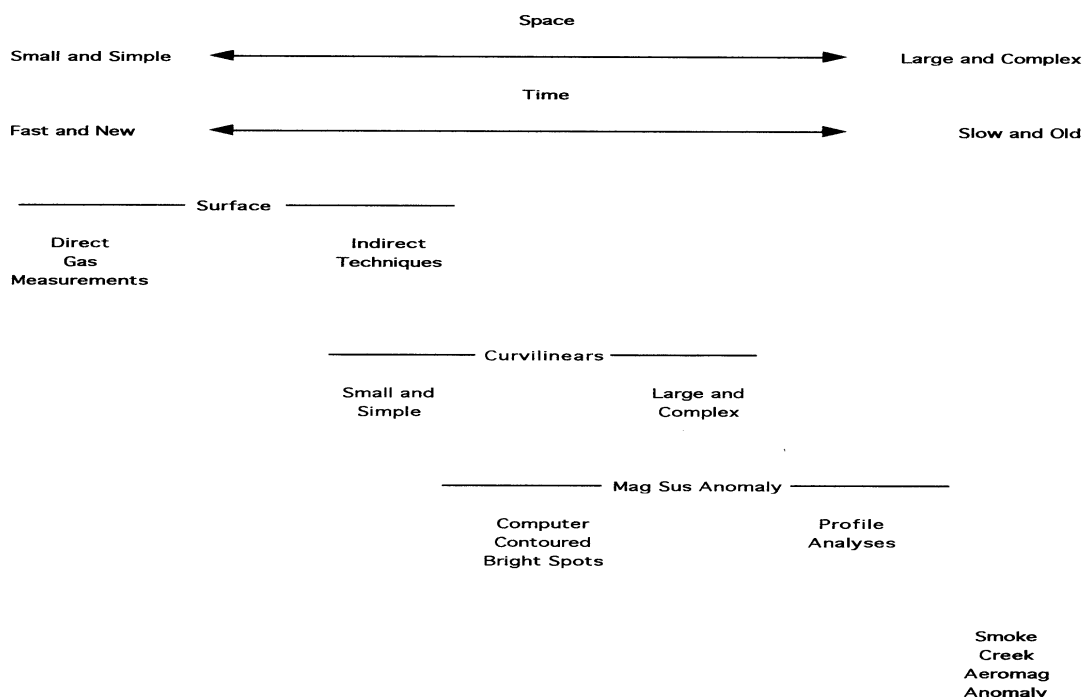
Figure 15. Cartoon illustrating a possible explanation for the distribution of small curvilinear features around the periphery of large magnetic susceptibility anomalies.

Figure 16. Sketch summarizing flux sources and plumbing geometries above the Smoke Creek Aeromagnetic Anomaly and in the surrounding domains defined by lineament zones.

Table 1
Summary of Map Observations
See Appendix I

	Domain 1	Domain 2	Domain 3	Domain 4	In	Out
Lineament Zone	None	NE	Both	NW	NA	NA
Area sq mi	54	114	61	60	70	219
Appendix Table A						
Curvilinears per sq mi	0.48	0.38	0.34	0.36	0.51	0.38
Bright spots per sq mi	0.06	0.07	0.07	0.05	0.09	0.06
Bright spots with curvilinears per sq mi	0.04	0.03	0.05	0.03	0.04	0.03
Appendix Table B						
Anomalous linear mi per sq mi	0.41	0.47	0.31	0.4	0.59	0.36
Non-anom linear mi per sq mi	0.5	0.3	0.21	0.25	0.43	0.27
Curvilinears touching anom line per sq mi	0.24	0.21	0.15	0.12	0.33	0.14
Curvilinears NOT touching anom line per sq mi	0.24	0.15	0.15	0.28	0.17	0.2
Appendix Table C						
Total anomalies per sq mi	0.19	0.16	0.13	0.07	0.2	0.11
Total anomalies with curvilinears per sq mi	0.11	0.08	0.18	0.05	0.07	0.06

TABLE 2.
Distribution of Data Types in Space and Time



Appendix Table A
Magnetic Susceptibility Ratio Contours and Landsat Curvilinears
Map Observations on Figures 8 and 9

	Domain 1	Domain 2	Domain 3	Domain 4	In	Out
Lineament Zone	None	NE	Both	NW	NA	NA
Area sq mi	54	114	61	60	70	219
Curvilinears count	26	43	21	22	36	76
Curvilinears count per sq mi	0.48	0.38	0.34	0.36	0.51	0.38
Bright spots count	3	8	4	3	6	12
Bright spots count per sq mi	0.06	0.07	0.07	0.05	0.09	0.06
Bright spots with curvilinears count	2	3	3	2	3	7
Bright spots with curvilinears count per sq mi	0.04	0.03	0.05	0.03	0.04	0.03

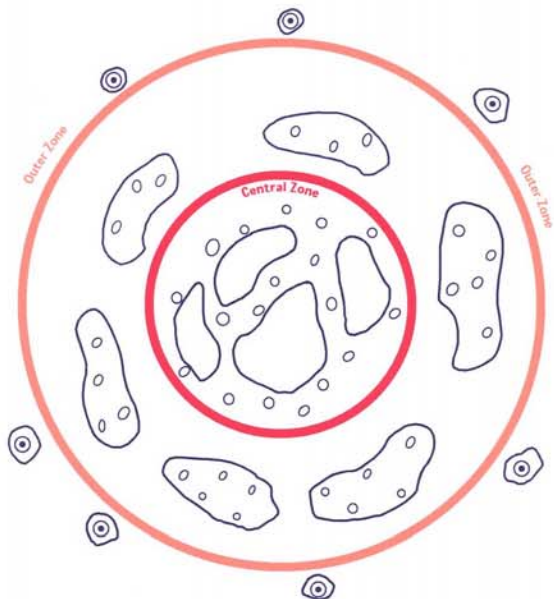
Appendix Table B
Magnetic Susceptibility Profiles and Landsat Curvilinears
Map Observations on Figure 10

	Domain 1	Domain 2	Domain 3	Domain 4	In	Out
Lineament Zone	None	NE	Both	NW	NA	NA
Area sq mi	54	114	61	60	70	219
Anomaly linear miles count	22	54	19	24	41	78
Anomaly linear miles per sq mi	0.41	0.47	0.31	0.4	0.59	0.36
Non-anomaly linear miles count	27	34	13	15	30	59
Non-anomaly linear miles per sq mi	0.5	0.3	0.21	0.25	0.43	0.27
Anomaly-Nonanomaly per sq mi	-0.9	0.17	0.1	0.15	0.16	0.09
Curvilinears touching anomaly line count	13	24	10	7	23	31
Curvilinears touching anomaly line per sq mi	0.24	0.21	0.15	0.12	0.33	0.14
Curvilinears NOT touching anomaly line count	13	17	9	17	12	44
Curvilinears NOT touching non-anomaly line per sq mi	0.24	0.15	0.15	0.28	0.17	0.2
Curvilinears touching/not touching per sq mi	0	0.6	0	-0.16	0.16	-0.06

Appendix Table C
Magnetic Susceptibility Profile Anomalies and Landsat Curvilinears
Map Observations on Figure 11

	Domain 1	Domain 2	Domain 3	Domain 4	In	Out
Lineament Zone	None	NE	Both	NW	NA	NA
Area sq mi	54	114	61	60	70	219
Major anomalies numbered	1	5	0	2	3	4
Minor anomalies unnumbered	9	13	8	2	11	20
Total anomalies count	10	18	8	4	14	24
Total anomalies per sq mi	0.19	0.16	0.13	0.07	0.2	0.11
Total anomalies with curvilinears count	6	9	5	3	5	13
Total anomalies with curvilinears per sq mi	0.11	0.08	0.08	0.05	0.07	0.06

**PRELIMINARY INTERPRETATIONS
OF
HYDROCARBON GAS CHIMNEYS
IN THE
SMOKE CREEK STUDY AREA**



**A Report Submitted to
Minerals Resources Office
Fort Peck Tribes
Poplar, MT**

by

**George W. Shurr
GeoShurr Resources, LLC
Ellsworth, MN**

December, 2002



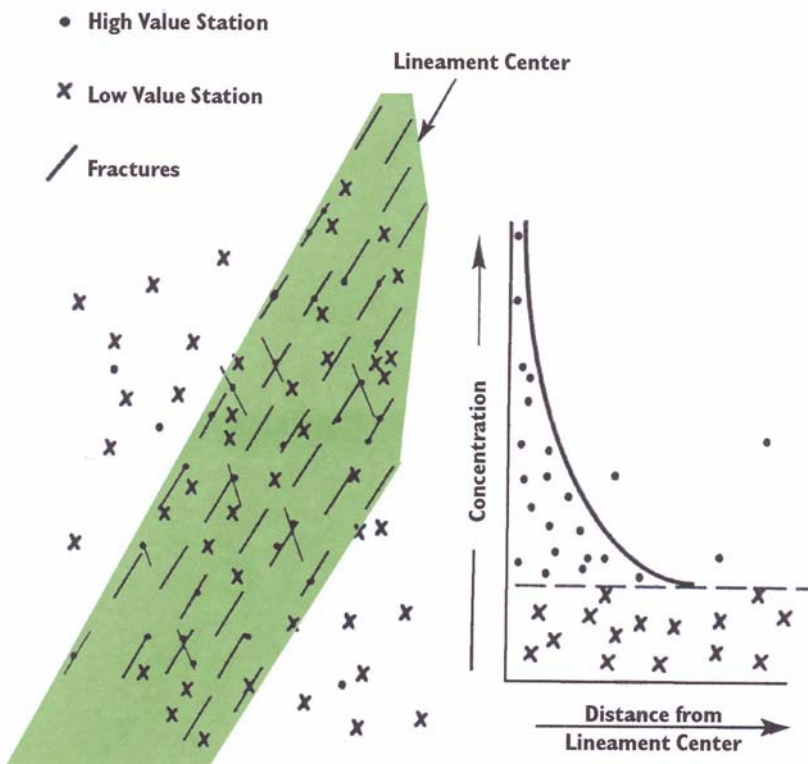


Figure 1

Distribution of high and low value soil gas stations relative to a lineament zone. Taken from Matthews (1996b).

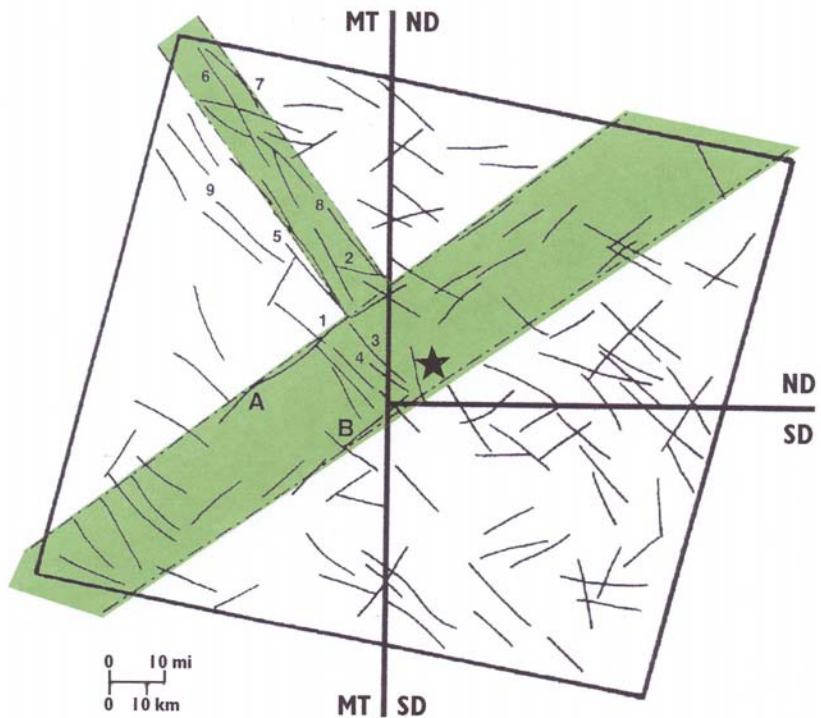


Figure 2

Lineament zones in green interpreted from Landsat linear features in the area of Cedar Creek Anticline. Specific faults and monoclines are associated with linear features (1-8). Linear features A and B are straight stream segments. Taken from Shurr (2000).

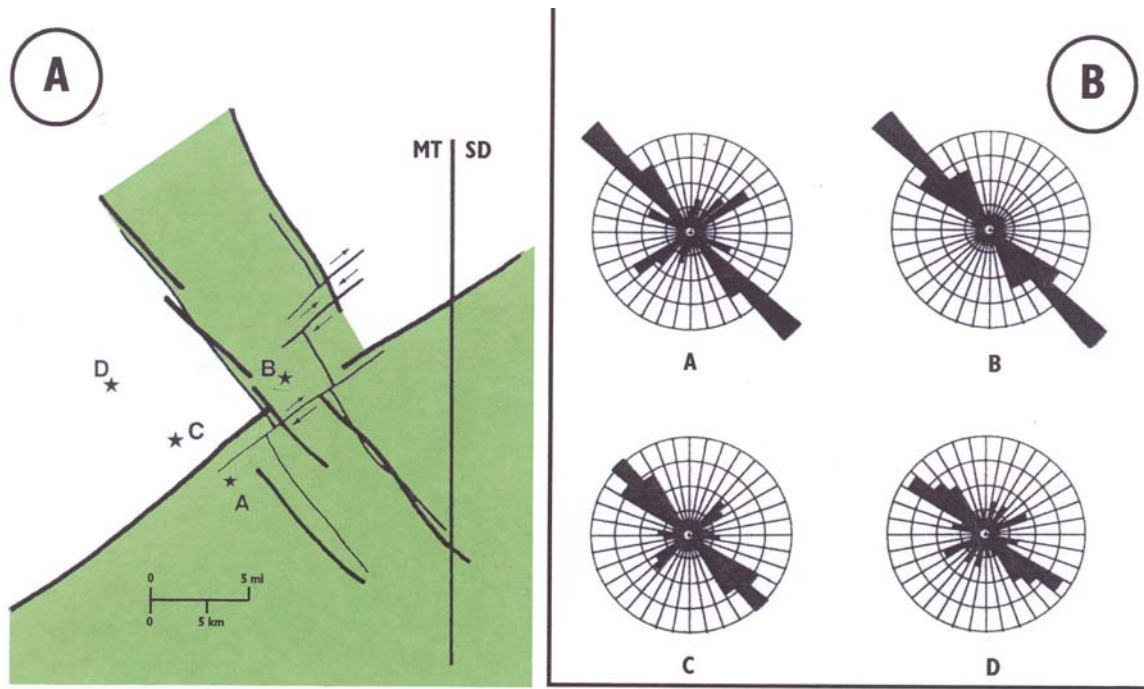


Figure 3

Patterns of linear features near the intersection of lineament zones. Taken from Shurr (2000).

- A. Sketch map of Landsat linear features (heavy lines), published surface faults (light lines), and air photo study areas.
- B. Rose diagrams of linear features mapped on high altitude air photos (NHAP) in 9 sq mi cells as located in Figure 3-A.

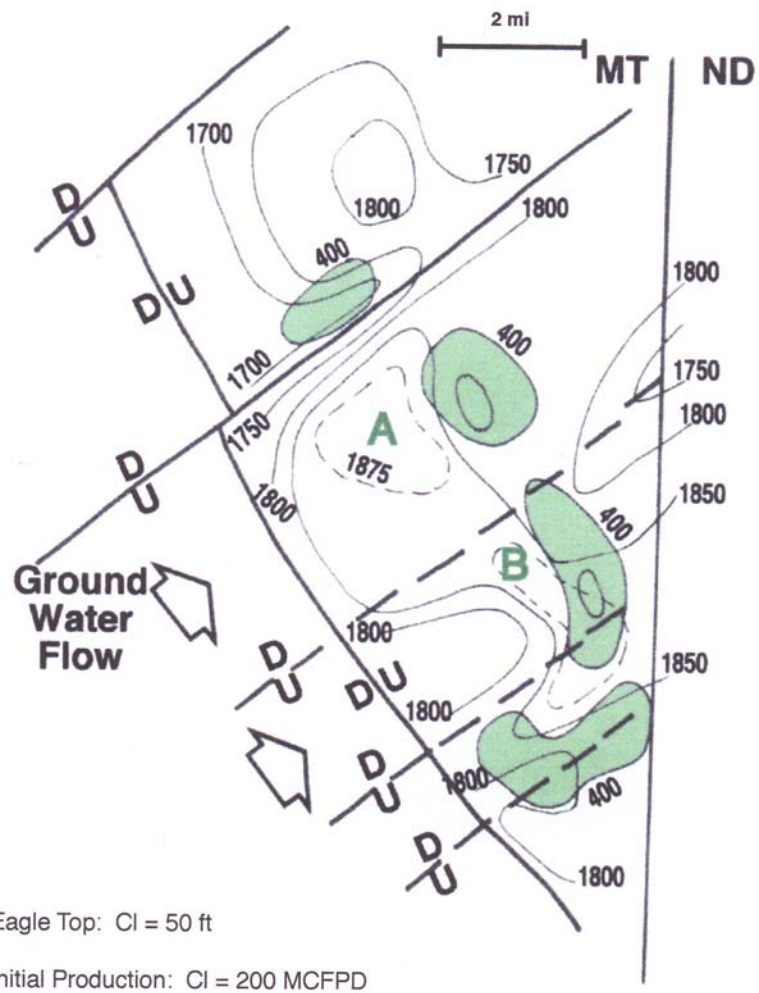


Figure 4

Shallow gas production from the Eagle is displaced to the northeast of structural highs (A and B) within the northeast lineament zone at the intersection with Cedar Creek Anticline. Ground water flow within this corridor of fractures is believed to have produced this pattern. Taken from Shurr (2002).

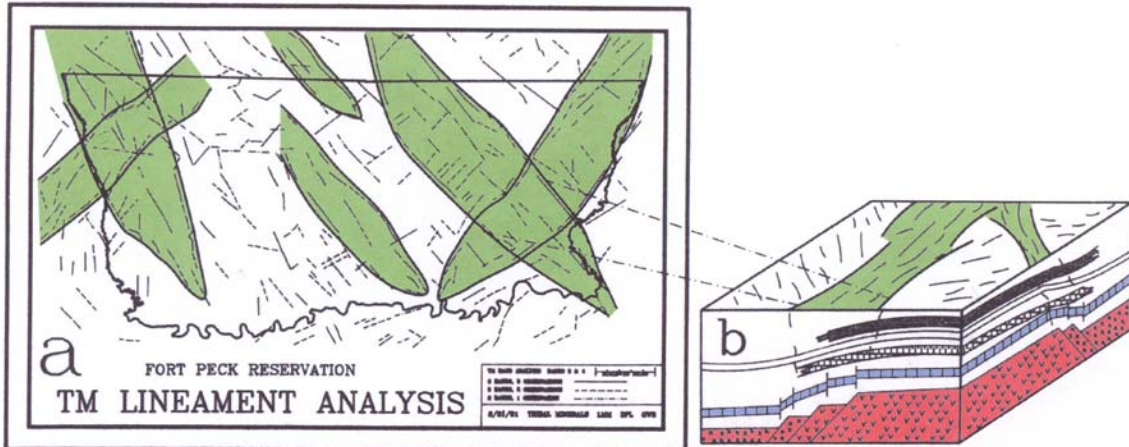


Figure 5

Landsat lineament zones shown in green on Fort Peck Reservation (map a) are the surface expressions of tectonic basement blocks (sketch b). Taken from Monson and Lund (1991).

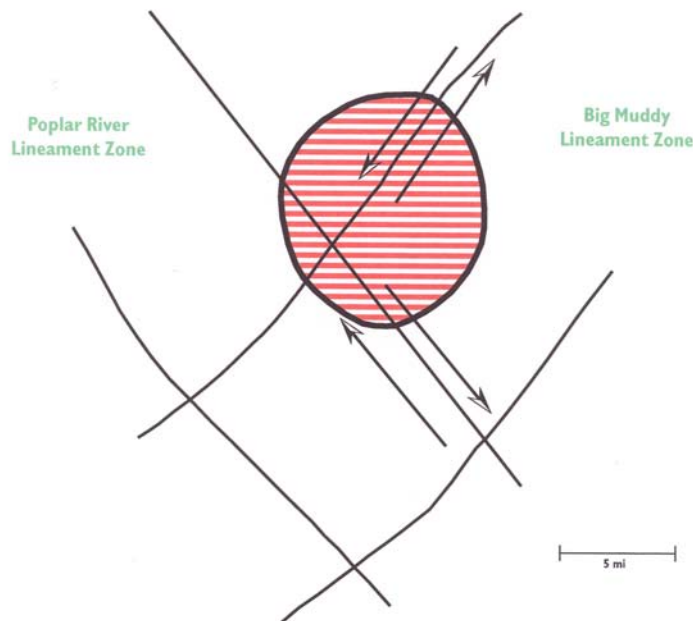


Figure 6

Sketch map of the Smoke Creek Aeromagnetic Anomaly located at the intersection of the Big Muddy and Poplar River Lineament Zones.

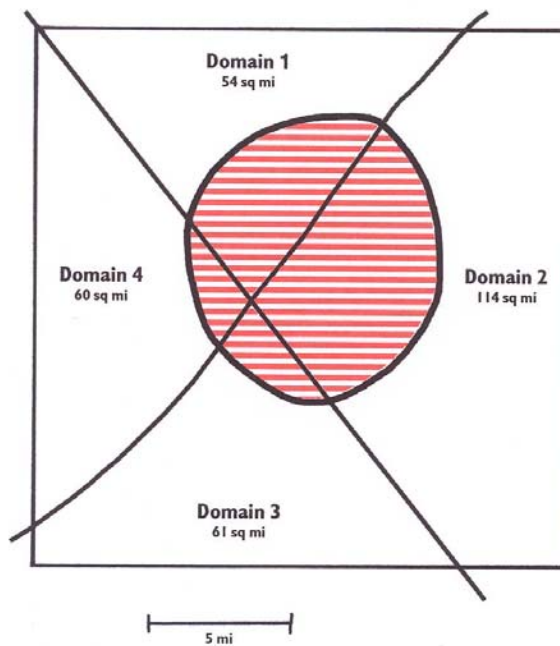


Figure 7

Geologic framework of the Smoke Creek Study Area. Domain 1 is outside lineament zones, Domains 2 and 4 are within lineament zones, and Domain 3 is at the intersection of lineament zones. The area within the outline of the Smoke Creek Aeromagnetic Anomaly is 70 sq mi and the area outside the anomaly is 219 sq mi.

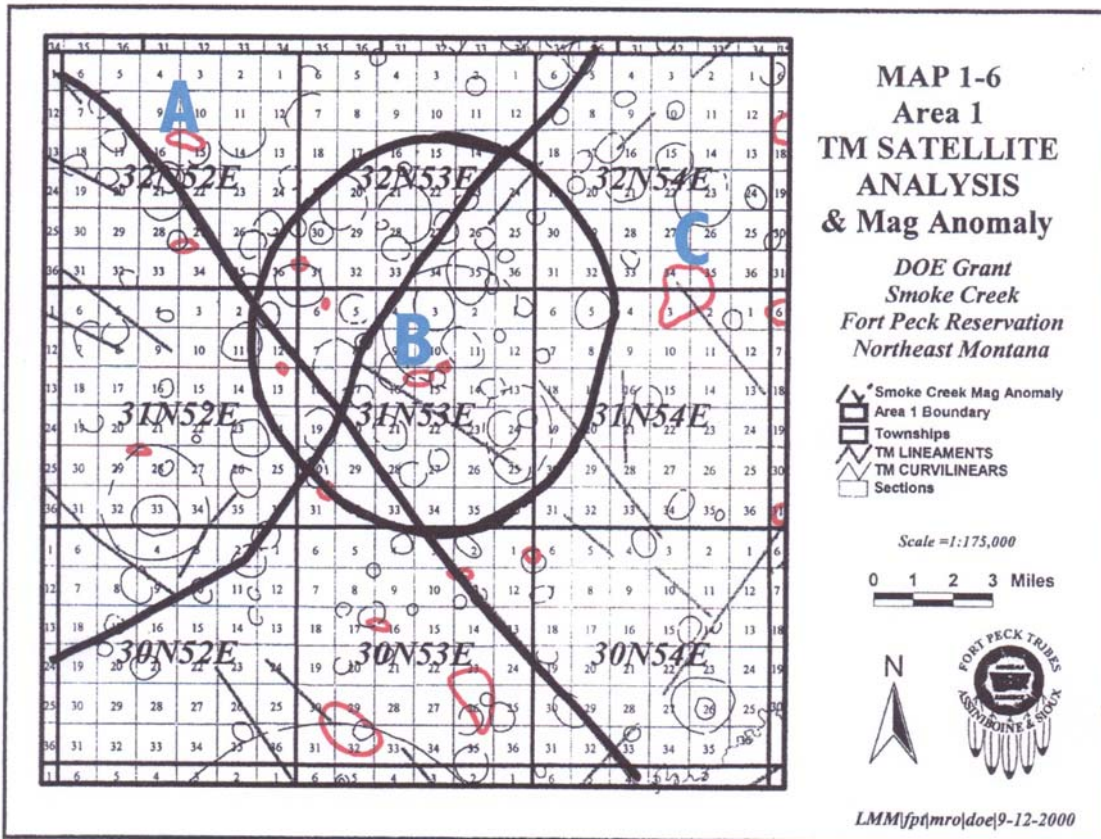


Figure 8

Curvilinears mapped on Landsat distributed through the lineament zone domains and Smoke Creek Aeromagnetic Anomaly (Monson, 2000). Small areas outlined in red are "bright spots" of high magnetic susceptibility values as mapped on the computer contoured magnetic susceptibility ratio (Monson, 2002, p. 53). A is Area 26; B is Smoke Creek Core; C is Lobo West.

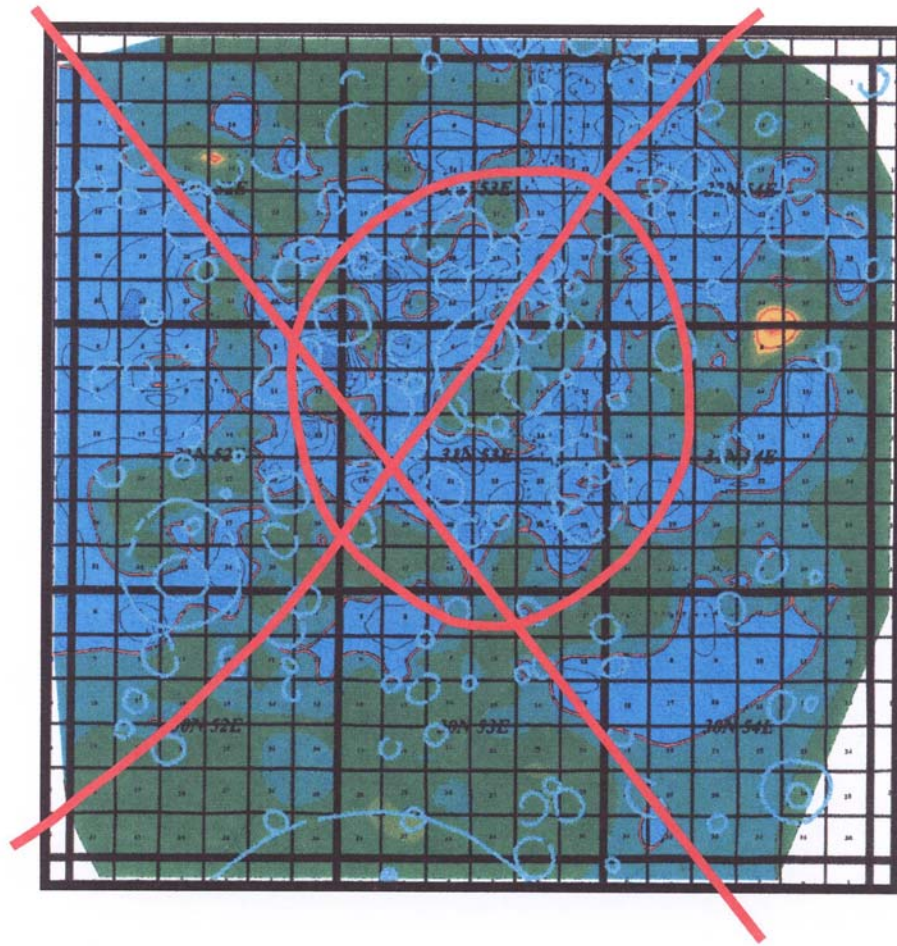


Figure 9

Landsat curvilinear features superimposed on the computer contoured map of magnetic susceptibility values (Monson, 2002, p. 52). Lineament domains and the central aeromagnetic anomaly are also shown.

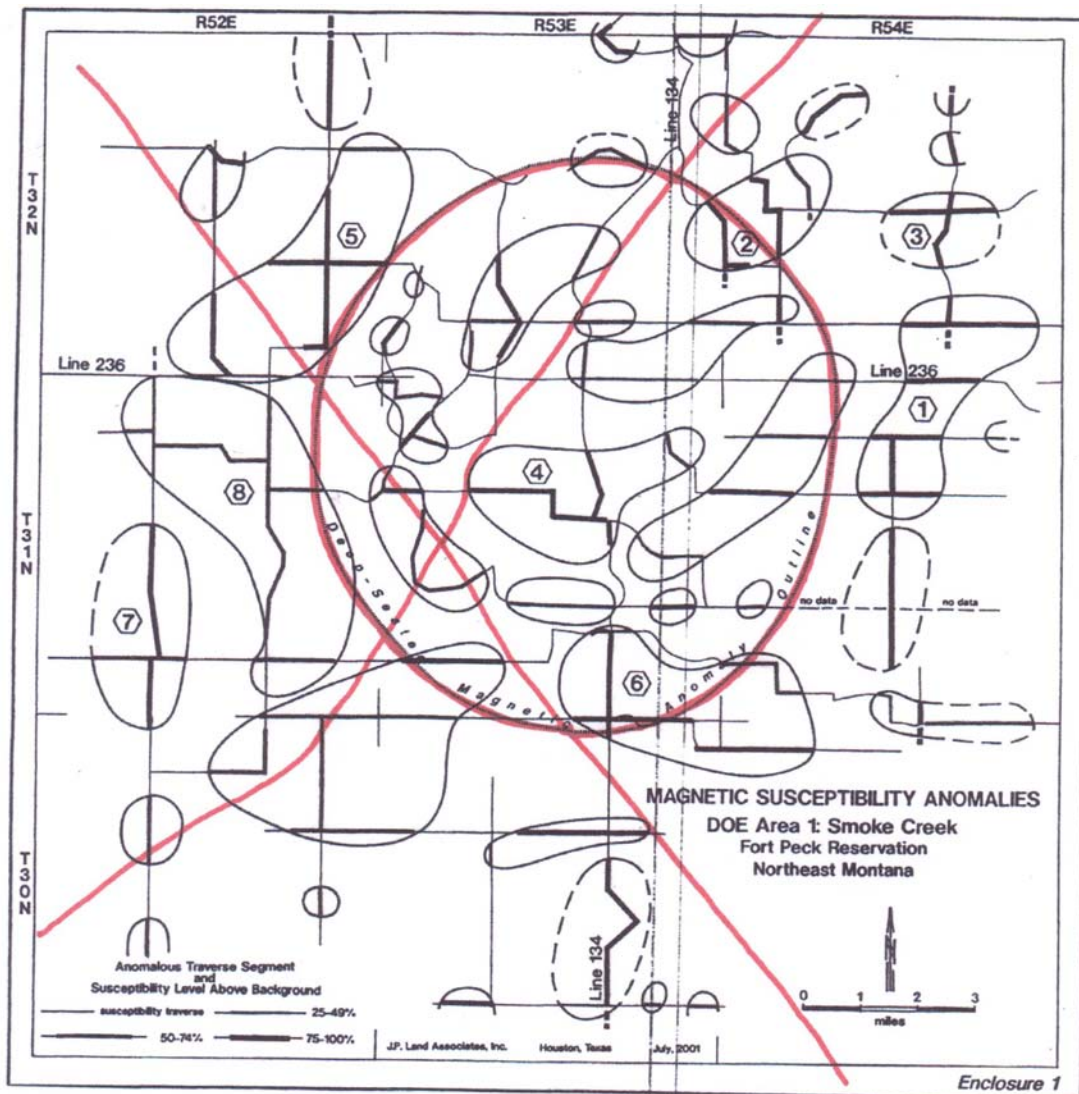


Figure 10

Anomalies interpreted from profile analysis of magnetic susceptibility data (Land, 2002). Lineament domains and the central aeromagnetic anomaly are shown in red. Anomalous traverse segments are taken as those with values 50% above background and non anomalous segments are less than 50%.

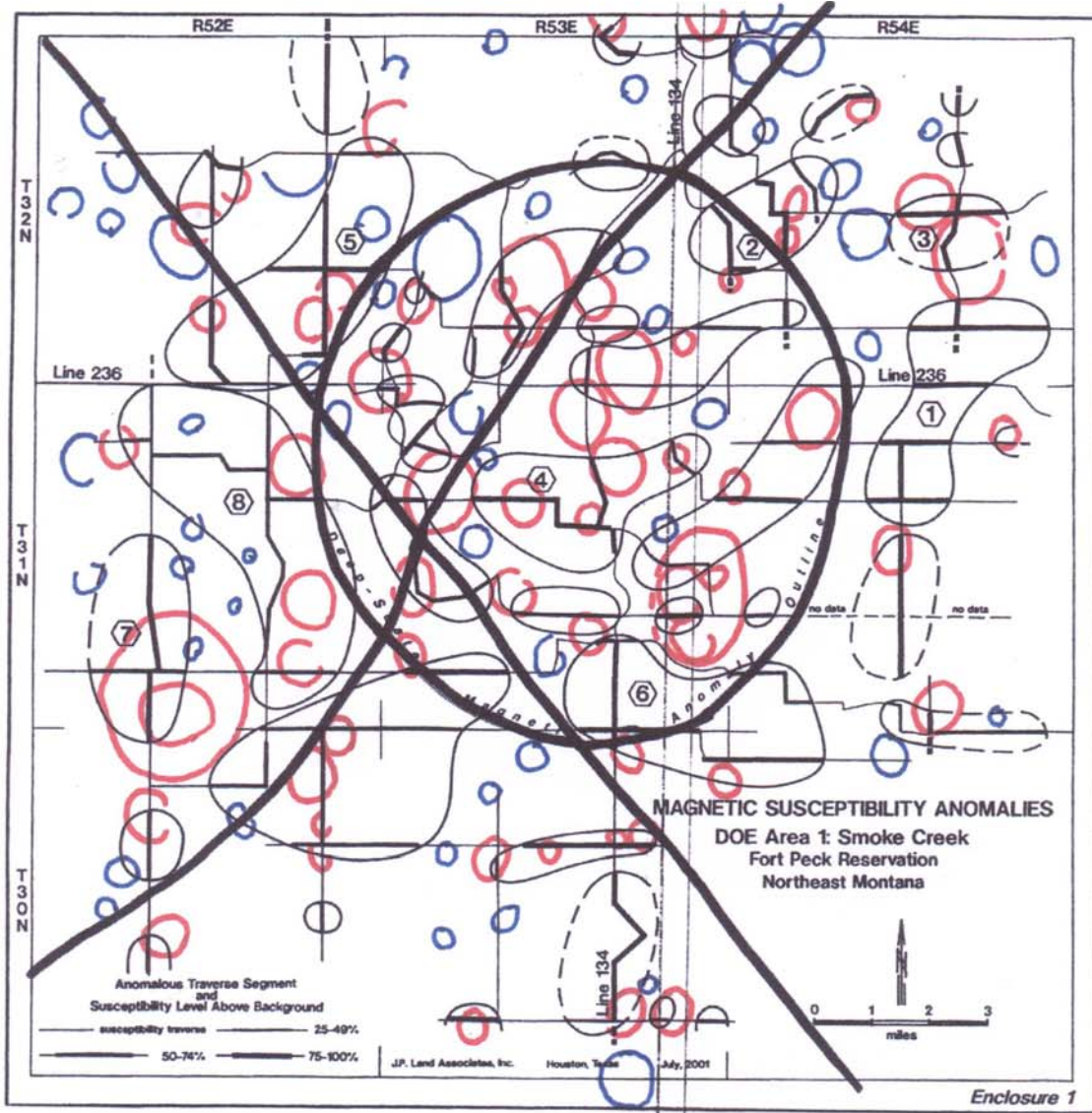


Figure 11

Landsat curvilinears, lineament domains, and the central aeromagnetic anomaly superimposed on anomalies interpreted from profile analysis (Land, 2002). Red curvilinears touch an anomalous traverse segment and blue curvilinears do not.

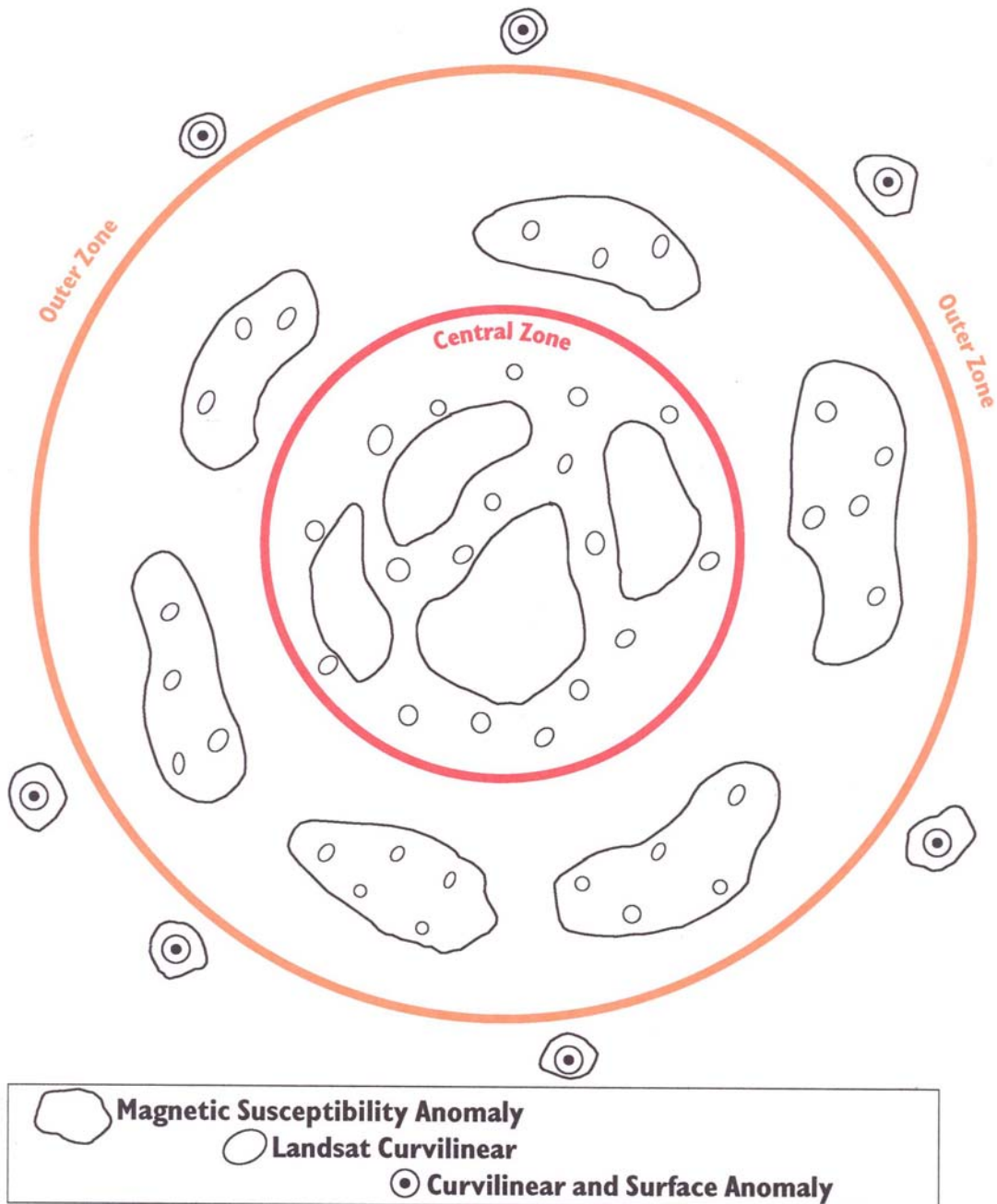


Figure 12

Summary sketch of the three zones of anomaly patterns above and around the central flux source associated with the Smoke Creek Aeromagnetic Anomaly.

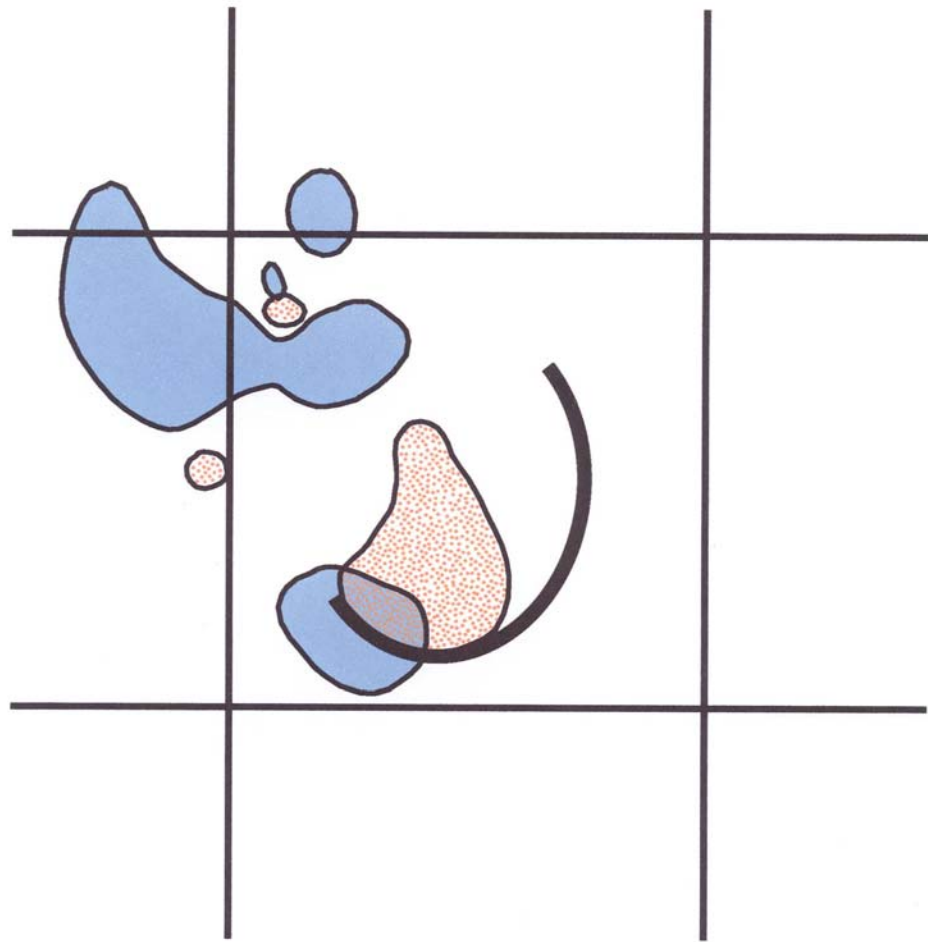


Figure 13

Cartoon summarizing the relationships of various data sets in Area 26. The heavy line is a Landsat curvilinear. Head gas propane is shown in blue and iodine is patterned in orange (Monson, 2002, p. 87 and 94 respectively).

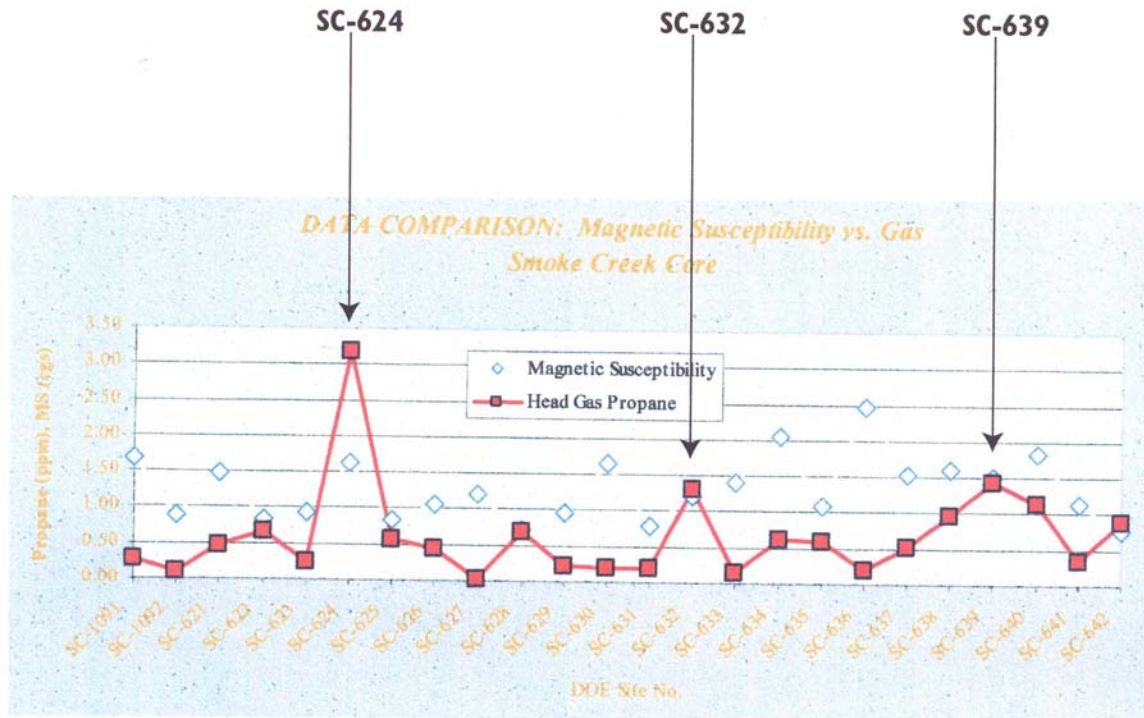


Figure 14

Comparison of magnetic susceptibility values and head gas propane along the profile through the Smoke Creek Core area (Monson, 2002, p. 119). Point SC-624 has high head gas propane and magnetic susceptibility and is located between curvilinear. Points SC-632 and SC-639 have high propane values and are at the edges of a diagenetic cap characterized by relatively high magnetic susceptibility.

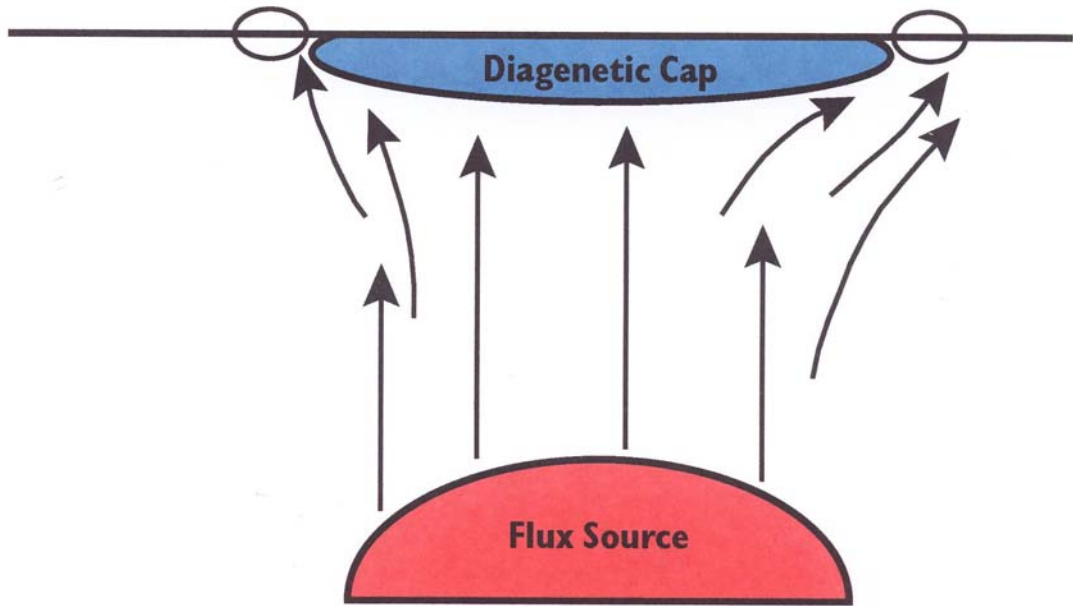


Figure 15

Cartoon illustrating a possible explanation for the distribution of small curvilinear features around the periphery of large magnetic susceptibility anomalies.

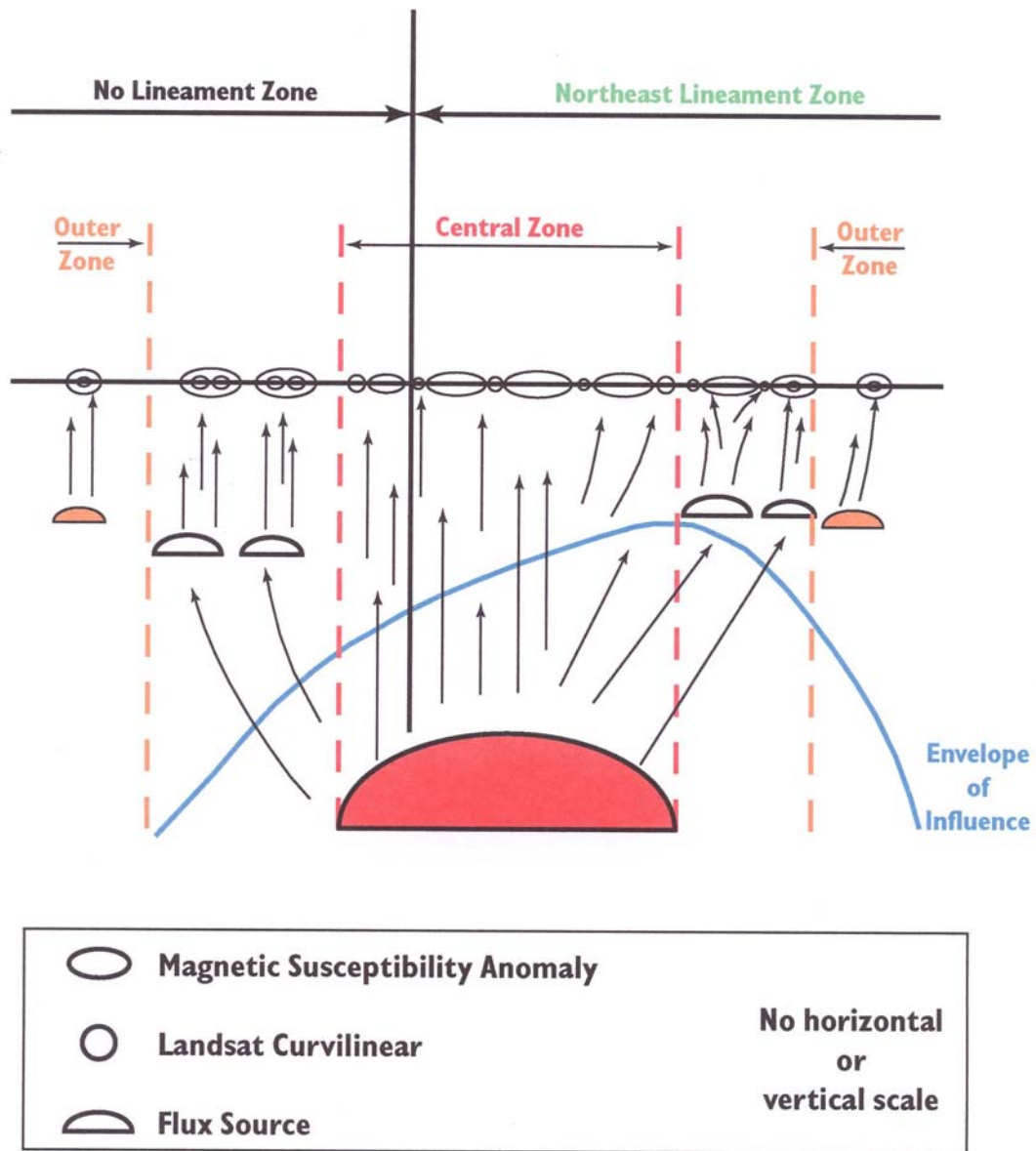


Figure 16

Sketch summarizing flux sources and plumbing geometries above the Smoke Creek Aeromagnetic Anomaly and in the surrounding domains defined by lineament zones.

APPENDIX C

TABLE WSW 1: WICAPE SOUTHWEST GPS SAMPLE SITES															
SITENO	VEG.	SLOPE	SOIL	MOIST.	TEMP	AIR P-psi	AIR UTM-Y	LONG UTM-X	ALT m	DEPTH-in. TOPO	(auger/probe)	DRAW-ml	SYRINGE	WEATHER	WIND
ws-w-aa1	grass	flat	silt	dry	55	28.6	5368876	470811.	730.	plain	3530	1.1	partly overcast	15-20n	
ws-w-aa2	grass	flat	silt	dry	60	28.7	5368871	471215.	726.	plain	3627	0.0	partly overcast	15-20n	
ws-w-aa3	grass	flat	silt	dry	58	28.5	5368868	471603.	721.	hillside	3630	0.7	partly overcast	15-20n	
ws-w-aa4	weeds	steep	loam	damp	62	28.5	5368869	472009.	718.	hillside	3630	0.0	partly overcast	15-20n	
ws-w-aa5	stubble	gentle	silt	dry	60	28.5	5368858	472403.	713.	hillside	3223	0.9	partly overcast	15-20n	
ws-w-aa6	stubble	flat	silt	dry	60	28.9	5368861	472818.	711.	plain	2630	2.5	partly overcast	15-20n	
ws-w-bb1	grass	flat	silt	dry	63	28.6	5368677	470616.	732.	plain	3622	1.7	partly overcast	10nw	
ws-w-bb2	grass	flat	loam	damp	63	28.5	5368672	471008.	727.	plain	3635	1.7	partly overcast	10nw	
ws-w-bb3	grass	flat	silt	dry	63	28.5	5368670	471416.	724.	plain	3628	0.9	partly overcast	10nw	
ws-w-bb4	grass	flat	loam	damp	63	28.6	5368650	471793.	721.	plain	3620	1.1	partly overcast	10nw	
ws-w-bb5	stubble	flat	loam	dry	60	28.4	5368658	472228.	716.	plain	3620	1.1	partly overcast	10nw	
ws-w-bb6	stubble	flat	silt	dry	65	28.4	5368650	472614.	711.	plain	3425	0.9	cloudy	10w	
ws-w-bb7	stubble	flat	silt	dry	65	28.4	5368646	473016.	711.	plain	3628	1.1	cloudy	10w	
ws-w-cc1	grass	flat	silt	dry	58	28.5	5368278	470615.	732.	plain	3630	2.6	cloudy	18-30nw	
ws-w-cc2	grass	flat	loam	damp	60	28.5	5368288	471008.	729.	plain	3628	0.7	cloudy	15-20w	
ws-w-cc3	grass	flat	silt	dry	59	28.5	5368285	471420.	727.	plain	3634	0.0	cloudy	15-20w	
ws-w-cc4	grass	flat	silt	dry	62	28.3	5368288	471813.	724.	plain	3630	1.2	cloudy	15-20w	
ws-w-cc5	stubble	flat	silt	dry	62	28.3	5368285	472233.	720.	plain	3621	1.0	cloudy	15-20w	
ws-w-cc6	stubble	flat	silt	dry	62	28.5	5368273	472609.	715.	plain	3322	2.6	cloudy	15-20w	
ws-w-cc7	stubble	flat	silt	dry	62	28.5	5368278	473023.	709.	plain	3530	0.4	cloudy	15w	
ws-w-r1	grass	gentle	sandy loam	damp	93	28.0	5370699	470618.	704.	bench	3636	0.0	partly cloudy	5sw	
ws-w-r2	grass	flat	clay	dry	92	27.8	5370693	470982.	703.	bench	3232	1.5	partly cloudy	calm	
ws-w-r3	grass	steep	sandy loam	dry	92	27.6	5370693	471414.	706.	hillside	3635	2.5	partly cloudy	calm	
ws-w-r4	grass	gentle	sandy loam	dry	92	27.5	5370694	471832.	700.	hillside	2420	3.5	partly cloudy	10sw	
ws-w-r5	grass	flat	silty	dry	91	27.7	5370687	472264.	689.	bench	3426	1.4	partly cloudy	5sw	
ws-w-r6	grass	flat	silt	dry	90	27.8	5370728	472562.	686.	bench	3626	0.6	partly cloudy	5-10sw	
ws-w-r7	grass	flat	silty	dry	90	27.7	5370686	473035.	686.	bench	3632	0.6	partly cloudy	5sw	
ws-w-s1	grass	gentle	gravel	dry	78	28.2	5370525	470028.	709.	hillside	1512	0.0	cloudy	5-10n	
ws-w-s2	grass	gentle	clay	dry	78	28.2	5370488	470459.	708.	bench	3424	3.5	cloudy	0-10	
ws-w-s3	grass	gentle	silt	dry	78	28.2	5370500	470838.	710.	hillside	3520	3.5	cloudy	0-10n	
ws-w-s4	grass	flat	silt	dry	78	28.2	5370497	471221.	722.	plain	3630	1.5	cloudy	0-10n	
ws-w-s5	grass	gentle	silt	dry	78	28.2	5370487	471659.	714.	hilltop	3628	0.0	cloudy	5-10nw	
ws-w-s6	grass	flat	silt	dry	78	28.2	5370483	472040.	710.	hilltop	3623	0.5	partly overcast	10-20nw	
ws-w-s7	grass	gentle	clay	dry	78	28.2	5370483	472426.	690.	hillside	3320	0.5	partly overcast	5-10nw	
ws-w-s8	grass	gentle	silt	dry	78	28.2	5370481	472786.	687.	hillside	3531	0.5	partly overcast	5-10nw	
ws-w-t1	summer	flat	loam	damp	76	27.9	5370307	469851.	729.	plain	3525	0.4	cloudy	15-25nw	
ws-w-t2	stubble	flat	silt	dry	76	27.9	5370241	470262.	728.	plain	3530	0.2	cloudy	15nw	
ws-w-t3	grass	flat	silt	dry	78	27.9	5370254	470674.	722.	plain	3621	0.0	cloudy	15nw	
ws-w-t4	grass	flat	silt	dry	82	27.8	5370268	471054.	718.	plain	2426	1.1	cloudy	10nw	
ws-w-t5	grass	flat	silt	dry	84	28.2	5370285	471424.	715.	plain	3618	0.0	cloudy	10nw	
ws-w-t6	grass	flat	silt	dry	84	28.2	5370275	471809.	712.	plain	3020	0.0	cloudy	10nw	
ws-w-t7	grass	flat	silt	dry	84	28.2	5370256	472259.	706.	hilltop	3628	1.6	partly overcast	10nw	
ws-w-t8	grass	flat	silt	dry	84	28.2	5370265	472630.	701.	plain	3218	2.6	partly overcast	10nw	
ws-w-t9	grass	gentle	silt	dry	78	28.2	5370278	473025.	684.	hillside	3028	0.5	partly overcast	5-10nw	
ws-w-u1	stubble	gentle	silt	dry	78	28.6	5370096	470067.	722.	hillside	3221	0.0	sunny	20nw	
ws-w-u2	stubble	flat	silt	dry	78	28.6	5370084	470452.	723.	plain	3628	3.6	sunny	20nw	
ws-w-u3	grass	gentle	silt	dry	78	28.6	5370072	470887.	717.	plain	3632	0.7	sunny	20nw	
ws-w-u4	grass	gentle	silt	dry	78	28.6	5370046	471253.	715.	hillside	2420	1.0	sunny	20nw	
ws-w-u5	grass	flat	silt	dry	78	28.6	5370055	471654.	713.	plain	2622	0.0	sunny	20nw	
ws-w-u6	grass	flat	silt	dry	70	28.6	5370035	472061.	711.	plain	3632	1.9	sunny	20nw	
ws-w-u7	grass	flat	silt	dry	68	28.6	5370053	472439.	707.	plain	3620	0.2	sunny	20nw	
ws-w-u8	grass	flat	loam	damp	68	28.6	5370057	472815.	695.	hilltop	3631	1.8	sunny	15nw	
ws-w-v1	grass	flat	silt	dry	48	29.0	5369902	469846.	723.	bench	3727	0.1	sunny	calm	
ws-w-v2	grass	flat	silt	damp	60	29.0	5369902	470220.	716.	bench	3628	1.5	sunny	calm	
ws-w-v3	stubble	steep	loam	damp	62	28.4	5369889	470605.	715.	hillside	3637	0.1	sunny	calm	
ws-w-v4	grass	gentle	silt	dry	62	28.4	5369862	471074.	711.	hillside	3624	1.2	sunny	0-5n	
ws-w-v5	grass	gentle	silt	dry	62	28.4	5369854	471424.	706.	hillside	3628	2.8	sunny	0-5n	
ws-w-v6	grass	flat	silt	damp	62	28.4	5369857	471830.	707.	hilltop	3628	2.6	sunny	15-20n	
ws-w-v7	grass	gentle	silt	dry	62	28.5	5369869	472288.	706.	hillside	3521	0.1	sunny	12n	
ws-w-v8	grass	gentle	silt	dry	67	28.5	5369868	472631.	698.	hillside	3421	2.1	sunny	12n	
ws-w-v9	grass	flat	silt	dry	67	28.6	5369865	473032.	684.	bench	3630	0.0	sunny	15nw	
ws-w-w1	stubble	gentle	loam	damp	74	28.3	5369674	470088.	722.	plain	3636	0.6	sunny	15-20w	
ws-w-w2	stubble	gentle	loam	damp	74	28.3	5369684	470417.	718.	plain	3636	1.0	sunny	15-20w	
ws-w-w3	grass	gentle	loam	dry	74	28.3	5369663	470845.	711.	bottom	3321	0.0	sunny	15-20w	
ws-w-w4	grass	flat	silt	dry	76	28.3	5369693	471241.	706.	hillside	3626	0.4	sunny	15-20w	
ws-w-w5	weeds	flat	silt	dry	76	27.9	5369625	471625.	709.	plain	3624	1.2	sunny	15-20w	
ws-w-w6	grass	gentle	loam	damp	80	27.9	5369647	472058.	693.	bottom	3627	1.1	sunny	10w	
ws-w-w7	grass	flat	silt	dry	80	27.9	5369662	472448.	690.	bench	3629	2.5	sunny	19w	
ws-w-w8	grass	flat	silt	dry	80	27.9	5369665	472884.	689.	hillside	3620	0.0	sunny	19w	
ws-w-x1	stubble	flat	loam	damp	69	28.0	5369502	469850.	732.	plain	3634	1.0	sunny	0-5sw	
ws-w-x2	stubble	gentle	loam	damp	70	28.0	5369498	470209.	725.	plain	3632	2.8	sunny	0-5sw	
ws-w-x3	stubble	flat	loam	damp	77	27.8	5369488	470618.	721.	plain	2632	0.0	sunny	15-10w	

wsw-x4	grass	flat	silt	dry	77	27.8	5369504,471114,712,plain	2430	1.0	sunny	8-18w
wsw-x5	grass	flat	silt	dry	77	27.8	5369482,471423,711,plain	3635	0.0	sunny	15-20w
wsw-x6	grass	flat	silt	dry	79	27.8	5369458,471845,709,hilltop	2635	0.0	sunny	15-20w
wsw-x7	grass	flat	silt	dry	79	27.8	5369408,472288,705,hilltop	2420	0.0	sunny	15-20w
wsw-x8	grass	gentle	silt	dry	80	27.7	5369418,472604,705,hilltop	2628	0.4	sunny	15-20w
wsw-x9	grass	flat	silt	dry	80	27.9	5369424,473026,703,hilltop	2421	0.0	sunny	19w
wsw-y1	stubble	gentle	loam	damp	60	28.8	5369260,470109,733,plain	3634	0.0	partly overcast	20-30w
wsw-y1	stubble	gentle	loam	damp	60	28.8	5369260,470109,733,plain	3634	0.0	partly overcast	20-30w
wsw-y2	grass	steep	loam	dry	60	28.8	5369274,470394,725,hillside	3226	0.0	partly overcast	20-30w
wsw-y2	grass	steep	loam	dry	60	28.8	5369274,470394,725,hillside	3226	0.0	partly overcast	20-30w
wsw-y3	grass	flat	silt	dry	60	28.0	5369284,470846,730,hilltop	2620	0.0	partly overcast	20-30w
wsw-y3	grass	flat	silt	dry	60	28.0	5369284,470846,730,hilltop	2620	0.0	partly overcast	20-30w
wsw-y4	grass	flat	silt	dry	60	28.0	5369284,471214,721,plain	2626	1.5	partly overcast	20-30w
wsw-y4	grass	flat	silt	dry	60	28.0	5369284,471214,721,plain	2626	1.5	partly overcast	20-30w
wsw-y5	grass	steep	silt	dry	64	28.2	5369311,471645,710,hillside	3426	0.0	cloudy	20-30w
wsw-y5	grass	steep	silt	dry	64	28.2	5369311,471645,710,hillside	3426	0.0	cloudy	20-30w
wsw-y6	grass	gentle	silt	dry	62	28.3	5369314,472046,701,hillside	2824	0.0	cloudy	20-30w
wsw-y6	grass	gentle	silt	dry	62	28.3	5369314,472046,701,hillside	2824	0.0	cloudy	20-30w
wsw-y7	grass	steep	silt	dry	62	28.3	5369290,472394,700,hillside	3531	0.2	cloudy	25-30w
wsw-y7	grass	steep	silt	dry	62	28.3	5369290,472394,700,hillside	3531	0.2	cloudy	25-30w
wsw-y8	grass	flat	silt	dry	62	28.3	5369268,472788,707,plain	2321	1.3	cloudy	35w
wsw-y8	grass	flat	silt	dry	62	28.3	5369268,472788,707,plain	2321	1.3	cloudy	35w
wsw-z1	stubble	flat	loam	damp	56	28.8	5369064,469860,744,plain	3531	1.6	partly overcast	15-20n
wsw-z2	stubble	flat	silt	dry	56	28.2	5369068,470216,737,plain	2829	0.0	partly overcast	15-20n
wsw-z3	stubble	flat	loam	damp	56	28.2	5369064,470602,733,plain	3636	3.9	partly overcast	15-20n
wsw-z4	stubble	flat	loam	dry	56	28.2	5369075,471026,728,plain	3629	2.7	partly overcast	15-20n
wsw-z5	grass	flat	silt	dry	56	28.2	5369066,471411,722,plain	3630	1.6	partly overcast	15-20n
wsw-z6	grass	gentle	silt	damp	56	28.2	5369053,471813,716,hilltop	3625	3.8	partly overcast	15-20n
wsw-z7	grass	gentle	silt	damp	57	28.2	5369078,472217,703,bottom	3632	2.6	partly overcast	15-20n
wsw-z8	stubble	flat	silt	dry	57	28.2	5369067,472618,710,plain	3623	0.9	partly overcast	15-20n
wsw-z9	stubble	flat	silt	dry	60	28.9	5369067,473018,704,plain	2823	1.7	partly overcast	15-20n

TABLE WSW 1: HEAD GAS DATA WICARE SOUTHWEST PROSPECT

X	Y	Client	Sample	Lab #	METHANE	ETHANE	ETHENE	PROPANE	PROPENE	i-BUTANE	n-BUTANE	i-PENTANE	PENTANE	EH	PH	COND.	c3 anomaly	c3ratio	EH ratio	
470619	5370659 wsw-1	R1	12640	30.217	2.443	5.535	1.25	0.149	0.149	0.13	0.169	-111	6.79	1184	0.69	-1.57				
470983	5370654 wsw-2	R2	12641	152.73	10.239	15.85	4.004	0.152	0.287	1.27	0.381	-142.8	6.95	1327	2.20	-2.02				
471412	5370653 wsw-3	R3	12642	14.458	0.931	0.944	0.427	0.151	0.013	0.163	0.085	125.4	7.35	5820	0.23	1.77				
471833	5370654 wsw-4	R4	12643	104.85	7.617	7.67	2.938	0.153	0.248	0.862	0.047	5.18	7.7	1427	1.61	-0.11				
472264	5370655 wsw-5	R5	12644	77.548	3.35	11.375	1.1763	0.123	0.157	1.168	0.209	0.542	-130	6.58	1278	0.97	-1.84			
472563	5370728 wsw-6	R6	12645	38.817	1.969	7.287	0.941	0.114	0.124	0.429	0.079	0.221	-40.1	6.75	963	0.52	-0.57			
473035	5370686 wsw-7	R7	12646	29.773	1.104	5.044	0.721	0.166	0.104	0.43	0.147	0.434	-39	6.73	1189	0.40	-0.55			
470029	5370526 wsw-8	S1	12647	115.02	7.202	30.505	4.929	0.113	0.369	2.055	0.531	2.001	-119.1	6.86	1534	2.71	-1.68			
470460	5370489 wsw-9	S2	12648	47.979	1.839	9.568	1.067	0.057	0.006	0.574	0.189	0.569	-84.4	6.56	1466	0.59	-1.19			
470839	5370501 wsw-10	S3	12649	55.647	1.243	11.226	0.845	0.065	0.01	0.679	0.159	0.282	-8	6.33	1018	0.46	-0.11			
471221	5370498 wsw-11	S4	12650	14.811	0.744	3.022	0.355	0.114	0.045	0.222	0.191	0.22	119.7	7	763	0.19	1.69			
471660	5370488 wsw-12	S5	12651	16.1	0.874	2.104	0.426	0.152	0.017	0.364	0.007	0.38	150.8	7.18	648	0.23	2.13			
472041	5370483 wsw-13	S6	12652	31.547	2.137	3.754	1.132	0.126	0.052	0.61	0.187	0.367	166.5	7.79	870	0.62	2.35			
472426	5370484 wsw-14	S7	12653	40.316	4.063	6.572	1.686	0.136	0.178	0.791	0.027	0.694	-1.6	7.12	1070	0.93	-0.02			
472786	5370482 wsw-15	S8	12654	67.663	2.716	9.736	1.44	0.139	0.148	0.866	0.025	0.723	-27.6	6.63	1091	0.79	-0.39			
498951	5370308 wsw-16	T1	12655	2.636	0.205	0.203	0.112	0.041	0.013	0.065	0.147	0.105	140.5	8.13	2390	0.00	1.99			
470263	5370241 wsw-17	T2	12656	12.541	0.738	1.113	0.437	0.102	0.087	0.407	0.229	0.163	171.7	7.45	757	0.24	2.43			
470675	5370259 wsw-18	T3	12657	11.189	0.747	1.135	0.465	0.125	0.091	0.582	0.021	0.218	186	7.55	1261	0.26	2.63			
471055	5370269 wsw-19	T4	12658	39.972	3.188	7.923	1.59	0.128	0.009	0.838	0.04	0.216	76.7	6.5	1166	0.87	-1.08			
471425	5370286 wsw-20	T5	12659	14.156	0.834	1.933	0.553	0.129	0.005	0.601	0.148	0.231	108.1	6.92	846	0.30	1.53			
471810	5370276 wsw-21	T6	12660	29.484	2.641	4.182	1.136	0.127	0.148	0.9	0.136	0.447	164.1	6.85	851	0.62	2.32			
472259	5370256 wsw-22	T7	12661	10.311	0.459	2.398	0.294	0.152	0.081	0.336	0.06	0.175	172.2	7.35	1030	0.16	1.93			
472626	5370268 wsw-23	T8	12662	50.911	3.581	6.944	1.585	0.037	0.165	0.746	0.218	0.667	-16.1	6.76	1136	0.87	-0.23			
472831	5370278 wsw-24	T9	12663	70.887	7.799	11.168	3.32	0.108	0.008	0.867	0.204	0.052	71.1	6.73	995	1.82	1.00			
473025	5370097 wsw-25	T10	12664	38.753	3.456	3.456	1.275	0.109	0.009	0.441	0.125	0.173	176.7	7.25	721	0.70	1.17			
470067	5370097 wsw-26	U1	12665	23.679	1.313	1.82	0.747	0.122	0.039	0.166	0.083	0.231	154.6	7.29	740	0.41	2.19			
470452	5370084 wsw-27	U2	12666	34.117	2.345	6.163	1.116	0.185	0.178	0.592	0.131	0.189	158.8	6.84	905	0.61	2.24			
470888	5370072 wsw-28	U3	12667	33.105	2.924	5.376	1.402	0.135	0.14	0.766	0.139	0.541	140.9	6.95	935	0.77	1.99			
471253	5370047 wsw-29	U4	12668	24.645	1.478	4.085	0.688	0.103	0.14	1.013	0.149	0.578	167.6	6.95	915	0.38	0.38			
471655	5370056 wsw-30	U5	12669	12.27	0.741	1.673	0.33	0.114	0.008	0.451	0.118	0.224	143.3	7.2	737	0.18	2.03			
472062	5370053 wsw-31	U6	12670	13.618	0.914	0.83	0.525	0.127	0.106	0.866	0.149	0.279	172.8	7.56	702	0.29	2.44			
472439	5370054 wsw-32	U7	12671	11.763	0.623	1.843	0.488	0.099	0.052	0.368	0.224	0.201	200.1	7.1	1025	0.41	2.83			
472816	5370057 wsw-33	U8	12672	18.22	1.037	2.121	0.606	0.128	0.098	0.572	0.013	0.209	157.2	6.97	836	0.33	2.22			
498947	5369847 wsw-34	U9	12673	41.865	3.982	3.223	0.532	0.03	0.242	0.768	0.246	0.359	167.6	7.47	687	0.84	2.37			
470221	5369802 wsw-35	V2	12674	41.507	2.619	16.296	2.004	0.26	0.285	0.323	0.031	0.578	16.7	7.75	1141	0.86	-0.67			
470606	5369866 wsw-36	V3	12675	25.69	1.357	3.898	0.733	0.121	0.041	0.525	0.163	0.307	96.7	6.86	884	0.40	1.37			
471075	5369862 wsw-37	V4	12676	18.456	0.798	3.32	0.49	0.131	0.084	0.647	0.125	0.383	115.9	7.31	849	0.27	1.64			
471424	5369855 wsw-38	V5	12677	9.496	0.849	0.723	0.4	0.115	0.006	0.877	0.05	0.057	160.1	7.8	686	0.22	2.26			
471830	5369857 wsw-39	V6	12678	37.801	3.826	5.985	1.736	0.083	0.142	0.877	0.152	0.476	142.2	6.9	1058	0.95	2.01			
472289	5369870 wsw-40	V7	12679	32.815	2.704	4.551	1.246	0.011	0.117	0.754	0.014	0.425	84.8	6.95	856	0.88	1.20			
472631	5369868 wsw-41	V8	12680	74.912	14.772	1.571	0.116	0.01	0.658	0.101	0.154	-25.7	6.75	1141	0.86	-0.67				
473033	5369866 wsw-42	V9	12681	4.974	0.434	0.273	0.203	0.097	0.045	0.078	0.045	0.436	138.2	6.28	963	0.58	1.95			
471077	5369865 wsw-43	W1	12682	6.644	0.341	0.499	0.282	0.12	0.075	0.084	0.813	0.58	0.588	-3.1	6.98	909	0.11	1.61		
470047	5369868 wsw-44	W2	12683	29.491	1.059	8.83	0.782	0.039	0.137	0.158	0.221	0.789	158.3	7.93	722	0.15	2.24			
470846	5369864 wsw-45	W3	12684	26.669	1.45	5.266	0.72	0.133	0.086	0.407	0.334	0.407	150.8	6.71	1536	0.43	1.57			
471241	5369864 wsw-46	W4	12685	16.549	0.707	2.776	0.46	0.027	0.036	0.301	0.445	1.111	106.6	6.7	896	0.25	1.51			
472058	5369847 wsw-46	W6	12686	48.521	2.206	13.905	1.065	0.072	0.127	0.922	0.319	0.436	113.8	6.28	963	0.58	1.95			
472448	5369862 wsw-47	W7	12687	62.895	4.784	5.898	1.828	0.108	0.2	0.813	0.58	0.588	-3.1	6.98	909	0.11	1.61			
472885	5369866 wsw-48	W8	12688	30.261	2.08	4.035	1.133	0.215	0.53	0.981	0.602	0.508	147.6	7.11	687	0.62	2.24			
469850	5369852 wsw-49	X1	12689	38.727	4.065	7.83	1.892	0.042	0.172	0.884	0.575	0.524	203.8	6.64	883	1.04	2.88			
470209	5369849 wsw-50	X2	12690	17.108	1.323	1.706	0.672	0.718	0.334	0.648	0.372	0.654	1.919	7.36	739	0.37	2.88			
470619	5369848 wsw-51	X3	12691	32.892	10.419	25.038	5.242	0.124	0.692	1.792	1.344	1.919	186.2	6.58	987	0.28	2.88			
471114	53698504 wsw-52	X4	12693	38.528	1.784	9.132	1.284	0.02	0.02	0.959	0.287	0.577	161.4	6.32	1081	0.70	2.28			

TABLE WSW 2

TABLE WSW1: HEAD GAS DATA, WICAPPE SOUTHWEST PROSPECT

X	Y	Client	SAMPLE LAB#	METHANE	ETHANE	ETHENE	PROPANE	PROPENE	i-BUTANE	n-BUTANE	i-PENTANE	PENTANE	EH	PH	COND.	c3 anomaly	c3 ratio	EH ratio	
471423	5369483	wsw-x5	X5	16.761	0.909	3.979	0.047	1.485	0.682	1.109	0.353	0.188	111.1	6.79	877	0.03	1.57		
471846	5369458	wsw-x6	X6	12695	29.383	3.711	4.179	1.653	0.127	0.181	0.88	0.185	0.528	160.8	7.05	939	0.91	2.27	
472289	5369409	wsw-x7	X7	12696	23.331	1.527	4.773	0.873	0.09	0.1	0.529	0.053	0.337	197.6	6.66	961	0.48	2.79	
472604	5369418	wsw-x8	X8	12697	11.461	0.836	4.767	0.773	0.142	0.131	0.613	0.072	0.361	198.1	7.36	1276	0.42	2.80	
473026	5369425	wsw-x9	X9	12698	30.186	2.248	7.97	1.224	0.155	0.077	0.854	0.365	0.447	71.7	6.45	983	0.67	1.01	
470110	5369261	wsw-y1	Y1	12699	19.041	1.842	1.762	0.995	0.072	0.121	0.589	0.211	0.29	156.5	7.27	674	0.55	2.21	
470395	5369275	wsw-y2	Y2	12700	23.863	2.066	8.966	1.161	0.114	0.105	0.584	0.135	0.846	170.2	6.93	1409	0.64	2.41	
470847	5369284	wsw-y3	Y3	12701	35.756	2.919	5.371	1.53	0.028	0.201	1.116	0.367	0.501	130.9	6.86	726	0.84	1.85	
471215	5369285	wsw-y4	Y4	12702	20.337	2.107	3.333	1.026	0.044	0.115	0.489	0.067	0.389	174.5	6.9	894	0.56	2.47	
471646	5369311	wsw-y5	Y5	12703	69.92	5.467	12.751	2.591	0.113	0.254	1.927	0.246	1.049	160.6	6.66	1020	1.42	2.27	
472046	5369314	wsw-y6	Y6	12705	1.601	9.733	0.825	0.107	0.102	0.78	0.161	0.842	197.7	6.1	820	0.45	2.79		
472395	5369280	wsw-y7	Y7	12706	33.04	1.656	10.439	0.984	0.111	0.088	0.632	0.132	0.549	202.1	6.34	854	0.54	2.86	
472788	5369268	wsw-y8	Y8	12715	32.342	1.267	8.979	0.737	0.046	0.098	0.811	0.101	0.3	172.3	6.57	1154	0.40	2.44	
469860	5369054	wsw-z1	Z1	12708	12.743	1.192	0.825	0.621	0.129	0.106	0.542	0.129	0.112	175.5	7.78	606	0.34	2.48	
470216	5369069	wsw-z2	Z2	12716	24.725	2.119	9.734	1.135	0.124	0.12	0.64	0.088	0.725	207.4	7.5	670	0.62	2.93	
470603	5369084	wsw-z3	Z3	12710	15.788	1.495	1.219	0.822	0.087	0.115	0.373	0.199	0.085	220.9	7.22	672	0.45	3.12	
471026	5369076	wsw-z4	Z4	12711	17.44	2.26	2.512	1.086	0.039	0.113	1	0.082	0.278	227.4	7.2	697	0.60	3.21	
471411	5369086	wsw-z5	Z5	12714	11.856	0.953	2.032	0.548	0.12	0.068	0.88	0.088	0.107	0.436	243.4	6.87	772	0.30	3.44
471813	5369053	wsw-z6	Z6	12713	6.876	0.587	0.384	0.233	0.087	0.057	0.412	0.071	0.243	213.9	7.74	449	0.13	3.01	
472218	5369079	wsw-z7	Z7	12717	44.289	5.007	6.742	2.109	0.073	0.206	1.318	0.253	0.733	257.5	6.49	798	1.16	3.64	
472619	5369067	wsw-z8	Z8	12718	10.255	0.693	1.508	0.411	0.104	0.07	0.378	0.105	0.155	247.1	6.97	768	0.23	3.49	
473019	5369067	wsw-z9	Z9	12719	96.079	12.303	13.931	5.303	0.07	0.489	2.172	0.552	1.156	247.4	6.93	971	2.91	3.50	
470812	5369877	wsw-aa1	AA1	12720	13.389	1.486	1.727	0.744	0.06	0.089	0.71	0.156	0.218	240.4	7.01	605	0.41	3.40	
471215	5369872	wsw-aa2	AA2	12721	8.825	0.618	0.516	0.429	0.017	0.091	0.658	0.118	0.14	240.6	7.24	564	0.24	3.40	
471603	5369869	wsw-aa3	AA3	12722	11.966	0.953	1.222	0.601	0.087	0.049	0.291	0.161	0.371	242.8	7.37	786	0.33	3.43	
472009	5369870	wsw-aa4	AA4	12723	9.741	0.879	0.747	0.624	0.09	0.01	0.444	0.135	0.12	241.2	7.38	758	0.34	3.41	
472403	5369859	wsw-aa5	AA5	12724	24.557	3.084	5.841	1.445	0.06	0.165	0.832	0.191	0.594	248.6	7.03	830	0.79	3.52	
472818	5369862	wsw-aa6	AA6	12725	19.652	1.568	2.396	0.797	0.058	0.107	0.492	0.129	0.188	257.3	6.93	784	0.44	3.64	
470617	5369878	wsw-bb1	BB1	12726	16.652	2.129	3.806	1.183	0.104	0.172	0.701	0.209	0.175	246	6.67	775	0.65	3.48	
471008	53698673	wsw-bb2	BB2	12727	24.705	3.433	3.074	1.815	0.007	0.178	0.973	0.267	0.382	230.6	7.53	680	1.00	3.26	
471417	53698670	wsw-bb3	BB3	12728	8.147	1.01	2.092	0.501	0.076	0.008	0.237	0.096	0.084	256.8	6.79	951	0.28	3.63	
471794	5369851	wsw-bb4	BB4	12729	12.297	2.098	2.074	1.292	0.102	0.154	1.208	0.18	0.388	238.2	7.7	625	0.71	3.37	
472229	5369859	wsw-bb5	BB5	12730	10.861	1.828	2.147	0.909	0.102	0.088	0.531	0.144	0.159	234.3	7.82	682	0.50	3.31	
472615	5369850	wsw-bb6	BB6	12731	22.145	5.563	5.634	1.448	0.095	0.006	0.763	0.025	0.184	263.8	6.96	749	0.73	3.73	
473016	5369846	wsw-bb7	BB7	12732	17.988	2.488	2.524	1.22	0.089	0.008	0.623	0.159	0.036	243.2	7.56	618	0.67	3.44	
470615	5369878	wsw-cc1	CC1	12734	11.379	0.903	0.945	0.477	0.136	0.096	0.863	0.164	0.168	246.6	7.42	593	0.28	3.49	
471008	5369828	wsw-cc2	CC2	12735	12.656	1.356	2.538	1.653	0.153	0.159	0.778	0.254	0.3	263.3	6.97	643	0.91	3.72	
471421	5369826	wsw-cc3	CC3	12736	13.678	1.741	2.524	0.86	0.124	0.075	0.663	0.113	0.245	256.5	7.31	719	0.47	3.61	
471813	5369829	wsw-cc4	CC4	12737	20.083	3.333	2.938	1.626	0.15	0.156	0.659	0.227	0.091	250.4	7.4	556	0.89	3.54	
472234	5369826	wsw-cc5	CC5	12738	13.308	1.613	1.51	0.837	0.127	0.128	0.379	0.091	0.069	248.9	7.47	611	0.46	3.52	
472609	53698274	wsw-cc6	CC6	12739	30.2	3.94	3.893	2.029	0.098	0.197	0.785	0.256	0.155	259	7.13	765	1.11	3.66	
473024	53698278	wsw-cc7	CC7	12740	21.368	2.544	3.136	1.256	0.071	0.154	1.572	0.217	0.295	259.4	7.29	713	0.69	3.67	
Harmonic Mean Anomaly (2xHM)																			
average																			
std dev																			
minimum																			
maximum																			
Anomaly (1.5 x mean)																			

TABLE WSW 2B

ANOMALY INDEX RATIO (AIR)												
Value / anomaly ratio (1.5 x mean)			[Except for Eh] Eh air = -1 x (Eh - mean) / (mean - min)/2									
METHANE	ETHANE	ETHENE	PROPANE	PROPENE	i-BUTANE	n-BUTANE	i-PENTANE	PENTANE	EH	PH	COND.	SAMPLE
0.65	0.67	0.69	0.69	0.81	0.76	0.46	0.44	0.28	1.73	0.89	0.82	R1
3.28	2.80	1.97	2.22	0.82	1.47	1.08	1.28	1.66	2.00	0.91	0.91	R 2
0.31	0.25	0.12	0.24	0.82	0.07	0.14	0.29	0.00	-0.26	0.96	4.01	R 3
2.25	2.08	0.95	1.63	0.83	1.27	0.74	0.16	0.86	0.86	0.92	0.98	R 4
1.67	0.92	1.45	0.98	0.66	0.81	1.00	0.70	0.90	1.89	0.86	0.88	R 5
0.83	0.54	0.91	0.52	0.62	0.64	0.37	0.27	0.37	1.13	0.88	0.66	R 6
0.64	0.30	0.63	0.40	0.90	0.53	0.37	0.49	0.72	1.12	0.88	0.82	R 7
2.47	1.97	3.79	2.73	0.61	1.89	1.75	1.79	3.33	1.80	0.90	1.06	S 1
1.03	0.50	1.19	0.59	0.31	0.03	0.49	0.67	0.95	1.51	0.86	1.01	S 2
1.20	0.34	1.39	0.47	0.35	0.05	0.58	0.53	0.47	0.86	0.83	0.70	S 3
0.32	0.20	0.38	0.20	0.62	0.23	0.49	0.64	0.37	-0.21	0.91	0.53	S 4
0.35	0.24	0.26	0.24	0.82	0.09	0.31	0.02	0.63	-0.48	0.94	0.45	S 5
0.68	0.58	0.47	0.63	0.68	0.27	0.52	0.63	0.61	-0.61	1.02	0.60	S 6
0.87	1.11	0.82	0.94	0.74	0.91	0.67	0.09	1.16	0.81	0.93	0.74	S 7
1.45	0.74	1.21	0.80	0.75	0.81	0.74	0.08	1.20	1.03	0.87	0.75	S 8
0.06	0.06	0.03	0.00	0.61	0.21	0.01	0.22	0.00	-0.39	1.06	1.65	T 1
0.27	0.20	0.14	0.24	0.55	0.45	0.35	0.77	0.27	-0.65	0.97	0.52	T 2
0.24	0.20	0.14	0.26	0.68	0.47	0.50	0.07	0.36	-0.77	0.99	0.87	T 3
0.86	0.87	0.98	0.88	0.69	0.05	0.71	0.13	0.36	1.44	0.85	0.80	T 4
0.30	0.23	0.24	0.31	0.70	0.03	0.51	0.50	0.38	-0.12	0.90	0.58	T 5
0.63	0.72	0.52	0.63	0.69	0.76	0.77	0.46	0.74	-0.59	0.89	0.59	T 6
0.22	0.13	0.30	0.16	0.82	0.42	0.29	0.20	0.29	-0.66	0.96	0.71	T 7
1.09	0.98	0.86	0.88	0.20	0.85	0.64	0.73	1.11	0.93	0.88	0.78	T 8
1.52	2.13	1.39	1.84	0.59	0.04	0.74	0.69	0.09	0.20	0.88	0.69	T 9
0.83	0.66	0.43	0.71	0.59	0.05	0.38	0.42	0.29	0.10	0.95	0.50	U 1
0.51	0.36	0.23	0.41	0.66	0.20	0.14	0.31	0.00	-0.51	0.95	0.51	U 2
0.73	0.64	0.77	0.62	1.00	0.91	0.51	0.44	0.31	-0.54	0.89	0.62	U 3
0.71	0.80	0.67	0.78	0.73	0.72	0.65	0.47	0.90	-0.39	0.91	0.64	U 4
0.53	0.40	0.51	0.38	0.56	0.72	0.86	0.50	0.96	0.57	0.91	0.63	U 5
0.26	0.20	0.21	0.18	0.62	0.04	0.30	0.40	0.00	-0.41	0.94	0.51	U 6
0.29	0.25	0.10	0.29	0.69	0.54	0.74	0.50	0.46	-0.66	0.99	0.48	U 7
0.25	0.17	0.23	0.27	0.54	0.27	0.31	0.00	0.37	-0.89	0.93	0.71	U 8
0.39	0.28	0.26	0.34	0.69	0.50	0.49	0.04	0.35	-0.53	0.91	0.58	V 1
0.90	1.09	0.40	0.85	0.16	1.24	0.66	0.83	0.60	-0.62	0.98	0.47	V 2
0.89	0.72	2.02	1.11	0.25	1.33	0.70	1.11	1.05	1.01	0.88	0.79	V 3
0.55	0.37	0.48	0.41	0.65	0.21	0.45	0.55	0.51	-0.02	0.90	0.61	V 4
0.40	0.22	0.41	0.27	0.71	0.43	0.55	0.42	0.64	-0.18	0.95	0.59	V 5
0.20	0.18	0.09	0.22	0.62	0.03	0.35	0.17	0.09	-0.55	1.02	0.47	V 6
0.81	1.05	0.74	0.96	0.50	0.73	0.75	0.51	0.79	-0.40	0.90	0.73	V 7
0.70	0.74	0.56	0.69	0.06	0.60	0.64	0.05	0.71	0.08	0.91	0.59	V 8
1.59	0.80	1.84	0.87	0.63	0.05	0.56	0.34	0.26	1.19	0.88	0.79	V 9
0.11	0.12	0.03	0.11	0.52	0.23	0.07	0.00	1.65	-0.16	1.08	1.10	W 1
0.14	0.09	0.06	0.16	0.65	0.38	0.07	1.15	1.31	-0.54	1.04	0.50	W 2
0.63	0.29	1.10	0.43	0.21	0.70	0.75	1.26	0.26	-0.14	0.88	1.06	W 3
0.57	0.40	0.65	0.40	0.72	0.44	0.35	1.12	0.37	-0.05	0.87	0.71	W 4
0.36	0.19	0.34	0.26	0.15	0.18	0.26	1.50	1.85	-0.10	0.88	0.62	W 5
1.04	0.60	1.73	0.59	0.39	0.65	0.79	1.07	0.73	-0.37	0.82	0.66	W 6
1.35	1.31	0.73	1.01	0.57	1.03	0.69	1.95	0.98	0.82	0.91	0.63	W 7
0.65	0.57	0.50	0.63	1.16	2.72	0.85	2.03	0.85	-0.45	0.93	0.47	W 8
0.83	1.11	0.97	1.05	0.23	0.88	0.75	1.93	0.87	-0.92	0.87	0.61	X 1
0.37	0.36	0.21	0.37	3.88	1.71	0.55	2.20	0.62	-0.92	0.96	0.51	X 2
2.30	3.88	3.11	2.91	0.67	3.55	6.14	4.52	3.20	-0.77	0.86	0.68	X 3
0.83	0.49	1.13	0.71	0.14	0.10	0.82	0.97	0.96	-0.57	0.83	0.75	X 4
0.36	0.25	0.49	0.03	8.03	3.50	0.95	1.19	0.31	-0.14	0.89	0.60	X 5
0.63	1.01	0.52	0.92	0.69	0.93	0.75	0.62	0.88	-0.56	0.92	0.65	X 6
0.50	0.42	0.59	0.48	0.49	0.51	0.45	0.18	0.56	-0.87	0.87	0.66	X 7
0.25	0.23	0.22	0.43	0.77	0.67	0.52	0.24	0.60	-0.88	0.96	0.88	X 8
0.65	0.61	0.99	0.68	0.84	0.39	0.73	1.23	0.74	0.19	0.84	0.68	X 9

0.41	0.50	0.22	0.55	0.39	0.62	0.50	0.71	0.48	-0.52	0.95	0.46	Y1
0.51	0.56	1.11	0.64	0.62	0.54	0.50	0.45	1.08	-0.64	0.91	0.97	Y2
0.77	0.80	0.67	0.85	0.15	1.03	0.95	1.23	0.83	-0.31	0.90	0.50	Y3
0.44	0.58	0.41	0.57	0.24	0.59	0.42	0.23	0.65	-0.68	0.90	0.62	Y4
1.50	1.49	1.58	1.44	0.61	1.30	1.64	0.83	1.75	-0.56	0.87	0.70	Y5
0.66	0.44	1.21	0.46	0.58	0.52	0.67	0.54	1.40	-0.87	0.80	0.57	Y6
0.71	0.45	1.30	0.55	0.60	0.45	0.54	0.44	0.91	-0.91	0.83	0.59	Y7
0.69	0.35	1.12	0.41	0.25	0.50	0.69	0.34	0.50	-0.66	0.86	0.80	Y8
0.27	0.33	0.10	0.34	0.70	0.54	0.46	0.43	0.19	-0.68	1.02	0.42	Z1
0.53	0.58	1.21	0.63	0.67	0.62	0.55	0.30	1.21	-0.95	0.98	0.46	Z2
0.34	0.41	0.15	0.46	0.47	0.59	0.32	0.67	0.14	-1.07	0.94	0.46	Z3
0.37	0.62	0.31	0.60	0.21	0.58	0.85	0.28	0.46	-1.12	0.94	0.48	Z4
0.26	0.26	0.25	0.30	0.65	0.35	0.75	0.36	0.73	-1.26	0.90	0.53	Z5
0.15	0.16	0.05	0.13	0.47	0.29	0.35	0.24	0.40	-1.00	1.01	0.31	Z6
0.95	1.37	0.84	1.17	0.39	1.06	1.12	0.85	1.22	-1.38	0.85	0.55	Z7
0.22	0.19	0.19	0.23	0.56	0.36	0.32	0.35	0.00	-1.29	0.91	0.53	Z8
2.06	3.36	1.73	2.94	0.38	2.41	1.85	1.86	1.93	-1.29	0.91	0.67	Z9
0.29	0.40	0.21	0.41	0.32	0.46	0.61	0.52	0.36	-1.23	0.92	0.42	AA1
0.19	0.17	0.06	0.24	0.09	0.47	0.56	0.40	0.23	-1.23	0.95	0.39	AA 2
0.26	0.26	0.15	0.33	0.47	0.25	0.25	0.54	0.62	-1.25	0.96	0.54	AA 3
0.21	0.24	0.09	0.35	0.49	0.05	0.38	0.45	0.20	-1.24	0.96	0.52	AA 4
0.53	0.84	0.73	0.80	0.32	0.85	0.71	0.64	0.99	-1.30	0.92	0.57	AA 5
0.42	0.43	0.30	0.44	0.31	0.55	0.42	0.43	0.28	-1.37	0.91	0.54	AA 6
0.36	0.58	0.47	0.66	0.56	0.88	0.60	0.70	0.29	-1.28	0.87	0.53	BB1
0.53	0.94	0.38	1.01	0.04	0.91	0.83	0.90	0.64	-1.15	0.98	0.45	BB 2
0.17	0.28	0.26	0.28	0.41	0.04	0.20	0.32	0.14	-1.37	0.89	0.66	BB 3
0.26	0.57	0.26	0.72	0.55	0.79	1.03	0.61	0.65	-1.21	1.01	0.43	BB 4
0.23	0.50	0.27	0.50	0.55	0.45	0.45	0.48	0.26	-1.18	1.02	0.46	BB 5
0.48	0.70	0.70	0.79	0.51	0.03	0.65	0.08	0.31	-1.43	0.91	0.52	BB 6
0.39	0.68	0.31	0.68	0.54	0.04	0.53	0.53	0.06	-1.26	0.99	0.43	BB 7
0.24	0.25	0.12	0.26	0.74	0.49	0.74	0.55	0.28	-1.28	0.97	0.41	CC1
0.51	0.86	0.65	0.92	0.83	0.82	0.66	0.85	0.50	-1.43	0.91	0.44	CC 2
0.29	0.48	0.31	0.48	0.67	0.38	0.57	0.44	0.41	-1.36	0.95	0.50	CC 3
0.43	0.91	0.37	0.90	0.81	0.80	0.59	0.76	0.15	-1.32	0.97	0.38	CC 4
0.29	0.44	0.19	0.46	0.69	0.66	0.32	0.31	0.11	-1.30	0.98	0.42	CC 5
0.65	1.08	0.48	1.13	0.54	1.01	0.67	0.86	0.26	-1.39	0.93	0.53	CC 6
0.46	0.70	0.39	0.70	0.38	0.79	1.34	0.73	0.49	-1.39	0.95	0.49	CC 7
0.39	0.36	0.25	0.05	0.38	0.18	0.32	0.10	0.03	#####	0.92	0.59	Harmonic Mean
0.78	0.73	0.50	0.09	0.76	0.37	0.63	0.21	0.06	#####	1.84	1.18	Anomaly (2xHM)
0.67	0.67	0.67	0.67	0.67	0.67	0.67	0.67	0.67	-0.40	0.92	0.67	average
0.56	0.64	0.64	0.55	0.86	0.64	0.65	0.62	0.58	0.88	0.06	0.40	std dev
0.06	0.06	0.03	0.00	0.04	0.03	0.01	0.00	0.00	-1.43	0.80	0.31	minimum
3.28	3.88	3.79	2.94	8.03	3.55	6.14	4.52	3.33	2.00	1.08	4.01	maximum
												Anomaly (1.5 x mean)

pH anomaly defined as mean x (max - mean)/2
Eh anomaly defined as mean / 1.5

TABLE WSW3: IN-HOUSE HEADGAS ANALYSIS
Wiecape SW Prospect Area

SAMPLE #	Raw Data in ppm				ANOMALY INDEX RATIO (AIR) Value / anomaly ratio (1.5 x mean)					
	C1	C2	C3	iC4	nC4	C1	C2	C3	iC4	nC4
R1	10.201	0.361	1.106	3.479	0.274	0.09	0.23	0.61	3.39	0.19
R2	85.309	0.858	8.341	0.182	2.279	0.78	0.55	4.58	0.18	1.58
R3	6.105	1.771	0.842	0.115	0.670	0.06	1.13	0.46	0.11	0.47
R4	42.824	2.846	0.723	0.152	0.163	0.39	1.82	0.40	0.15	0.11
R5	20.371	0.553	0.723	0.289	1.134	0.19	0.35	0.40	0.28	0.79
R6	23.431	0.508	0.788	0.111	1.664	0.21	0.33	0.43	0.11	1.16
S1										
S2	165.323		0.137		0.149	1.51		0.08		0.10
S3	152.989					1.40				
S4	9.094	0.075	0.457	0.079	0.356	0.08	0.05	0.25	0.08	0.25
S5	2.246	0.796	0.810	0.021	0.148	0.02	0.51	0.45	0.02	0.10
S6	21.428	0.228		0.188	0.799	0.20	0.15		0.18	0.56
S7	128.322		0.613	0.597	1.046	1.17		0.34	0.58	0.73
S8	46.095	0.256	0.425		0.525	0.42	0.16	0.23		0.37
T1	12.060	0.163	0.231		0.337	0.11	0.10	0.13		0.23
T2	4.645	2.219		2.169	3.243	0.04	1.42		2.11	2.26
T3	3.857	3.739	1.366	3.006	2.731	0.04	2.40	0.75	2.93	1.90
T4	153.015		0.116	0.558	1.067	1.40		0.06	0.54	0.74
T5	9.157	0.092		0.574	0.08	0.08				0.40
T6	8.244	0.498	1.687	0.620	1.772	0.08	0.32	0.93	0.60	1.23
T6	7.024	0.492	1.400	0.510	1.171	0.06	0.32	0.77	0.50	0.81
T7	38.353		0.346	0.334	0.661	0.35		0.19	0.33	0.46
T8	52.766			0.435	1.641	0.48			0.42	1.14
T9	70.281	1.545	1.218	0.772	1.455	0.64	0.99	0.67	0.75	1.01
U1	102.628		0.522	0.861	1.452	0.94	0.29	0.84	1.01	
U2	3.158	0.157		0.497		0.03	0.10		0.35	

TABLE WSW 3: IN-HOUSE HEADGASS ANALYSIS
Wicape SW Prospect Area

SAMPLE #	Raw Data in ppm					ANOMALY INDEX RATIO (AIR)				
	C1	C2	C3	iC4	nC4	C1	C2	C3	iC4	nC4
U3	67.522	0.175				0.62	0.11			0.81
U4	529.756					4.84				1.29
U5	166.990	1.719	1.770	1.809		1.52			0.94	1.73
U6	27.132	0.163	0.364	0.374		0.25	0.10			1.26
U7	10.147	0.190	0.324	1.017	1.757	0.09	0.12	0.18	0.35	0.26
U8	13.158	0.474	0.776	0.217	1.403	0.12	0.30	0.43	0.21	1.22
V1	45.699	0.158	0.438	3.628		0.42	0.10		0.43	0.98
V2	150.984	0.768	1.285	2.507		1.38			0.42	0.43
V3	336.683	0.305	0.117			3.07			1.25	2.52
V4	68.553	0.180	0.716			0.63	0.12		0.42	1.74
V5	12.055	0.311	0.673	0.132	1.048	0.11	0.20		0.17	0.08
V6	30.633			0.088	1.175	0.28			0.39	
V7	66.429	0.545	0.747		2.064	0.61	0.35		0.20	
V8	150.984					1.38			0.37	
V9	248.054	4.705	0.971	2.224		2.27			0.13	0.73
W1	3.930	1.475	1.794	0.435		0.04	0.94		0.99	0.30
W2	6.729	0.188	0.893	0.963	2.013	0.06	0.12		0.49	1.40
W3	293.354	0.258	0.485	1.360		2.68			0.14	0.47
W4	99.802	0.760	1.238	0.456	1.637	0.91	0.49		0.68	0.95
W5	45.027	0.344	0.500	0.606	1.774	0.41	0.22		0.27	1.14
W6	79.065	0.958	1.783		0.915	0.72	0.61		0.98	1.23
W7	72.361	2.510	1.785	0.167	1.542	0.66	1.61		0.98	0.44
W8	8.961	0.237	0.614	0.667	1.698	0.08	0.15		0.34	1.18
X1	65.240	0.205		1.873	0.816	0.60	0.13		1.83	0.57
X2	85.977		0.402	2.217	0.534	0.79	0.22		2.16	0.37
X3	6.483	0.177		0.378		0.06	0.11		0.22	0.26

TABLE WSW 3: IN-HOUSE HEADGAS ANALYSIS
Wicape SW Prospect Area

SAMPLE #	Raw Data in ppm						ANOMALY INDEX RATIO (AIR)				
	C1	C2	C3	iC4	nC4	Value / anomaly ratio (1.5 x mean)	C1	C2	C3	iC4	nC4
X4	213.859			0.052	0.228		1.95			0.05	0.16
X5	10.169	0.816	0.103			0.09	0.45	0.10			
X6	175.840	0.756	0.361			1.61	0.42				0.25
X7	52.588	0.206	0.441	0.603		0.48	0.13	0.24	0.59		
X8	65.240	0.390	0.837		0.189	0.60	0.25	0.46			
X9	189.666		0.468	0.072		1.73			0.46		
Y1	8.846	0.838		3.352	3.150	0.08	0.54		3.27		
Y2	217.316	0.563	0.566	1.822		1.98		0.31	0.55		
Y3	85.977	6.957	2.268	0.035		0.79		3.82	2.21		
Y4	52.029	0.157	0.315	0.443	0.243	0.48	0.10	0.17	0.43		
Y5	65.240	0.556	1.139	0.586	1.215	0.60	0.36	0.63	0.57		
Y6	535.293					4.89					
Y7	521.468	0.386		0.191		4.76		0.21			
Y8	286.441					2.62					
Z1	13.123	0.029	0.249	0.565	0.896	0.12	0.02	0.14	0.55		
Z2	18.749	0.383	0.737	0.187	0.162	0.17	0.25	0.40	0.18		
Z3	5.174	1.438	0.408	0.466	1.094	0.05	0.92	0.22	0.45		
Z4	5.320			0.558	1.129	0.05					
Z5	15.188		0.130	0.188	0.204	0.14		0.07	0.18		
Z6	5.269	2.786		0.444	0.618	0.05	1.78		0.43		
Z7	16.741	0.105	1.852	0.672	0.818	0.15	0.07	1.02	0.65		
Z8	13.353	0.048	0.570	0.058	0.138	0.12	0.03	0.31	0.06		
Z9	99.908		1.194	0.249	1.308	0.91		0.66	0.24		
AA1	15.096	2.682		0.741	0.666	0.14	1.72		0.72		
AA2	9.396	1.134		0.306	0.093	0.09	0.73		0.30		
AA3	9.786	2.877	2.532	1.083	1.356	0.09	1.84	1.39	1.06		

TABLE WSW 3: IN-HOUSE HEADGAS ANALYSIS
Wicape SW Prospect Area

SAMPLE #	Raw Data in ppm							ANOMALY INDEX RATIO (AIR)			
	C1	C2	C3	iC4	nC4	C1	C2	C3	iC4	nC4	
AA4	5.073	1.728	2.805	0.135	0.060	0.05	1.11	1.54	0.13	0.04	
AA5	17.691	4.524	2.391	0.504	1.110	0.16	2.90	1.31	0.49	0.77	
AA6	30.780	0.096	0.822	0.588	0.258	0.28	0.06	0.45	0.57	0.18	
BB1	29.180	0.168	1.123	0.270	0.515	0.27	0.11	0.62	0.26	0.36	
BB2	8.243	0.348	1.003	0.218	0.265	0.08	0.22	0.55	0.21	0.18	
BB3	30.300	0.318	1.525	0.453	1.423	0.28	0.20	0.84	0.44	0.99	
BB4	9.355	3.410	1.975	0.323	0.438	0.09	2.18	1.09	0.31	0.30	
BB5	8.340	3.200	2.873	1.545	0.513	0.08	2.05	1.58	1.51	0.36	
BB6	27.080	0.535	1.353	0.508	0.485	0.25	0.34	0.74	0.49	0.34	
BB7	10.830	5.108	2.843	0.660	0.558	0.10	3.27	1.56	0.64	0.39	
CC1	5.654	1.480	1.856	0.506	0.442	0.05	0.95	1.02	0.49	0.31	
CC2	40.958	0.254	0.094	0.326	0.262	0.37	0.16	0.05	0.32	0.18	
CC3	10.922	2.032	1.432	0.288	0.10	1.30	0.79	0.20			
CC4	6.854	2.128	0.044	0.056	0.056	0.06	1.36	0.02			
CC5	5.528	2.932	0.866	0.054	0.196	0.05	1.88	0.48	0.05		
CC6	12.420	0.272	0.578	0.338	0.11	0.17	0.32				
CC7	25.382	0.312	0.832	0.174	0.380	0.23	0.20	0.46	0.17	0.26	
Harmonic Mean	14.220	0.266	0.480	0.234	0.338	0.130	0.170	0.264	0.228	0.235	
Anomaly (2xHM)	28.441	0.531	0.960	0.468	0.676	0.260	0.340	0.527	0.456	0.470	
average	73.003	1.041	1.213	0.684	0.959	0.667	0.667	0.667	0.667	0.667	
std dev	110.295	1.205	1.376	0.747	0.808	1.007	0.772	0.756	0.728	0.562	
minimum	2.246	0.029	0.044	0.021	0.035	0.021	0.019	0.024	0.020	0.024	
maximum	535.293	5.108	8.341	3.479	3.628	4.888	3.272	4.583	3.391	2.523	
Anomaly (1.5 x mean)	109.505	1.561	1.820	1.026	1.438	1.000	1.000	1.000	1.000	1.000	

ws wsgas

TABLE WSW 4: PROBE SOIL GAS (ppm)
Wicape SW Prospect Area

sample#	TABLE WSW 4: PROBE SOIL GAS (ppm)					ANOMALY INDEX RATIO (AIR)				
	Wicape SW Prospect Area					Value / anomaly ratio (1.5 x mean)				
	C1	C2	C3	iC4	nC4	C1	C2	C3	iC4	nC4
R1	11.763	0.337	0.284			1.30	0.10	0.12		
R2	8.178	0.206	0.295	0.432		0.90	0.06	0.13	0.29	
R3	12.347	0.369	0.241	0.135	0.088	1.36	0.11	0.10	0.09	0.04
R4	6.911	2.623	2.584	1.122	1.682	0.76	0.80	1.10	0.77	0.73
R5	32.806	0.364	0.438	2.445	2.163	3.61	0.11	0.19	1.67	0.94
R6	7.204	1.903	0.976			0.79	0.58	0.42		
R7	7.127	2.220	1.268	0.130	0.639	0.79	0.68	0.54	0.09	0.28
S1	5.029	0.112	0.134	0.087		0.55	0.03	0.06	0.06	
S2	7.054	1.156		2.340	1.403	0.78	0.35		1.60	0.61
S3	5.559		0.199	0.541	1.262	0.61		0.08	0.37	0.55
S4	6.453	1.980	1.144	0.157	0.200	0.71	0.61	0.49	0.11	0.09
S5	6.293	3.185	1.899	0.244	0.381	0.69	0.97	0.81	0.17	0.17
S6	6.315	2.724	1.791			0.70	0.83	0.76		
S7	6.730	3.098	2.073	1.319	1.548	0.74	0.95	0.89	0.90	0.67
S8	5.806	2.443	1.416	0.172	0.490	0.64	0.75	0.60	0.12	0.21
T1	5.256	2.979	1.336		0.279	0.58	0.91	0.57		0.12
T2	6.016	3.017	3.484	1.779	3.168	0.66	0.92	1.49	1.21	1.37
T3	5.559	2.799	2.468	0.940	1.367	0.61	0.86	1.05	0.64	0.59
T4	6.687	2.852	3.637	1.832	4.252	0.74	0.87	1.55	1.25	1.85
T5	5.928	2.819	2.860	1.329	2.148	0.65	0.86	1.22	0.91	0.93
T6	5.858		1.904	1.667	2.947	0.65		0.81	1.14	1.28
T7	9.904				0.091	1.09				0.04
T8	7.303		0.799		0.107	0.80		0.34		0.05
T9	5.009	1.645			1.545	0.55	0.50			0.67
U1	7.333			1.009		0.81			0.69	
U2	5.435	2.377			1.157	0.60	0.73			0.50
U3	6.051	2.614			0.073	0.67	0.80			0.03
U4			0.419		2.208			0.18		0.96
U5	5.188	2.679		1.462		0.57	0.82		1.00	
U6	5.580	3.075	3.476	0.503		0.61	0.94	1.48	0.34	
U7	5.486	2.296	1.959	1.454	1.793	0.60	0.70	0.84	0.99	0.78
U8	5.190	2.382	0.803	0.209	0.268	0.57	0.73	0.34	0.14	0.12
V1	5.576	4.186	2.007	2.806	1.699	0.61	1.28	0.86	1.91	0.74
V2	6.554	1.757	1.781	1.089	3.558	0.72	0.54	0.76	0.74	1.54
V3	5.590	2.816	1.865		2.388	0.62	0.86	0.80		1.04
V4	6.186	2.405	1.458	0.455	0.410	0.68	0.74	0.62	0.31	0.18
V5	6.021	3.283	1.354	0.273		0.66	1.00	0.58	0.19	
V6	9.684		2.118	0.845	2.184	1.07		0.90	0.58	0.95
V7	6.050	2.695	1.809	1.388	2.197	0.67	0.82	0.77	0.95	0.95
V8	5.687			1.206	2.106	0.63			0.82	0.91
V9	5.535	1.188	1.820	1.333		0.61	0.36	0.78	0.91	
W1	5.580				0.247	0.61				0.11
W2	5.924	1.650	3.045	0.851	1.186	0.65	0.51	1.30	0.58	0.51
W3	5.976	1.960			0.887	0.66	0.60			0.38
W4	5.513	2.384	1.280	0.140	0.085	0.61	0.73	0.55	0.10	0.04
W5	5.237		2.499	0.020	0.066	0.58		1.07	0.01	0.03
W6	5.509	1.333	0.893	1.055	0.638	0.61	0.41	0.38	0.72	0.28
W7	5.565	1.737	2.428	1.491	0.869	0.61	0.53	1.04	1.02	0.38
W8	5.338	2.110	0.952	1.013	1.413	0.59	0.65	0.41	0.69	0.61
X1	5.078	1.679	1.441	0.230	0.045	0.56	0.51	0.62	0.16	0.02
X2	5.332		0.883	0.547	0.545	0.59		0.38	0.37	0.24
X3	5.748	3.994	1.380		3.605	0.63	1.22	0.59		1.56
X4	7.196		1.669		1.311	0.79		0.71		0.57
X5	5.504	3.788	1.895	1.963		0.61	1.16	0.81	1.34	
X6	5.014		2.540	1.643	1.294	0.55		1.08	1.12	0.56
X7	4.814	3.156	1.243			0.53	0.97	0.53		
X8	7.471		2.228	0.473		0.82		0.95	0.32	

X9	4.698	3.450	2.709	1.672	11.458	0.52	1.06	1.16	1.14	4.97
Y1	8.940		1.073		0.129	0.042	0.98	0.46		
Y2	8.431					0.93			0.09	0.02
Y3	5.824	3.335	1.528	0.410	0.107	0.64	1.02	0.65	0.28	0.05
Y4	5.841	3.699	1.811	2.219		0.64	1.13	0.77	1.51	
Y5	8.482					0.93				
Y6	5.606	3.144	2.764	2.308	3.209	0.62	0.96	1.18	1.57	1.39
Y7	4.416	1.999		0.072	0.044	0.49	0.61		0.05	0.02
Y8	5.910	2.982	1.757	1.817	2.977	0.65	0.91	0.75	1.24	1.29
Z1	2.833	1.051	0.140	0.049	0.169	0.31	0.32	0.06	0.03	0.07
Z2	4.530	3.162		0.437	0.288	0.50	0.97		0.30	0.12
Z3	3.003		0.082			0.33		0.04		
Z4	5.442	2.086	1.536	0.652	2.128	0.60	0.64	0.66	0.44	0.92
Z5	4.931	1.484	1.696		7.959	0.54	0.45	0.72		3.45
Z6	4.240					0.47				
Z7	5.594	2.475	1.861	0.158		0.62	0.76	0.79	0.11	
Z8	4.128		2.171	1.026	1.291	0.45		0.93	0.70	0.56
Z9	4.360				0.126	0.48				0.05
AA1	3.049	1.004		0.084	5.911	0.34	0.31		0.06	2.57
AA2	3.601			0.169	0.937	0.40			0.12	0.41
AA3	4.062		1.128			0.45		0.48		
AA4	4.404	2.151	2.051	3.486	1.635	0.49	0.66	0.88	2.38	0.71
AA5	3.096	0.260		2.151		0.34	0.08		1.47	
AA6	3.732		1.603		0.397	0.41		0.68		0.17
BB1	3.752			0.044		0.41			0.03	
BB2	5.552	2.961	1.107	1.864	0.015	0.61	0.91	0.47	1.27	0.01
BB3	7.259	1.569		0.796	2.873	0.80	0.48		0.54	1.25
BB4	3.739	2.991			0.753	0.41	0.92			0.33
BB5	3.915	1.805	0.481		0.253	0.43	0.55	0.21		0.11
BB6	4.613		3.126		0.972	0.51		1.33		0.42
BB7	4.347	1.125				0.48	0.34			
CC1	4.922	2.238	0.862	0.590		0.54	0.68	0.37	0.40	
CC2	7.735				0.968	0.85				0.42
CC3		0.121	0.128	0.531	1.777		0.04	0.05	0.36	0.77
CC4	4.997	1.691		1.221	0.632	0.55	0.52		0.83	0.27
CC5	3.169	0.600	0.915		2.410	0.35	0.18	0.39		1.05
CC6			0.784		1.701			0.33		0.74
CC7	2.613		1.487	0.522	0.042	0.29		0.64	0.36	0.02
Harmonic Mean	5.354	1.051	0.731	0.256	0.222	0.590	0.322	0.312	0.175	0.096
Anomaly (2xHM)	10.708	2.103	1.462	0.512	0.444	1.179	0.644	0.624	0.349	0.193
average	6.052	2.178	1.561	0.977	1.536	0.667	0.667	0.667	0.667	0.667
std dev	3.294	1.008	0.872	0.802	1.857	0.363	0.309	0.373	0.547	0.806
minimum	2.613	0.112	0.082	0.020	0.015	0.288	0.034	0.035	0.014	0.007
maximum	32.806	4.186	3.637	3.486	11.458	3.614	1.281	1.553	2.378	4.973
Anomaly (1.5 x mean)	9.078	3.267	2.342	1.466	2.304	1.000	1.000	1.000	1.000	1.000

APPENDIX D

TABLE MS1: WEST SMOKE CREEK														
GPS Sample sites: Phase III, Smoke Creek Revisited														
SITENO	VEGETATION	SLOPE	SOIL	MOIST.	TEMP	P-psi	AIR	AIR	LAT	LONG	ALT	TOPO	AUGER	
							UTM-Y	UTM-X	m			DEPTH-in.	WEATHER	WIND
doe1-cp1-1	grass	gentle	silt	dry	64	29.2	5359824	502756	727.31	bench	36	partly overcast	0-5w	
doe1-cp1-2	grass	gentle	clay	dry	64	29.2	5359918	502902	736.20	hillside	25	partly overcast	0-5w	
doe1-cp1-3	grass	gentle	silt	dry	60	29.2	5360026	503027	743.36	hillside	36	partly overcast	0-5w	
doe1-cp1-4	grass	gentle	silt	dry	63	28.8	5360147	503158	755.33	hillside	38	partly overcast	0-5w	
doe1-cp1-5	grass	gentle	loam	dry	63	28.8	5360317	503308	758.94	hilltop	36	partly overcast	0-5w	
doe1-cp1-6	grass	gentle	loam	dry	63	28.8	5360455	503391	750.16	hilltop	38	partly overcast	0-5w	
doe1-cp1-7	grass	gentle	loam	dry	63	28.8	5360574	503496	738.33	hillside	35	partly overcast	0-5w	
doe1-cp2-1	stubble	flat	loam	damp	56	29.3	5370298	503500	706.00	plain	38	cloudy	10nw	
doe1-cp2-2	stubble	flat	loam	dry	56	29.3	5370449	503497	708.70	plain	38	cloudy	10nw	
doe1-cp2-3	stubble	flat	silt	dry	55	29.3	5370609	503501	710.30	plain	38	cloudy	10nw	
doe1-cp2-4	grass	flat	silt	dry	55	29.3	5370786	503499	712.66	plain	38	cloudy	5nw	
doe1-cp2-5	grass	flat	loam	damp	53	29.3	5370940	503498	714.97	plain	38	cloudy	5nw	
doe1-cp2-6	grass	flat	loam	dry	50	29.3	5371133	503497	721.20	plain	38	cloudy	5-10n	
doe1-cp2-7	grass	flat	loam	dry	50	29.3	5371294	503498	725.09	plain	38	cloudy	5-10n	
doe1-cp2-8	grass	flat	loam	dry	50	29.3	5371451	503498	726.75	plain	38	partly overcast	5-10n	
doe1-cp2-9	grass	flat	loam	dry	50	29.3	5371584	503497	730.45	plain	38	partly overcast	5-10n	
doe1-cp3-1	summerfallow	gentle	silty loam	damp	65	28.3	5375634	501374	750.53	hillside	35	cloudy	10w	sandy, pebbles
doe1-cp3-10	CRP	flat	clay	dry	61	28.7	5374281	500877	719.03	bench	38	cloudy	5-10nw	sand then dk clay
doe1-cp3-2	stubble	gentle	silty loam	damp	65	28.3	5375431	501064	747.12	hillside	36	cloudy	10w	grayish tan
doe1-cp3-3	stubble	gentle	silty loam	dry	65	28.3	5375280	501015	741.00	hillside	42	cloudy	5-10nw	buffy tan
doe1-cp3-4	stubble	gentle	loam	damp	65	28.3	5375133	500975	735.70	hillside	38	cloudy	5-10nw	dk brown
doe1-cp3-5	summerfallow	gentle	loam	damp	65	28.3	5374990	500925	733.75	hillside	30	cloudy	5-10nw	dk brown
doe1-cp3-6	summerfallow	gentle	loam	damp	61	28.7	5374844	500880	729.73	hillside	35	cloudy	5-10nw	dk brown
doe1-cp3-7	summerfallow	flat	loam	damp	61	28.7	5374684	500876	725.25	plain	36	cloudy	5-10nw	dk clay then silt
doe1-cp3-8	CRP	flat	sand	dry	61	28.7	5374531	500860	721.65	bottom	39	cloudy	5-10nw	creamy tan
doe1-cp3-9	CRP	flat	sand	dry	61	28.7	5374379	500876	722.34	bottom	35	cloudy	5-10nw	creamy tan
doe1-cp4-1	stubble	gentle	loam	dry	55	28.7	5375601	500272	754.80	hillside	32	partly overcast	2nw	brown
doe1-cp4-10	stubble	gentle	loam	damp	67	28.7	5376981	500268	772.91	hillside	35	partly overcast	2nw	dk brown;clay rich
doe1-cp4-11	grass	gentle	loam	dry	67	28.7	5377346	500268	779.56	hillside	37	partly overcast	calm	dk brown
doe1-cp4-2	stubble	gentle	loam	damp	57	28.7	5375759	500272	760.21	hillside	32	partly overcast	2nw	light brown
doe1-cp4-2	stubble	gentle	loam	damp	57	28.7	5375911	500272	760.44	hillside	32	partly overcast	2nw	light brown
doe1-cp4-4	stubble	gentle	loam	dry	57	28.7	5376059	500271	762.87	hillside	32	partly overcast	2nw	light brown loamie silt!!
doe1-cp4-5	grass	flat	loam	dry	57	28.7	5376210	500270	765.76	hillside	32	partly overcast	2nw	tan to gray
doe1-cp4-6	stubble	flat	loam	damp	65	28.7	5376365	500270	765.67	plain	30	partly overcast	2nw	lt brn, clay rich
doe1-cp4-7	stubble	flat	loam	damp	65	28.7	5376520	500269	765.45	plain	36	partly overcast	2nw	dk brown
doe1-cp4-8	stubble	gentle	loam	damp	65	28.7	5376675	500269	769.19	hillside	32	partly overcast	2nw	dk brown
doe1-cp4-9	stubble	gentle	loam	damp	65	28.7	5376828	500269	772.17	hillside	38	partly overcast	2nw	dk brown;clay rich
doe1-cv1-1	grass	gentle	clay	damp	60	29.2	5360036	503494	740.51	hillside	38	partly overcast	0-5w	
doe1-cv1-2	grass	gentle	loam	damp	60	29.2	5360207	503394	752.20	hillside	38	partly overcast	0-5w	
doe1-cv1-3	grass	flat	loam	dry	58	29.2	5360440	503190	758.88	hilltop	35	partly overcast	5-10w	
doe1-cv1-4	grass	flat	loam	dry	58	29.3	5360543	503044	757.77	plain	34	cloudy	10nw	
doe1-cv1-5	grass	flat	loam	dry	58	29.3	5360577	502853	750.54	plain	36	cloudy	10nw	
doe1-cv2-1	grass	gentle	clay	damp	69	28.8	5370712	503687	715.76	plain	37	sunny	15sw	loam in top 30"
doe1-cv2-2	grass	gentle	loam	dry	69	28.8	5370909	503800	721.55	plain	30	sunny	15sw	gray
doe1-cv2-3	grass	gentle	loam	dry	73	28.8	5371125	503737	721.57	plain	33	sunny	15sw	gray
doe1-cv2-4	grass	gentle	loam	dry	73	28.8	5371299	503625	725.90	plain	39	sunny	15sw	cream color
doe1-cv2-5	grass	gentle	silt	dry	65	28.8	5370631	503154	703.80	bench	40	sunny	15sw	light gray
doe1-cv2-6	grass	flat	silty loam	dry	65	28.8	5370861	503031	704.32	bench	40	sunny	15sw	brown
doe1-cv2-7	grass	flat	loam	dry	65	28.8	5371087	503079	709.46	bench	38	sunny	15sw	brown
doe1-cv2-8	stubble	flat	loam	dry	66	28.7	5371301	503185	714.88	plain	40	sunny	12sw	tan
doe1-cv3-1	CRP	flat	sand	dry	64	28.9	5374555	500756	721.12	bench	32	cloudy	5-10nw	med brown w/clay
doe1-cv3-10	grass	flat	silt	dry	49	29.0	5374667	500583	721.42	bench	25	cloudy	5-10nw	sw cv3 bench edge, gray
doe1-cv3-2	summerfallow	flat	silty loam	wet	64	28.9	5374547	501098	723.96	bench	38	cloudy	5-10nw	sandy then clay
doe1-cv3-3	CRP	gentle	silty loam	dry	57	28.9	5374820	501334	737.08	hillside	38	cloudy	5-10nw	tan powder
doe1-cv3-4	CRP	flat	silty loam	dry	57	28.9	5375088	501311	742.42	hilltop	30	cloudy	5-10nw	light gray
doe1-cv3-5	CRP	flat	silty loam	dry	57	29.0	5375305	501189	741.87	plain	35	cloudy	5-10nw	tan
doe1-cv3-6	stubble	flat	loam	dry	53	29.0	5375419	500799	744.37	plain	29	cloudy	5-10nw	gray
doe1-cv3-7	summerfallow	flat	loam	wet	53	29.0	5375332	500509	736.72	plain	36	cloudy	5-10nw	dk brown
doe1-cv3-8	summerfallow	gentle	loam	wet	50	29.0	5375177	500289	725.86	plain	36	cloudy	5-10nw	west side follows drainage
doe1-cv3-9	stubble	flat	silt	dry	52	29.0	5374821	500403	722.35	bench	26	cloudy	5-10nw	sw cv3 bench edge, gray
doe1-cv4-1	stubble	gentle	loam	dry	67	28.7	5376957	500631	778.76	hillside	32	cloudy	calm	light brown
doe1-cv4-10	stubble	flat	loam	dry	52	28.2	5376223	500686	773.92	hillside	40	cloudy	calm	brown, clumpy
doe1-cv4-2	stubble	gentle	loam	dry	69	28.5	5376966	500380	775.27	hillside	30	partly overcast	calm	light brown
doe1-cv4-3	stubble	gentle	loam	damp	69	28.5	5376899	500113	767.85	hillside	35	partly overcast	calm	light brown
doe1-cv4-4	grass	steep	loam	dry	67	28.5	5376729	499887	762.16	hillside	32	cloudy	calm	gray
doe1-cv4-5	grass	flat	clay	wet	58	28.9	5376495	499796	753.85	bottom	42	cloudy	calm	gray muck
doe1-cv4-6	grass	flat	silty loam	dry	58	28.9	5376312	499832	755.96	bench	36	cloudy	calm	tan
doe1-cv4-7	grass	flat	silty loam	dry	55	28.9	5376155	499935	756.24	bench	33	cloudy	7nw	tan
doe1-cv4-8	stubble	gentle	loam	damp	52	28.9	5375910	500386	768.86	hillside	36	cloudy	calm	lt brn

doe1-cv4-9	stubble	flat	loam	dry	52	28.3	5376080.	500603	779.54	hilltop	37	cloudy	calm	brown, clumpy
doe1-11-1	stubble	gentle	loam	dry	66	28.7	5374108	502292	724.44	hillside	40	sunny	12sw	dk brown
doe1-11-2	stubble	gentle	silty loam	dry	63	28.7	5374353	502115	735.59	plain	32	sunny	12sw	brown
doe1-11-3	stubble	gentle	silty loam	dry	63	28.7	5374606	501934	735.90	plain	34	sunny	12sw	gray w/ clay
doe1-11-4	CRP	gentle	silty loam	dry	63	28.7	5374869	501746	742.18	plain	3	sunny	12sw	gray w/ clay
doe1-11-5	CRP	gentle	silty loam	dry	63	28.7	5375144	501551	748.43	plain	35	sunny	12sw	tan-loam-silt
doe1-11-6	CRP	gentle	silt	dry	63	28.7	5375389	501374	746.83	hillside	38	sunny	12sw	light tan silt
doe1-11-7	summerfallow	gentle	loam	damp	58	28.7	5375609.	501218	752.41	hillside	40	sunny	12sw	dk brown
doe1-11-8	stubble	gentle	silty loam	dry	56	28.7	5375842	501050	758.34	hillside	26	sunny	10sw	tan
doe1-11-9	stubble	flat	silty loam	dry	56	28.7	5376072	500885	764.05	plain	36	sunny	10sw	light brown
doe1-nes8	summerfallow	flat	loam	wet	57	28.2	5376050	501684	786.20	plain	38	cloudy	calm	dk brown
doe1-nwse8	summerfallow	gentle	loam	damp	57	28.2	5376047	501306	776.54	hillside	40	cloudy	calm	brown
doe1-sese8	summerfallow	flat	loam	wet	55	28.2	5375640	501683	776.98	plain	38	cloudy	calm	dk brown

SITENO	VEGETATION	SLOPE	SOIL	AIR MOIST.	AIR TEMP	LAT UTM-Y	LONG UTM-X	ALT m	TOPO	AUGER	DEPTH in.	WEATHER	WIND	COMMENTS
doe1-I2-1	grass	gentle	loam	dry	64	28.2	5374416.	5156320.	695.:	hillside	40	sunny	calm	golden tan
doe1-I2-2	grass	gentle	loam	dry	66	28.2	5374168.	516143.	707.:	hillside	38	sunny	calm	tan
doe1-I2-3	grass	gentle	loam	dry	70	28.4	5373917.	515964.	704.:	hillside	30	sunny	calm	tan
doe1-I2-4	grass	steep	silty loam	dry	70	28.4	5373696.	515806.	695.:	hillside	27	sunny	calm	tan
doe1-I2-5	grass	gentle	loam	dry	70	28.4	5373438.	515621.	684.:	hillside	40	sunny	calm	dk brown
doe1-I2-6	grass	flat	clay	wet	69	28.7	5373189.	515443.	681.:	bottom	36	sunny	calm	dark play dough
doe1-I2-7	grass	flat	clay	damp	69	28.7	5372876.	515220.	681.:	bottom	37	sunny	calm	dk gray, CV also
doe1-I2-8	stubble	flat	clay	damp	64	28.9	5372634.	515047.	680.:	bottom	37	sunny	calm	black
doe1-I2-9	grass	flat	clay	dry	62	28.9	5372283.	514796.	681.:	bottom	34	sunny	0-5sw	dk gray, on CV
doe1-I2-10	grass	flat	silty loam	dry	61	28.8	5371982.	514581.	683.:	bench	38	sunny	calm	tan, s of CV (gravel)
doe1-I2-11	grass	flat	loam	dry	61	28.8	5371610.	514315.	681.:	bench	35	sunny	calm	tan
doe1-I2-12	grass	gentle	loam	dry	61	28.8	5371366.	514136.	679.:	hillside	39	sunny	calm	brown
doe1-I2-13	grass	flat	loam	dry	56	29.1	5371008.	513883.	675.:	bottom	39	sunny	calm	dk brown, on CV
doe1-I2-14	grass	flat	loam	dry	56	29.1	5370739.	513706.	674.:	bottom	38	sunny	calm	gray, damp at bottom
doe1-I2-15	grass	flat	clay	damp	72	29.0	5370497.	513519.	673.:	bottom	40	sunny	0-5sw	dk gray
doe1-I2-16	grass	gentle	loam	dry	70	28.8	5370228.	513326.	676.:	bench	38	sunny	0-5sw	tan
doe1-I2-17	grass	gentle	loam	dry	70	28.8	5370087.	513225.	683.:	hillside	36	sunny	0-5sw	creamy tan, anticline axis
doe1-I2-18	grass	flat	loam	dry	70	28.8	5369835.	513045.	685.:	hilltop	36	sunny	0-5sw	creamy tan, anticline axis
doe1-I2-19	grass	gentle	loam	dry	72	28.6	5369578.	512860.	672.:	hillside	39	sunny	0-5sw	brown to gray
doe1-I2-20	grass	gentle	clay	wet	72	28.6	5369323.	512678.	667.:	bottom	37	sunny	0-5sw	reddish brown
doe1-I2-21	grass	gentle	silty loam	dry	72	28.6	5369196.	512587.	680.:	hilltop	36	sunny	10-15sw	light brown, on large CV also
doe1-I2-22	grass	gentle	silty loam	dry	72	28.6	5368943.	512406.	679.:	hillside	39	sunny	15sw	light brown rocky
doe1-I2-23	grass	gentle	loam	dry	72	28.7	5368697.	512230.	669.:	hillside	40	sunny	15sw	light gray powder
doe1-I2-24	grass	flat	clay	wet	74	28.7	5368449.	512052.	661.:	bottom	37	sunny	15sw	silty, red brown
doe1-I2-25	grass	flat	clay	damp	74	28.6	5368115.	511813.	662.:	bottom	37	sunny	15sw	on CV, brown silty
doe1-I2-26	grass	flat	silty loam	damp	72	28.6	5367862.	511631.	661.:	bottom	38	sunny	15sw	brown clay a bottom
doe1-I2-27	grass	flat	silty loam	damp	72	28.6	5367617.	511457.	661.:	plain	38	sunny	5-10w	bottom plain, light brown
doe1-I2-28	grass	flat	clay	dry	72	28.6	5367362.	511273.	659.:	plain	35	sunny	5-10w	bottom plain, brown
doe1-I2-29	grass	steep	clay	damp	70	28.6	5367198.	511156.	668.:	hillside	35	sunny	0-5w	CV edge, steep round hill, 2pi
doe1-I2-30	grass	gentle	loam	dry	70	28.6	5367039.	511042.	666.:	hillside	39	sunny	0-5w	CV cent, round hill
doe1-I2-31	grass	flat	clay	dry	69	28.8	5366881.	510929.	666.:	plain	33	sunny	0-5w	CV cent
doe1-CP5-5	grass	flat	loam	dry	69	28.8	5366759.	510851.	664.:	plain	40	sunny	0-5w	CV cent, cont L2 line
doe1-CP5-6	grass	flat	loam	dry	68	28.8	5366646.	510769.	662.:	plain	37	sunny	0-5w	CV edge, med gray
doe1-CV6-1	grass	gentle	silty loam	dry	73	28.2	5367345.	513920.	711.:	hillside	36	sunny	2sw	tan
doe1-CV6-2	grass	gentle	silty loam	dry	73	28.2	5367435.	513626.	716.:	hillside	37	sunny	5sw	light brown
doe1-CV6-3	grass	gentle	loam	dry	71	28.0	5367720.	513286.	720.:	hilltop	33	partly overcast	5sw	light brown
doe1-CV6-4	grass	gentle	loam	dry	71	28.3	5368228.	513065.	709.:	hillside	37	partly overcast	5sw	tan gray
doe1-CV6-5	grass	gentle	loam	dry	71	28.3	5368818.	513123.	696.:	hillside	32	partly overcast	5sw	tan
doe1-CV6-6	grass	steep	loam	dry	71	28.3	5369100.	513579.	690.:	hillside	40	sunny	2sw	gray to brown
doe1-CV6-7	grass	steep	loam	dry	73	28.1	5369110.	513919.	700.:	hillside	36	sunny	2sw	dk brown, clay rich
doe1-CP6-1	grass	flat	loam	dry	73	28.1	5369424.	513980.	706.:	hilltop	34	sunny	2sw	tan
doe1-CP6-2	grass	steep	loam	dry	73	28.1	5369263.	513960.	697.:	hillside	35	sunny	2sw	brown
doe1-CP6-3	grass	gentle	loam	dry	73	28.1	5368955.	513913.	708.:	hillside	34	sunny	2sw	cream color
doe1-CP6-4	grass	flat	loam	dry	73	28.1	5368799.	513917.	712.:	plain	35	sunny	2sw	grayish tan
doe1-CP6-5	grass	flat	loam	dry	71	28.1	5368647.	513921.	709.:	plain	35	cloudy	2sw	dk brown
doe1-CP6-6	grass	flat	loam	dry	70	28.1	5368491.	513916.	715.:	plain	40	cloudy	2sw	grayish tan
doe1-CP6-7	grass	flat	silty loam	dry	70	28.1	5368336.	513918.	714.:	plain	36	cloudy	0-2sw	light brown
doe1-CP6-8	grass	flat	silty loam	dry	70	28.1	5368182.	513917.	716.:	plain	40	cloudy	3-5sw	tan
doe1-CP6-9	grass	flat	loam	dry	70	28.1	5368027.	513911.	715.:	plain	36	cloudy	3-5sw	tan
doe1-CP6-10	grass	flat	loam	dry	70	28.2	5367872.	513917.	720.:	plain	40	partly overcast	calm	tan
doe1-CP6-11	grass	flat	loam	dry	70	28.2	5367720.	513917.	717.:	plain	37	cloudy	calm	dk brown
doe1-CP6-12	grass	flat	loam	dry	70	28.2	5367566.	513919.	715.:	plain	33	cloudy	calm	brown
doe1-CP6-13	grass	flat	loam	dry	70	28.2	5367412.	513921.	715.:	plain	40	cloudy	calm	tan
doe1-CP6-14	grass	gentle	loam	dry	70	28.2	5367193.	513921.	714.:	hilltop	30	cloudy	calm	light brown, clay rich
doe1-CP6-15	grass	flat	loam	dry	70	28.2	5367038.	513921.	714.:	hilltop	38	cloudy	calm	tan
DOE1-L3-1	grass	flat	silty loam	dry	48	29.0	5366561.	508124.	729.:	hilltop	34	cloudy	15w	tan;gritty soil
DOE1-L3-2	CRP	flat	loam	dry	46	29.0	5366310.	508304.	708.:	bottom	38	cloudy	15-20nw	tan-very fine
DOE1-L3-3	grass	gentle	loam	dry	46	29.0	5366054.	508487.	701.:	hillside	34	cloudy	15-20nw	gray-tan
DOE1-L3-4	summerfallow	flat	loam	damp	45	29.0	5365805.	508665.	687.:	plain	37	cloudy	15-20nw	br-hvy glay base
DOE1-L3-5	stubble	flat	loam	damp	45	29.1	5365558.	508842.	674.:	plain	35	cloudy	5-10nw	reddish orange Sand with loam
DOE1-L3-6	stubble	flat	loam	damp	45	29.1	5365220.	509084.	669.:	plain	37	cloudy	5-10nw	dark brn
DOE1-L3-7	summerfallow	gentle	loam	damp	45	29.1	5364965.	509266.	662.:	plain	37	cloudy	5-10nw	dark brn;lot of clay
DOE1-L3-8	grass	gentle	silt	dry	45	29.1	5364559.	509556.	659.:	hillside	32	cloudy	10-20nw	gray-tan
DOE1-CP7-1	grass	flat	silt	dry	58	29.4	5367716.	509900.	706.:	plain	42	partly overcast	20nw	It brn
DOE1-CP7-2	grass	flat	loam	dry	58	29.4	5367564.	509902.	703.:	plain	36	partly overcast	20nw	It brn
DOE1-CP7-3	grass	gentle	loam	dry	58	29.4	5367421.	509899.	699.:	hillside	42	partly overcast	20nw	tan;creamy
DOE1-CP7-4	grass	gentle	loam	dry	60	29.2	5367272.	509900.	698.:	hillside	42	partly overcast	20nw	It brn
DOE1-CP7-5	grass	gentle	loam	dry	60	29.2	5367121.	509900.	690.:	hillside	40	partly overcast	20nw	It brn
DOE1-CP7-6	grass	steep	silty loam	dry	60	29.2	5366962.	509900.	677.:	bottom	40	partly overcast	20nw	brn

DOE1-CP7-7	summerfallow	flat	silty loam	damp	56	29.0	5366807.	509901.677.:plain	40	partly overcast	20nw	dk brn
DOE1-CP7-8	summerfallow	flat	silty loam	damp	56	29.0	5366659.	509901.676.(plain	42	partly overcast	20nw	gold
DOE1-CP7-9	summerfallow	flat	silty loam	damp	56	29.2	5366501.	509901.675.:plain	42	partly overcast	20nw	gold-mostly loam
DOE1-CP7-10	summerfallow	flat	loam	damp	56	29.2	5366348.	509901.674.(plain	41	partly overcast	20nw	gold-mostly loam
DOE1-CP7-11	summerfallow	flat	silty loam	damp	56	29.2	5366191.	509901.671.:plain	42	partly overcast	20nw	gold-mostly loam
DOE1-CP7-12	summerfallow	flat	loam	damp	56	29.0	5366042.	509901.669.:plain	42	partly overcast	20nw	lt brn
DOE1-CP7-13	summerfallow	flat	loam	damp	56	29.0	5365890.	509901.668.:plain	42	partly overcast	20nw	with hyv clay base
DOE1-CP7-14	stubble	flat	loam	dry	56	29.0	5365737.	509904.667.:plain	42	partly overcast	20nw	dk brn not totally dry harddi
DOE1-CP7-15	stubble	flat	loam	dry	56	29.0	5365584.	509904.668.:plain	42	partly overcast	20nw	dk brn not totally dry harddi
DOE1-CP7-16	stubble	gentle	silty loam	dry	50	29.3	5365427.	509905.665.(hillside	cloudy	calm	tan	
DOE1-CP7-17	stubble	gentle	loam	damp	50	29.3	5365274.	509906.664.(hillside	cloudy	calm	bk brn clay base	
DOE1-CP7-18	stubble	gentle	silty loam	damp	50	29.3	5365117.	509906.667.(hillside	cloudy	calm	gray:brn alot of clay	
DOE1-CP7-19	stubble	gentle	silty loam	dry	52	29.0	5364962.	509907.671.(hillside	cloudy	calm	lt brn	
DOE1-CP7-20	stubble	gentle	silty loam	dry	53	29.0	5364807.	509907.671.(hilltop	cloudy	calm	tan	
DOE1-CP7-21	stubble	steep	silt	dry	50	29.0	5364659.	509907.666.(hillside	cloudy	calm	lt brn; a lot of gravel	
DOE1-CP7-22	stubble	flat	silt	damp	50	29.0	5364505.	509909.659.:bottom	cloudy	calm	tan somewhat sandy	
DOE1-CP7-23	grass	flat	silt	dry	50	28.0	5364356.	509911.661.:bottom	cloudy	3nw	creamy,whitish; somewhat sanc	
DOE1-CP7-24	grass	gentle	silt	dry	50	29.3	5364206.	509910.660.(hillside	cloudy	5nw	ground froze 2ft down	
DOE1-CV7-1	summerfallow	flat	loam	dry	23.0	29.5	53655803.	508969.680.:plain	40.0	partly overcast	5-12nw	ground froze 2ft down
DOE1-CV7-2	grass	gentle	loam	dry	23.0	29.5	53655954.	508981.681.(hillside	36.0	partly overcast	5-16nw	ground frozen6" tan verydry
DOE1-CV7-3	grass	gentle	loam	dry	23.0	29.5	5366102.	509017.689.(hillside	42.0	partly overcast	5-16nw	ground frozen6" tan verydry
DOE1-CV7-4	grass	gentle	loam	dry	45.0	29.5	5366247.	509065.691.(hillside	42.0	partly overcast	5-16nw	frozen 2" drk brn
DOE1-CV7-5	grass	gentle	loam	dry	44.0	28.8	5366400.	509086.693.:hillside	40.0	partly overcast	5-10w	gravel on top; wet loam-gray:
DOE1-CV7-6	summerfallow	flat	loam	wet	43.0	29.0	5366545.	509143.701.(hilltop	39.0	partly overcast	5-10w	dk brn silty loam
DOE1-CV7-7	grass	gentle	loam	dry	43.0	29.0	5366670.	509239.688.:bottom	35.0	partly overcast	5-10w	dk brn;sandy/some loam
DOE1-CV7-8	summerfallow	flat	silt	wet	43.0	29.0	5366771.	509353.687.:bench	40.0	partly overcast	5nw	dk loam hvy clay
DOE1-CV7-9	summerfallow	steep	silty loam	damp	43.0	29.0	5366856.	509493.689.(hillside	42.0	partly overcast	5-10w	dk loam hvy clay??
DOE1-CV7-10	summerfallow	gentle	loam	damp	43.0	29.0	5366919.	509635.683.(hillside	42.0	partly overcast	5w	dk brn almost black
DOE1-CV7-11	summerfallow	gentle	loam	damp	42.0	29.3	5366972.	509787.679.:hillside	40.0	partly overcast	5-11nw	redish brown very fine;rocks!!
DOE1-CV7-12	grass	steep	silty loam	dry	38.0	29.6	5367003.	509922.678.:bottom	30.0	partly overcast	5-11nw	dk brown: some clay
DOE1-CV7-13	stubble	steep	loam	damp	38.0	29.0	5366954.	510113.673.:bottom	38.0	cloudy	0-5w	
DOE1-CV7-14	stubble	flat	loam	dry	38.0	29.0	5366879.	510244.671.:bench	42.0	cloudy	0-5w	
DOE1-CV7-15	stubble	flat	loam	damp	35.0	29.2	5366812.	510383.669.:plain	42.0	cloudy	5-15nw	
DOE1-CV7-16	stubble	gentle	silty loam	damp	40.0	29.4	5366722.	510508.664.:bench	42.0	sunny	0-5NW	
DOE1-CV7-17	stubble	gentle	silty loam	damp	40.0	29.4	5366628.	510631.663.:plain	42.0	sunny	0-5NW	
DOE1-CV7-18	CRP	flat	silt	dry	41.0	28.7	5366518.	510740.660.:plain	42.0	partly overcast	0-5NW	
DOE1-CV7-19	CRP	flat	silt	damp	42.0	28.7	5366391.	510823.658.:plain	42.0	partly overcast	0-5NW	
DOE1-CV7-20	CRP	flat	silty loam	damp	42.0	28.7	5366240.	510903.656.:plain	42.0	partly overcast	0-5NW	
DOE1-CV7-21	CRP	flat	silty loam	dry	42.0	28.7	5366090.	510942.655.:plain	42.0	partly overcast	0-5NW	
DOE1-CV7-22	CRP	flat	loam	dry	42.0	28.5	5365938.	510932.657.:hillside	42.0	partly overcast	0-5NW	
DOE1-CV7-23	CRP	gentle	silty loam	dry	40.0	28.5	5365792.	510881.661.:hillside	36.0	partly overcast	0-5NW	
DOE1-CV7-24	CRP	gentle	silty loam	dry	45.0	28.5	5365648.	510823.661.:hillside	38.0	partly overcast	0-5NW	
DOE1-CV7-25	CRP	gentle	silt	dry	45.0	28.5	5365502.	510775.660.:hillside	42.0	partly overcast	0-5NW	
DOE1-CV7-26	summerfallow	gentle	loam	damp	45.0	28.5	5365351.	510706.665.:hillside	40.0	partly overcast	0-5NW	
DOE1-CV7-27	summerfallow	gentle	loam	damp	45.0	28.5	5365227.	510620.670.:hillside	39.0	partly overcast	0-5NW	
DOE1-CV7-29	summerfallow	gentle	loam	damp	45.0	28.5	5365115.	510518.676.:hillside	39.0	partly overcast	0-5NW	
DOE1-CV7-30	summerfallow	flat	loam	damp	45.0	28.6	5365012.	510402.677.:hilltop	30.0	partly overcast	0-5NW	
DOE1-CV7-31	summerfallow	flat	silty loam	damp	45.0	28.6	5364918.	510276.677.:hilltop	42.0	partly overcast	0-5NW	
DOE1-CV7-32	summerfallow	flat	silty loam	damp	44.0	28.9	5364825.	510157.677.:hilltop	42.0	partly overcast	0-5NW	
DOE1-CV7-33	grass	flat	silt	damp	44.0	29.0	5364760.	510002.672.:hilltop	42.0	partly overcast	0-5NW	
DOE1-CV7-34	stubble	flat	silty loam	damp	46.0	29.0	5364728.	509847.671.:plain	42.0	cloudy	0-5NW	
DOE1-CV7-35	stubble	gentle	loam	damp	45.0	29.1	5364735.	509680.664.:bottom	40.0	cloudy	0-5NW	
DOE1-CV7-36	stubble	gentle	loam	damp	40.0	29.4	5364792.	509540.667.:hillside	38.0	cloudy	0-5w	
DOE1-CV7-37	summerfallow	flat	loam	damp	35.0	29.1	5364859.	509401.661.:plain	42.0	cloudy	dk brn with alott of clay	
DOE1-CV7-38	summerfallow	flat	loam	damp	35.0	29.1	5365081.	509168.663.:plain	40.0	partly overcast	5-10nw	
DOE1-CV7-39	stubble	flat	sand	dry	35.0	29.1	5365318.	509042.670.:plain	42.0	partly overcast	5-10nw	
DOE1-CV7-40	stubble	flat	silt	damp	35.0	29.1	5365458.	508995.673.:plain	42.0	partly overcast	5-10nw	
DOE1-CV7-41	stubble	flat	silty loam	damp	35.0	29.1	5365619.	508969.676.:plain	42.0	partly overcast	10nw	
DOE1-CV8-1	grass	gentle	silt	dry	40.0	30.0	5362596.	516706.670.:plain	42.0	cloudy	5-8W	
DOE1-CV8-2	grass	flat	silty loam	dry	40.0	29.8	5362634.	516556.672.:hilltop	42.0	cloudy	TAN;lt brn	
DOE1-CV8-3	grass	steep	clay	dry	40.0	29.8	5362700.	516422.658.:hillside	42.0	cloudy	clay : gray;	
DOE1-CV8-4	grass	steep	silty loam	dry	40.0	29.8	5362799.	516295.666.:hillside	42.0	cloudy	more silt than loam	
DOE1-CV8-5	grass	steep	silty loam	dry	40.0	29.8	5362909.	516205.665.:hillside	42.0	cloudy	more silt than loam	
DOE1-CV8-6	grass	flat	silty loam	dry	38.0	30.0	5363050.	516124.671.:hillside	42.0	cloudy	brn; alot of big rocks here	
DOE1-CV8-7	weeds	steep	silt	dry	37.0	30.0	5363199.	516089.660.:bottom	35.0	cloudy	lt brn hit gravel or something	
DOE1-CV8-8	weeds	steep	silt	dry	32.0	29.8	5363350.	516081.672.:hillside	42.0	cloudy	cream! lt yellow;very fine	
DOE1-CV8-9	weeds	steep	silty loam	damp	40.0	29.0	5363700.	516143.671.:hilltop	37.0	raining	BRN in steep cooly	
DOE1-CV8-10	grass	gentle	silty loam	dry	38.0	29.5	5363936.	516373.695.:hilltop	40.0	cloudy	lt brn	
DOE1-CV8-11	stubble	flat	loam	damp	37.0	29.7	5363947.	517033.700.:plain	42.0	cloudy	dk brn streaks of gray;clay	
DOE1-CV8-12	summerfallow	gentle	loam	damp	37.0	29.7	5363643.	517338.689.:plain	42.0	cloudy	good brown soil	
DOE1-CV8-13	grass	gentle	silty loam	dry	36.0	29.7	5363290.	517385.684.:plain	42.0	cloudy	tan with gray tent	
DOE1-CV8-14	grass	flat	silt	dry	35.0	29.8	5362723.	517045.673.:plain	42.0	snowing	10-16nw	
DOE1-CV9-1	stubble	flat	silty loam	dry	41.0	29.9	5372268.	518110.727.:plain	36.0	sunny	5-10nw	
DOE1-CV9-2	stubble	flat	loam	dry	41.0	29.9	5372222.	517782.723.:plain	37.0	sunny	fine tan silt	
DOE1-CV9-3	stubble	gentle	loam	dry	41.0	29.9	5371976.	517620.724.:hillside	37.0	sunny	calm-0-5w	
											hard dry;dk brn almost black	

DOE1-CV9-4	stubble	flat	silty loam	dry	38.7	29.8	5371730.	517749.	720.	hillside	37.0	sunny	calm-0-5w	brn
DOE1-CV9-5	stubble	gentle	silty loam	dry	36.5	29.8	5371723.	518189.	718.	hillside	37.0	sunny	calm-0-5w	brn
DOE1-CV9-6	stubble	gentle	silty loam	dry	34.0	29.8	5371923.	518353.	720.	hillside	37.0	partly overcast	calm-0-5w	cream;lt brn very fine
DOE1-CP9-1	stubble	flat	silty loam	dry	48.0	28.5	5372228.	518618.	729.	plain	37.0	partly overcast	10W	LT BRN very fine
DOE1-CP9-2	stubble	gentle	silty loam	dry	48.0	28.5	5372180.	518474.	726.	hillside	37.0	partly overcast	10-15nw	brown
DOE1-CP9-3	stubble	gentle	silty loam	dry	34.0	29.9	5372136.	518325.	726.	plain	37.0	partly overcast	CALM	dk brn
DOE1-CP9-4	stubble	flat	silty loam	dry	34.0	29.9	5372060.	518212.	722.	plain	37.0	partly overcast	CALM	lt brn
DOE1-CP9-5	stubble	flat	silty loam	dry	35.0	29.0	5372003.	518073.	723.	plain	37.0	cloudy	6-12NW	DK BRN
DOE1-CP9-6	stubble	flat	silty loam	dry	35.0	29.0	5371932.	517940.	724.	plain	37.0	cloudy	15-20NW	BRN
DOE1-CP9-7	stubble	flat	silty loam	dry	35.0	29.0	5371888.	517801.	721.	plain	37.0	cloudy	15-20NW	cream;tan; a lot of silt
DOE1-CP9-8	stubble	gentle	silty loam	dry	35.0	29.0	5371840.	517660.	720.	hillside	37.0	cloudy	20NW	brown
DOE1-CP9-9	stubble	gentle	silty loam	damp	46.0	28.5	5371764.	517528.	721.	hillside	37.0	partly overcast	10-15nw	brown
DOE1-CP9-10	stubble	gentle	loam	dry	46.0	28.5	5371686.	517391.	717.	hillside	37.0	partly overcast	10-15nw	brown; HEAVY on the clay
DOE1-CV13-1	stubble	flat	loam	damp	32.0	29.8	5368771.	519836.	711.	plain	42.0	partly overcast	0-5NW	DK BRN almost black
DOE1-CV13-2	stubble	gentle	silt	dry	32.0	29.8	5369043.	520372.	710.	plain	36.0	partly overcast	0-5NW	tan very fine;bent 42"auger
DOE1-CV13-3	stubble	gentle	loam	damp	32.0	30.0	5368790.	520944.	707.	hilltop	37.0	sunny	0-5NW	dk brn may be some silt
DOE1-CV13-4	stubble	flat	silty loam	dry	40.0	30.0	5367848.	521044.	695.	plain	37.0	sunny	CALM	tan somewhat sandy
DOE1-CV13-5	stubble	flat	silt	dry	40.0	30.0	5367537.	520633.	698.	plain	36.0	sunny	CALM	brn some loam
DOE1-CV13-6	stubble	flat	loam	damp	40.0	30.0	5367438.	520134.	701.	plain	36.0	sunny	CALM	dk brn
DOE1-CV13-7	stubble	gentle	loam	dry	40.0	30.0	5367743.	519740.	715.	plain	36.0	partly overcast	15-20NW	brown may be some clay??
DOE1-CP13-1	stubble	flat	silty loam	dry	50.0	29.3	5368353.	521410.	698.	plain	37.0	partly overcast	15-20NW	LT BRN a lot of silt
DOE1-CP13-2	stubble	flat	loam	damp	50.0	29.3	5368358.	521254.	698.	plain	37.0	partly overcast	15-20NW	brown:gray?? lots of clay
DOE1-CP13-3	stubble	flat	silty loam	dry	30.0	30.0	5368361.	521095.	699.	plain	42.0	cloudy	8nw	tan
DOE1-CP13-4	grass	flat	silt	dry	30.0	30.0	5368370.	520940.	700.	plain	42.0	cloudy	8nw	lt brn
DOE1-CP13-5	stubble	flat	silt	dry	30.0	30.0	5368322.	520790.	700.	plain	42.0	cloudy	8nw	tan
DOE1-CP13-6	stubble	gentle	silty loam	dry	30.0	30.0	5368274.	520645.	704.	plain	42.0	cloudy	8nw	brn
DOE1-CP13-7	stubble	gentle	loam	damp	30.0	30.0	5368252.	520492.	708.	plain	42.0	cloudy	calm	brn
DOE1-CP13-8	stubble	gentle	silty loam	dry	30.0	30.0	5368246.	520340.	710.	plain	42.0	cloudy	calm	brn
DOE1-CP13-9	stubble	gentle	loam	dry	30.0	29.8	5368246.	520185.	711.	plain	42.0	cloudy	calm	dk brn
DOE1-CP13-11	summerfallow	flat	loam	wet	30.0	30.0	5368249.	520209.	711.	plain	38.0	cloudy	calm	
DOE1-CP13-1	stubble	gentle	silty loam	dry	30.0	30.0	5368251.	519875.	715.	plain	42.0	cloudy	calm	lt brn:possible sandy
DOE1-CP13-11	summerfallow	flat	silty loam	damp	30.0	30.0	5368250.	519641.	718.	plain	42.0	cloudy	calm	tan
DOE1-CP13-1	stubble	gentle	loam	dry	50.0	28.8	5368247.	519488.	719.	plain	37.0	cloudy	15-20NW	brown
DOE1-CP13-1	stubble	flat	silty loam	dry	50.0	28.8	5368244.	519334.	722.	plain	37.0	cloudy	10-15nw	brown
DOE1-F1-1	grass	gentle	silty loam	damp	44.0	29.0	5366535.	515647.	708.	hillside	42.0	cloudy	10-20NW	soil was a rusty color
DOE1-F1-2	grass	gentle	silty loam	dry	44.0	29.0	5366391.	515702.	704.	hillside	42.0	cloudy	15-20nw	rusty; veryfine almost clayish
DOE1-F1-3	grass	steep	silty loam	dry	44.0	29.0	5366250.	515755.	699.	hillside	42.0	partly overcast	15-20nw	lt brn
DOE1-F1-4	grass	gentle	silty loam	damp	30.0	29.9	5366082.	515819.	699.	hillside	40.0	snowing	5-10W	REDISH BROWN;yellowish on reddish yellow;rust color
DOE1-F1-5	grass	gentle	silt	dry	30.0	29.9	5365934.	515875.	705.	hillside	41.0	cloudy	5-10W	
DOE1-F1-6	grass	steep	loam	damp	30.0	29.9	5365792.	515929.	698.	hillside	42.0	cloudy	5-10W	brown
DOE1-F1-7	grass	gentle	silt	dry	30.0	29.9	5365641.	515986.	702.	hillside	42.0	cloudy	5-10W	dk brn
DOE1-F1-8	grass	gentle	silt	dry	30.0	29.7	5365500.	516040.	702.	hillside	42.0	cloudy	5-10W	tan
DOE1-F1-9	grass	gentle	silty loam	damp	30.0	29.6	5365359.	516093.	697.	hilltop	38.0	cloudy	5-10W	brn
DOE1-F1-10	grass	flat	silty loam	damp	30.0	29.7	5365217.	516147.	698.	hilltop	42.0	cloudy	5-10W	brn
DOE1-F1-11	grass	flat	silty loam	dry	30.0	29.7	5365088.	516202.	697.	hilltop	42.0	cloudy	5-10W	lt brn
DOE1-F1-12	grass	flat	silt	dry	30.0	29.7	5364933.	516279.	691.	hilltop	38.0	cloudy	5-10W	lt brn
DOE1-F1-13	weeds	steep	silty loam	dry	30.0	29.7	5364803.	516343.	672.	bottom	34.0	cloudy	5-10W	dk brn
DOE1-F1-14	grass	gentle	silty loam	dry	30.0	29.5	5364615.	516436.	673.	hillside	42.0	cloudy	5-10W	tan
DOE1-F1-15	grass	flat	silt	dry	32.0	29.6	5364478.	516504.	697.	hilltop	36.0	partly overcast	5-10W	lt brn
DOE1-F1-16	grass	flat	silty loam	dry	32.0	29.6	5364338.	516573.	701.	hilltop	42.0	partly overcast	5-10W	brn
DOE1-F1-17	grass	gentle	silty loam	dry	32.0	29.6	5364205.	516642.	692.	hillside	42.0	partly overcast	5-10W	tan
DOE1-F1-18	grass	gentle	silty loam	dry	32.0	29.5	5364043.	516719.	694.	hillside	42.0	partly overcast	5-10W	tan
DOE1-F1-19	stubble	flat	silty loam	damp	38.0	29.5	5363899.	516790.	700.	plain	42.0	partly overcast	5-10W	dk brn some sand & pebbles
DOE1-F1-20	stubble	flat	silty loam	damp	38.0	29.5	5363757.	516862.	697.	plain	42.0	partly overcast	5-10W	dk brn
DOE1-F1-21	summerfallow	gentle	silty loam	damp	38.0	29.5	5363628.	516927.	693.	plain	42.0	partly overcast	5-10W	dk brn
DOE1-F1-22	summerfallow	flat	loam	damp	38.0	29.5	5363500.	516993.	690.	hilltop	42.0	partly overcast	5-10W	dk brn some gray clay???
DOE1-F1-23	grass	flat	silty loam	dry	38.0	29.5	5363354.	517068.	682.	bottom	42.0	partly overcast	5-10W	dk brn some gray clay???
DOE1-F1-24	grass	flat	silty loam	dry	38.0	29.5	5363215.	517139.	684.	hilltop	42.0	partly overcast	5nw	dk brn
DOE1-F1-25	grass	flat	silty loam	dry	30.0	29.8	5363071.	517212.	680.	plain	42.0	cloudy	8NW	LT BRN; a lot of silt
DOE1-F1-26	grass	flat	silty loam	dry	30.0	29.8	5362966.	517266.	672.	plain	42.0	cloudy	8NW	LT BRN; a lot of silt
DOE1-F1-27	grass	flat	silt	dry	31.0	29.7	5362831.	517335.	674.	plain	40.0	cloudy	5w	tan
DOE1-F1-28	weeds	flat	silty loam	dry	31.0	29.7	5362530.	517489.	666.	bottom	42.0	cloudy	5w	dark brn
DOE1-F1-29	grass	gentle	silt	dry	31.0	29.7	5362407.	517555.	665.	hillside	42.0	cloudy	5w	tan
DOE1-F1-30	grass	gentle	silt	damp	31.0	29.7	5362274.	517625.	660.	hillside	42.0	cloudy	5w	tan
DOE1-F1-31	grass	flat	silt	dry	31.0	29.7	5362138.	517698.	655.	bottom	42.0	cloudy	5w	reddish tan;real # 31
DOE1-F1-32	grass	steep	silty loam	dry	31.0	30.1	5361995.	517774.	658.	hillside	42.0	cloudy	5w	rusty;lt brn;more silt th loam
DOE1-F1-33	grass	gentle	loam	dry	35.0	30.1	5361863.	517845.	652.	hillside	42.0	cloudy	5w	brn;gray; a lot of clay
DOE1-F1-34	stubble	flat	loam	damp	35.0	30.0	5361726.	517918.	649.	bottom	42.0	cloudy	5w	reddish brn clay???
DOE1-F1-35	summerfallow	gentle	loam	damp	35.0	30.1	5361590.	517990.	649.	bench	42.0	cloudy	5w	tan
DOE1-F1-36	summerfallow	flat	loam	damp	35.0	30.1	5361452.	518064.	659.	hilltop	37.0	cloudy	5w	lt brn
DOE1-F1-37	stubble	gentle	sand	damp	38.0	30.1	5361255.	518169.	651.	bottom	42.0	cloudy	5w	tan

TABLE MS3: NORTHEAST SMOKE CREEK
GPS Sample sites: Phase III, Smoke Creek Revisited

DOESITENO	VEGETATION	SLOPE	SOIL	MOIST.	AIR TEMP	P-psi	LAT	LONG	ALT	AUGER DEPTH	WEATHER	WIND	COMMENTS	
DOE1-Cv10-1	CRP	gentle	silty loam	dry	51	29.5	5376261.518629.715.	i bench	37	sunny	5nw	dk brn		
DOE1-Cv10-2	CRP	steep	clay	damp	51	29.5	5376301.519247.719.	i hillside	37	sunny	5nw	greenish-gray		
DOE1-Cv10-3	grass	steep	sand	dry	51	29.5	5375918.519230.734.	i hillside	37	sunny	5nw	sandy; tan		
DOE1-Cv10-4	grass	flat	silt	dry	47	29.5	5375759.518975.736.	i plain	37	sunny	5nw	It brn		
DOE1-Cv10-5	CRP	flat	silty loam	dry	45	29.5	5375881.518677.730.	i hilltop	37	partly overcast	5nw	It brn		
DOE1-CP10-1	grass	gentle	loam	dry	51	29.4	5376115.519593.726.	i hillside	36	sunny	5W	DK BRN		
DOE1-CP10-2	CRP	gentle	silt	dry	51	29.4	5376117.519439.726.	i hillside	37	sunny	5W	It brn		
DOE1-CP10-3	CRP	gentle	sand	damp	51	29.4	5376103.519283.730.	i hilltop	37	sunny	5W	tan		
DOE1-CP10-4	CRP	steep	sand	dry	51	29.4	5376101.519135.721.	i bottom	37	sunny	5W	tan		
DOE1-CP10-5	CRP	gentle	silty loam	dry	51	29.2	5376101.518998.731.	i hilltop	37	sunny	5W	It brn		
DOE1-CP10-6	CRP	gentle	silty loam	dry	51	29.2	5376089.518808.726.	i hilltop	37	sunny	5W	tan		
DOE1-CP10-7	CRP	gentle	silty loam	dry	51	29.2	5376088.518613.718.	i hillside	37	sunny	5nw	It brn		
DOE1-CP10-8	CRP	gentle	silty loam	dry	51	29.2	5376079.518459.727.	i hillside	37	sunny	5nw	dk brn		
DOE1-CP10-9	CRP	gentle	sand	dry	51	29.2	5376074.518304.733.	i hillside	37	sunny	5nw	sandy??		
DOE1-CV11-1	grass	flat	gravel	damp	35	30.0	5376743	523701.641	bench	40	partly overcast	5W	SAND & gravel	
DOE1-CV11-2	weeds	steep	clay	damp	35	30.0	5376574	523450.636	hillside	40	partly overcast	calm	SANDY clay tan with red tent	
DOE1-CV11-3	weeds	steep	silt	dry	35	30.0	5376106	523388.635	hillside	38	cloudy	5w	very sandy silt dk brn	
DOE1-CV11-4	grass	flat	sand	dry	34	30.0	5375983	523655.633	bottom	42	cloudy	5w	dk brn	
DOE1-CV11-5	bare	steep	silt	dry	34	30.0	5376136	523930.647	hillside	42	cloudy	calm	Gray	
DOE1-CV11-6	grass	steep	silty loam	dry	28	30.0	5376563	523995.654	hillside	42	cloudy	8sw	tan	
DOE1-CP11-1	weeds	flat	silty loam	damp	48	28.6	5376341.524311.654.	i plain	42	cloudy	25-30NW	DK BRN LOOKS LIKE CRP??		
DOE1-CP11-2	grass	flat	silty loam	dry	48	29.0	5376341.524169.658.	i plain	42	cloudy	25-30NW	BROWN ALOT OF SILT		
DOE1-CP11-3	grass	gentle	silty loam	dry	48	29.0	5376341.524009.655.	i hillside	42	partly overcast	25-30NW	BROWN		
DOE1-CP11-4	grass	steep	silty loam	dry	48	29.0	5376340.523838.645.	i bottom	39	partly overcast	25-30NW	dk brn;in a valley steep sides		
DOE1-CP11-5	grass	gentle	loam	dry	48	29.0	5376339.523665.641.	i bottom	42	partly overcast	25-30NW	dk brn;alot of clay hard packe		
DOE1-CP11-6	grass	flat	silt	dry	48	29.0	5376339.523501.636.	i bottom	42	partly overcast	25-30NW	very fine,dk brn		
DOE1-CP11-7	weeds	steep	silty loam	dry	48	28.8	5376338.523337.653.	i hillside	42	partly overcast	25-30NW	dk br almost blk very steep		
DOE1-CP11-8	grass	flat	silt	dry	50	28.7	5376338.523175.665.	i plain	42	sunny	25-30NW	cream;lt tan;maybe some loam		
DOE1-CP11-9	grass	gentle	silty loam	dry	50	29.0	5376337.523010.664.	i plain	42	sunny	25-30NW	lt brn		
DOE1-CV12-1	grass	flat	clay	damp	35	29.5	5374654.524314.650.	i hilltop	40	partly overcast	5-10NW	DK BRN LOAN TURNED RED!!		
DOE1-CV12-2	grass	flat	silty loam	wet	35	29.5	5374038.524365.655.	i plain	36	partly overcast	5-10NW	dk brn		
DOE1-CV12-3	grass	gentle	silty loam	damp	38	29.1	5373632.524073.657.	i hillside	40	partly overcast	5-10NW	tan;blkspots;grayblueClaybotte		
DOE1-CV12-4	stubble	gentle	loam	damp	38	29.1	5373582.523296.674.	i plain	40	partly overcast	calm	dk brn some clay		
DOE1-CV12-5	stubble	gentle	loam	dry	38	29.1	5373900.523020.689.	i plain	40	partly overcast	calm	rust; very fine;like clay-loam		
DOE1-CV12-6	weeds	steep	silt	dry	38	29.8	5374630.522984.655.	i hillside	49	partly overcast	5-8w	redish brn;scory rock al arou		
DOE1-CV12-7	grass	flat	silt	dry	38	29.5	5375003.523657.655.	i plain	49	partly overcast	25-30NW	tan;lt brn gravel on bottom		
DOE1-CP12-1	grass	gentle	silty loam	dry	52	29.0	5374369.524703.639.	i bench	42	partly overcast	25-30NW	lt brn		
DOE1-CP12-2	grass	steep	silt	dry	49	29.0	5374376.524556.650.	i hillside	37	partly overcast	25-30NW	tan very fine soil		
DOE1-CP12-3	grass	flat	gravel	dry	49	29.3	5374367.524413.655.	i plain	37	partly overcast	30NW	dk brn silt		
DOE1-CP12-4	grass	gentle	silty loam	dry	48	29.3	5374355.524260.652.	i plain	42	partly overcast	30NW	dk brn loam?		
DOE1-CP12-5	grass	gentle	silty loam	dry	48	29.3	5374349.524101.657.	i hilltop	42	partly overcast	15-25SW	LT BRN/With reddish tent		
DOE1-CP12-6	grass	flat	silty loam	dry	47	29.3	5374348.523939.658.	i plain	42	partly overcast	15-25SW	tan partly rocky		
DOE1-CP12-7	grass	gentle	silty loam	dry	47	29.3	5374346.523781.658.	i hillside	42	partly overcast	15-25SW	dk brn		
DOE1-CP12-8	grass	gentle	silty loam	dry	42	30.0	5374346.523609.(659.	i bench	42	cloudy	15-25SW	LT BRN/With reddish tent		
DOE1-CP12-9	grass	gentle	silty loam	dry	45	30.0	5374342.523434.666.	i bench	42	cloudy	15-25SW	tan partly rocky		
DOE1-CP12-10	grass	gentle	silty loam	dry	52	29.7	5374342.523244.670.	i bottom	42	cloudy	15-25SW	dk brn		
DOE1-CP12-11	grass	gentle	silt	dry	52	29.7	5374336.523075.677.	i hillside	42	cloudy	15-25SW	cream; or tan very fine		
DOE1-CP12-12	weeds	steep	silt	dry	52	30.0	5374333.522921.666.	i hillside	42	cloudy	15-25sw	cream; or tan very fine		
DOE1-CP12-13	grass	gentle	clay	dry	53	30.0	5374334.522765.(670.	i hillside	42	cloudy	15-25sw	dkbrnloan/rustGray clay lst2in		
DOE1-CP12-14	grass	steep	silty loam	dry	53	30.0	5374332.522611.672.	i hillside	42	cloudy	calm	lt brn ; tan ; fine		
MSC1-L4-1	stubble	gentle	silty loam	damp	32	29.2	5379310.526018.665.	i plain	40	partly overcast	7w	BRN		
MSC1-L4-2	stubble	flat	silty loam	damp	32	29.2	5379100.525791.661.	i plain	40	partly overcast	5w	dk brn		
MSC1-L4-3	grass	flat	silty loam	damp	32	29.2	5378889.525562.656.	i plain	40	partly overcast	5w	dk brn		
MSC1-L4-4	CRP	flat	silty loam	dry	40	28.6	5378660.525313.655.	i plain	40	partly overcast	5w	lt brn		
MSC1-L4-5	CRP	gentle	silty loam	dry	40	28.6	5378424.525058.653.	i plain	40	partly overcast	calm	tan more silt slightly rockie		
MSC1-L4-6	summerfallow	flat	loam	damp	39	29.0	5378192.524806.645.	i plain	40	partly overcast	calm	brn loam with lt brn sand		
MSC1-L4-7	stubble	flat	loam	damp	34	28.8	5377978.524574.645.	i plain	40	partly overcast	8w	gray brn clayish loam.Lot of c		
MSC1-L4-8	summerfallow	gentle	loam	damp	33	28.5	5377758.524335.646.	i hillside	40	partly overcast	8w	dk brn loam with sand		
MSC1-L4-9	grass	gentle	loam	dry	33	28.5	5376242.522840.664.	i plain	37	partly overcast	8w	dk brn and very hard		
DOE1-L4-10	stubble	flat	loam	damp	35	29.4	5376032.522626.668.	i plain	40	partly overcast	10sw	?#10;brngry some clay		
DOE1-L4-11	bare	steep	silt	dry	35	29.4	5375778.522370.663.	i plain	42	partly overcast	10sw	dk brn very fine by road& hill		
DOE1-L4-12	bare	steep	silt	dry	35	29.4	5375577.522161.672.	i hillside	42	partly overcast	10sw	yellow;yellowTan veryfine loam		
DOE1-L4-13	grass	steep	silty loam	dry	35	29.4	5375313.521892.682.	i hillside	42	partly overcast	10sw	yellow;yellowTan veryfine loam		
DOE1-L4-14	grass	flat	silty loam	dry	35	29.4	5374993.521565.677.	i hilltop	38	partly overcast	10sw	tan on a plateau		
DOE1-L4-15	weeds	flat	loam	wet	35	29.4	5374778.521344.667.	i hilltop	39	partly overcast	10sw	dk brn stream mud!		

TABLE MS4: HEAD GAS DATA
Phase III, More Smoke Creek

CV = Curvilinear, CP = Curvilinear Perpendicular
L = Lineament

DOE #	X	Y	SAMPLE	METHANE	ETHANE	PROPANE	IBUTANE	BUTANE	IPENTANE	PENTANE	EH	PH	UMHOS	
CV1-1	53494	53636	38	3.438	0.320	0.211	0.500	0.930				173	7.380	433
CV1-2	53395	53628	39	43.734	8.294	3.899	0.369	1.686	0.398	1.182	22	7.460	83	
CV1-3	5319	53644	4	36.270	5.985	2.490	0.221	1.230	0.285	1.246	212	7.330	73	
CV1-4	5344	536543	41	27.411	5.120	2.100	0.163	0.841	0.270	0.960	27	6.950	78	
CV1-5	52854	536577	42	17.544	3.560	1.376	0.980	0.487	0.122	0.130	28	7.490	729	
CV2-1	53688	537713	43	16.541	2.824	1.220	0.133	0.928	0.184	0.410	21	7.480	474	
CV2-2	538	53799	44	19.118	3.530	1.640	0.120	0.570	0.124	0.173	7	7.820	625	
CV2-3	53737	5371126	45	2.383	1.927	0.410	0.128	1.100	0.129	0.560	228	6.830	671	
CV2-4	53625	5371299	46	27.823	4.966	2.223	0.187	0.865	0.249	0.555	21	7.700	74	
CV2-5	53155	537631	47	32.454	3.695	1.748	0.500	0.432	0.780	0.580	11	6.790	496	
CV2-6	5331	537862	48	2.336	0.145		0.310	0.230			161	8.250	259	
CV2-7	5379	537187	49	317.470	63.848	27.970	2.778	11.363	3.391	7.455	38	6.490	964	
CV2-8	53186	537132	5	4.870	0.744	0.438	0.890	0.338	0.510		2	7.660	755	
CV3-1	5756	5374555	51	47.956	2.748	1.240	0.140	0.273			142	8.230	266	
CV3-2	5199	5374548	53	8.345	1.326	0.473	0.180	0.185	0.990		196	8.900	534	
CV3-3	51335	5374821	54	33.253	6.554	2.869	0.265	1.128	0.254	1.370	-55	7.680	69	
CV3-4	51312	537588	55	24.813	5.272	2.444	0.226	0.811	0.210	0.131	88	7.950	685	
CV3-5	51189	537535	56	24.619	4.685	2.270	0.260	0.810	0.234	0.498	14	7.760	675	
CV3-6	5799	5375419	57	6.549	11.584	5.520	0.418	1.690	0.440	0.765	48	7.540	663	
CV3-7	559	5375333	58	38.620	6.840	3.400	0.284	1.140	0.345	0.543	-64	7.900	645	
CV3-8	529	5375177	59	63.720	8.543	3.471	0.310	1.233	0.351	0.683	28	7.410	633	
CV3-9	544	5374822	6	29.561	4.325	2.180	0.185	0.938	0.211	0.384	179	7.610	549	
CV3-10	5584	5374687	52	5.610	7.610	3.500	0.227	1.756	0.224	0.444	3	7.000	689	
CV4-1	5631	5376957	61	1.585	1.370	0.723	0.124	0.338	0.145	0.160	123	7.910	68	
CV4-2	538	5376967	63	18.868	2.381	1.262	0.154	0.959	0.197	0.372	86	7.690	589	
CV4-3	5114	5376899	64	39.197	5.730	2.493	0.260	0.927	0.286	0.477	29	7.600	632	
CV4-4	499888	5376729	65	3.491	5.817	2.582	0.211	1.300	0.296	0.635	-66	7.790	658	
CV4-5	499797	5376495	66	4.181	0.191		0.560	0.300	0.530		232	7.380	726	
CV4-6	499833	5376312	67	21.284	1.749	0.937	0.131	0.898		0.277	145	7.900	56	
CV4-7	499935	5376156	68	9.737	1.161	0.557	0.850	0.540	0.160	0.230	-73	7.590	763	
CV4-8	5387	5375911	69	6.227	0.672	0.381	0.900	0.280			193	7.730	527	
CV4-9	564	537681	7	13.380	1.392	0.759	0.990	0.530	0.147	0.710	-154	7.620	627	
CV4-10	5687	5376224	62	16.770	1.839	0.816	0.190	0.357	0.183	0.166	-4	7.550	538	
CV6-1	513921	5367346	116	39.292	4.896	2.328	0.235	0.991	0.258	0.668	214	6.750	814	
CV6-2	513626	5367435	117	9.987	1.496	0.790	0.130	0.899	0.112	0.720	-37	8.900	658	
CV6-3	513286	5367721	118	4.253	0.570	0.410	0.790	0.157	0.140		153	8.500	642	
CV6-4	51366	5368228	119	21.288	1.744	0.953	0.120	0.182	0.325	0.588	227	6.910	785	
CV6-5	513123	5368818	12	1.659	1.570	0.679	0.320	0.430	0.113	0.500	98	7.820	732	
CV6-6	513579	53691	121	2.132	0.950	0.764	0.137	1.420	0.121	0.258	232	7.000	85	
CV6-7	51392	5369111	122	12.100	1.646	1.360	0.138	0.460	0.159	0.100	3	7.760	695	
CV7-1	536584	58969	171	73.572	6.430	2.867	0.360	0.985	0.325	0.530	-4	7.200	937	
CV7-2	5365955	58981	172	89.459	11.896	5.767	0.649	2.539	0.739	1.580	-218	6.700	958	
CV7-3	536613	5917	173	12.328	0.756	0.376	0.610	0.520	0.210	0.230	-23	7.540	71	
CV7-4	5366247	5966	174	16.994	0.929	0.565	0.350	0.345	0.940	0.400	29	7.190	793	
CV7-5	5366461	5987	175	35.521	3.665	1.555	0.228	0.939	0.287	0.646	45	6.660	712	
CV7-6	5366546	59143	176	23.100	4.300	1.882	0.241	0.574	0.187	0.510	-133	7.920	53	
CV7-7	5366667	59239	177	73.338	6.952	3.226	0.345	1.516	0.430	0.782	-156	6.400	84	
CV7-8	5366771	59356	178	32.593	2.625	1.314	0.200	0.619	0.240	0.117	-17	7.290	677	
CV7-9	5366857	59493	179	11.967	1.298	0.679	0.128	0.256	0.650	0.700	-170	8.100	571	
CV7-10	5366919	59635	18	8.722	0.595	0.350	0.100	0.200	0.164		-119	7.910	622	
CV7-11	5366972	59788	181	2.773	2.121	0.999	0.153	0.760	0.133		48	7.490	917	
CV7-12	53673	59923	182	29.277	1.210	1.190	0.165	0.764	0.233	0.570	-270	6.670	1191	
CV7-13	5366955	51113	183	43.972	3.489	1.891	0.241	1.780	0.264	0.346	-81	7.180	85	
CV7-14	5366879	51245	184	16.319	0.882	0.576	0.970	0.391	0.173		-8	7.450	666	
CV7-15	5366812	51384	185	8.569	0.513	0.187	0.490	0.168	0.280	0.820	18	8.220	63	
CV7-16	5366722	5158	186	12.931	0.795	0.411	0.580	0.281	0.114	0.130	31	8.160	658	
CV7-17	5366628	51632	187	8.259	0.416	0.220	0.290	0.620	0.129	0.280	47	7.860	595	
CV7-18	5366519	51741	188	17.611	0.433	0.312	0.550	0.356	0.760	0.169	27	7.200	823	
CV7-19	5366391	51824	189	1.990	0.490	0.393	0.500	0.765	0.250	0.195	35	7.130	84	
CV7-20	536624	5194	19	5.385	0.200	0.460	0.500	0.173		0.460	43	7.830	956	
CV7-21	536691	51942	191	8.293	0.513	0.210	0.220	0.229		0.273	72	7.800	231	
CV7-22	5365938	51934	192	22.438	2.640	1.217	0.189	0.577	0.134	0.398	54	7.840	349	
CV7-23	5365792	51881	193	25.297	2.576	1.320	0.161	0.731	0.214	1.520	56	7.110	838	
CV7-24	5365648	51825	194	11.370	0.573	0.361	0.370	0.184	0.870	0.180	72	7.400	672	
CV7-25	5365552	51777	195	11.326	0.966	0.266	0.180	0.234	0.137		14	8.110	743	
CV7-26	5365352	5176	196	35.234	4.387	1.866	0.240	0.543	0.273	0.178	69	7.610	625	

TABLE MS4: HEAD GAS DATA
Phase III, More Smoke Creek

CV = Curvilinear, CP = Curvilinear Perpendicular
L = Lineament

DOE #	X	Y	SAMPLE	METHANE	ETHANE	PROPANE	IBUTANE	BUTANE	IPENTANE	PENTANE	EH	PH	UMHOS
CV7-27	5365227	51621	197	2.511	2.131	1.182	0.183	0.447	0.129	0.159	74	7.890	657
CV7-29	5365115	51518	198	23.947	2.520	1.178	0.410	0.479	0.560	0.180	7	7.620	658
CV7-30	536512	5143	199	22.890	2.379	1.670	0.165	0.400	0.114	0.620	12	7.670	75
CV7-31	5364919	51277	2	14.510	1.789	0.661	0.130	0.680	0.162		113	7.930	655
CV7-32	5364826	51158	21	19.723	2.440	1.121	0.163	0.160	0.230	0.300	126	7.920	653
CV7-33	5364761	512	22	29.685	1.670	1.400	0.151	0.672	0.100	0.214	-247	7.910	128
CV7-34	5364729	59847	23	13.360	1.883	0.757	0.151	0.370	0.280	0.580	-117	6.780	76
CV7-35	5364735	5988	24	33.698	0.912	0.322	0.530	0.660	0.640	0.280	-6	7.980	1592
CV7-36	5364792	5954	25	26.240	3.527	1.646	0.162	0.133	0.940	0.240	9	7.450	765
CV7-37	5364848	5942	26	9.152	1.173	0.157	0.320	0.380	0.450	0.350	96	7.790	1332
CV7-38	536581	59168	27	13.855	1.465	0.644	0.118	0.930	0.490	0.280	129	7.850	229
CV7-39	5365318	5942	28	3.722	0.278	0.131	0.330	0.690	0.370		159	7.420	629
CV7-40	5365459	58995	29	15.810	2.283	0.922	0.940	0.315	0.130	0.760	173	7.540	759
CV7-41	536562	5897	21	12.435	1.566	0.935	0.410	0.660	0.190	0.360	19	7.860	279
CV8-1	5362596	51677	211	34.223	4.740	1.998	0.110	0.634	0.240	0.470	26	7.330	626
CV8-2	5362634	516557	212	9.140	0.590		0.470	0.183	0.560	0.167	21	7.720	689
CV8-3	536271	516423	213	6.817	0.249		0.220	0.188	0.910	0.620	172	8.400	447
CV8-4	5362799	516295	214	6.937	9.394	3.869	0.565	1.513	0.156	0.451	140	6.880	872
CV8-5	536291	51625	215	14.260	2.198	1.860	0.750	0.467	0.230	0.242	-17	7.940	74
CV8-6	53635	516124	216	8.364	0.459		0.420	0.490	0.250	0.240	13	7.720	784
CV8-7	5363199	51689	217	91.664	11.523	5.445	0.471	1.798	0.300	1.238	149	6.770	985
CV8-8	536335	51681	218	9.830	0.568	0.440	0.330	0.610	0.170	0.251	192	6.840	742
CV8-9	53637	516143	219	29.561	2.467	1.519	0.120	0.757	0.391	0.678	76	6.630	986
CV8-10	5363937	516373	22	3.898	0.213	0.100	0.190	0.270	0.450	0.150	156	7.790	947
CV8-11	5363947	51735	221	23.784	3.352	1.433	0.185	0.437	0.122	0.138	214	7.330	63
CV8-12	5363644	517338	222	11.214	1.160	0.269	0.151	0.241	0.156	0.660	236	7.350	452
CV8-13	536329	517386	223	18.977	2.875	1.380	0.380	0.610	0.610	0.230	247	7.620	769
CV8-14	5362724	51745	224	16.458	1.377	0.669	0.160	0.670	0.460	0.450	247	7.930	758
CV9-1	5372269	51811	225	19.734	2.549	1.177	0.232	0.159	0.260	0.680	263	7.670	61
CV9-2	5372223	517782	226	13.476	1.784	0.948	0.370	0.383	0.127	0.950	222	6.940	572
CV9-3	5371976	51762	227	17.870	2.210	1.720	0.184	0.477	0.194	0.252	-75	7.610	67
CV9-4	5371731	517749	228	18.936	2.160	1.425	0.280	0.644	0.348	0.274	-133	7.310	73
CV9-5	5371723	518189	229	11.561	1.750	0.720	0.400	0.331	0.158	0.930	-24	7.710	611
CV9-6	5371924	518353	23	7.334	0.460	0.378	0.200	0.180		147	7.580	61	
CV10-1	518629	5376261	333	43.333	1.936	1.200	0.214	0.820	0.246	0.575	65.600	6.800	41.000
CV10-2	519247	537632	334	9.353	0.770	0.266	0.940	0.460	0.131	0.182	9.500	7.120	875.000
CV10-3	51923	5375918	335	41.990	7.894	4.118	0.550	1.596	0.446	0.758	96.300	7.310	273.000
CV10-4	518975	537576	336	2.634	2.546	1.170	0.249	0.869	0.272	1.388	112.000	6.860	917.000
CV10-5	518677	5375882	337	15.477	1.868	0.950	0.640	0.552	0.253	0.489	12.100	7.830	745.000
CV11-1	52371	5376743	338	31.669	2.762	2.214	0.261	0.938	0.278	0.724	-11.400	7.500	77.000
CV11-2	52345	5376574	339	9.174	0.958	0.362	0.920	0.250	0.720	0.116	39.500	7.670	872.000
CV11-3	523388	537616	34	71.889	11.243	6.780	0.659	2.660	0.680	1.513	-53.000	6.770	131.000
CV11-4	523655	5375983	341	2.532	1.694	1.218	0.196	0.841	0.210	0.448	-81.600	6.880	962.000
CV11-5	52393	5376136	342	5.923	0.238	0.760	0.290	0.250	0.520		53.400	8.800	518.000
CV11-6	523995	5376563	343	48.271	7.196	3.531	0.380	1.573	0.393	1.950	38.100	6.990	975.000
CV12-1	524314	5374654	344	8.700	1.262	0.587	0.163	0.256	0.960	0.134	-21.300	8.630	1612.000
CV12-2	524366	537439	345	58.851	9.250	4.480	0.560	2.800	0.577	1.191	54.600	7.140	17.000
CV12-3	52473	5373632	346	11.923	1.900	0.557	0.320	0.444	0.127	0.224	91.500	7.110	358.000
CV12-4	523296	5373582	347	9.711	1.563	0.552	0.780	0.350	0.114	0.120	92.700	8.140	497.000
CV12-5	52321	53739	348	7.979	0.730	0.329	0.230	0.235	0.930	0.300	-28.400	7.970	957.000
CV12-6	522984	5374631	349	2.193	2.733	1.714	0.110	1.350	0.396	0.697	-3.500	6.640	1131.000
CV12-7	523658	53753	35	55.854	11.227	5.139	0.477	2.370	0.565	1.462	-5.800	6.920	681.000
CV13-1	5368772	519836	231	14.358	1.810	0.910	0.210	0.160	0.151		217	6.960	639
CV13-2	536943	52373	232	19.690	2.432	1.368	0.170	0.647	0.225		-172	7.440	614
CV13-3	536879	52945	233	4.139	0.626	0.926	0.300	0.570	0.160	0.226	-174	7.790	571
CV13-4	5367849	52144	234	16.331	1.973	1.159	0.300	0.578	0.192	0.710	145	7.440	561
CV13-5	5367538	52633	235	18.700	2.155	0.896	0.900	0.491	0.173	0.154	182	7.710	562
CV13-6	5367438	52134	236	44.548	6.456	3.800	0.459	1.194	0.540	0.229	239	7.410	589
CV13-7	5367744	519741	237	8.898	1.110	0.820	0.270	0.583	0.212	0.220	-165	7.720	559
Harmonic Mean				8.954	1.103	0.693	0.244	0.440	0.229	0.315	#NUM!	7.489	214.190
Anomaly (2xHM)				17.907	2.206	1.386	0.487	0.881	0.458	0.631	#NUM!	14.977	428.380
average				23.026	3.390	1.710	0.367	0.799	0.353	0.581	47.573	7.522	564.408
std dev				32.179	6.117	2.758	0.319	1.092	0.362	0.772	113.971	0.502	334.647
minimum				1.585	0.145	0.100	0.100	0.133	0.100	0.100	-269.500	6.400	17.000
maximum				317.470	63.848	27.970	2.778	11.363	3.391	7.455	263.200	8.900	1612.000
Anomaly (1.5 x mean)				34.538	5.084	2.565	0.551	1.198	0.530	0.871	31.7	8.211	846.612
COUNT				125									

pH anomaly defined as mean x (max - mean)/2

TABLE MS4: HEAD GAS DATA
Phase III, More Smoke Creek

CV = Curvilinear, CP = Curvilinear Perpendicular
L = Lineament

DOE #	X	Y	SAMPLE	METHANE	ETHANE	PROPANE	IBUTANE	BUTANE	IPENTANE	PENTANE	EH	PH	UMHOS
Eh anomaly defined as mean / 1.5													
CP1-1	52756	5359825	1	3.496	4.160	2.133	0.222	1.100	0.270	0.640	229	6.980	146
CP1-2	5292	5359918	2	18.812	1.285	1.510	0.510	0.296		0.110	23	7.300	985
CP1-3	5327	53626	3	21.423	1.200	0.778	0.133	0.594	0.181	0.375	26	6.670	643
CP1-4	53158	536148	4	26.842	4.167	1.794	0.232	1.259	0.342	1.270	217	7.690	76
CP1-5	5339	536317	5	32.247	4.668	2.252	0.183	0.747	0.226	0.474	221	7.480	88
CP1-6	53392	536455	6	18.822	2.330	0.960	0.115	0.716	0.190	0.385	217	7.390	89
CP1-7	53496	536574	7	27.467	4.378	2.310	0.293	0.979	0.211	0.462	184	7.730	685
CP2-1	5351	537299	8	16.434	2.770	0.950	0.157	0.273	0.112	0.320	23	7.290	626
CP2-2	53498	537449	9	49.323	4.283	2.397	0.800	0.880	0.258	0.463	15	6.880	636
CP2-3	5352	53769	1	25.395	2.480	1.214	0.181	0.799	0.135	0.320	215	6.910	555
CP2-4	53499	537787	11	77.337	1.819	4.655	0.320	1.680	0.133	0.969	129	6.960	1919
CP2-5	53498	53794	12	19.196	3.260	1.430	0.150	1.148	0.312	0.324	-96	7.190	26
CP2-6	53498	5371134	13	44.675	7.745	3.666	0.517	2.118	0.290	0.711	29	7.420	683
CP2-7	53498	5371295	14	46.220	5.571	2.481	0.700	0.733	0.191	0.394	199	7.340	81
CP2-8	53499	5371451	15	17.394	2.398	1.910	0.930	0.382		0.112	190	7.970	875
CP2-9	53497	5371585	16	27.681	3.844	1.986	0.171	1.855	0.165	0.255	217	7.310	619
CP3-1	51374	5375634	17	22.140	2.982	1.615	0.270	0.760	0.169	0.210	228	7.220	52
CP3-2	5165	5375432	19	14.550	2.168	1.200	0.156	0.522	0.182	0.370	213	7.610	579
CP3-3	5116	537528	2	4.456	0.384	0.271	0.600	0.577	0.390		220	7.500	445
CP3-4	5075	5375133	21	27.563	4.187	1.940	0.257	0.817	0.270	0.282	236	7.400	697
CP3-5	5025	537499	22	15.894	2.279	1.117	0.131	0.464	0.152	0.120	221	7.700	635
CP3-6	5881	5374845	23	38.512	6.270	2.872	0.242	0.922	0.284	0.463	222	7.670	63
CP3-7	5876	5374685	24	1.853	1.423	0.780	0.111	0.322		0.780	238	7.800	578
CP3-8	586	5374532	25	34.622	5.364	1.760	0.175	1.700	0.170	6.417	161	6.550	987
CP3-9	5878	5374379	26	39.730	6.212	2.643	0.190	0.768	0.190	0.652	219	7.300	486
CP3-10	5877	5374282	18	14.667	1.261	0.873	0.800	0.950	0.289	0.480	193	8.240	65
CP4-1	5273	537581	27	8.351	1.286	0.549	0.320	0.180			232	7.110	55
CP4-2	5272	5375759	3	3.767	6.679	2.680	0.218	0.790	0.133	0.376	-155	8.600	667
CP4-3	5272	5375911	31	12.344	2.336	1.110	0.180	0.349	0.810	0.680	117	7.710	721
CP4-4	5271	537659	32	22.587	3.699	1.684	0.176	0.790	0.187	0.385	213	7.620	578
CP4-5	5271	5376211	33	7.188	0.665	0.499	0.640	1.259		0.300	24	7.420	598
CP4-6	527	5376366	34	9.524	19.415	7.482	0.631	3.300	0.834	1.595	229	6.930	575
CP4-7	527	537652	35	15.822	2.891	1.230	0.145	0.579		0.620	-189	7.980	687
CP4-8	5269	5376675	36	12.670	1.333	0.561	0.123	0.480	0.910	0.770	22	7.440	677
CP4-9	527	5376828	37	15.890	1.999	0.915	0.990	0.860	0.113	0.710	-96	7.870	659
CP4-10	5268	5376981	28	19.736	3.457	1.348	0.260	0.816	0.265	0.454	25	7.110	245
CP4-11	5268	5377347	29	28.523	5.700	2.172	0.212	1.296	0.259	0.174	217	7.480	754
CP5-5	51851	536676	114	4.350	0.463	0.246	0.210	0.136			98	7.960	76
CP5-6	5177	5366646	115	12.840	1.380	0.555	0.114	0.325	0.128	0.159	216	7.550	558
CP6-1	513981	5369424	123	9.272	0.771	0.485	0.240	0.280	0.400	0.370	200	7.810	67
CP6-2	513961	5369264	124	14.970	0.864	0.180	0.290	0.444	0.190	0.900	246	6.520	548
CP6-3	513914	5368956	125	7.316	0.771	0.294	0.190	0.341	0.570	0.182	40	7.870	672
CP6-4	513917	5368799	126	13.720	0.945	0.573	0.550	0.419	0.510	0.167	23	7.540	788
CP6-5	513921	5368648	127	14.539	0.861	0.642	0.240	0.518	0.400	0.190	223	7.300	752
CP6-6	513917	5368491	128	32.550	2.811	1.563	0.231	0.994	0.191	0.637	231	6.960	865
CP6-7	513919	5388337	129	22.653	2.958	1.282	0.135	0.522	0.150	0.850	172	7.530	683
CP6-8	513917	5368183	13	8.913	0.800	0.454	0.800	0.230			139	7.690	142
CP6-9	513911	536827	131	17.287	1.600	0.867	0.960	0.425	0.840	0.352	233	6.910	851
CP6-10	513917	5367873	132	12.464	1.161	0.647	0.470	0.382	0.470	0.220	19	7.650	76
CP6-11	513917	536772	133	2.338	1.239	0.879	0.100	0.700	0.131	0.760	247	6.460	621
CP6-12	513919	5367587	134	19.910	0.851	0.596	0.340	0.428	0.310	0.334	229	6.680	772
CP6-13	513921	5367412	135	8.464	1.790	0.574	0.880	0.133		0.135	27	7.740	798
CP6-14	513922	5367194	136	16.586	2.219	1.246	0.161	0.671	0.161	0.230	162	7.570	715
CP6-15	513921	536738	137	4.167	0.496	0.297	0.510	0.176	0.230	0.460	159	8.130	687
CP7-1	5991	5367716	146	12.400	1.563	0.662	0.700	0.227		0.880	175	7.480	476
CP7-2	5992	5367565	147	8.962	0.900	0.320	0.480	0.368	0.700	0.190	24	7.660	681
CP7-3	599	5367421	148	11.938	0.872	0.540	0.270	0.666		0.110	6	7.330	654
CP7-4	5991	5367272	149	5.840	0.553	0.321	0.580	0.720	0.410	0.170	162	8.130	675
CP7-5	599	5367122	15	6.251	0.634	0.312	0.460	0.440	0.150	0.330	89	8.000	681
CP7-6	5991	5366963	151	7.240	0.788	0.377	0.410	0.286	0.120	0.150	53	7.860	63
CP7-7	5992	536687	152	8.955	0.926	0.560	0.138	0.239	0.310	0.160	144	7.610	621
CP7-8	5991	5366659	153	4.310	0.281	0.187	0.240	0.180	0.290		3	7.920	551
CP7-9	5991	5366551	154	9.286	1.113	0.397	0.510	0.770	0.740		164	7.870	62
CP7-10	5991	5366348	155	6.824	0.377	0.191	0.380	0.264	0.210	0.700	-5	7.590	64
CP7-11	5991	5366192	156	7.964	0.622	0.148	0.160	0.850		0.370	24	7.510	652
CP7-12	5991	536642	157	5.269	0.428	0.500	0.180	0.300	0.120	0.420	21	7.410	752

TABLE MS4: HEAD GAS DATA
Phase III, More Smoke Creek

CV = Curvilinear, CP = Curvilinear Perpendicular
L = Lineament

DOE #	X	Y	SAMPLE	METHANE	ETHANE	PROPANE	IBUTANE	BUTANE	IPENTANE	PENTANE	EH	PH	UMHOS		
CP7-13	5992	5365891	158	3.723	0.430	0.173	0.710	0.680				219	7.220	349	
CP7-14	5995	5365738	159	6.100	0.653	0.380	0.220	0.200	0.250	0.210		226	7.900	413	
CP7-15	5994	5365584	16	15.593	1.430	0.886	0.142	0.846	0.540	0.126		235	6.770	1254	
CP7-16	5996	5365427	161	4.364	0.386	0.930	0.160	0.250			2	7.840	1497		
CP7-17	5996	5365275	162	6.566	1.324	0.479	0.900	0.218	0.660			229	7.310	368	
CP7-18	5997	5365118	163	22.926	5.550	1.753	0.415	0.543	0.212	0.114		211	7.720	389	
CP7-19	5997	5364962	164	13.490	1.460	0.440	0.147	0.990	0.440	0.120		197	8.500	843	
CP7-20	5997	5364888	165	2.579	2.116	0.953	0.120	0.863	0.900	0.570		88	7.950	66	
CP7-21	5998	5364666	166	7.271	0.789	0.494	0.100	0.380	0.820			-154	7.610	44	
CP7-22	5991	5364555	167	32.139	4.195	1.877	0.268	1.480	0.350	0.572		185	7.680	575	
CP7-23	59911	5364356	168	8.372	0.771	0.451	0.114	0.850	0.990	0.246		177	7.450	539	
CP7-24	59911	536426	169	24.270	3.420	1.538	0.197	1.269	0.170	0.615		181	6.850	651	
CP8-1	516574	5364339	277	5.831	0.281		0.12	0.1				-165.8	7.76	973	
CP8-2	516643	536425	278	9.497	0.54		0.75	0.595				0.169	73.5	7.48	565
CP8-3	51672	536443	279	9.955	0.977	0.63	0.18	0.56	0.96	0.26		-258.7	7.77	529	
CP8-4	516791	53639	28	18.294	2.55	1.388	0.196	0.39	0.23	0.35		-21.7	6.69	457	
CP8-5	516863	5363757	281	2.225	2.39	1.28	0.145	0.349	0.148	0.15		-116.9	7.83	621	
CP8-6	516928	5363629	282	25.622	3.28	1.415	0.16	0.519	0.17	0.2		-112.6	7.85	5.23	
CP8-7	516993	536351	283	19.667	3.158	1.337	0.25	0.525	0.169	0.116		-252.7	7.45	678	
CP8-8	51768	5363354	284	26.154	1.771	1.189	0.169	0.61	0.151	0.497		-27.5	7.3	1179	
CP8-9	517139	5363215	285	9.55	0.71	0.474	0.8	0.2				14.7	6.21	842	
CP8-10	517213	536371	286	5.998	0.624	0.454	0.6	0.329	0.96			12	7.74	649	
CP8-11	517267	5362966	287	35.23	1.459	0.851	0.14	0.66				0.376	-8.5	8.8	1732
CP8-12	517335	5362831	288	28.91	0.836	0.525	0.4	0.251				0.1	-6.4	7.71	956
CP9-1	5372229	518619	238	13.525	1.726	1.580	0.241	0.695	0.130	0.276		-252	7.490	534	
CP9-2	5372181	518475	239	12.711	1.828	1.196	0.195	0.457	0.165	0.163		-35	7.240	475	
CP9-3	5372137	518325	24	15.563	1.417	0.754	0.166	0.374	0.167			26	7.470	577	
CP9-4	53726	518212	241	3.830	0.344	0.316	0.300	0.228	0.170			216	6.790	57	
CP9-5	53723	51874	242	12.980	1.617	0.879	0.130	0.384	0.180	0.126		-59	7.740	584	
CP9-6	5371932	51794	243	5.827	0.653	0.374	0.400	0.150	0.149			-148	7.690	71	
CP9-7	5371888	51782	244	5.577	0.338	0.231	0.760	0.230				-259	7.550	474	
CP9-8	5371841	51766	245	4.613	0.450	0.370	0.610	0.270				44	7.320	675	
CP9-9	5371764	517528	246	1.756	1.371	0.753	0.900	0.288	0.133	0.280		-251	6.720	546	
CP9-10	5371687	517392	247	8.100	0.947	0.678	0.650	0.267	0.127			-53	7.130	536	
CP10-1	519593	5376115	31	45.747	4.553	2.392	0.321	1.694	0.335	1.340	-89.500	6.520	838.000		
CP10-2	51944	5376118	32	15.370	1.798	1.170	0.142	0.486	0.148	0.184	58.200	7.530	647.000		
CP10-3	519283	537614	33	6.647	0.990	1.210	0.118	0.530	0.175	0.239	72.700	7.620	229.000		
CP10-4	519135	537612	34	22.850	0.879	0.650	0.117	0.547		0.249	45.300	6.620	747.000		
CP10-5	518998	537612	35	1.384	1.391	0.833	0.179	0.451		0.151	84.200	7.960	624.000		
CP10-6	51888	537689	36	1.740	1.430	0.798	0.132	0.420	0.136		88.000	7.930	625.000		
CP10-7	518613	537688	37	2.918	2.224	1.254	0.183	0.832	0.229		99.800	7.330	744.000		
CP10-8	518459	537688	38	18.630	1.484	0.780	0.129	0.654	0.199	0.398	75.400	6.710	695.000		
CP10-9	51835	537675	39	14.335	1.340	0.911	0.162	0.514	0.139	0.138	49.000	7.900	486.000		
CP11-1	524312	5376341	31	1.321	1.890	0.715	0.860	0.386	0.700	0.210	75.800	7.870	747.000		
CP11-2	52417	5376341	311	13.458	0.632	0.524	0.190	0.494	0.160	0.337	93.100	7.000	79.000		
CP11-3	5241	5376342	312	4.677	0.165	0.137	0.420	0.182	0.133	0.190	85.700	7.880	692.000		
CP11-4	523838	537634	313	22.399	1.530	0.774	0.125	0.628	0.171	0.341	-111.200	6.840	964.000		
CP11-5	523665	537634	314	8.365	0.579	0.243	0.760	0.280			45.100	7.900	878.000		
CP11-6	52351	5376339	315	19.330	0.733	0.729	0.160	0.410		0.110	-142.800	7.700	891.000		
CP11-7	523337	5376339	316	4.546	1.442	1.394	0.390	0.451	0.970	0.173	-83.300	6.800	1277.000		
CP11-8	523175	5376338	317	8.243	0.412	0.251	0.550	0.320	0.100	0.280	51.400	7.510	989.000		
CP11-9	5231	5376338	318	2.918	1.840	1.430	0.165	0.572	0.121	0.276	76.600	7.560	751.000		
CP12-1	52474	537437	319	28.746	1.500	0.539	0.129	0.510	0.191	0.442	-74.600	6.830	961.000		
CP12-2	524556	5374377	32	11.228	0.729	0.560	0.132	0.477	0.117	0.234	22.200	7.460	387.000		
CP12-3	524413	5374368	321	42.380	0.871	0.724	0.270	0.478	0.113	0.490	-147.600	6.810	1183.000		
CP12-4	52426	5374355	322	43.413	3.545	1.838	0.218	1.277	0.265	0.696	-132.500	7.300	118.000		
CP12-5	52411	5374349	323	9.914	0.600	0.473	0.970	0.415	0.890	0.144	19.900	7.340	89.000		
CP12-6	52394	5374348	324	12.576	0.998	0.527	0.100	0.335	0.119	0.244	59.100	7.600	728.000		
CP12-7	523781	5374347	325	19.571	2.470	1.141	0.920	0.478	0.180	0.256	-134.300	6.970	128.000		
CP12-8	52369	5374347	326	14.197	0.727	0.521	0.900	0.799	0.122	0.168	-18.400	7.140	357.000		
CP12-9	523435	5374342	327	22.340	2.365	1.136	0.124	0.757	0.900	0.271	6.000	7.000	842.000		
CP12-10	523245	5374342	328	23.398	1.686	0.840	0.122	0.663	0.170	0.365	44.700	6.870	923.000		
CP12-11	52376	5374337	329	18.599	0.844	0.622	0.640	0.534	0.123	0.187	-98.400	6.880	856.000		
CP12-12	522921	5374334	33	25.870	1.481	1.315	0.160	0.599	0.129	0.444	-113.600	6.900	167.000		
CP12-13	522786	5374335	331	44.970	2.377	1.298	0.373	0.492	0.244	0.610	74.800	6.900	55.000		
CP12-14	522612	5374333	332	9.364	0.462	0.287	0.260	0.634	0.192	0.246	88.000	7.170	1765.000		
CP13-1	5368353	521411	248	1.345	1.131	0.856	0.142	0.333	0.141	0.130	18	7.400	533		
CP13-2	5368358	521254	249	3.141	0.423	0.595	0.800	0.259	0.136		-36	7.870	674		

TABLE MS4: HEAD GAS DATA
Phase III, More Smoke Creek

CV = Curvilinear, CP = Curvilinear Perpendicular
L = Lineament

DOE #	X	Y	SAMPLE	METHANE	ETHANE	PROPANE	IBUTANE	BUTANE	IPENTANE	PENTANE	EH	PH	UMHOS
CP13-3	5368361	52196	25	33.312	2.230	1.723	1.690	1.165	0.292	0.430	-199	7.850	1191
CP13-4	5368371	52941	251	16.878	1.894	0.953	0.152	0.613	0.133	0.248	128	7.630	341
CP13-5	5368322	52791	252	2.372	0.260	0.190	0.190	0.310	0.160		-120	8.180	657
CP13-6	5368275	52645	253	5.911	0.350		0.530	0.500			3	7.470	971
CP13-7	5368253	52493	254	6.891	0.794	0.535	0.900	0.850			85	7.570	553
CP13-8	5368247	5234	255	14.287	1.513	0.827	0.121	0.194	0.180		81	7.660	68
CP13-9	5368246	52185	256	7.954	1.100	0.598	0.110	0.180	0.131		21	7.330	674
CP13-10	536825	523	257	5.865	0.660	1.360	0.118	0.275			229	7.610	72
CP13-11	5368251	519876	258	17.289	2.140	0.920	0.600	0.393	0.185		259	7.450	673
CP13-12	536825	519641	259	9.495	1.230	0.956	0.270	0.130	0.130		-25	7.340	632
CP13-13	5368247	519489	26	33.240	4.616	2.710	0.240	0.619	0.276	0.315	-99	7.790	684
CP13-14	5368244	519334	261	25.956	3.637	1.997	0.249	0.620	0.258	0.236	-252	7.810	65
Harmonic Mean				7.762	1.001	0.618	0.222	0.411	0.202	0.257	#NUM!	7.417	180.831
Anomaly (2xHM)				15.524	2.002	1.237	0.444	0.822	0.404	0.514	#NUM!	14.833	361.662
average				15.842	1.980	1.068	0.354	0.604	0.298	0.428	60.073	7.444	582.817
std dev				12.319	2.100	0.913	0.278	0.429	0.241	0.623	136.244	0.449	359.315
minimum				1.321	0.165	0.137	0.100	0.100	0.100	0.100	-259.100	6.210	5.230
maximum				77.337	19.415	7.482	1.690	3.300	0.990	6.417	259.300	8.800	1919.000
Anomaly (1.5 x mean)				23.763	2.970	1.602	0.531	0.907	0.447	0.642	40.0	8.122	874.225
COUNT			146										

pH anomaly defined as mean x (max - mean)/2
Eh anomaly defined as mean / 1.5

L1-1	52292	537419	71	38.731	7.570	3.457	0.400	1.461	0.570	1.610	24	6.600	51
L1-2	52116	5374354	72	27.353	4.474	1.981	0.174	0.640	0.156	0.930	8	7.810	59
L1-3	51934	537467	73	42.138	6.580	2.746	0.270	0.830	0.236	0.155	-22	7.760	637
L1-4	51747	537487	74	26.128	4.254	2.310	0.210	0.749	0.157	0.576	45	7.870	626
L1-5	51551	5375145	75	21.764	3.631	1.812	0.143	0.740	0.160	0.115	212	7.960	594
L1-6	51375	537539	76	26.285	3.937	1.692	0.145	0.632	0.136	0.490	79	7.760	381
L1-7	51218	537569	77	28.979	2.980	1.437	0.172	0.642	0.295	0.455	190	7.380	714
L1-8	5151	5375843	78	66.445	1.189	4.857	0.355	2.137	0.441	1.170	215	6.940	799
L1-9	5886	537672	79	18.863	2.670	1.487	0.250	0.722	0.230	0.169	-8	7.510	631
L2-1	51632	5374416	83	11.598	0.550	0.389	0.800	0.348	0.150	0.360	225	7.400	963
L2-2	516143	5374168	84	3.785	0.264	0.230	0.140	0.460			94	7.960	713
L2-3	515864	5373917	85	16.568	1.380	0.885	0.120	0.556	0.570	0.145	217	7.560	695
L2-4	51586	5373696	86	56.278	6.926	3.167	0.316	1.348	0.369	0.866	154	6.720	671
L2-5	515622	5373438	87	27.799	2.868	1.350	0.140	0.564	0.178	0.865	245	6.350	3
L2-6	515444	5373189	88	7.980	0.222	0.190	0.130	0.360	0.250		27	7.380	263
L2-7	51522	5372877	89	73.715	2.296	1.600	0.700	0.271	0.280	0.350	220	6.980	518
L2-8	51548	5372634	9	12.234	0.225	0.118	0.800	0.180	0.130	0.110	219	7.280	1421
L2-9	514797	5372283	91	7.240	1.578	0.989	0.600	0.340	0.160	0.930	22	7.100	124
L2-10	514581	5371983	92	35.650	5.660	2.476	0.289	1.135	0.164	0.345	222	7.190	721
L2-11	514315	5371611	93	32.647	4.349	2.880	0.230	0.735	0.210	0.500	29	7.490	779
L2-12	514137	5371367	94	19.825	0.921	0.472	0.700	0.269	0.110		197	7.900	246
L2-13	513884	53718	95	17.442	1.230	0.688	0.130	0.438			231	6.860	1146
L2-14	51377	53776	96	8.160	0.465	0.362	0.290	0.523	0.720		189	7.740	32
L2-15	513519	537498	97	14.540	0.740	0.513	0.800	0.757	0.660	0.880	184	7.970	382
L2-16	513326	5372229	98	8.651	1.480	0.535	0.120	0.462	0.121		158	8.130	787
L2-17	513225	53787	99	22.130	3.288	1.445	0.136	0.530	0.138	0.320	214	7.670	64
L2-18	51345	5369835	1	35.397	3.100	1.391	0.830	0.749	0.137	0.279	238	6.940	928
L2-19	51286	536958	11	12.523	1.144	0.637	0.400	0.394		0.162	218	7.260	49
L2-20	512678	5369323	12	12.518	0.888	0.371	0.530	0.287	0.650		176	8.400	439
L2-21	512588	5369198	13	23.967	2.960	1.439	0.125	0.644	0.164	0.477	225	7.470	487
L2-22	51246	5368944	14	36.478	4.662	2.360	0.267	2.282	0.327	0.914	191	7.500	641
L2-23	512231	5368697	15	22.300	2.461	1.225	0.430	0.660	0.460	0.240	24	7.670	773
L2-24	51252	5368449	16	9.229	0.784	0.315	0.200	0.243	0.180		183	8.330	489
L2-25	511813	5368115	17	28.532	4.922	2.140	0.283	1.210	0.277	0.564	174	7.460	93
L2-26	511632	5367862	18	8.526	0.680	0.331	0.450	0.290			118	8.180	587
L2-27	511457	5367618	19	21.630	1.723	0.779	0.190	0.758	0.178	0.393	212	7.550	626
L2-28	511273	5367362	11	9.559	0.917	0.478	0.760	0.336	0.600	0.135	218	7.300	388
L2-29	511156	53672	111	5.689	0.264	0.200	0.390	0.161		0.160	22	7.620	842
L2-30	51143	53674	112	4.721	0.444	0.335	0.650	0.247		0.174	29	7.640	478
L2-31	51929	5366882	113	21.570	3.537	1.736	0.193	0.699	0.210	0.244	213	7.440	696
L3-1	58124	5366562	138	9.330	1.370	0.531	0.780	0.422	0.470	0.116	218	7.340	715
L3-2	5834	536631	139	4.670	0.390	0.194	0.320	0.236	0.240		22	7.140	611
L3-3	58487	536655	14	28.540	2.862	1.338	0.133	0.565	0.410	0.570	215	7.400	672
L3-4	58666	536585	141	25.326	4.787	1.660	0.298	0.486	0.125	0.139	37	7.830	689
L3-5	58842	5365558	142	18.911	2.735	1.242	0.151	0.580	0.140	0.116	222	7.270	247

TABLE MS4: HEAD GAS DATA
Phase III, More Smoke Creek

CV = Curvilinear, CP = Curvilinear Perpendicular
L = Lineament

DOE #	X	Y	SAMPLE	METHANE	ETHANE	PROPANE	IBUTANE	BUTANE	IPENTANE	PENTANE	EH	PH	UMHOS
L3-6	5984	5365221	143	2.681	2.980	1.580	0.160	0.590	0.140	0.182	22	7.300	644
L3-7	59267	5364965	144	6.634	0.699	0.255	0.680	0.146	0.220	20	8.800	697	
L3-8	59557	536456	145	37.315	3.770	1.780	0.166	1.149	0.160	0.647	198	6.890	698
L4-1	52619	537931	351	16.630	2.882	1.261	0.910	0.471	0.540	78.200	7.460	493.000	
L4-2	525791	53791	352	6.433	8.938	3.913	0.513	1.573	0.525	0.859	99.000	7.130	558.000
L4-3	525563	537889	353	26.576	3.180	1.750	0.191	1.240	0.270	0.568	19.400	6.790	153.000
L4-4	525314	537866	354	54.132	12.490	5.328	0.672	2.164	0.570	1.190	113.200	7.900	527.000
L4-5	52558	5378425	355	27.416	4.989	2.162	0.282	1.250	0.246	0.440	119.900	7.190	491.000
L4-6	52487	5378193	356	46.388	9.627	3.687	0.463	1.415	0.380	0.656	121.800	7.780	399.000
L4-7	524574	5377979	357	31.566	6.839	2.968	0.568	1.724	0.319	0.230	128.900	7.820	698.000
L4-8	524335	5377759	358	4.546	8.776	3.325	0.431	1.140	0.428	0.624	-79.100	7.840	1516.000
L4-9	52284	5376242	359	47.831	9.219	4.480	0.515	2.100	0.489	1.528	92.000	6.680	154.000
L4-10	522627	537633	36	15.947	2.873	1.374	0.164	0.678	0.160	0.294	13.800	7.460	454.000
L4-11	522371	5375778	361	62.366	4.263	1.813	0.143	0.660	0.143	0.334	143.900	6.850	847.000
L4-12	522161	5375578	362	5.821	0.228	0.168	0.170	0.380	0.170	113.600	8.510	532.000	
L4-13	521893	5375314	363	6.000	0.650	0.331	0.110	0.520	0.100	0.680	137.000	7.680	966.000
L4-14	521568	5374993	364	7.567	0.791	0.320	0.370	0.270	0.110	0.132	23.400	7.490	318.000
L4-15	521344	5374779	365	4.713	0.230	0.150	0.300	0.150	0.150	19.600	7.370	394.000	
Harmonic Mean				12.202	1.040	0.639	0.242	0.486	0.213	0.286	#NUM!	7.459	111.758
Anomaly (2xHM)				24.403	2.080	1.278	0.484	0.972	0.426	0.571	#NUM!	14.917	223.517
average				22.586	3.108	1.537	0.359	0.744	0.290	0.498	125.817	7.488	555.698
std dev				16.620	2.760	1.249	0.233	0.526	0.173	0.372	87.709	0.473	310.693
minimum				2.681	0.222	0.118	0.110	0.146	0.100	0.110	-79.100	6.350	3.000
maximum				73.715	12.490	5.328	0.910	2.282	0.720	1.610	244.600	8.800	1516.000
Anomaly (1.5 x mean)				33.879	4.661	2.305	0.538	1.116	0.435	0.747	83.9	8.144	833.548
COUNT			63										

pH anomaly defined as mean x (max - mean)/2

Eh anomaly defined as mean / 1.5

F1-1	515647	5366535	262	1.6	0.587	0.315	0.23	0.27	0.38	-16	7.85	398	
F1-2	51572	5366391	263	5.386	0.247	0.45	0.269	0.162	-292.9	7.12	417		
F1-3	515755	536625	264	7.47	1.87	0.563	0.24	0.327	0.13	-177.9	6.86	1824	
F1-4	515819	536683	265	9.864	0.815	0.437	0.55	0.273	0.37	0.141	-197.8	6.92	347
F1-5	515875	5365935	266	19.25	1.181	0.569	0.134	0.223	0.6	0.156	-158.1	6.74	446
F1-6	515929	5365792	267	34.941	2.757	1.632	0.151	0.583	0.225	0.422	-66.8	7.78	549
F1-7	515987	5365642	268	27.58	0.729	0.482	0.75	1.124	0.8	0.37	-275.3	8.28	133
F1-8	5164	536551	269	53.54	1.768	1.53	0.125	0.593	0.131	0.424	18.5	7.86	129
F1-9	51694	536536	27	28.21	2.494	1.2	0.158	0.963	0.123	0.589	-316	6.55	833
F1-10	516148	5365218	271	27.45	3.195	1.713	0.21	0.924	0.239	0.119	-199.8	7.11	686
F1-11	51623	536589	272	9.876	1.512	0.658	0.16	0.277	0.9	0.17	-59.5	7.23	885
F1-12	516279	5364934	273	16.723	1.882	0.941	0.16	0.476	0.189	0.397	-253.6	8.17	796
F1-13	516344	536483	274	139.1	9.739	5.143	0.613	2.33	0.731	1.769	0.1	7.72	16
F1-14	516437	5364615	275	14.159	1.118	0.79	0.18	0.821	0.122	-125.1	7.68	213	
F1-15	51654	5364479	276	28.13	3.988	2.91	0.21	1.42	0.87	0.624	-273.5	7.69	811
F1-16	516574	5364339	277	5.831	0.281	0.12	0.1	0.595	0.169	-165.8	7.76	973	
F1-17	516643	536425	278	9.497	0.54	0.75	0.595	0.169	73.5	7.48	565		
F1-18	51672	536443	279	9.955	0.977	0.63	0.18	0.56	0.96	0.26	-258.7	7.77	529
F1-19	516791	53639	28	18.294	2.55	1.388	0.196	0.39	0.23	0.35	-21.7	6.69	457
F1-20	516863	5363757	281	2.225	2.39	1.28	0.145	0.349	0.148	0.15	-116.9	7.83	621
F1-21	516928	5363629	282	25.622	3.28	1.415	0.16	0.519	0.17	0.2	-112.6	7.85	5.23
F1-22	516993	536351	283	19.667	3.158	1.337	0.25	0.525	0.169	0.116	-252.7	7.45	678
F1-23	51768	5363354	284	26.154	1.771	1.189	0.169	0.61	0.151	0.497	-27.5	7.3	1179
F1-24	517139	5363215	285	9.55	0.71	0.474	0.8	0.2	0.12	14.7	6.21	842	
F1-25	517213	536371	286	5.998	0.624	0.454	0.6	0.329	0.96	0.376	-8.5	7.74	649
F1-26	517267	5362966	287	35.23	1.459	0.851	0.14	0.66	0.169	0.1	7.71	1732	
F1-27	517335	5362831	288	26.91	0.836	0.525	0.4	0.251	0.14	0.1	-6.4	7.71	956
F1-28	51749	5362531	289	51	13.663	3.572	0.124	0.92	0.328	0.55	16.9	7.48	64
F1-29	517555	536248	29	6.538	0.792	0.95	0.75	0.548	0.63	-149.4	6.59	1794	
F1-30	517626	5362275	291	1.349	0.88	0.557	0.162	0.56	0.124	-44.7	7.31	133	
F1-31	517699	5362139	292	8.474	0.697	0.331	0.74	0.243	0.112	17.7	7.63	78	
F1-32	517775	5361996	293	2.214	0.188	0.36	0.19	0.562	0.443	-8	7.38	495	
F1-33	517845	5361863	294	16.895	1.23	0.859	0.12	0.562	0.443	14.7	7.63	396	
F1-34	517919	5361726	295	11.476	0.651	0.373	0.27	0.57	0.14	0.11	183.8	8.6	216
F1-35	517991	536159	296	1.394	1.871	0.726	0.1	0.42	0.9	0.224	7.99	588	
F1-36	51865	5361452	297	16.997	2.2	1.191	0.51	0.41	0.211	0.275	147.7	8.1	634
F1-37	51817	5361255	298	4.94	0.385	0.33	0.51	0.8	0.216	0.225	162.7	7.5	432
Harmonic Mean			37.000	6.749	0.875	0.715	0.214	0.389	0.216	0.225	#NUM!	7.481	103.117

TABLE MS4: HEAD GAS DATA
Phase III, More Smoke Creek

CV = Curvilinear, CP = Curvilinear Perpendicular
L = Lineament

DOE #	X	Y	SAMPLE	METHANE	ETHANE	PROPANE	IBUTANE	BUTANE	IPENTANE	PENTANE	EH	PH	UMHOS	
Anomaly (2xHM)				46.200	8.600	3.764	0.482	1.148	0.374	1.020	-265.800	15.840	106.000	
average				19.986	2.027	1.131	0.321	0.567	0.375	0.370	-72.943	7.523	608.033	
std dev				23.995	2.580	1.013	0.227	0.410	0.313	0.332	140.711	0.561	458.907	
minimum				1.349	0.188	0.315	0.100	0.100	0.112	0.100	-316.000	6.210	5.230	
maximum				139.100	13.663	5.143	0.800	2.330	0.960	1.769	224.000	8.800	1824.000	
Anomaly (1.5 x mean)				29.979	3.041	1.696	0.482	0.851	0.562	0.556	-48.6	8.162	912.050	
COUNT			37											
pH anomaly defined as mean x (max - mean)/2														
Eh anomaly defined as mean / 1.5														
NW8ad	51684	537651	8	12.756	1.951	0.551	0.820	0.353	0.740		219	7.870	582	
NW8bd	5137	537647	81	19.740	2.838	1.659	0.178	0.741	0.265	0.188	-74	7.580	62	
NW8dd	51684	5375641	82	29.655	5.800	2.234	0.400	0.554	0.139	0.770	-95	7.770	525	
CV														
Harmonic Mean				8.954	1.103	0.693	0.244	0.440	0.229	0.315	#NUM!	7.489	214.190	
Anomaly (2xHM)				17.907	2.206	1.386	0.487	0.881	0.458	0.631	#NUM!	14.977	428.380	
average				23.026	3.390	1.710	0.367	0.799	0.353	0.581	47.573	7.522	564.408	
std dev				32.179	6.117	2.758	0.319	1.092	0.362	0.772	113.971	0.502	334.647	
minimum				1.585	0.145	0.100	0.100	0.133	0.100	0.100	-269.500	6.400	17.000	
maximum				317.470	63.848	27.970	2.778	11.363	3.391	7.455	263.200	8.900	1612.000	
Anomaly (1.5 x mean)				34.538	5.084	2.565	0.551	1.198	0.530	0.871	31.715	8.211	846.612	
CP														
Harmonic Mean				7.762	1.001	0.618	0.222	0.411	0.202	0.257	#NUM!	7.417	180.831	
Anomaly (2xHM)				15.524	2.002	1.237	0.444	0.822	0.404	0.514	#NUM!	14.833	361.662	
average				15.842	1.980	1.068	0.354	0.604	0.298	0.428	60.073	7.444	582.817	
std dev				12.319	2.100	0.913	0.278	0.429	0.241	0.623	136.244	0.449	359.315	
minimum				1.321	0.165	0.137	0.100	0.100	0.100	0.100	-259.100	6.210	5.230	
maximum				77.337	19.415	7.482	1.690	3.300	0.990	6.417	259.300	8.800	1919.000	
Anomaly (1.5 x mean)				23.763	2.970	1.602	0.531	0.907	0.447	0.642	40.049	8.122	874.225	
L														
Harmonic Mean				12.202	1.040	0.639	0.242	0.486	0.213	0.286	#NUM!	7.459	111.758	
Anomaly (2xHM)				24.403	2.080	1.278	0.484	0.972	0.426	0.571	#NUM!	14.917	223.517	
average				22.586	3.108	1.537	0.359	0.744	0.290	0.498	125.817	7.488	555.698	
std dev				16.620	2.760	1.249	0.233	0.526	0.173	0.372	87.709	0.473	310.693	
minimum				2.681	0.222	0.118	0.110	0.146	0.100	0.110	-79.100	6.350	3.000	
maximum				73.715	12.490	5.328	0.910	2.282	0.720	1.610	244.600	8.800	1516.000	
Anomaly (1.5 x mean)				33.879	4.661	2.305	0.538	1.116	0.435	0.747	83.878	8.144	833.548	
F														
Harmonic Mean				6.749	0.875	0.715	0.214	0.389	0.216	0.225	#NUM!	7.481	103.117	
Anomaly (2xHM)				46.200	8.600	3.764	0.482	1.148	0.374	1.020	-265.800	15.840	106.000	
average				19.986	2.027	1.131	0.321	0.567	0.375	0.370	-72.943	7.523	608.033	
std dev				23.995	2.580	1.013	0.227	0.410	0.313	0.332	140.711	0.561	458.907	
minimum				1.349	0.188	0.315	0.100	0.100	0.112	0.100	-316.000	6.210	5.230	
maximum				139.100	13.663	5.143	0.800	2.330	0.960	1.769	224.000	8.800	1824.000	
Anomaly (1.5 x mean)				29.979	3.041	1.696	0.482	0.851	0.562	0.556	-48.629	8.162	912.050	
PROPANE COMPARISON				CV	CP	L	F			Eh COMP	CV	CP	L	F
Harmonic Mean				0.693	0.618	0.639	0.715			#NUM!	#NUM!	#NUM!	#NUM!	
Anomaly (2xHM)				1.386	1.237	1.278	3.764			#NUM!	#NUM!	#NUM!	#NUM!	-265.800
average				1.710	1.068	1.537	1.131			47.573	60.073	125.817	-72.943	
std dev				2.758	0.913	1.249	1.013			113.971	136.244	87.709	140.711	
minimum				0.100	0.137	0.118	0.315			-269.500	-259.100	-79.100	-316.000	
maximum				27.970	7.482	5.328	5.143			263.200	259.300	244.600	224.000	
Anomaly (1.5 x mean)				2.565	1.602	2.305	1.696			31.715	40.049	83.878	-48.629	

TABLE MS5: IN-HOUSE HEAD GAS DATA

Phase III, More Smoke Creek

CV = Curvilinear

CP = CV Perpendicular

L = Lineament, F = Fold

moresmoke #	C1	C2	ETHENE	C3	IC4	NC4	PROPENE
CV1-1	8.533		3.280	2.461		2.731	4.204
CV1-2	91.356	9.968	14.034	12.007		0.832	3.399
CV1-3			2.737	3.082	0.501	0.675	0.059
CV1-4		2.402	4.400	1.899	0.215	0.986	0.623
CV1-5	36.556	4.431	6.869		3.320	3.436	2.155
CV2-1	17.269	8.199	6.966	3.511	0.172	1.493	1.787
CV2-2	4.590	0.207	1.791	0.533		1.888	
CV2-3	17.129	0.140	2.967	0.758		0.541	
CV2-4	4.463		1.529	0.351			
CV2-5			0.823				
CV2-6	8.177	0.113	0.902				
CV2-7			0.87	0.332		1.436	1.715
CV2-8	7.416		1.027	0.217			
CV3-1	95.511	2.207	1.718	2.203	1.52	2.083	2.09
CV3-2	2.596		0.928				
CV3-3	4.081	0.116	1.831				
CV3-4	3.384		0.676				
CV3-5	10.235	1.31	2.22	1.582	0.479	1.624	1.674
CV3-6	42.972	5.412	2.493	4.538	1.184	2.73	1.872
CV3-7	5.036		5.406	2.827		2.361	2.227
CV3-8	5.263	0.139	1.842				
CV3-9	13.107	0.570	16.172	8.407			
CV3-10	21.152	0.151					
CV4-1						0.499	
CV4-2	7.569		1.523				
CV4-3	10.371		1.954				
CV4-4	8.717	0.455	1.679	0.602			
CV4-5	3.67		4.012				
CV4-6	9.354		1.392				
CV4-7	7.386		1.856				
CV4-8	6.171	2.527	3.452				
CV4-9	13.452	3.129	2.712	1.785	0.475	1.399	1.857
CV4-10	5.89		1.565				
CV6-1			1.575				
CV6-2	10.601	0.797	0.801	0.825	0.732	1.366	1.508
CV6-3	3.461		1.939				
CV6-4	9.558	0.08	2.391	0.406			
CV6-5	6.991	0.339	1.983	0.897		1.551	
CV6-6	63.819	1.3	7.8	2.054	0.443	1.449	1.912
CV6-7	4.517		4.487				
CV7-1	20.87	0.523	2.402	0.966		1.338	
CV7-2			1.86	0.762		1.188	3.786
CV7-3	59.099		0.747				
CV7-4	8.419		2.192				
CV7-5	13.214	0.113	2.418	1.222			
CV7-6	6.664	3.619	5.395	2.818			

TABLE MS5: IN-HOUSE HEAD GAS DATA
Phase III, More Smoke Creek

CV = Curvilinear
 CP = CV Perpendicular
 L = Lineament, F = Fold

moresmoke #	C1	C2	ETHENE	C3	IC4	NC4	PROPENE
CV7-7				0.758		0.188	1.385
CV7-8	28.992	0.776	1.718	0.772		0.963	
CV7-9	8.62	0.289	1.033	1.245			
CV7-10	9.43	0.182	0.959	0.928			
CV7-11	26.946	0.509	2.45	0.517		0.559	
CV7-12							
CV7-13			0.496	0.399		0.155	
CV7-14	22.401	0.442	1.852	0.478			
CV7-15	6.289		0.633	2.209			
CV7-16	5.928		3.679				
CV7-17	3.514		1.216				
CV7-18	13.448		1.506	0.285			
CV7-19	4.308		1.258				
CV7-20	4.793		3.071				
CV7-21	21.335	0.194	1.354	1.509			
CV7-22	8.287	0.448	1.189	0.475		0.768	
CV7-23	12.846	0.139	1.775	1.211			
CV7-24	4.377		5.672				
CV7-25	7.211	0.786	0.682	0.591		1.042	
CV7-26	71.799	1.177	1.189	2.064	1.416	1.836	2.707
CV7-27							
CV7-29	5.501	3.279	5.675	3.056			
CV7-30	4.078		4.577				
CV7-31	4.393	2.829	2.853	1.341			
CV7-32	3.877						
CV7-33	208.266	0.165	1.391	0.377		0.788	
CV7-34	4.415	3.025	4.666	3.781			
CV7-35	180.582	0.661	1.206	1.239		0.152	
CV7-36	4.425	3.084	4.271	3.065	2.597	2.964	
CV7-37	4.671	3.22	5.144	5.682			
CV7-38	14.111	0.684	1.486	1.603	1.369	2.096	3.061
CV7-39	4.182		5.756				
CV7-40	2.731		1.287				
CV7-41	3.989		5.068				
CV8-1	7.369	0.206	1.617	0.862		2.185	
CV8-2	4.769		3.448				
CV8-3	4.416		1.496				
CV8-4	84.669	0.25	1.657	0.481		1.354	
CV8-5	4.755	2.906	3.933	2.991			
CV8-6	4.823						
CV8-7				1.245	0.415	1.834	1.897
CV8-8	4.279		1.704				
CV8-9							
CV8-10	35.406	0.733	0.785	1.163	1.088	1.858	2.107
CV8-11	11.329		0.93	0.314			
CV8-12	10.243		1.645	0.355			

TABLE MS5: IN-HOUSE HEAD GAS DATA

Phase III, More Smoke Creek

CV = Curvilinear

CP = CV Perpendicular

L = Lineament, F = Fold

moresmoke #	ppm						
	C1	C2	ETHENE	C3	IC4	NC4	PROPENE
CV8-13	8.1	0.199	1.586	1.365		1.701	
CV8-14	7.885	3.618	5.776	4.142			
CV9-1	3.897						
CV9-2	7.178		4.253				
CV9-3	4.196			2.801			
CV9-4	157.166		1.616	1.135		1.469	
CV9-5	3.982						
CV9-6	3.777		6.263				
CV10-1			1.629				
CV10-2	5.888		1.678				
CV10-3	5.896	3.185	5.994				
CV10-4			2.111	0.322			
CV10-5	5.851	3.476	5.242	3.98		2.144	
CV11-1	4.136		0.845				
CV11-2	8.044		1.34				
CV11-3		0.217	2.087	0.744	0.502	1.473	
CV11-4	31.624	0.442	1.476	0.601		1.207	
CV11-5	11.523	0.309	0.331	0.192			
CV11-6		0.593	2.528	0.877	0.467	1.485	2.035
CV12-1	11.493	0.651	0.759	2.033	1.409		
CV12-2				4.332	0.862	2.318	3.365
CV12-3		0.487	1.421	2.031	1.482	2.112	1.685
CV12-4	58.855	0.461	0.458	0.394			
CV12-5	4.405		2.634				
CV12-6			3.566	0.429		1.049	2.477
CV12-7			1.706	0.402		1.484	
CV13-1	5.438		5.237	4.39			
CV13-2	5.447	0.171	1.111	0.984		2.231	
CV13-3	5.484	3.238	4.618	3.144		2.358	
CV13-4	7.086		5.321				
CV13-5	10.679	0.179	0.96	0.519		1.257	
CV13-6			0.737				
CV13-7	4.956		4.893	2.363			
Harmonic Mean	6.932	0.361	1.612	0.803	0.590	0.909	
Anomaly (2xHM)	13.864	0.722	3.225	1.606	1.180	1.817	
average	18.829	1.524	2.751	1.803	1.032	1.513	
std dev	34.127	1.974	2.412	1.915	0.805	0.740	
minimum	2.596	0.080	0.331	0.192	0.172	0.152	
maximum	208.266	9.968	16.172	12.007	3.320	3.436	
Anomaly (1.5 x mean)	28.244	2.286	4.127	2.704	1.549	2.270	
CP1-1	96.580	2.154	1.890	0.819		1.050	2.345
CP1-2	5.577		2.084				
CP1-3			1.873				
CP1-4	6.079		3.052				
CP1-5	15.130	1.028	4.148	4.185		3.248	2.860

TABLE MS5: IN-HOUSE HEAD GAS DATA

Phase III, More Smoke Creek

CV = Curvilinear

CP = CV Perpendicular

L = Lineament, F = Fold

moresmoke #	C1	C2	ETHENE	C3	IC4	NC4	PROPENE
CP1-6	7.901	0.290	3.533	5.459			
CP1-7	4.815		6.010				
CP2-1	9.605	0.161	3.433	0.740			
CP2-2			1.969				2.181
CP2-3			1.956	0.261			
CP2-4	38.486	0.271	3.160	0.590			
CP2-5	38.771	0.698	4.096	0.761		0.875	1.805
CP2-6	36.353		2.273				
CP2-7	4.563		1.592				
CP2-8	48.979	0.111	1.787	0.316			
CP2-9	39.147	0.138	2.211	0.207			
CP3-1	4.547		3.89				
CP3-2	4.474		5.178				
CP3-3	4.454		5.829			3.185	
CP3-4	18.391	0.121	2.513	2.379		1.557	
CP3-5	4.145		3.424				
CP3-6	3.196		3.79				
CP3-7	5.447		2.216				
CP3-8	10.492		1.799				
CP3-9	7.702	14.573	30.128				
CP3-10	12.500	0.799	8.311	0.970		2.981	3.277
CP4-1			3.653	0.703		1.451	
CP4-2	6.242	3.251	5.189	5.563		2.62	
CP4-3	4.491	0.176	1.642	0.414			
CP4-4	25.594	1.789	1.928	1.992	0.512	1.546	1.573
CP4-5	7.373		2.086			1.119	
CP4-6			1.991	0.518		1.111	
CP4-7	4.705		2.645				
CP4-8	5.765		1.542	0.495			
CP4-9	26.157	1.764	0.921	1.108	0.384	1.299	1.91
CP4-10	39.35	1.649	1.448	1.968	1.463	2.209	2.227
CP4-11	8.34	3.381	5.128	3.529		3.012	
CP5-5	3.849		3.593		0.437		
CP5-6	7.232	0.125	1.813				
CP6-1	4.58	0.111	1.184				
CP6-2	198.437		2.319	0.445			
CP6-3	7.486	0.495	1.214	0.558		1.219	2.041
CP6-4	8.882	0.184	1.991	0.66			
CP6-5	11.17	0.118	1.395				
CP6-6			1.661	0.428		1.246	2.104
CP6-7	5.112		2.063				
CP6-8	5.48		1.723				
CP6-9	143.658		1.399	0.337		1.256	
CP6-10	7.006	0.182	1.451	0.343			
CP6-11	131.53	0.627	3.622	1.435		1.721	2.349
CP6-12	29.081	0.203	2.53	1.22			

TABLE MS5: IN-HOUSE HEAD GAS DATA

Phase III, More Smoke Creek

CV = Curvilinear

CP = CV Perpendicular

L = Lineament, F = Fold

moresmoke #	C1	C2	ETHENE	C3	IC4	NC4	PROPENE
CP6-13	4.891		3.577				
CP6-14	5.012	0.373	1.137	1.773			
CP6-15	2.637		0.641				
CP7-1	5.439		1.929				
CP7-2	46.143	0.763	3.22	1.874		2.454	2.74
CP7-3	15.341	0.287	4.393				
CP7-4	4.42		5.503				
CP7-5	4.148		4.212				
CP7-6	4.795		1.755				
CP7-7	4.8		5.619				
CP7-8	6.032		6.079				
CP7-9	6.865	0.319	1.755	0.861			
CP7-10	49.484	0.628	2.126	1.495		1.915	2.38
CP7-11	11.163		1.596	0.424			
CP7-12	11.575	0.172	1.645	2.098			
CP7-13	4.937	3.307	4.984	3.026			
CP7-14	4.302	0.56	0.757	2.238			
CP7-15		0.156	2.069	3.075		2.306	
CP7-16	4.38		5.277				
CP7-17	5.585	0.96	1.105	1.388		1.79	2.488
CP7-18	4.12	0.268	0.548	0.228			
CP7-19	5.306		5.256	2.551			
CP7-20	4.334		5.313				
CP7-21	4.644		3.613	1.303			
CP7-22	81.53	0.449	1.267	0.57			2.105
CP7-23	14.295	0.074	2.475	1.456			
CP7-24			1.304				
CP8-1	2.226						
CP8-2	60.765		1.173				
CP8-3			0.709				
CP8-4	3.676						
CP8-5	4.711						
CP8-6	227.947		1.039	0.312			
CP8-7	39.162						
CP8-8							
CP8-9	5.704	0.19	0.588	0.187			
CP8-10	5.081		3.949				
CP8-11	39.266	0.22	0.737	0.316			
CP8-12		0.204	1.735	0.48			
CP9-1	31.182	0.273	2.075	1.664		2.12	
CP9-2	6.931		4.335				
CP9-3	3.797			1.21			
CP9-4	4.004		4.337				
CP9-5	7.097	3.359	5.929	4.681		3.4	
CP9-6	161.729	0.444	1.429	0.841		1.367	
CP9-7	6.308		4.081	2.177			

TABLE MS5: IN-HOUSE HEAD GAS DATA

Phase III, More Smoke Creek

CV = Curvilinear

CP = CV Perpendicular

L = Lineament, F = Fold

moresmoke #	C1	C2	ETHENE	C3	IC4	NC4	PROPENE
CP9-8	6.826		6.815				
CP9-9	3.664		3.419	1.183			
CP9-10	7.028	2.918	3.703	1.908		0.657	
CP10-1							
CP10-2	33.169	0.075	1.351	0.467			
CP10-3	46.87		1.205				
CP10-4	137.523		2.328	0.471			
CP10-5	7.373		0.563				
CP10-6	4.453		1.127	0.848			
CP10-7	10.864		1.898	1.546		1.66	
CP10-8			2.022	0.397		1.441	
CP10-9	7.505		1.942	1.366			
CP11-1	3.663						
CP11-2	24.145		1.492	0.32			
CP11-3	6.08		4.703				
CP11-4	118.747	0.107	1.866	0.629		1.627	
CP11-5	7.592		0.462				
CP11-6			1.104	1.47		2.537	
CP11-7	19.119	0.121	1.94	2.334			
CP11-8	5.684		1.289				
CP11-9	9.991	0.168	1.568	1.949		2.12	
CP12-1	75.488	0.272	2.934	0.615		1.482	1.556
CP12-2	5.681	0.175	1.238	0.418			
CP12-3							
CP12-4			0.691	0.252		1.052	
CP12-5	8.52	2.581	4.046	1.429			
CP12-6			1.867	0.508		0.168	
CP12-7							
CP12-8	36.339	0.699	3.129	0.505		0.978	
CP12-9	22.555	0.252	1.312	0.309		1.548	
CP12-10	36.002	0.431	2.401	0.413		1.581	
CP12-11			0.906	0.148			
CP12-12	23.564	0.335	3.51	0.796		1.537	1.505
CP12-13	50.023	1.26	4.271	1.31	0.271	0.171	0.364
CP12-14	20.216	0.331	2.179	1.853			1.711
CP13-1	4.126		5.982				
CP13-2	3.843		0.644				
CP13-3							
CP13-4	8.384	0.37	1.824	1.485			
CP13-5	5.626		6.203	4.418			
CP13-6	4.401		5.481				
CP13-7	4.122		0.564				
CP13-8	4.262		5.671				
CP13-9	3.737						
CP13-10	5.615		6.438	7.351			
CP13-11	9.69		1.18	0.477		2.202	

TABLE MS5: IN-HOUSE HEAD GAS DATA

Phase III, More Smoke Creek

CV = Curvilinear

CP = CV Perpendicular

L = Lineament, F = Fold

moresmoke #	C1	C2	ETHENE	C3	IC4	NC4	PROPENE
CP13-12	4.131		6.155				
CP13-13	40.655	2.392	2.058	1.861	1.501	2.453	2.718
CP13-14	88.419	0.305	1.451	0.901	0.391	0.198	
Harmonic Mean	7.307	0.264	1.811	0.654	0.485	1.006	1.700
Anomaly (2xHM)	14.613	0.528	3.622	1.309	0.969	2.011	3.401
average	23.574	0.987	2.929	1.380	0.708	1.702	2.112
std dev	38.895	2.005	2.912	1.358	0.533	0.808	0.622
minimum	2.226	0.074	0.462	0.148	0.271	0.168	0.364
maximum	227.947	14.573	30.128	7.351	1.501	3.400	3.277
Anomaly (1.5 x mean)	35.361	1.480	4.393	2.071	1.063	2.552	3.168
 L1-1	 4.476	 1.479					
L1-2	47.658	3.417	1.619	3.036	1.9	2.342	1.712
L1-3	24.092	2.062	1.259	1.585	0.539	1.694	1.396
L1-4	3.789		2.923	0.961			
L1-5	4.855		2.985				
L1-6	4.35		4.48				
L1-7	5.788	0.22	1.884	0.937			
L1-8	14.017	0.256	1.55	0.608		1.149	
L1-9	4.216	0.157	1.542	1.002			
L2-1	13.752	0.206	1.626	0.383			
L2-2	5.695	0.566	1.363	1.434		1.718	
L2-3	4.539		1.344				
L2-4							
L2-5			2.219				
L2-6	63.838	0.212	1.145				
L2-7	12.667	0.107	1.017				
L2-8	95.864		1.18				
L2-9						1.312	2.125
L2-10			0.889				1.454
L2-11	49.816			1.239		1.878	
L2-12	36.811	0.897	2.319	0.679		1.631	1.475
L2-13							
L2-14	57.092	0.802	2.467	0.778		1.551	1.38
L2-15	46.021	0.652	1.058	0.614		1.132	1.22
L2-16	16.945						
L2-17	11.851	0.694	1.249	0.463			1.664
L2-18			1.361	0.403		0.95	
L2-19	8.303		1.417				
L2-20	46.609	0.33	0.88	3.42			1.371
L2-21	34.043		0.965				
L2-22			0.863				
L2-23	5.747		1.349				
L2-24	4.349		0.911				
L2-25	37.195	1.366	0.866	0.89		1.391	1.464
L2-26	4.439						

TABLE MS5: IN-HOUSE HEAD GAS DATA

Phase III, More Smoke Creek

CV = Curvilinear

CP = CV Perpendicular

L = Lineament, F = Fold

moresmoke #	C1	C2	ETHENE	C3	IC4	NC4	PROPENE
L2-27	52.621	1.516	2.231	1.735	1.491	1.948	1.627
L2-28	40.164	1.207		1.053		1.415	1.695
L2-29	4.13						
L2-30	3.705		1.352				
L2-31	3.922		1.36	0.907			
L3-1	10.126		1.722				
L3-2	7.272		2.043				
L3-3	9.503		1.075				
L3-4	5.344		1.407	0.296			
L3-5	3.992		4.268	1.614			
L3-6	43.345		1.781	0.337			
L3-7	4.347						
L3-8							
L4-1	4.901	0.148	1.083	1.072			
L4-2	7.732	0.794	0.772	1.104	0.452	1.641	1.596
L4-3			1.552	0.282		1.039	
L4-4	44.191		1.309	0.216			
L4-5	6.94	0.191	1.37				
L4-6	4.939		6.274	5.153			1.342
L4-7	3.627		0.998	0.441			
L4-8	40.379	0.814	0.45	0.72	0.796	1.116	
L4-9		0.784	2.479	1.037	0.398	1.78	1.335
L4-10	5.061		7.968				
L4-11							
L4-12	11.157						
L4-13	5.401		1.383				
L4-14	3.324						
L4-15	5.826	0.145	1.212	1.344			
Harmonic Mean	7.548	0.331	1.359	0.682	0.664	1.425	1.497
Anomaly (2xHM)	15.097	0.662	2.719	1.365	1.328	2.851	2.994
average	19.246	0.763	1.806	1.153	0.929	1.511	1.524
std dev	21.085	0.774	1.359	1.035	0.623	0.373	0.223
minimum	3.324	0.107	0.450	0.216	0.398	0.950	1.220
maximum	95.864	3.417	7.968	5.153	1.900	2.342	2.125
Anomaly (1.5 x mean)	28.868	1.144	2.709	1.730	1.394	2.267	2.286
F1-1	12.789	0.284	1.556	2.301			
F1-2	50.804						
F1-3	84.424		0.698				
F1-4	2.482	0.239	1.196				
F1-5	6.608		1.242				
F1-6	9.597		1.484				1.366
F1-7							
F1-8			0.996				
F1-9							
F1-10	7.718	0.193	0.854	0.367		1.513	

TABLE MS5: IN-HOUSE HEAD GAS DATA

Phase III, More Smoke Creek

CV = Curvilinear

ppm CP = CV Perpendicular

L = Lineament, F = Fold

moresmoke #	C1	C2	ETHENE	C3	IC4	NC4	PROPENE
F1-11	4.325	0.103	0.447				
F1-12	3.852	0.167	1.038	1.261			
F1-13				0.445		1.277	1.315
F1-14	239.276		0.992	0.196			
F1-15	12.711	0.115	0.977	0.351		2.061	
F1-16	2.226						
F1-17	60.765		1.173				
F1-18			0.709				
F1-19	3.676						
F1-20	4.711						
F1-21	227.947		1.039	0.312			
F1-22	39.162						
F1-23							
F1-24	5.704	0.19	0.588	0.187			
F1-25	5.081		3.949				
F1-26	39.266	0.22	0.737	0.316			
F1-27		0.204	1.735	0.48			
F1-28	8.702	0.111	1.21				
F1-29	81.368	1.134	1.479	1.157	0.169	0.244	0.943
F1-30	6.888						
F1-31	26.584		1.069				
F1-32	3.548		3.623				
F1-33	131.536	0.984		1.078		1.078	1.844
F1-34	9.434	0.175	1.809	1.003			
F1-35	5.559		1.463	0.747			
F1-36	183.877		1.293	0.39			
F1-37	17.282				1.409		
Harmonic Mean	7.900	0.189	1.058	0.433	0.302	0.719	1.292
Anomaly (2xHM)	13.328	7.238	10.790	5.636	0.000	0.000	0.000
average	43.263	0.317	1.334	0.706	0.789	1.235	1.367
std dev	66.745	0.335	0.816	0.572	0.877	0.665	0.370
minimum	2.226	0.103	0.447	0.187	0.169	0.244	0.943
maximum	239.276	1.134	3.949	2.301	1.409	2.061	1.844
Anomaly (1.5 x mean)	64.895	0.475	2.001	1.059	1.184	1.852	2.051
SESE 8	6.862	0.308	1.349	0.431		1.162	
NWSE 8	5.31	0.173	1.141	1.525			
NESE 8	4.848	2.941	3.326				
PROPANE COMPARISON		CV	CP	L	F		
Harmonic Mean		0.803	0.654	0.682	0.433		
Anomaly (2xHM)		1.606	1.309	1.365	5.636		
average		1.803	1.380	1.153	0.706		
std dev		1.915	1.358	1.035	0.572		
minimum		0.192	0.148	0.216	0.187		
maximum		12.007	7.351	5.153	2.301		

TABLE MS5: IN-HOUSE HEAD GAS DATA

Phase III, More Smoke Creek

ppm

CV = Curvilinear

CP = CV Perpendicular

L = Lineament, F = Fold

moresmoke # Anomaly (1.5 x mean)	C1	C2 2.704	ETHENE 2.071	C3 1.730	IC4 1.059	NC4	PROPENE
MINIMUM		0.192	0.148	0.216	0.187		
AVERAGE		1.803	1.380	1.153	0.706		
MAXIMUM		12.007	7.351	5.153	2.301		